Mechanism of Valproic Acid Induced Dysmorphogenesis *Via* Oxidative Stress and Epigenetic Regulation at the *Hoxa2* Gene Promoter

A Thesis Submitted to the College of

Graduate Studies and Research

In Partial Fulfillment of the Requirements

For the Degree of Doctor of Philosophy

In the College of Pharmacy and Nutrition

University of Saskatchewan

Saskatoon

By

Xia Wang

PERMISSION TO USE

In presenting this thesis in partial fulfillment of the requirements for a postgraduate degree from the University of Saskatchewan, I agree that the libraries of this University make it freely available for inspection. I further agree that permission for copying of this thesis in any manner, in whole or in part, for scholarly purposes may be granted by Dr. Adil J. Nazarali, who supervised my thesis work or, in his absence, by the Dean of the College of Pharmacy and Nutrition in which my thesis work was done. It is understood that any copy or publication or use of this thesis or parts thereof for financial gain shall not be allowed without my written permission. It is also understood that due recognition shall be given to me and to the University of Saskatchewan in any scholarly use which may be made of any material in my thesis.

Requests for permission to copy or to make other use of material in this thesis in whole or part should be addressed to:

Dean of the College of Pharmacy and Nutrition
University of Saskatchewan
110 Science Place
Saskatoon, Saskatchewan S7N 5C9
Canada

ABSTRACT

Valproic acid (2-propylpentanoic acid, VPA) is a clinically used anti-epileptic drug and an effective mood stabilizer. VPA is also a histone deacetylase inhibitor and can induce embryonic malformations in both humans and mice. The mechanism(s) of VPA-induced teratogenicity are not well characterized. The objectives of my study were three fold, to: (i) investigate the effect of VPA on mouse embryonic development, (ii) characterize the putative mechanism(s) of VPA-induced teratogenicity and, (iii) investigate VPA associated epigenetic regulation of *Hoxa2* gene in cell lines and in developing embryos. Whole mouse embryo cultures were treated with VPA at doses of 0, 50 (0.35 mM), 100 (0.70 mM), 200 (1.4 mM), and 400 µg/mL (2.8 mM), encompassing the therapeutic range of 0.35 mM to 0.70 mM. Van Maele-Fabry's morphologic scoring system was used to quantitatively assess embryonic organ differentiation and development. *Hoxa2* gene expression was measured by quantitative real-time RT-PCR (Reverse Transcriptase-Polymerase Chain Reaction). To assess epigenetic changes on the *Hoxa2* gene promoter, DNA methylation was determined by bisulfite (BSP) sequencing and pyrosequencing. Histone "bivalent domains" H3K4me3 (histone 3 lysine 4 trimethylation) and H3K27me3 (histone 3 lysine 27 trimethylation) associated with gene activation and repression, respectively, were analyzed with qChIP-PCR (quantitative chromatin immunoprecipitation-PCR). Telomere length and telomerase activity were analyzed in mouse embryos and in NIH3T3 cell line treated with VPA.

Results indicate significantly increased incidence of dysmorphogenesis in embryos (11.8%, 35.3%, 47.0% and 88.3%) exposed to increasing doses of VPA (0.35 mM, 0.70 mM, 1.4 mM and 2.8 mM respectively). Van Maele-Fabry's quantitative differentiation assessment of developing embryos demonstrated a significantly lower score for the circulation system, central nervous system, craniofacial development and limb development in VPA treated embryos (0.35 mM to 2.8 mM) compared to the untreated control group. Glutathione homeostasis was altered as indicated by decreased total glutathione content and increased GSSG/GSH ratio in all VPA treatment groups. In addition, a dose-dependent inhibition of *Hoxa2* gene expression was observed in embryos and in the NIH3T3 cell line exposed to VPA. Pre-treatment with ascorbic acid [1000 µg/mL (5 mM)] restored

glutathione level and normalized *Hoxa2* gene expression in embryos exposed to VPA. DNA methylation status was characterized on the *Hoxa2* gene promoter at the three CpG islands; CpG island 1 (-277 to -620 bp), CpG island 2 (-919 to -1133 bp), and CpG island 3 (-1176 to -1301 bp) in the two cells lines (NIH3T3 and EG7) and in developing embryos. CpG sites remained unmethylated on the *Hoxa2* gene promoter in the NIH3T3 cell line which expresses the *Hoxa2* gene, whereas these same CpG sites were methylated in EG7 cells that did not express *Hoxa2*. CpG island 1 is closest to *Hoxa2* transcription start site and its methylation status was most affected. In developing embryos, CpG island 1 was found to be highly methylated at E6.5 when *Hoxa2* is not expressed, whereas the methylation status of CpG sites on the CpG island 1 declined between E8.5 and E10.5 when *Hoxa2* expression is present. VPA induced methylation of several CpG sites on CpG island 1 in NIH3T3 cell line and in E10.5 embryos when *Hoxa2* expression was down regulated following VPA exposure. In addition, embryos and the NIH3T3 cell line treated with VPA impacted the "bivalent domains" resulting in increased H3K27me3 enrichment and decreased H3K4me3 enrichment on *Hoxa2* promoter. Pre-treatment with ascorbic acid normalized *Hoxa2* expression and histone bivalent domain changes and prevented increased DNA methylation following VPA exposure. Moreover, the telomerase activity and telomere length were both impacted by changes in glutathione redox potential induced by VPA. Oxidative stress following VPA treatment reduced telomerase activity and accelerated telomere shortening.

These results are the first to demonstrate: (i) a correlation between VPA dose and total morphologic score in the developing mouse embryos. VPA impacted embryonic tissue differentiation and neural system development in the dose range of 0.35 mM to 2.8 mM; (ii) VPA altered glutathione homeostasis in cultured mouse embryos and inhibited *Hoxa2* gene expression; (iii) Histone bivalent domains of H3K27 and H3K4 trimethylation and DNA methylation status at the *Hoxa2* gene promoter region were altered following treatment with VPA. This appears to be the epigenetic event in transcriptional silencing of *Hoxa2* gene expression after VPA exposure; and (iv) Ascorbic acid normalizes glutathione homeostasis, H3K27 and H3K4 trimethylation and DNA methylation status, restoring *Hoxa2* gene expression following VPA exposure. Taken together our results show VPA-induced altered glutathione homeostasis, telomere shortening and telomerase dysfunction, and an

inhibition of *Hoxa2* gene expression leads to developmental abnormalities. Exposure to ascorbic acid had a protective effect on developing embryos exposed to VPA.

ACKNOWLEDGEMENT

I remembered it's in June 2003 that I transferred my master's program from Chemistry Department to Dr. Nazarali's lab at the College of Pharmacy and Nutrition. This marked the date that I started working in the biomedical research areas, the area that I will never regret in life.

The first week Dr. Nazarali had to explain to me on a blackboard what the RT-PCR is, and at the moment I didn't think I could have gone this far.

My first debt of gratitude must go to my supervisor, both my Master's and Ph.D. supervisor, Dr. Adil J. Nazarali. I couldn't imagine how much I have learned, grown and discovered with him over the last few years. He provided the vision, encouragement and advises necessary for me to proceed through my doctoral program and complete my dissertation. He has been a strong and supportive adviser to me throughout my graduate studies, and has always given me great freedom to pursue work independently. I owe him my heartfelt appreciation in my life for having some insights and taking big acts of courage to bring me into this field.

I would like to show my greatest appreciation to Dr. Alfred Remillard. I can't say "thank you" enough for his tremendous support and help. It has been a great privilege for me to spend several years in the College of Pharmacy and Nutrition, and its people and members will always be dear to me.

Special thanks to my graduate chairs Dr. Jane Alcorn and Dr. Ed. Krol, and my external examiner Dr. James Davie; and my committee: Dr. Brian Bandy, Dr. C. Ron Geyer, Dr. Jian Yang, for their guidance, support and helpful suggestions on my Ph. D. project and my thesis work, and also to Ms. Christine Ruys, who did so much formatting work on my thesis.

Past and present members of Dr. Nazarali's lab also deserve my sincerest thanks: Rhonda Sobchishin, Dr. Shaoping Ji, Ran Bi, Dr. Tara Smith, Jotham Gan, Paul Pown Raj, Merlin Paul, Muath Helal, Dennis Okello. Their friendship and assistance has meant more to me than I could ever express.

I take this opportunity also to express my gratitude to the people in the lab at the Department of Ophthalmology and Visual Sciences at UBC: Dr. Cheryl Gregory-Evans, Xianghong Shan, Naif Sannan, Elham Mohammadi and Dr. Ishaq Ahmed. I am grateful for their constant support and help.

I couldn't complete this work without invaluable help from the people and friends in Saskatoon and Vancouver and at VCAC, thank you for all your prayers.

Finally, I wish to thank my parents. Their love and help had generated inspiration to me and was my driving force. I owe them everything and I wish I could show them how much I love and appreciate them. I hope this work makes you proud of me.

TABLE OF CONTENTS

LIST OF TABLES

LIST OF FIGURES

ABBREVIATIONS

5-Aza	5-Azacytidine
AEDs	Antiepileptic drugs
ALS	Amyotrophic lateral sclerosis
ALT	Alternative telomere-lengthening
AML	Acute myeloid leukemia
AP-1	Activator protein-1
A-P	Anterior-posterior
ASD	Autistic spectrum disorder
ASH	Abundant Src homology
ASK 1	Apoptosis signal regulating kinase 1
ATPase	Adenosine triphosphatase
Bcl-2	B-cell lymphoma 2
Bid	BH3 interacting-domain death agonist
bFGF	Basic fibroblast growth factor
Blimp1	B-lymphocyte-induced maturation protein 1
BMI1	B lymphoma Mo-MLV insertion region 1 homolog
BMP4	Bone morphogenetic protein 4
bp	Base pair
BRCA1	Breast cancer type 1 susceptibility protein
BSO	L-Buthionine-sulfoximine
BSP	Bisulfite specific PCR
CBP	CREB binding protein
CCA	cholangiocarcinoma
Cdx2	Caudal-related homeobox 2
CG	Cytosine and guanine
CGIs	CpG islands
ChIP-qPCR	Chromatin immunoprecipitation and quantitative real-time PCR assays

ChIP-on-chip	Chromatin immunoprecipitation with microarray (chip)
CM-H2DCFDA	Chloromethyl-2',7'-dichlorofluorescein diacetate
CNS	Central nervous system
COMPASS	Complex Proteins Associated with Set1
CoR	Corepressors
CoREST	REST corepressor 1
CpG	Cytosine and guanine separated by a phosphate
CREB	c-AMP response element-binding
CTCF	CCCTC-binding factor
Daz1	Deleted in azoospermia-like
DBD	DNA-binding domain
DC	Dyskeratosis congenital
DDR	DNA damage response
Ddx4	DEAD box polypeptide 4
Dhx38	DEAH box polypeptide 38
Dicer	Endoribonuclease in the RNase III family
DKC1	Dyskerin gene
DNMTs	DNA methyltransferases
DNMT3	DNA methyltransferase 3
DNMT3a	DNA methyltransferase 3 alpha
DNMT3b	DNA methyltransferase 3 beta
Dpc	days post coitum
dRING	*Drosophila* Really Interesting New Gene (zinc finger)
DTNB	5,5'-dithiobis-2-nitrobenzoic acid
ERK	Extracellular signal-regulated kinase
E	Embryonic stage
E2	Ubiquitin-conjugating enzymes
E3	Ubiquitin ligase

EED	Embryonic ectoderm development
EGs	Embryonic germ cells
ES	Embryonic stem cells
ESC	Extra sex combs
ESET	ERG-associated protein with SET domain
E(Z)	Enhancer of zeste
EZH2	Enhancer of zeste homolog 2 (histone lysine N- methyltransferase)
Exe	Extraembryonic ectoderm
FCS	Fuculose
FGF	Fibroblast growth factor
Fgf2	Fibroblast growth factor 2
Fragilis	First gene to be implicated in acquisition of germ cell competence (An interferon-inducible gene coding for a transmembrane protein)
GABA	γ-aminobutyric acid
GABA-T	GABA transaminase
GAD	Glutamic acid decarboxylase
Gal10	*H. jecorina* uridine 5'-diphosphate (UDP)-glucose 4-epimerase
GCN5	General control nonderepressible
GNAT	GCN5-related N- acetyltransferases
GSH	Glutathione
GSSG	Oxidized glutathione
GST	Glutathione S-transferase
H	Histone
HATs	Histone acetyltransferases (now called KATs)
γH2AX	Phosphorylation of histone H2AX
HBSS	Hank's balanced salt solution
HDAC1	Histone deacetylase 1

HDACi/HDACI	Histone deacetylase inhibitor
HDACs	Histone deacetylases
H3K4	Histone 3 lysine 4
H3K4me3/me2	tri-methylated or dimethylated H3K4
H3K9	Histone 3 lysine 9
H3K27	Histone 3 lysine 27
H3K27(me3)	tri-methylated H3K27
H3K36	Histone 3 lysine 36
H3K79	Histone 3 lysine 79
H4K5	Histone 4 lysine 5
5hmc	5-hydroxymethylcytosine
HMG	High mobility group proteins
HMTase	Histone methyltransferase
Hox gene	Homeobox gene of the Antennapedia class
HP1	Heterochromatin protein 1
H3P38	Histone 3 proline 38
H3S10	Histone 3 serine 10
H3T6	Histone 3 threonine 6
Hst	Homologue of Sir2
ICM	Inner cell mass of blastocyst
Ifitm3	Interferon induced transmembrane protein 3
IL-2	Interleukin-2
i. p.	Intraperitoneal
IUGR	Intrauterine growth restriction
JARID1B	Lysine (K)-specific demethylase 5B (Jumonji/ARID domain-containing protein 1B)
Kap1	A corepressor for Krüppel-associated box domain
KATs	Lysine (K) acetyltransferases (formerly called histone acetyltransferase

	(HAT)
kb	Kilobase
LC-pTP	Leucocyte-phosphotyrosine phosphatase
LIF	Leukemia inhibitory factor
lncRNAs	Long non-coding RNAs
LBD	Ligand-binding domain
LSD1	Lysine-specific demethylase 1
MBDs	methyl-CpG binding domain proteins
5mc	5-methylcytosine
MDA	Malondialdehyde
MDS	Myelodysplastic syndrome
MeDIP	Methylated DNA immunoprecipitation
Me2/3	Di/tri methylation
MeCP2	Methyl CpG binding protein 2
MES	(N-morpholino) ethanesulphonic acid
MLL	Mixed lineage leukemia
MMP	Matrix metalloproteinases
MSP	Methylation specific PCR
MYST	Named for the founding members MOZ, Ybf2/Sas3, Sas2, and Tip60
NAD-dependent	Nicotinamide adenine dinucleotide-dependent
Nanog	Homeobox protein Nanog
NCH-51	Non-hydroxamic acid HDAC inhibitor
NCoR	Nuclear receptor co-repressor 1
NMDA	N-methyl-D-aspartate
NRs	Nuclear receptors
NTDs	Neural tube defects
NuRD	Nucleosome remodeling and deacetylase

NURF-55	Nucleosome remodeling factor 55
ODNs	Oligodeoxynucleotides
ORF	Open reading frame
Oct4	Ornithine carbamoyltransferase 4
Orc2	Origin recognition complex 2
P160	160 kDa protein
p300	E1A binding protein p300
Paf1	Polymerase associated factor 1
PBMC	Peripheral blood mononuclear cells
PBS	Phosphate buffer saline
PC	Polycomb
PCAF	P300/CBP-associated factor
PcG	Polycomb group
PCR	Polymerase chain reaction
PECAM	Platelet-derived endothelial cell adhesion molecule
PEct	Primitive ectoderm cell
PGCs	Primordial germ cells
PKC	Protein kinase
Ph	Polyhomeotic
PHD	Plant Homeo Domain
PhoRC	Pho-repressive complex
POT1	Protection of telomeres 1
PRC1	Polycomb repressive complex 1
PRC2/3	Polycomb repressive complex 2/3
PRDM1	PR domain containing 1
PRE/TREs	Polycomb/Trithorax response elements
PRMT5	Protein arginine methyltransferase 5
Psc	Posterior sex combs

PTMs	Post-translational modifications
RA	Retinoic acid
RAD51	A protein family highly similar to bacterial RecA and *Saccharomyces cerevisiae* Rad51
RAP1	Repressor and activator protein 1
Ring1B	RING finger protein member of Polycomb group
REST	repressor element-1 silencing transcription factor
RLIM	ring finger protein, LIM domain interacting
RNAi	RNA interference
RNAPII	RNA polymerase II
RNP	Ribonucleoprotein
ROS	Reactive oxygen species
Rpd3	Reduced potassium dependency 3
Rtt109	Regulator of Ty1 transposition protein 109
RT	Reverse transcription
SAHA	Vorinostat (suberoylanilide hydroxamic acid)
SAM	S-adenosyl methionine
s.c.	Subcutaneous
SET	Suppressor of variegation-Enhancer of zeste-Trithorax (A 130-160 amino acid motif, found in proteins that are members of PcG, trxG and SU(VAR). Names after the genes *Su(var)3-9, Enhancer of zeste [E(z)]* and *trithorax (tr*x))
Set1/KMT2	SET domain-containing protein 1/Histone-lysine N-methyltransferase
SIN3A	Switch Independent 3 homolog A (Yeast)
SIR2	Sirtuins 2 (Silencing information regulator) 2
siRNAs	Small interfering RNAs
Sox2	(Sex determining region Y)-box 2

SPT10	Sequence-specific putative histone acetylase (*S. Cerevisiae*)
SSAD	Succinic semialdehyde dehydrogenase
ssDNA	single stranded DNA
Su(var)3-9	Suppressor of variegation 3-9 *(Drosophila)*
SUZ12	Suppressor of zeste 12 homolog *(Drosophila)*
SW1/SNF	Multicomponent complex of *Saccharomyces cerevisiae*
Sycp3	Synaptonemal complex protein 3
TAFII250	TATA-binding protein-associated factors
TBP2	Trx binding protein
TERT	Telomerase reverse transcriptase subunit
TET	Ten-eleven-translocation oxygenase
TFIID	Transcription factor II D
TIN2	TRF1-interacting nuclear protein 2
TPP1	POT1-and TIN2-interacting protein
TRF	Repeat-binding factor 1
Trx	Thioredoxin
trxG	Trithorax group
TSR	Ratio of telomere repeat copy number to single gene copy number
TSA	Trichostatin A
R	Rhomobomere
TNB	5-thio-2-nitrobenzoic acid
H2A119ub	Ubiquitylation of core histone 2A at 119
Ubc8	Ubiquitin conjugating enzyme 8
Ubx	Ultrabithorax
VYS	Visceral yolk sac
VPA	Valproic acid
VE	Visceral endoderm
VEGF	Vascular endothelial growth factor

Wk	Week
Wnt	Wingless-type MMTV integration site family member
YY1	Yin Yang-1

CHAPTER 1: OBJECTIVES AND HYPOTHESES

HYPOTHESES

1. Valproic acid (VPA) is teratogenic and induces oxidative stress in mouse embryo organ culture *in vitro*. Change in embryonic antioxidant status will affect *Hoxa2* gene expression during VPA-induced teratogenesis.

2. Exposure to VPA will lead to alterations in histone bivalent modification patterns at *Hoxa2* gene promoter and inhibit *Hoxa2* gene expression. Hence, an increase in trimethylated histone 3 lysine 27 (H3K27me3) will be accompanied by a decrease in trimethylation of H3K4 (H3K4me3) at *Hoxa2* gene promoter inducing transcriptional repression.

3. VPA will induce DNA methylation at *Hoxa2* CpG-enriched-promoter region in NIH3T3 cell line and in mouse embryos with active *Hoxa2* gene transcription and inhibit *Hoxa2* gene expression.

4. Depletion of GSH and changes in GSSG/GSH redox potential induced by VPA will reduce the telomerase activity and telomere length. This will be blocked by the addition of ascorbic acid in VPA treated NIH3T3 cell line and in developing embryos.

OBJECTIVES

1. To determine the effect of VPA-induced teratogenicity and VPA-induced oxidative stress on *Hoxa2* gene expression in mouse embryo cultures *in vitro.*

2. To determine the effect of VPA on DNA methylation status and histone modifications at the *Hoxa2* gene promoter in a cell culture system and in the developing mouse embryo.

3. To investigate the role of redox potential impacted by VPA on the regulation of the telomerase activity and the telomere length.

CHAPTER 2: LITERATURE REVIEW

2.1. Valproic acid: an antiepileptic drug

Valproic acid (2-*n*-propylpentanoic acid; VPA) is one of the most widely prescribed antiepileptic drug (AED) since its introduction into clinical use in 1974 (Fig.2.1).

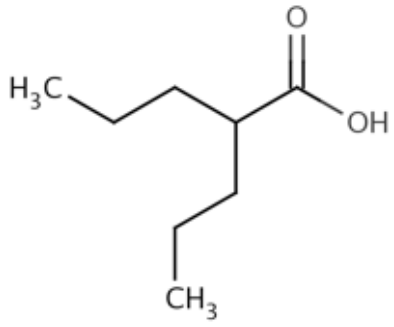

Fig. 2.1 Chemical structure of valproic acid (2-*n*-propylpentanoic acid; VPA)

VPA is used to treat a wide spectrum of seizures including absence seizures, tonic-clonic seizures, complex partial seizures, and juvenile myoclonic epilepsy. It is also used in the treatment of bipolar disorder, migraine headaches, addiction, amyotrophic lateral sclerosis (ALS), and neuropathic pain (Chateauvieux et al., 2010; Loscher, 1999). In the recent years, VPA has been associated with treatment or clinical trials for other neurological disorders, such as mood disorders, schizophrenia, and attention deficit hyperactivity disorder (Chateauvieux et al., 2010). The neurochemical and neurophysiological mechanisms of VPA on anticonvulsive action are complex and not well-defined. One mode of action of VPA is to increase levels of the neurotransmitter γ-aminobutyric acid (GABA) in the brain. GABA is an important inhibitor of seizures and a reduction in GABA levels potentiate seizures (Owens and Nemeroff, 2003; Perucca, 2002; Shorvon, 1990). However, it is not known whether the effect of VPA on GABA is due to activation of the GABA synthesizing enzyme, glutamic acid decarboxylase (GAD), or due to inhibition of the catabolic enzymes, succinic semialdehyde dehydrogenase (SSAD) and GABA transaminase (GABA-T) (Davis et al., 1994; Sztajnkrycer, 2002). VPA can reduce the release of the epileptogenic γ-hydroxybutyric

acid and attenuates neuronal excitation mediated by activation of N-methyl-D-aspartate (NMDA)-type glutamate receptors (Porter and Meldrum, 2001). VPA also exerts a direct effect on the potassium channels of the neuron membrane (Porter and Meldrum, 2001). For daily seizure control, VPA doses range between 300 mg to 2 g to achieve therapeutic plasma levels of 50-100 μg/mL [0.35 mM-0.70 mM] (Ornoy, 2009). Lower doses are usually used in the treatment of bipolar disorder and migraine (Ornoy, 2009).

VPA is a histone deacetylase inhibitor (HDACI) (Phiel et al., 2001), that has wide implications in the treatment of various cancers including multiple myeloma (Schwartz et al., 2007), glioma (Ciusani et al., 2007), and melanoma (Valentini et al., 2007). Most of the clinical data on the antitumor effect of VPA has come from studies of combining VPA and DNA methylation inhibitors. Recently, some completed phase I/II studies included combined action of decitabine and VPA (Garcia-Manero et al., 2006), or azacitidine, VPA and retinoic acid (Soriano et al., 2007) in hematological malignancies. VPA shows potent antitumor effect in a wide variety of cancers in preclinical studies, both *in vitro* and *in vivo*, by modulating multiple pathways including cycle arrest, angiogenesis, apoptosis, differentiation and senescence (Chateauvieux et al., 2010).

The use of VPA in monotherapy or polytherapy for leukemia diseases is promising. VPA exerts different effects in different cell types, including inducing proliferation in early stem cells and inhibiting angiogenesis, which could be beneficial in the treatment of leukemic pathologies (Chateauvieux et al., 2010). Clinical studies on the use of VPA have shown the beneficial effect especially on myelodysplastic syndrome (MDS) (Batty et al., 2009; Chateauvieux et al., 2010; Kuendgen et al., 2005; Kuendgen et al., 2006).

2.2. Teratogenic effects of VPA

2.2.1. Effect of VPA during pregnancy

Many anti-epileptic drugs (AEDs) are teratogenic to the embryo and fetus when used during pregnancy (Diav-Citrin et al., 2008; Dravet et al., 1992; Kaneko et al., 1999; Kini et al., 2006; Kultima et al., 2004; Morrow et al., 2006; Ornoy, 2003). In a majority of epileptic women, even when pregnancy is planned, AEDs cannot be discontinued because the risk of seizures during pregnancy can be harmful to both mother and child (Ornoy, 2006). As a result, adverse effects of AEDs on fetuses are a major concern for millions of women with epilepsy (Perucca, 2005). Studies have suggested that the rate of malformation among the offspring of women with untreated epilepsy is similar to that in non-epileptic control women (Fried et al., 2004), which indicate that epilepsy by itself was not associated with a high risk of congenital malformations in the offspring. VPA can cross the human placenta, and is likely the most potent teratogenic anticonvulsant drug (Diav-Citrin et al., 2008; Dravet et al., 1992; Kaneko et al., 1999; Kini et al., 2006; Morrow et al., 2006). VPA clearance is increased during pregnancy, and the accumulated VPA levels in placental cord serum are often up to 5 times higher than levels in maternal serum at term (Albani et al., 1984; Nau, 1982). Intrauterine exposure to AEDs can result in increased rate of major and minor congenital anomalies, especially if exposure occurred during the first trimester of pregnancy (Ornoy, 2009). Many studies have described an association between the VPA administration in the first trimester and the occurrence of fetal anomalies (Ardinger et al., 1988; DiLiberti et al., 1984). These anomalies can be anatomical or functional or both, and can include neurological, behavioural and cognitive defects (Ardinger et al., 1988; DiLiberti et al., 1984).

Teratogenic effects of VPA could be due to impaired methionine synthesis (Alonso-Aperte et al., 1999), as VPA interrupts the folic acid cycle and subsequent synthesis of methionine (Ubeda-Martin et al., 1998) and/or due to the induced oxidative stress, to which the brain is more susceptible than the other fetal organs (Ornoy, 2009; Zhang et al., 2010).

2.2.2. Valproate syndrome

VPA associated facial dysmorphic features in the developing embryo and fetus were first described by DiLiberti et al., (1984). The use of VPA during pregnancy causes a 1-2% incidence of neural tube defects (NTDs) mainly associated with spina bifida aperta and is 10-20 times higher than in the general population (Bjerkedal et al., 1982; Dalens et al., 1980; Fried et al., 2004; Gomez, 1981; Lindhout et al., 1992; Omtzigt et al., 1992; Robert et al., 1983). Many of the children affected by VPA developed a typical "fetal valproate syndrome". Features of VPA exposure *in utero* include intrauterine growth restriction (IUGR) and facial dysmorphism recognized by mid-facial hypoplasia, hypertelorism, epicanthal folds, short nose with a broad nasal bridge, thin upper lip but thick lower lip, and micrognathia; and other abnomalies found in limbs, heart and brain (Dean et al., 2000; DiLiberti et al., 1984). Animal studies in monkeys, mice, rats, hamsters and rabbits have also documented VPA-induced teratogenic effects including craniofacial, skeletal, cardiac, limb, renal, and central nervous system anomalies including NTDs and encephaloceles (Lyon et al., 2003; Nulman et al., 1997).

2.2.3. VPA-induced neurodevelopmental defects

VPA associated intellectual ability studies have noted children exposed *in utero* exhibit developmental delay including reduced cognitive function, attention deficit disorder and learning difficulties. Most of them have the typical facial dysmorphic features as part of the "valproate syndrome" (Christianson et al., 1994; Dean et al., 2002; Dean et al., 2000; Eriksson et al., 2005; Kini et al., 2006; Koch et al., 1996; Langer et al., 1994; Moore et al., 2000; Perucca and Tomson, 2006; Viinikainen et al., 2006). Christianson et al., (1994) first described a relationship that may exist between VPA exposure and autistic spectrum disorder (ASD). In their study, four children exposed *in utero* to VPA demonstrated developmental delay, and one of these children also had ASD. Later studies on children associated with typical facial features of VPA embryopathy were also described to have developed typical features of autism (Williams et al., 2001). Recently, more findings of VPA exposure

associated with ASD have been reported (Adab et al., 2004; Dean et al., 2002; Meador, 2006; Moore et al., 2000; Rasalam et al., 2005; Viinikainen et al., 2006).

2.2.4. VPA in animal studies

Many animal studies attempting to mimic effects of VPA on human embryos were carried out to elucidate mechanisms of VPA teratogenicity (Arndt et al., 2005; Wagner et al., 2006; Wegner and Nau, 1991; Wegner and Nau, 1992; Zhang et al., 2010). VPA induces multiple organ malformations in mice, rats, and gerbils; kidney and skeletal defects in rabbits; NTDs in mice and hamsters; and craniofacial and appendicular skeletal defects in primates (Binkerd et al., 1988; Ehlers et al., 1996; Ehlers et al., 1992; Emmanouil-Nikoloussi et al., 2004; Holmes et al., 2005; Narotsky et al., 1994). High doses of VPA in rhesus monkeys are associated with IUGR and craniofacial and skeletal anomalies, all of which are similar to effects demonstrated in the human fetus (Hendrickx et al., 1988).

A number of animal studies have been conducted to further characterize VPA-induced ASD (Ingram et al., 2000; Rodier et al., 1996). When VPA is administered to pregnant mice and rats, a set of behavioural changes in the offspring that resemble the behavioural changes in human ASD were observed (Ingram et al., 2000; Rodier et al., 1996). Recently, one study showed mice exposed to VPA at embryonic day 12.5 (E12.5) exhibited social interaction deficits, anxiety-like behaviour and memory deficits at age 4-8 week (wk). VPA treatment also decreased the number of Nissl-positive cells in the prefrontal cortex and somatosensory cortex in mice at 8 wk of age (Kataoka et al., 2011). Furthermore, VPA exposure caused a transient increase in histone acetylation in the embryonic brain. It was followed by increased cell death in the neocortex and decreased cell proliferation in the ganglionic eminence. This study implicated a dysfunction in HDAC activity during pregnancy as a key risk factor of ASD in the offspring (Kataoka et al., 2011).

These findings strengthen the possible relationship between *in utero* VPA exposure and ASD that has been suggested in humans (Arndt et al., 2005; Wagner et al., 2006). Furthermore, VPA has a toxic effect on the development of central nervous system (CNS) in

animals, with respect to biochemical and morphological changes such as reduced number of neurons in motor cranial nerve nuclei in the brain (Arndt et al., 2005; Emmanouil-Nikoloussi et al., 2004; Rodier et al., 1996; Ingram et al., 2000). Interestingly, the timing of the effect of VPA that increased the risk of ASD is coincident with the timing of neural tube closure (Wagner et al., 2006).

2.3. Proposed mechanism(s) of VPA-induced teratogenicity

2.3.1. Folic acid deficiency

One mechanism of AED-induced birth defects is believed to be due to a reduction in folic acid level that occurs after treatment with VPA and other AEDs. Lower folic acid levels in embryos can result in disruption of gene expression and changes in protein syntheses and also induce embryonic oxidative stress (Wegner and Nau, 1991; Wegner and Nau, 1992). VPA appears to interfere with the metabolism of folic acid, whereas other AEDs appear to act specifically on the intestine and reduce intestinal absorption of folic acid (Wegner and Nau, 1991; Wegner and Nau, 1992; Yerby, 2003). However, the mechanism of the disturbances in folic acid metabolism only plays a partial role in VPA-induced teratogenicity (Graf et al., 1998; Ornoy, 2009).

2.3.2. Oxidative stress

2.3.2.1. Redox homeostasis and glutathione

Redox homeostasis is very important for vital cellular functions. The disruption of redox homeostasis is accompanied by an increase in the level of reactive oxygen species (ROS), and causes oxidative damage to lipids, DNA, and proteins (Oktyabrsky and Smirnova, 2007).

Glutathione (GSH), a widely distributed thiol in animal organisms, is the major redox buffer in cells (Zuelke et al., 2003). It has antioxidative properties and protects eukaryotic cells against ROS (Luberda, 2005). GSH also plays a role during oocyte maturation, fertilization and the pre-implantation stage of embryo development. The GSH level in a cell

is determined by the rate of its synthesis and the rate of export and conjugation. Apoptosis is an important process in the cell and can be initiated by alterations in redox homeostasis (Ghibelli et al., 1998; Gulbins et al., 2000; Kern and Kehrer, 2005; Kwon et al., 2003). An early event during apoptosis is the efflux of reduced GSH from cells through specific channels across the cytoplasmic membrane. GSH efflux can cause disruption of redox balance and ultimately lead to oxidative stress (Kern and Kehrer, 2005).

2.3.2.2. Teratogenic effect of oxidative stress

Similar to diabetic teratogenicity, the intermediate metabolites of AEDs can induce oxidative stress, and increased oxidative stress can cause irreversible damage to the developing fetus especially since the embryonic antioxidant defense systems are immature and develop slowly with the advancement in gestational stage (Danielsson et al., 2007; Ornoy, 2007). Studies conducted in rats have suggested enhanced oxidative stress is more harmful to the developing brain than to other fetal organs (Ornoy, 2007).

2.3.2.3. Oxidative stress induced by VPA

There is a growing body of evidence indicating VPA exposure can cause excessive oxidative stress, as a result of VPA biotransformation or alterations in GSH homeostasis or cofactors required for antioxidant reactions (Cotariu et al., 1990; Graf et al., 1998; (Hurd et al., 1984; Tabatabaei and Abbott, 1999; Yuksel et al., 2001; Zhang et al., 2010). VPA-induced testicular toxicity is reported to be associated with elevated oxidative stress and an over-production of free radicals, accounting at least in part the testicular injury associated with VPA exposure (Hamza and Amin, 2007). Children with epilepsy treated with VPA showed increased oxidative stress that linked to obesity (Verrotti et al., 2008).

Oxidative stress has also been implicated in VPA-induced idiosyncratic hepatotoxicity (Tabatabaei and Abbott, 1999; Weber et al., 1991). *In vitro* studies have revealed decreased GSH content in liver homogenates from rats administered with a single intraperitoneal (i.p) dose of VPA (Cotariu et al., 1990; Seckin et al., 1999). Interestingly, VPA toxicity in

cultured rat hepatocytes could be attenuated by antioxidants such as ascorbic acid (Jurima-Romet et al., 1996). Recently, it has been demonstrated that VPA is capable of producing elevated levels of mitochondrial ROS in glioma cells, leading to loss of matrix metalloproteinases (MMP) and mitochondrial injuries and causing cytotoxicity and ultimately cell death (Fu et al., 2010). Another study was also the first to directly localize ROS in mouse embryos by whole-mount immunofluorescence with CM-H2DCFDA (chloromethyl-2',7'-dichlorofluorescein diacetate), a dye sensitive to ROS (Tung and Winn, 2011). A significant increase in fluorescent staining was observed in the heads of mouse embryos that were exposed to VPA, and these increased ROS levels were attenuated by coculture with PEG-catalase (Polyethylene glycol – catalase). PEG-catalase catalyzes the decomposition of hydrogen peroxide to water and molecular oxygen, preventing VPA-induced ROS formation (Tung and Winn, 2011). The incidence of embryonic and fetal defects induced by VPA was prevented by catalase in both whole-embryo culture and *in vivo* models (Tung and Winn, 2011). Increased apoptosis in the neuroepithelium caused by VPA-induced ROS production and alterations in embryonic signaling may be the underlying causes of NTDs in this model. They postulated that VPA may be mediating teratogenesis by alterations in redox-sensitive signaling pathways (Tung and Winn, 2011).

Study reported in this thesis on VPA induced teratogenicity in whole mouse embryo culture system showed that VPA decreased GSH content, increased GSSG/GSH ratio and induced oxidative stress. VPA also inhibited *Hoxa2* gene expression in a dose-dependent manner (see section 4.1). Pre-treatment with the antioxidant, ascorbic acid, prevented VPA-induced reduction in GSH and normalized *Hoxa2* expression in the whole mouse embryo cultures (see Section 4.1)(Zhang et al., 2010)

2.3.3 VPA as an inhibitor of histone deacetylase (HDAC)

Phiel et al. (2001) were the first to describe VPA induced inhibition of histone deacetylase (HDAC). They demonstrated in HeLa cell lines that VPA is a potent inhibitor of histone deacetylases and reduced the level of histone deacetylation, resulting in the change of

chromatin structure and the accessibility of transcription factors and RNA polymerase to the DNA to regulate gene expression (Orney, 2009).

There is good congruency between VPA's teratogenic potency and its HDAC inhibition (Eikel et al., 2006b), prompting the widely known term "valproate syndrome" for consideration to be renamed as the "HDACi syndrome" (Eikel et al., 2006a). Indeed, there is direct correlation between the axial abnormalities and the specific hyperacetylation levels in the embryonic axial organs such as the somites (Eikel et al., 2006a; Menegola et al., 2005). Mouse embryos between E8 and E10 stage of development exposed to VPA *in utero* induced hyperacetylation of histone 4 (H4) and caused embryonic tissues to be hyperacetylated in the caudal neural tube and somites (Eikel et al., 2006a; Menegola et al., 2005). VPA induces growth retardation and a number of congenital anomalies in *Xenopus* and zebrafish embryos as a result of its inhibition of HDAC (Wiltse, 2005). HDAC inhibitors can interrupt cell cycle, arrest cell growth, and induce apoptosis (Ornoy, 2009). Hence, inhibition of cell proliferation after VPA could be one mechanism for its teratogenicity (Ornoy, 2009). This has been demonstrated in cultured brain microglial cells obtained from 2-day-old rats exposed to VPA which induces apoptosis, suggesting specific brain damage can occur in the offspring of rats exposed to VPA *in utero* (Chen et al., 2007; Ornoy, 2009).

VPA specifically targets 2 of the 4 classes of HDACs: class I (HDAC 1, 2, 3 and 8) and class IIb (HDAC6 and 10), components of HDAC complexes [REST corepressor 1 (CoREST), NuRD, Sin3, Nuclear receptor co-repressor 1 (NCoR) complex], and putative novel complex components or targets (Bradbury et al., 2005; Bantscheff et al., 2011). It is interesting to mention that HDAC classes I and II have been reported to be strongly implicated in neuronal function, which could partially explain the action of VPA in neural pathologies (Chateauvieux et al., 2010).

2.3.4 VPA or HDAC inhibitor and oxidative stress

HDAC inhibitors cause histone hyperacetylation and influence chromatin stability by inducing profound changes in chromatin structure (Eot-Houllier et al., 2009). These changes can release tightly packed DNA, thereby increasing exposure to potential damage (Eot-Houllier et al., 2009; Rajendran et al., 2011).

HDAC inhibition may also disrupt the expression of DNA repair genes by affecting the timing of their expression, leading to improper cellular responses to DNA damage and accumulation of strand breaks and modified bases (Eot-Houllier et al., 2009). HDAC inhibitors such as vorinostat, PCI-24781 (a broad-spectrum phenyl hydroxamic acid HDAC inhibitor) (Adimoolam et al., 2007) and VPA (Kachhap et al., 2010) have been shown to decrease the expression of DNA repair proteins such as Ku70 (a protein that binds to DNA double-strand break ends and is required for the non-homologous end joining pathway of DNA repair) (Chen et al., 2007), BRCA1 (breast cancer type 1 susceptibility protein) (Zhang et al., 2007), RAD51 (a protein family highly similar to bacterial RecA and *Saccharomyces cerevisiae* Rad51)(Adimoolam et al., 2007), and CtIP (C-terminal-binding protein 1)(Robert et al., 2011). Moreover, these studies have found that DNA damage was related to ROS generation and GSH depletion (Sestili et al., 2010).

ROS, hydrogen peroxide, and hydroxyl radicals, represent major sources of endogenous DNA damage (Eot-Houllier et al., 2009). Normal cells control ROS concentrations through the actions of enzymatic and non-enzymatic ROS scavengers (Eot-Houllier et al., 2009). However, cells with particularly high ROS concentrations, or with defective or damaged ROS scavengers, enter a state of genotoxic oxidative stress that eventually leads to apoptosis (Sancar et al., 2004). A number of studies have reported that HDAC inhibition by several HDAC inhibitors, such as Vorinostat, MS-275 (a benzamide HDAC inhibitor), or NCH-51 (non-hydroxamic acid HDAC inhibitor) lead to accumulation of ROS (Ruefli et al., 2001; Rosato et al., 2003; Sanda et al., 2007; Ungerstedt et al., 2005; Xu et al., 2006). The resulting oxidative stress seems to be involved in HDAC-induced apoptotic effects, since co-treatment

with ROS scavengers, such as N-acetylcysteine decreased HDAC inhibitor-induced cell death (Ruefli et al., 2001; Rosato et al., 2003; Sanda et al., 2007). The HDAC inhibitor, LAQ-824, also triggered ROS production, with increased γH2AX (phosphorylation of histone H2AX) and Ku70 acetylation (Rosato et al., 2008).

Consequently, HDAC inhibitors may enhance oxidative DNA damage by changing the chromatin conformation or inducing histone hyperacetylation of DNA repair proteins (Eot-Houllier et al., 2009), causing ROS accumulation, disrupting intracellular redox balance and impacting mechanisms involved in the repair of oxidative DNA lesions (Driscoll et al., 2007). HDAC inhibition may also disrupt the regulation of ROS concentration or mitotic progression. Thus, HDAC inhibitors can likely induce extensive oxidative DNA damage (Eot-Houllier et al., 2009).

HDACIs also alter cellular functions through having effects on non-histone proteins (Tang et al., 2013). These non-histone proteins were involved in the regulation of gene expression, pathways of apoptosis, cell-cycle progression, mitotic division, redox pathways, DNA repair, cell migration and angiogenesis (Seuter et al., 2012; Shan et al., 2012). Therefore, HDACIs might have an effect on immune responses, inflammation, cell survival, cellular differentiation and proliferation (Tang et al., 2013).

2.3.5 Impact of VPA exposure on gene expression

Many molecular approaches have been used to evaluate the expression of genes vital for normal and abnormal neural tube closure in intact, mutant, and chemically induced NTD mouse models (Finnell et al., 2002). A significant increase in the expression of transforming growth factors α and β which regulate the maintenance of neural viability has been reported in the neural tube of mouse embryos exposed to VPA. Okada et al. (2004) employed a GeneChip system to catalog the expression of genes in mouse embryos that exhibited VPA-induced failure of neural tube closure. They report an increase in expression of *Gadd45b, Ier5, Per1, Phf13, Pou3f1,* and *Sox4,* and decrease in *Ccne2, Ccnl, Gas5, Egr2, Sirt1* and

Zfp105 expression in the heads of mouse embryos after 1 h of i.p. injection of VPA (600 mg/kg at E8.0). These changes of gene expression are strongly correlated with VPA's teratogenic potency. *Egr2* and *Zfp105* are zinc finger protein genes, which are DNA-binding transcription factors (Gommans et al., 2005). *Sir1* is an HDAC enzyme protein that exhibits NAD-dependent activity, regulating transcription, apoptosis and stress resistance (North and Verdin, 2004). *Sir1* binds directly to p53 and suppresses p53-dependent apoptosis in response to DNA damage (Gasser and Cockell, 2001; Guarente, 2000; Imai et al., 2000). An analysis of these genes demonstrates VPA disrupts gene expression that is essential for the regulation of the cell cycle and the apoptosis pathways of the neural tube cells during neurulation in mice. Mechanism of VPA-induced teratogenicity has also involved investigations on changes in gene expression (Chen et al., 2007; Menegola et al., 2006; Stodgell et al., 2006; Wiltse, 2005). For example, VPA induces down-regulation of *protein kinase C* isoforms (Menegola et al., 2006), and up-regulation of *Bcl-2* (Chen et al., 2007), *Hoxa1* (Stodgell et al., 2006) and activated Wnt-dependent gene expression (Wiltse, 2005). In our study, we found VPA induces a dose-dependent down-regulation of *Hoxa2* gene in whole mouse embryo culture system (see Section 6.1).

In a recent study, researchers used CodeLink whole-genome expression microarrays in undifferentiated R1 mouse embryonic stem cells exposed to VPA to define VPA-responsive genes that correlate with teratogenicity (Jergil et al., 2011). Many of the genes that were found to be deregulated by VPA and correlating with teratogenicity, appear to related to embryonic development and morphogenesis including neural tube formation and closure. This indicates genes that are important in embryonic development are putative teratogen targets of VPA in this *in vitro* system (Jergil et al., 2011). Genes important for cell division and cell differentiation were downregulated and upregulated by VPA, respectively, in agreement with cellular effects of VPA for inhibiting proliferation and promoting differentiation (Jergil et al., 2011). A large number of genes that are crucial for neural tube morphogenesis (Harris and Juriloff, 2007; Harris and Juriloff, 2010) were significantly deregulated by VPA. Taken together, Jergil et al., (2011) concluded that an accumulation of

minor anomalies in the expression of several developmentally important genes leads to disturbances in embryonic development following VPA exposure. VPA also induced an increase in the acetylation of histones H3 and H4 in R1 cells and imply that HDAC inhibition may be a key factor responsible for changes in a majority of gene expression patterns induced by VPA (Jergil et al., 2011). It has been demonstrated that VPA triggers proteasome-mediated degradation of HDAC2 (Kramer et al., 2003). A significant decrease of HDAC2 protein levels is found *in vivo* in the mice treated with VPA. The results have suggested VPA-induced overexpression of Ubiquitin conjugating enzyme 8 (Ubc8) is most likely a determining factor for the degradation of HDAC2 (Kramer et al., 2003). This VPA-induced HDAC2 turnover specifically depends on the E2 ubiquitin conjugase Ubc8 and the E3 ubiquitin ligase RLIM (ring finger protein, LIM domain interacting). This study has provided evidence that the response of HDAC2 protein levels to VPA is indirect rather than being a direct response (Kramer et al., 2003).

2.4. Telomere and telomerase activity

2.4.1. Telomere

2.4.1.1 Structure and Function

Eukaryotic nuclear genome is packed condensely into linear chromosomes. The natural ends of linear chromosomes resemble DNA breaks; however, their ends differ from DNA breaks and avoid DNA repair processes that would result in chromosome end-to-end fusions, illegitimate recombination, and genomic instability (Cesare and Reddel, 2010; Savage and Bertuch, 2010). A specialized ribonucleoprotein structure termed telomere is assembled at the ends of chromosome to avoid inappropriate DNA repairs (O'Sullivan and Karlseder, 2010).

In most eukaryotes, telomeric DNA has short tandem repeats that can be synthesized *de novo* by a reverse transcriptase enzyme, telomerase (Rhodes and Giraldo, 1995). The 3′ end of telomere is G-rich sequence and referred to as the G-strand, whereas the 5′-end containing complementary strand is referred to as the C-strand. In all vertebrates the telomeric repeat

sequence is 5′-TTAGGG-3′. The length of the duplex telomeric tract ranges from < 30 bp in some ciliates, to 200-300 bp in budding yeast, to 5-15 kb in humans, and up to ~50 kb in mice (Chai et al., 2006; Klobutcher et al., 1981).

For linear chromosomes, the second fundamentally important problem is their ends cannot be fully replicated by the DNA-replication machinery. Due to this 'end-replication problem', telomeres shorten in each round of DNA replication (Olovnikov, 1973; Watson, 1972). However, in stem cells, germ cells and lineage progenitor cells, this telomere shortening can be compensated by the telomerase enzyme complex, which use the 3′OH of the G-overhang as its substrate to add newly synthesized repeats (Griffith et al., 1999).

Moreover, telomere can fold back on itself, and the single-stranded terminus can enter into duplex telomeric DNA, forming a telomere loop called T-loop (Blasco, 2007). The configuration of the telomeric T-loop provides a protective cap that not only defines the natural end of the chromosome, but also masks the telomere from DNA damage response (DDR) machinery. Therefore, the generation and manipulation of the telomeric G-overhang by telomerase in telomerase-positive cells is an important convergence both for chromosome end protection and telomere length maintenance (O'Sullivan and Karlseder, 2010).

2.4.1.2. Shelterin organizes and defines telomeres

In mammals, telomere structure and function is maintained and associated with a protein complex called shelterin. This complex consists of six individual proteins: telomeric repeat-binding factor 1 (TRF1), TRF2, repressor and activator protein 1 (RAP1), TRF1-interacting nuclear protein 2 (TIN2), protection of telomeres 1 (POT1) and TIN2-interacting protein (TPP1) (Palm and de Lange, 2008). TRF1 and TRF2 bind to the double–stranded telomeric repeats, whereas POT1 attaches to the single-stranded G-overhang. These DNA binding modules are then bridged by TPP1 and TIN2 (Bianchi et al., 1997; Griffith et al., 1998). Recent studies have shown that although consisting of only six proteins, the shelterin plays an immensely complex role in protecting chromosome ends from enzymatic attack, regulation of telomere length, recruitment of telomerase complex, and control of signalling cascades from

the natural chromosome ends (O'Sullivan and Karlseder, 2010). Moreover, telomerase activity is regulated by telomere-binding proteins to achieve telomere length homeostasis (Lingner and Hug, 2006). Recently, there are a growing number of proteins found to localize to telomeres that are involved in the assembly and regulation of telomerase in cells (Park et al., 2009; Venteicher et al., 2009; Venteicher et al., 2008).

2.4.1.3. Telomere-lengthening mechanisms

In somatic cells, telomeres natural lack of length-maintenance machinery is due to (1) the inability of conventional polymerases to completely replicate the telomeric parent DNA by lagging-strand synthesis (termed the end replication problem) (Watson, 1972), and (2) the requirement to enzymatically generate G-overhangs on both leading and lagging replication product strands. As a result, chromosomes lose 100-200 bp of telomeric sequence in every cell division during the process of replication and the post-replicative restoration of the protective cap at chromosome ends (Makarov et al., 1997; McElligott and Wellinger, 1997; Wright et al., 1997). Because of this so called replication-associated telomere shortening, a somatic cell only undergoes a defined number of doublings before telomeres become critically short (Bodnar et al., 1998; Meyerson et al., 1997), which is visualized as a mechanism to limit the proliferative ability of the dividing cells (Bianchi and Shore, 2008).

Therefore, a critical length of telomere repeats is required to ensure proper telomere function and avoid the activation of DNA damage pathways that result in replicative senescence of cell death (Smogorzewska and de Lange, 2004). Cancer cells and some human cells, such as stem cells, germ cells and activated lymphocytes, are able to maintain and/or extend their telomere lengths by two independent mechanisms: synthesis of telomere DNA by the holo-enzyme telomerase (Counter et al., 1992), or homologous recombination of telomeres by an alternative telomere-lengthening mechanism (ALT) (Bryan et al., 1997; Bryan et al., 1995). However, the heterogeneity of telomere length in chromosomes of normal cells is complicated for identifying the role of factors that regulate telomere length. The length of telomere repeats reflects the balance between additions and losses of telomere

repeats. In most somatic cells, additions of telomere repeats by telomerase are outbalanced by losses from the proteins that bind to telomeres, telomerase levels, and telomeric chromatin status (Aubert and Lansdorp, 2008).

2.4.2. The telomerase complex

The most common way to conquer the end replication problem of chromosome occurs through the ribonucleoprotein (RNP) enzyme called telomerase. The enzyme was discovered in the holotrichous ciliate *Tetrahymena thermophila* by Carol Greider and Elizabeth Blackburn in 1985 (Greider and Blackburn, 1985), and the components of the telomerase complex vary depending on the organism (Collins, 2006). In most species, the enzyme complex contains an RNA moiety (Greider and Blackburn, 1987) with a complementary sequence to the telomeric repeats (Greider and Blackburn, 1989), serving as a template for repeat addition (Feng et al., 1995; Nakamura et al., 1997). The complex also contains the protein dyskerin that is required for proper folding and stability of telomerase RNA and ribonucleoprotein maturation (Mitchell et al., 1999). The telomerase reverse transcriptase subunit (TERT) composed of enzyme complex catalyzes reverse transcription of the RNA template into telomeric repeats (Lingner et al., 1997b). The telomere elongation steps include the enzyme complex binds to the telomere end, associates with ssDNA at 3′ telomere terminus containing the TTAGGG repeat, and finally adds successive telomeric repeats to the ends (Autexier and Lue, 2006; Ouellette et al., 2000; Westin et al., 2007).

The elongation analysis of single telomere molecules suggests that not all telomeres are elongated by telomerase in every cell cycle (Teixeira et al., 2004). The expression of telomerase is limited in human and mice fibroblasts, suggesting telomerase notably exhibits a significant preference for telomeres as their lengths go shorter (Liu et al., 2002; Ouellette et al., 2000; Teixeira et al., 2004). However, the mechanisms that govern the correct timing of the recruitment of telomerase enzyme to the telomeres have remained unknown (Stern and Bryan, 2008). More recently, regulation of telomerase activity has been found not only controlled at the TERT transcriptional level, but also determined at the post-transcriptional

level (Liu et al., 1999). Phosphorylation of telomerase and followed nuclear translocation play an important role in the post-transcriptional regulation of telomerase (Liu et al., 2001; Zhu et al., 2011).

New roles of telomerase have also been recently suggested. For example, loss of TERT does not alter short-term telomere integrity but, instead, affects the overall configuration of chromatin and impairs the DNA damage response (Masutomi et al., 2005). Moreover, telomerase serves as a cofactor in a β-catenin transcriptional complex and directly modulates Wnt/β-catenin signalling pathway (Park et al., 2009). Wnt/β-catenin signalling plays a crucial role during embryogenesis and the normal adult tissue genesis involved in cardiac differentiation and development (Gessert and Kuhl, 2010), angiogenesis, cardiac hypertrophy, and cardiac failure and aging (Rao and Kuhl, 2010).

2.4.3 Telomere and telomerase dysfunction

2.4.3.1 Telomere shortening

Telomere structures are essential for chromosome end protection (Martinez and Blasco, 2011). As a consequence of loss of telomere protection, chromosome ends could activate DNA damage response pathway, causing cell cycle arrest, senescence, or even apoptosis (Karlseder et al., 1999; Smogorzewska et al., 2002; van Steensel et al., 1998).

Shortening telomeres within each replication cycle could subsequently activate DNA damage signals (d'Adda di Fagagna et al., 2003; Takai et al., 2003; Verdun and Karlseder, 2006). As telomere length decreases with age, the effect of DNA damage originating from shorterning telomeres is expected to increase.

Defects in shelterin or telomerase components directly and adversely affect telomere structure and telomere length (Martinez and Blasco, 2011). Telomerase deficiencies were first implicated in the inherited genetic disorder dyskeratosis congenital (DC, a rare and progressive bone marrow failure syndrome) with the discovery of mutations in the dyskerin

gene (*DKC1*) associated with the X-linked inheritance form of the disease (Heiss et al., 1998; Mitchell et al., 1999).

Telomerase activity in all eukaryotes is directly linked to cellular proliferation and maintenance of telomeric DNA relies on telomerase activity. Loss of telomerase activity results in an even shorter telomere that finally leads to cell cycle arrest or cell death (Lundblad and Szostak, 1989; Nakamura et al., 1997). In humans, telomerase activity varies in different cell types during development. In germ line cells, telomerase activity is stable to allow telomere length to be maintained throughout the life. However, in most other cells or fully differentiated cells, telomerase is down-regulated, having little or no detectable telomerase as a result of decreased TERT expression, and the limited telomerase is not sufficient to entirely compensate cell-cycle associated telomere shortening (Aubert and Lansdorp, 2008; Flores et al., 2006; Geserick and Blasco, 2006).

2.4.3.2 Telomere dysfunction and genomic instability

Genomic instability is a prominent characteristic of tumorigenesis by accelerating the accumulation of genetic changes that are responsible for cancer cell progression (Hanahan and Weinberg, 2000; Lengauer et al., 1998). The acquisition of malignant traits through the alteration of key genes as a result of genomic instability thus fuels cancer evolution (Artandi and DePinho, 2010; Halazonetis et al., 2008; Tsantoulis et al., 2008). Critical telomere shortening that is associated with excessive proliferation of preneoplastic cells might be an important source of genomic instability (Engelhardt et al., 1997a; Engelhardt et al., 1997b; Meeker et al., 2004a; Meeker et al., 2004b; Odagiri et al., 1994; van Heek et al., 2002). Studies in cells and mice that are deficient for telomerase or some of the shelterin proteins support a model in which the telomere dysfunction either due to the loss of telomeric repeats or to the loss of the telomere protective structure, induces genome instability and thereby affect tumorigenesis (Artandi et al., 2000; Blanco et al., 2007; Blasco et al., 1997; Chin et al., 1999; Else et al., 2009; Martinez et al., 2009; Munoz et al., 2005; Tejera et al., 2010) .

Decreasing telomere function in the aged life may even promote genome instability and therefore contribute to the higher incidence of cancer (Maser and DePinho, 2002; Wright and Shay, 2000). In humans, telomere length has been tied to several types of cancers. Compared to control, the shorter telomeres of leukocytes have been implicated as a risk factor or biomarker for solid tumors (Lundblad, 2003; Reichenbach et al., 2003). Studies in colorectal cancer suggested the shortening telomere length contributes to tumorigenesis and genetic instability of cancer cells (Hughes et al., 2000). Patients with ulcerative colitis or developed cancer were associated with telomere shortening (Lingner et al., 1997a).

2.4.3.3 Aging

Telomere and telomerase have received considerable attentions because any changes in their structure and function can lead to the development of cancers and aging (Zhu et al., 2011). Aging can be defined as the progressive functional decline of tissues and organs or cell senescence that eventually results in mortality (Aubert and Lansdorp, 2008). The role of telomere biology in the development of aging-related diseases is only partly understood (Zhu et al., 2011).

Studies of increasing generations of telomerase-null mice (Kim et al., 1999) indicated that telomere shortening along successive mouse generations (Espejel et al., 2002a; Espejel et al., 2002b; Herrera et al., 1999) was accompanied by a progressive decrease in both median and maximum longevity (Donate and Blasco, 2011).

Additionally, telomerase-deficient mice developed premature aging pathologies with increasing mouse generations, in agreement with inheritance of shortening telomeres after each generation in humans (Donate and Blasco, 2011).

2.4.3.4 Telomere shortening and oxidative stress

Recently, telomeres have emerged as sensitive indicators of inflammation and cumulative oxidative stress that accumulates in human body *in vivo* (Georgin-Lavialle et al. 2010). These

factors are associated with telomere shortening acceleration (von Zglinicki, 2002), suggesting a connection between the telomere/telomerase system and autoimmune and/or inflammatory disease.

Chronic life stress is linked to shorter telomeres and has been associated with reduced telomerase activity (Hsu et al., 2006).

For instance, compared to age-matched healthy individuals, the telomere length of peripheral blood mononuclear cells (PBMC) is shorter in patients with systemic lupus erythematosus (Fritsch et al., 2006; Honda et al., 2001; Kurosaka et al., 2003; Kurosaka et al., 2006; Wu et al., 2007), rheumatoid arthritis (Koetz et al., 2000; Salmon and Akbar, 2004; Schonland et al., 2003; Steer et al., 2007), Wegener's granulomatosis (Vogt et al., 2003), sarcoidosis (Guan et al., 2007), systemic sclerosis (Artlett et al., 1996), idiopathic pulmonary fibrosis (Armanios et al., 2007; Tsakiri et al., 2007) and type I diabetes (Fyhrquist et al.; Jeanclos et al., 1998). It is suggested oxidative stress induces shortened telomeres and decreased telomerase activity in blood cells during aging (Aubert and Lansdorp, 2008; von Zglinicki et al., 2005). *In vitro* studies demonstrate that oxidative stress and inflammation reduce telomerase activity and shorten telomere length in cultured endothelial progenitor cells, human-derived fibroblasts and neoplastic cells (Dixit et al., 2009; Makpol et al. 2010; Scalera et al., 2009). Stress and senescence affect telomerase levels in lymphocytes (Saretzki, 2009; Choi et al., 2008).

It has also been demonstrated that mitochondrial dysfunction via induction of telomere damage is an important component in the occurrence of senescence within dividing cellular process (Hsu et al., 2006; Passos et al., 2007; Saretzki, 2009; Xia et al., 2008). Telomerase activity is associated with cellular homeostasis as it maintains the length of the telomeres (Indran et al., 2009). Telomerase activity is reported to be modulated by a shift in glutathione redox potential, and changes in telomerase activity are coordinated with changes in cell cycle proteins (Borras et al., 2004). The relationship between telomerase activity, cell cycle regulatory proteins and GSH contents revealed a mechanism that connects telomerase-

mediated cell survival, cell proliferation control and oxidative stress (Borras et al., 2004). Minamino et al. (2001) also reported that hypoxia up-regulates telomerase activity in vascular smooth muscle cells. Furthermore, antioxidants are known to inhibit nuclear export of telomerase reverse transcriptase and can delay replicative senescence of endothelial cells (Haendeler et al., 2004).

2.5. Whole mouse embryo cultures

2.5.1. Culturing embryos at gastrulation and early organogenesis

The ability to grow *in vitro* cultures of whole post-implantation mouse embryos provides an unique opportunity to study development through direct experimental manipulation (Tam, 1998). The developmental stages during which whole embryo culture can be applied range from egg cylinder to about 60 pairs of somites. However, the highest efficiency and reliability of this technique is obtained from early somite (E7.5-8.0 in the mouse) to organogenetic stage (E10.5-11.5; 30-40 pairs of somites), allowing normal embryonic development to continue for up to 2 days in culture. During this period of time, major processes of differentiation and organ development take place, including neurulaton, somitogenesis, and development of the cardiovascular, digestive, and locomotor systems (Calegari et al., 2004; Tam, 1998) (Table 3.1).

2.5.2 Applications of whole mouse embryo culture

2.5.2.1 Teratological studies in whole mouse embryo cultures

Whole embryo culture has mostly been applied to teratological and toxicological studies (Calegari et al., 2004). Such studies constitute the majority of experiments seeking to elucidate the effects of metabolic compounds and teratogenic agents on mouse development (Bavik et al., 1996; New, 1978). Since the early 1970s, the whole embryo culture system has become particularly popular in the study of teratogenic mechanisms, without having interference from maternal absorption, distribution, metabolism and excretion (Cockroft, 1980; Cockroft, 1987; New, 1978).

However, recently several sophisticated techniques have been successfully applied to whole embryo culture, such as cell or tissue transplantation, antibody interference, cell lineage tracing, infection with viral vectors, and electroporation of nucleic acids (Drake and Little, 1991; Inoue et al., 2000; Lee et al., 2012; Oback et al., 2000; Osumi and Inoue, 2001; Pryor et al., 2012; Tam, 1998). These techniques combined with whole embryo culture has offered novel opportunities to study mammalian development at the morphological, cellular, and molecular levels (Calegari et al., 2004; Gray and Ross, 2011; Huang et al., 2012).

2.5.3. Gene targeting with antisense oligodeoxynucleotides and siRNA

A mechanism of disrupting gene expression has been devised by injecting antisense oligodeoxynucleotides (ODNs) into the amniotic cavity of day 9 (plug day = day 1), 4-6 somite mouse embryos (Augustine et al., 1993). The ODNs are 20-25 bases long and are directed to specific sequences of targeted mRNA (Fakler et al., 1994). The probes are phosphorothioated to resist degradation by nucleases, begin to enter cells 30-45 min after injection by endocytosis (Loke et al., 1989; Yakubov et al., 1989), and are distributed throughout the embryo (Augustine et al., 1993). By 3 h they reach a peak concentration and remain high for at least an additional 9 h (Augustine et al., 1993).

The recent findings that small interfering RNA (siRNAs) can be used to knock down gene expression (Betancur et al., 2012; Elbashir et al., 2001) led to the application of siRNAs in whole mouse embryo cultures (Calegari et al., 2002; Calegari et al., 2004; Gratsch et al., 2003; Calegari et al., 2004). The technology of topical injection and directional electroporation of siRNAs induces silencing of gene expression during the mouse post-implantation embryonic development. This offers several advantages as compared to classical techniques of gene knock-down (Calegari et al., 2004). First, the technique constitutes a practical approach to obtain silencing of gene expression in post-implantation mouse embryos without the labor-intensive generation of genetically modified transgenic animals. In addition, the temporal limitation of whole embryo culture can be overcome by *in utero* electroporation (Takahashi et al., 2002).

2.5.4. Application of *in vivo* electroporation in functional studies of genes important in neural tube development

Electroporation is a standard method used to deliver molecules into cells (Calegari et al., 2004). *In vivo* electroporation as a means of gene transfer for functional studies has been applied to the developing neural tube both in mouse and chick embryos in culture. This is because the onset of neurogenesis in neural development coincides with the time period during which whole embryo culture is carried out with a high rate of success. Moreover, electroporation is particularly easy and effective when nucleic acids ONDs, siRNA, or gene DNA are injected into the lumen of the neural tube (Inoue and Krumlauf, 2001). Hence the whole embryo culture technology allows researchers to study the effects of the introduced nuclei acids ODN, siRNA or gene DNA, such as the functional consequences of a given transgene expression or loss of gene expression, on embryonic neural tube development (Calegari et al., 2004).

2.5.5. Micro-manipulation *in vitro*

The direct micro-manipulation of the embryo includes: the micro-surgical ablation of groups of cells or parts of the conceptus; labelling of single embryonic cells, groups of cells or the entire germ layer; transplantation of cells or embryonic fragments; and the retroviral transfection of embryonic cells (Beddington and Lawson, 1990).

2.5.5.1 Elucidation of mouse gastrulation through micro-manipulation

An important contribution of the micro-manipulation experiments of post-implantation embryos is the construction of fate maps of cells in the germ layers of the mouse gastrulae. Cells in specific regions of the germ layer can be labelled *in situ* with enzymes or fluorescent dyes (Lawson et al., 1986; Lawson et al., 1991). The fate of the cells is then assessed by studying certain types of embryonic tissues colonized by the descendants of cells that have been marked (Tam, 1998).

2.5.5.2 Cell fate mapping and establishment of body plan

Fate-mapping studies performed on mouse embryos *in vitro* have led to the construction of fate maps of the epiblast and the primitive endoderm of the early-primitive-streak-stage embryo (El Ouakfaoui et al., 2012; Hang et al., 2012; Lawson et al., 1986; Lawson et al., 1991; Lawson and Pedersen, 1987; Parameswaran and Tam, 1995; Quinlan et al., 1995), the mesoderm of the early-, mid- and late-primitive-streak-stage embryos (Quinlan et al., 1995), and the ectoderm of the late-primitive-streak-stage embryos (Beddington, 1982; Beddington, 1981; Hang et al., 2012; Tam, 1989). These fate maps can provide a description of the geographical distribution of the precursor cells of specific lineages in the germ layers at successive stages of gastrulation (Tam and Behringer, 1997). The study of the cell fate maps can be further analyzed for the functional role of the primitive streak and the organizer in the establishment of the body plan (Gray and Ross, 2011; Lawson et al., 1991; Pryor et al., 2012).

Table 2.1 Fundamental development events occurring during the early organogenesis stages in mouse embryos (E8.5-10.5)

Embryonic Stages	Developmental Events
E 8.0	• Start of regionalization of the heart • Closed neural tube from a point opposite the outflow tract to the proximal port of the tail
E 9.0	• Closed rostral extremity of neural tube • 1st branchial arch of mandibular process is visible
E 9.5	• Formation of posterior neuropore • Subdivision of forebrain vesicle into telecephalic and diencephalic vesicles • Formation of forelimb bud and appearance of a distinct condensation of hind limb bud • Lung development begins
	• Closure of posterior neuropore • Hind limb bud is visible, and tail bud appears as a short stump • 3rd and 4th branchial arches are distinctly concave.

E 10	• Formation of Rathke's pouch and nasal processes
E 10.5	• Conspicuous division of 1st branchial arch into maxillary and mandibular components • Advanced development of the brain tube • Elongation of the tail • Appearance of pancreatic bud

(Summary from http://embryology.med.unsw.edu.au/OtherEmb/mouse1.htm)

2.6. Epigenetic regulation

2.6.1 Role of chromatin during transcription

2.6.1.1 Nuclear architecture

The nuclear structure of eukaryotic cells is well-organized and the architectural integrity and organization of the nucleus is related to how the genome is organized, and how this dynamic arrangement is reflected in genome function (Francastel et al., 2000; Lamond and Earnshaw, 1998; Parada and Misteli, 2002). Genomes are distinct non-randomly organized structures within cell nuclei (Parada and Misteli, 2002) and nuclear positioning of the genome is closely associated with its function (Kumaran and Spector, 2008). In eukaryotes, chromosomes are organized in distinct territories of the nucleus and have an essential role in cell division to ensure genetic diversity and survival of cell progeny (Cremer et al., 1982). Gene-rich chromosomes tend to reside in the centre of the nucleus, whereas gene-poor chromosomes tend to localize towards the nuclear periphery (Gilbert et al., 2005; Sproul et al., 2005). Such spatial organization of chromosomes and genes in the nucleus correlates with genomic activities that have been documented in numerous cell differentiation systems and in embryonic development (Marshall, 2003; Taddei et al., 2004).

2.6.1.2 Chromatin structure and organization

a) Dynamics of chromatin structure

The eukaryotic genome is assembled into chromatin structures that can undergo various forms of dynamic changes. The lowest order of chromatin structure is like 'beads on a string',

consisting of the basic repeat element nucleosomal unit that is wrapped around by DNA. This structure can be further assembled into higher-order structures through the interactions of protein effectors, RNA and surrounding cations (Meshorer and Misteli, 2006). The spatial organization of chromatin into a higher-order structure has recently emerged as a key contributor to genomic regulation (Loden and van Steensel, 2005). The physiological chromatin structure plays a vital role in DNA function in which chromatin regulates DNA accessibility through its structural variation, ranging between 'condensed' heterochromatin and more 'open' euchromatin (Cremer et al., 1982; Parada et al., 2004).

b) Maintenance of chromatin organization

Chromatin structure within the nucleus is determined and largely maintained by the binding of chromatin structural proteins as well as other regulatory proteins. Chromatin structural proteins include six classes of histones (H1, H2A, H2B, H3, H4, and H5) that are organized into two super groups: core histones (H2A, H2B, H3 and H4) and linker histones (H1 and H5). Two copies of each of the core histones assemble together to form an octamer as a nucleosome core particle, which is wrapped around by 146 base pairs of DNA (Luger et al., 1997; Phair et al., 2004; Shigetomi et al., 2011). Linker histone H1 locks DNA into place by binding the nucleosome with the entry and exit sites of DNA, resulting in the formation of the proteinaceous structural backbone of the chromatin (Luger et al., 1997). At the same time, many other DNA-binding proteins interact with chromatin *in vivo*. For most transcription factors, chromatin remodelers, and structural proteins such as heterochromatin protein (HP1) and the high mobility group (HMG) proteins, their residence time on chromatin can range from a few minutes to just a few seconds (Kimura and Cook, 2001; Phair et al., 2004). Although the functional relationship between protein effectors and chromatin has not been completely elucidated, recent observations in embryonic stem (ES) cells have indicated that the dynamic interplay of structural proteins on the chromatin is crucial for genome function (Meshorer et al., 2006). Furthermore, the highly compacted DNA within chromatin in each mammalian cell reveals hierarchical levels of complexity in genome regulation.

Epigenetic regulation is part of a highly complex and interwoven genetic network, including multiple feed-forward and feedback pathways (Cedar and Bergman, 2009; Graff et al., 2011; Latham and Dent, 2007; Lee et al., 2006a) that occur at the DNA and the histone level as well as higher order chromatin structure. On many occasions, several epigenetic modifications can be jointly altered or facilitated, however the precise mechanisms behind these observations remain not completely understood (Graff et al., 2011).

2.6.2. Epigenetic modifications in mammalian genomes

Epigenetics is an inheritable event where a change in phenotype or gene expression can occur without a change in DNA sequence (Szyf, 2009). At least three mechanisms associated with chromatin include: DNA methylation, histone modifications, and ATP-dependent nucleosome remodeling (Bernstein et al., 2007; Cairns, 2007; Graff et al., 2011).

Nucleosome remodeling refers to a process by which change in the structure of chromatin is produced. The process is carried out by nucleosome remodeling complexes that are catalytically dependent on ATP. In eukaryotes, ATP-dependent complexes contain SWI2/SNF2-like ATPases and regulate the position of nucleosomes on DNA (Eisen et al., 1995). They facilitate the sliding of histone octamers to adjacent DNA sequences and thereby enrich transcription factors to accessible DNA on the surface of nucleosomes (Becker and Horz, 2002).

2.6.2.1. DNA methylation

In vertebrates a major component of epigenetic regulation is the pattern of DNA methylation of the genome. DNA methylation is a covalent modification where methylation occurs primarily at the cytosine residue in the di-nucleotide CG sequence (Kar et al., 2012; Razin and Riggs, 1980; Straussman et al., 2009) (Fig. 2.2). In vertebrates, different CG sites are methylated in different tissues, creating a pattern of DNA methylation which is gene and tissue specific (Razin and Riggs, 1980; Straussman et al., 2009). Hence, the pattern and distribution of DNA methylation in different cells and tissues have produced a layer of

information that gives a specific cell type identity to its genome. More importantly, patterning of DNA methylation in vertebrates is tightly correlated with histone post-translational modifications that regulate chromatin structure and modulate DNA transcriptional states. In general, the active regions on chromatin with loose chromatin structure are associated with hypomethylated DNA, enabling gene expression, whereas inactive and condensed chromatin regions are associated with hypermethylated DNA and repress gene expression (Razin and Cedar, 1977; Straussman et al., 2009).

The unmethylated CpG dinucleotides regions are generally characterised by transcriptionally permissive chromatin and punctuate the genome at transcription start sites at approximately 70% of gene promoters (Illingworth and Bird, 2009; Straussman et al., 2009). However, the mechanisms that establish and maintain unmethylated CpG islands (CGIs) remain largely unknown, although DNA methyltransferases (DNMTs), histone modifications, transcription factors and chromatin-modifying complexes are known to be involved (Blackledge and Klose, 2011; Brenner and Fuks, 2007; Fuks, 2005; Illingworth and Bird, 2009; Ndlovu et al., 2011; Straussman et al., 2009).

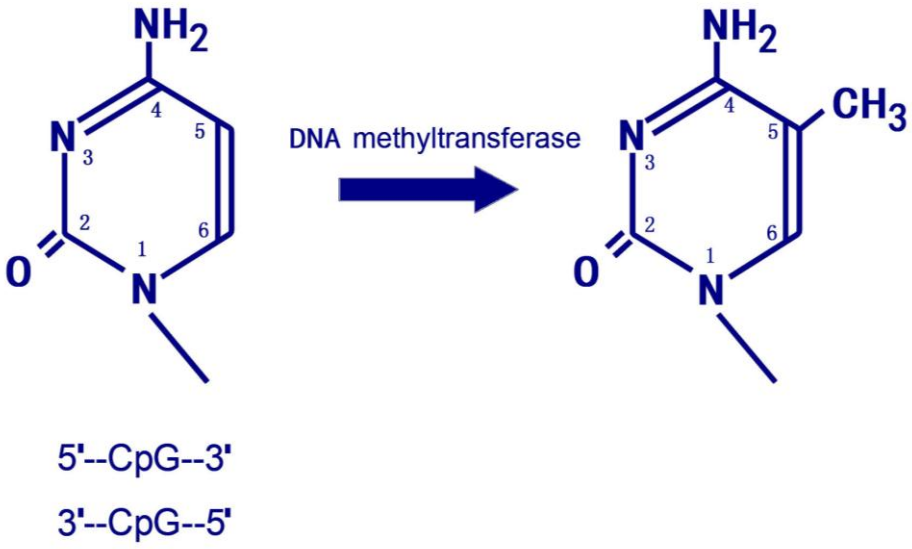

Fig. 2.2 DNA methylation occurs at the 5′ position of the cytosine pyrimidine.

The latest technological advances have revealed new insights into the dynamics of DNA methylation . First, the bisulfite ultra-deep sequencing methods have confirmed the presence of extensive $5^{me}C$ in a non-CpG sequence context (Laurent et al., 2010; Lister et al., 2009; Ramsahoye et al., 2000). These studies have shown methylation of CpHpG and CpHpH trinucleotides (H=A, T, C) was present in both human embryonic stem cells (hESCs) and differentiated cells. In addition, the methylation profile for 5^{me}CpA was found to be conserved in differentiated cells and hESCs at the same sites (Ndlovu et al., 2011).

A second confounding factor in DNA modifications of the genome is the identification of a novel DNA nucleotide, 5-hydroxymethylcytosine ($5^{hm}C$), which is generated from $5^{me}C$ within a CpG context in the regulation of gene expression (Feng et al., 2010; Laurent et al., 2010; Lister et al., 2009). Moreover, the studies have revealed a diverse genomic distribution of eukaryotic DNA methylation in which intragenic DNA methylation plays a major role in mammalian gene regulation (Maunakea et al., 2010; Medvedeva et al., 2010).

DNA methylation is catalyzed by a family of enzymes called DNA methyltransferases (DNMTs) (Razin and Cedar, 1977; Szyf, 2009). Methylation of DNA occurs immediately after DNA replication. The reaction is catalyzed by DNMT and completed by transfer of a methyl group from the methyl donor S-adenosyl-L-methionine (SAM) to 5′carbon position of cytosine (Razin and Cedar, 1977; Szyf, 2009). Three distinct DNA methyltransferases have been identified in mammals. DNMT1 is the most abundant DNA methyltransferase and has been found to be the key methyltransferase in mammalian cells. DNMT1 functions as both a *de novo* methylation and a maintenance methyltransferase, showing preference of methylation on hemimethylated CpG di-nucleotides *in vitro.* It has been suggested that DNMT1 shares a conserved function with the methylation binding co-factor ubiquitin-like containing PHD and ring finger domains in maintaining gene-body methylation in various organisms (Feng et al., 2010). DNMT2 is the first RNA cytosine methyltransferase identified in humans (Goll et al., 2006). Since 2006, DNMT2 has been renamed to TRDMT1 (tRNA aspartic acid methyltransferase 1) (Goll et al., 2006). DNA methyltransferase 3 (DNMT3)

includes DNA methyltransferase 3 alpha (DNMT3a), DNA methyltransferase 3 beta (DNMT3b) and DNMT3L (DNMT3-like). All three (DNMT3a, DNMT3b and DNMT3L) can methylate the unmethylated and hemimethylated DNA at the same rate (Okano et al., 1998). DNMT3a and DNMT3b can interact with DNMT1, acting as co-operators during DNA methylation. DNMT3L is required for establishing maternal genomic imprints during early embryonic development. Although both DNMT1 and DNMT3 classes of enzymes are required for DNA methylation, a distinction between *de novo* and maintenance DNMTs is not always evident and studies have indicated that these two classes of enzymes may participate in both *de novo* and maintenance methylation (Szyf, 2009).

2.6.2.2 Mechanisms of DNA methylation to silence gene expression

DNA methylation is an effective mechanism for epigenetic silencing of gene expression in mammals. It is a key factor that can induce formation of heterochromatin and inhibit binding of transcription factors to target DNA sequences (Comb and Goodman, 1990; Graff et al., 2011; Inamdar et al., 1991). DNA methylation represses gene expression also by attracting methylated DNA-binding proteins (MBDs) to block the binding sites on DNA (Graff et al., 2011; Nan et al., 1997). MBD family is composed of five members including Methyl CpG binding protein 2 (MeCP2), MBD1, MBD2, MBD3 and MBD4. Each protein contains a methyl-CpG binding domain that can recognize methylated CG dinucleotide (Hendrich and Bird, 1998). These MBD family members share a similar mechanism for suppression of gene expression (Fujita et al., 1999; Graff et al., 2011; Hendrich and Bird, 1998; Ng et al., 1999). In addition, MBD proteins can recruit other histone modifying proteins such as SIN3A (Switch Independent 3 homolog A) and chromatin remodeling complexes to methylated sites, resulting in the formation of more condensed chromatin structures to silence gene expression (Nan et al., 1997; Szyf, 2009; Ndlovu et al., 2011). For instance, MBD3 is associated with the nucleosome remodeling and deacetylase complex (such as NurD) that contains MBD2 as the methylated DNA-binding factor, indirectly binding to methylated DNA (Zhang et al., 1999).

However, as highly methylated stretches of DNA have also been found both in the promoter and coding regions of actively transcribed genes, the functional impact of DNA methylation on transcriptional activity (Ndlovu et al., 2011) is not that clear-cut (Suzuki and Bird, 2008; Weber et al., 2007). Indeed, many questions remain regarding the details of the extent and how 5meC residues specifically distribute on the promoters to affect their transcriptional activity (Graff et al., 2011).

2.6.2.3 Histone modifications and gene transcription

2.6.2.3.1 Post-translational modifications of histone

The eukaryotic genome is packed into chromatin, and the nucleosome serves as its fundamental organization unit, which is composed of an octamer of core histone proteins (two copies of H2A, H2B, H3 and H4) wrapped by ~146 bp of DNA (Ruthenburg et al., 2007). The superhelical turn of DNA is hidden under the radial-like surface of histone octamer, and the histone unstructured N-terminal 'tails' is projected from the α-helical protein core of the nucleosome (Fig. 2.3). Investigations on histone modifications have found the majority of histone post-translational modifications (PTMs) occur on the unstructured tails, particularly at the N termini (Cosgrove, 2007). However, recent studies have suggested a growing number of modifications can also take place on residues within the secondary helical structure and loops of folded histones (Cosgrove, 2007). It appears that histone isoforms which are diversified from nucleosome core particle and commonly known as histone variants play essential roles in various stages of DNA management as well (Bernstein and Hake, 2006; Clarkson et al., 1999; Henikoff and Ahmad, 2005; Pidoux and Allshire, 2005).

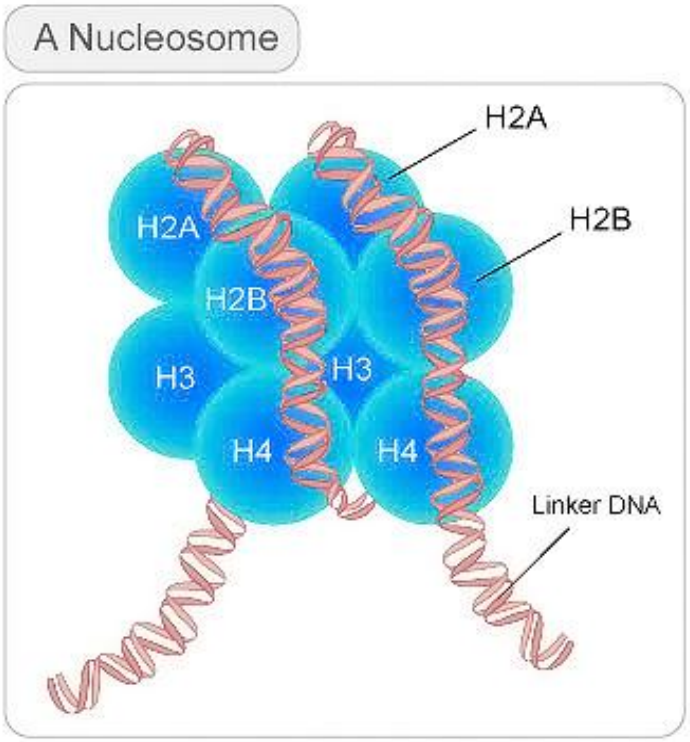

Fig. 2.3 Nuclear DNA resides in a nucleosomal structure where approximately 146 bp of DNA are wrapped around a histone octamer consisting of two molecules of H2A, H2B, H3 and H4) (Adapted from the figure at http://www.fastbleep.com/biology-notes/40/116/1191).

2.6.2.3.2 Functions of histone modifications

a) Global chromatin environments

The functions of histone modifications are to establish either globally modified chromatin environments or genomic DNA transcription-based processes (see section below for description) (Kouzarides, 2007). Globally modified chromatin environments are achieved by forming distinct chromatin domains through histone modifications, which occur on positively charged amino acids lysine and arginine within histone tails (Berger, 2002). Global chromatin environments specify distinct chromatin domains such as euchromatin, on which DNA is kept "accessible" for transcription; or heterochromatin where DNA is "inaccessible" and results in gene silencing (Berger, 2002).

Euchromatin structure formed by histone modifications has been demonstrated to represent a high proportion in the genome. The pattern of modification to euchromatin reflects an open choice for DNA activity. Hence, DNA in euchromatin state has flexibility as to its biological consequences (Kouzarides, 2007). For instance, DNA can be "unraveled" for replication or repair, or held in a transcriptional active or repressive state, ready for gene expression to be turned "on" or turned "off". It has been suggested that low levels of histone acetylation, methylation (depends on type of PTM) , and phosphorylation are associated and observed on genes in the transcriptionally inactive state, whereas high levels of histone acetylation and trimethylation at histone 3 lysine 4 (H3K4), histone 3 lysine 36 (H3K36), and histone 3 lysine 79 (H3K79) are typically found in actively transcribed euchromatin (Kouzarides, 2007). Heterochromatin structure, on the contrary, is a tightly packed DNA silent state, and believed to have functions in both gene regulation and the protection of chromosome integrity. DNA in heterochromatin state is densely packed, making it less accessible for protein regulators and other associated factors. Mainly, heterochromatin limits gene expression through the repression of transcription initiation (Fisher and Merkenschlager, 2002). In mammals, heterochromatic state is associated with low levels of histone acetylation and high levels of histone methylation at specific sites such as H3K9, H3K27, and H4K20 (Zhang and Reinberg, 2001). However, histone bivalent domains, histone 3 lysing 27 (H3K27) and H3K4 trimethylation, have recently been shown to coordinate activating and repressive effects on developmental genes (Bernstein et al., 2005). The enrichment of bivalent domains is associated with low-level of gene expression (Bernstein et al., 2005). In addition, CCCTC-binding factor (CTCF) is found at boundary elements, forming a chromatin barrier between silent heterochromatin and active euchromatin by preventing the spread of heterochromatin structures (Kim et al., 2007; Xie et al., 2007). Studies in fission yeast indicate heterochromatin boundaries are established by the presence of methylation at H3K4 and histone 3 lysine 9 (H3K9) in adjacent euchromatic regions. Therefore, one critical function of chromatin modifications is to establish and maintain the different chromatin environments (Kouzarides, 2007).

b) Genomic DNA-based functions of histone modifications

DNA-based functions of histone modifications refer to the unraveling of chromatin to expose DNA for either more genome wide or more local effect on such events as DNA replication, gene transcription or DNA repair (Kouzarides, 2007). It is known that these biological tasks require well-organized recruitments of protein regulators to unravel and manipulate DNA in a proper chromatin state (Kouzarides, 2007). Within euchromatin environments, the regulation of gene expression requires the binding of transcription factors to the promoter of the gene, followed by the delivery of chromatin-modifying enzymes to initiate a cascade of modification events (Kouzarides, 2007). The term "histone code" is used to describe the combination of histone modifications specifying the transcriptional output of genes. The information constituted from these marks can be read by transcriptional effectors to determine its association with DNA activity (Jenuwein and Allis, 2001; Liu et al., 2005; Verrier et al., 2011).

Post translational modifications (PTMs) function as a single platform to recruit effectors to local chromatin. It is the effectors as "readers" that ultimately determine the functional outcome of certain PTM (Grzenda et al., 2011). So far a number of protein domains have been identified to interact with specific PTMs, such as bromodomain for acetylated lysines, chromodomain for methylated lysines, and Plant Homeo Domain (PHD) for methylated lysines and arginines (Bottomley, 2004). The interactions between histone modifications and proteins could be classified as: 1) cooperative for two or more marks act together to facilitate protein stabilization or recruitment; 2) independent for several modifications existing together but do not interfere with each other's associated proteins; or 3) antagonistic for the present modification will block interaction with an adjacent modified residue (Oliver and Denu, 2011; Seet et al., 2006).

There is still no comprehensive understanding of how transcription factors cope with chromatin (Margueron and Reinberg, 2011). However, interesting examples have highlighted their potential sensitivity and interaction with DNA in the context of nucleosomes (Schwartz

et al., 2006). Most transcription factors require exposure of their binding sites either within linkers or by nucleosome remodeling (Hawkins et al., 2010; Leeb et al.; Rosenfeld et al., 2009; Tolhuis et al., 2006). A diverse set of transcription factors involved in liver differentiation has been found with markedly different extents of mitotic chromosome binding (Caravaca et al., 2013). FoxA1, one of the pioneer factors exhibits the greatest extent of mitotic chromosome binding. The study reveals ~15% of the FoxA1 interphase target sites are bound in mitosis, including at genes that are important for liver differentiation (Caravaca et al., 2013). Results from biophysical, genome mapping, and mutagenesis studies of FoxA1 have shown two different modes of FoxA1 binding to mitotic chromatin: specific binding of FoxA1 in mitosis occurs at sites that continue to be bound at interphase; nonspecific binding of FoxA1 in mitosis occurs across the chromosome due to the intrinsic chromatin affinity of FoxA1. Both specific and nonspecific binding are implicated to contribute to reactivation of post-mitosis target genes in a time specific manner (Caravaca et al., 2013).

Histone modification patterns can be widely found on a gene within the upstream region of the promoter, the core promoter region, the 5′ end of the open reading frame (ORF) and the 3′ end of the ORF. Within these regions histone marks are notably distributed (Vakoc et al., 2005) and the location of a specific modification is tightly regulated and is crucial for its effect on gene transcription (Li et al., 2007).

2.6.2.3.3. Several types of histone modifications

a) Histone Acetylation

This modification occurs by adding an acetyl group to specific lysine residues at N-terminal tail of the histone protein (Allfrey et al., 1964; Pan et al., 2012; Roth et al., 2001). It is one of the major histone modifications and plays a positive role in gene transcription (Roth et al., 2001; Sterner and Berger, 2000). Histone acetylation has been associated with transcriptional activation. The addition of the acetyl group neutralizes the positive charge of the ε-amino group of the lysine, thereby weakening the interaction between the histone tail

and the negatively charged DNA (Brownell and Allis, 1996) and increasing nucleosome fluidity (Workman and Kingston, 1998).

Histone acetylation is catalyzed by enzymes called lysine acetyltransferases (KATs). KATs are divided into three main families, based on their sequence homologies and the similarities in their biological functions, GCN5-related N- acetyltransferases (GNAT), MYST (named for the founding members MOZ, Ybf2/Sas3, Sas2, and Tip60), and p160 coactivator (Sterner and Berger, 2000). The GNAT family is the best characterized nuclear KATs. It includes GCN5 (general control nonderepressible 5) and PCAF (P300/CBP-associated factor) as well as related proteins. Each member of GNAT protein family contains a C-terminal catalytic HAT domain and a 110-residue bromodomain that specifically interacts with lysine-acetylated histone tails (Sterner and Berger, 2000; Roth et al., 2001). Members of MYST family possess a highly conserved 370 residue MYST domain (Ikura et al., 2000). Their functions demonstrate a variety of DNA-mediated reactions including promoter-driven transcriptional regulation, double-stranded DNA break repair and licensing of DNA replication (Iizuka et al., 2006; Ikura et al., 2000; Utley and Cote, 2003). Finally, p160 coactivators are involved in nuclear hormone receptor-dependent gene transcription (Sterner and Berger, 2000; Roth et al., 2001). Other groups such as p300/CBP (protein p300/CREB binding protein, each contain a histone acetyltransferase domain and a bromodomain) and TAFII250 (TATA-binding protein-associated factors) have also been shown to act as KATs to regulate transcription of many genes (Bannister and Kouzarides, 1996; Mizzen et al., 1996; Ogryzko et al., 1996).

b) Histone Deacetylation

Histone acetylation is a highly dynamic event particularly since the presence of histone deacetylase (HDAC) can catalyze the removal of acetyl groups (Yang and Seto, 2003), leading to repression of transcriptional activity (Santini et al., 2007). HDACs are a group of enzymes conserved in mammals, plants, bacteria and fungi (Santini et al., 2007). There are four distinct families of HDACs in mammals, based on structural homologies with yeast

HDACs: class I HDACs (HDAC1, 2, 3 and 8) have homology with the yeast protein reduced potassium dependency 3 (Rpd3); class II HDACs (HDAC 4, 5, 6, 7, 9 and 10) have a high degree of homology to the yeast HDAC1 protein (Fischle et al., 2001); class III HDACs are homologous to the yeast silencing information regulator 2 (Sir2)/homologue of Sir2 (Hst) and include SIRT 1 to 7 in mammals , and HDAC11 is the sole member of the class IV HDAC (de Ruijter et al., 2003; Mehnert and Kelly, 2007). The classes I, II and IV contain an active zinc domain site and their structures are closely related, whereas the class III are NAD^+-dependent enzymes of Sirtuin (Sirt) family and consists of two distinct domains that bind NAD and acetyl-lysine substrate, respectively, and is shared with catalytic domain among all sirtuins (Grozinger and Schreiber, 2002). The role of HDACs is not limited to histone modifications and is also involved in multiple signaling pathways. Class I HDACs also control cell proliferation and survival; class II HDACs are capable of shuttling between the nucleus and cytoplasm, and have been implicated in cell maturation and differentiation (de Ruijter et al., 2003; Grozinger and Schreiber, 2002; Leipe and Landsman, 1997); class III HDACs or sirtuins can also deacetylate cytoplasmic proteins with some family members being localized in the nucleus, cytoplasm or mitochondria (Luo et al., 2001). In general, these enzymes are present in numerous repressive chromatin complexes in mammals, but may not show faithful specificity of any particular residues on histone proteins (Vaquero et al., 2006).

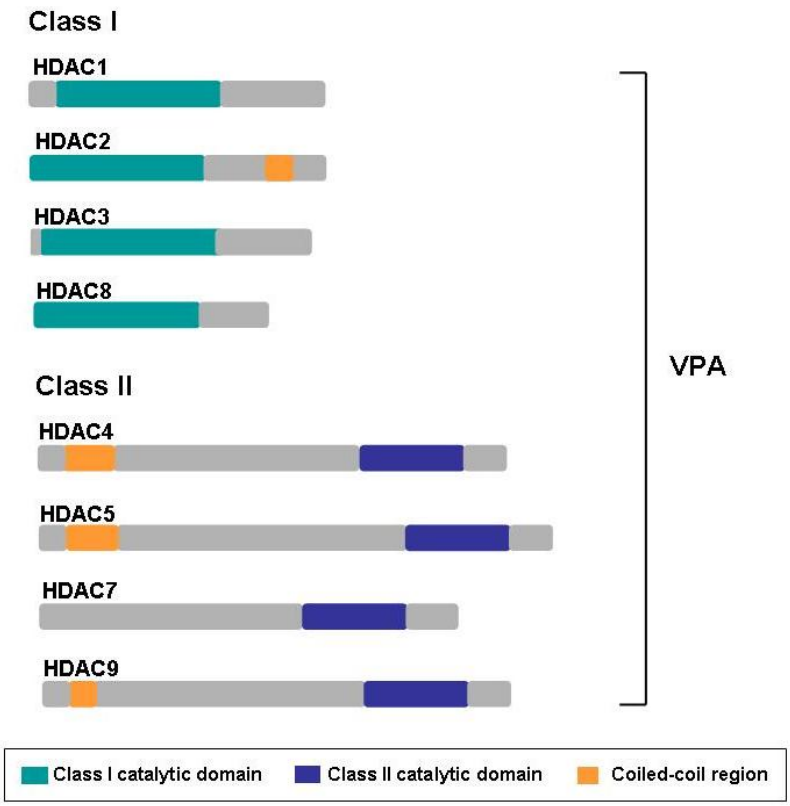

Fig. 2.4 The figure shows the capacity of VPA to inhibit the activity of HDAC classes I and II [Redrawn from (Bolden et al., 2006)]

c) Lysine methylation

Lysine methylation involves transfer of a methyl group from the methyl donor SAM to lysine residues within histones, and this modification commonly occurs on histones H3 and H4 (Kouzarides, 2002; Shilatifard, 2006). Unlike histone acetylation, which generally correlates with transcriptional activation, histone methylation can induce either transcriptional activation or transcriptional repression depending on the specific modified residues within histone proteins. Compared to other modifications, histone methylation is more stable under physiological conditions, and lysine residue can be mono-, di-, or tri-methylated by lysine methyltransferases (Bannister and Kouzarides, 2005; Cuthbert et al., 2004; Margueron and Reinberg, 2011; Shi et al., 2004; Wang et al., 2004b; Whetstine et al., 2006; Yamane et al., 2006). All identified lysine methyltransferases have been found to

contain a 140 amino acid catalytic region known as SET domain (Suppressor of variegation-Enhancer of zeste-Trithorax). In addition, lysine methyltransferases have more extensive specificity than histone acetyltransferases (Santos et al., 2002). Methylation at H3K4, H3K36, and H3K79 is associated with transcriptional activation and in particular, H3K4me and H3K36me are involved in transcriptional elongation (Kouzarides, 2007). Methylation of K36 at H3 is conserved from yeast to human (Barski et al., 2007). H3K36me has been suggested in several processes including RNA splicing, DNA repair, repression of cryptic transcription and histone exchange (Wagner and Carpenter, 2012). In contrast, methylation at H3K9, H3K27, and H4K20 are linked to transcriptional repression, which results from either silencing of euchromatic genes or forming a heterochromatin structure in combination with other enzyme factors (Vakoc et al., 2005).

d) Histone deacetylases **(**HDACs) in early mouse development

Genome activation in early mouse development occurs by the 2-cell stage in the transition from highly differentiated oocyte into totipotent blastomeres (Schultz, 2002). Epigenetic regulation of genome activation during this early stage is suggested to develop a chromatin-mediated transcriptionally repressive state, which results in reprogramming and correct pattern of gene expression that are required for continued embryonic development (Schultz, 2002).

Transcript profiling has suggested that oocytes and preimplantation mouse embryos express most class I and II HDACs including HDACs 1, 2, 3, 4, 5, 6, 9, and Sir2, and possibly HDAC7 and 11, although no convincing signal is detected for HDAC8 (Pan et al., 2005; Verdel et al., 2003; Zeng et al., 2004; Zeng and Schultz, 2005). It has also suggested that class II HDACs (e.g., 4 and 6) are not linked to transcription repression following genome activation (Pan et al., 2005; Kageyama et al., 2006; Verdel et al., 2003). Thus, class I HDACs may be involved in development of the transcriptionally repressive state, and among these, HDAC1 may participate in numerous interactions in a gene network that could contribute to development of the transcriptionally repressive state (Zeng and Schultz, 2005).

Previous studies in somatic cells have shown that acetylation of histone H4 occurs initially on K16, and then on K8 or K12, and ultimately on K5 (Ren et al., 2005; Turner and Fellows, 1989). This is an order that is also observed in mouse embryonic stem cells (Keohane et al., 1996). Thus, acetylation of histone 4 lysine 5 (H4K5) reflects hyperacetylated histone H4, which is strongly correlated with transcriptionally permissive chromatin (Urnov and Wolffe, 2001). *Hdac1* gene expression has been implicated in development of transcriptionally repressive state that is initiated during the 2-cell stage (Davis et al., 1996; Wiekowski et al., 1993) and becomes more crucial with further embryonic development (Christians et al., 1994; Henery et al., 1995). Treatment of 2-cell embryos with VPA results in an increase in acetylation of H4K5 and a global increase in transcription (Aoki et al., 1997).

2.6.2.4 Mechanisms of histone modification and regulation

Although the fundamental role of histone modification has been recognized, detailed mechanism(s) of what impact this modification has is still not clear. One of the mechanisms considered for histone modification is that it disrupts the affinity between nucleosomes to "unravel" chromatin. DNA can thus be accessed by enzyme regulators (Kouzarides, 2007). A second more characterized mechanism of the impact of histone modification is recruitment of nonhistone proteins (Kouzarides, 2007). This model suggests a sequential binding or exclusion of a group of protein regulators on chromatin based on the components of specific histone modifications. Protein regulators are associated with enzymatic activities [e.g., remodeling adenosine triphosphatases (ATPases**)**] which can further modify chromatin structures (Kouzarides, 2007). Investigations have revealed certain transcription regulators consist of a chromodomain which can bind to specific histone lysine methylation site (An, 2007). One characterized example is the recognition of heterochromatin protein 1 (HP1) to tri-methylated H3K9 triggering chromatin reorganization (Bannister et al., 2001; Jacobs and Khorasanizadeh, 2002; Lachner et al., 2001; Nakayama et al., 2001). Chromatin compaction and gene repression involves recruitment of HP1 (HP1α and HP1β) (Margueron and Reinberg, 2011; Verschure et al., 2005). HP1 specifically recognizes and binds methylated H3K9 and can oligomerize to bridge nearby nucleosomes. Thus, H3K9me-dependent

repression is thought to involve nucleosome remodeling by HP1. This can generate a condensed chromatin template, thereby reducing protein accessibility to the genomic template (Karanikolas et al., 2009; Kleer et al., 2003; Varambally et al., 2002). HP1 proteins not only promote the propagation of heterochromatin but also recruit protein complexes with various enzymatic activities that are essential for the assembly of repressed chromatin (Grewal and Jia, 2007).

Histone modifications also have influence on higher-order chromatin structure by impacting connections between different histones or the interaction between histones and underlying DNA (Kouzarides, 2007). Although chromatin structure activity is difficult to observe *in vivo*, biophysical analysis has demonstrated internucleosomal contacts are important for stabilizing a higher-order chromatin structure (Kouzarides, 2007).

Moreover, a given histone methylation mark is often associated with specific positions along DNA sequence (Verrier et al., 2011). For example, methylation of histone H3 at Lys-9 (H3K9me3/me2) on promoters and methylation of histone H3 at Lys-27 (H3K27me3) on promoters as well as on the gene coding region correlate with transcriptional repression. In contrast, methylation of histone H3 at Lys-4 (H3K4me3) around the transcription start site and methylation of Lys-79 (me1, me2 or me3) and Lys-36 (me3) on the gene coding region are associated with gene activation (Campos and Reinberg, 2009; Kouzarides, 2007; Li et al., 2007).

2.6.2.4.1 Enzymatic machinery associated with histone methylation

During the past few years, significant progress has been made in identifying the enzymatic machinery that catalyzes the modification of histones methylation (Kouzarides, 2007). These enzymes have been grouped into several classes, including (1) the lysine-specific SET domain-containing histone methyltransferases (HMTases) involved in methylation of lysines 4, 9, 27, and 36 of histone H3 and lysine 20 of histone H4; (2) non-SET domain-containing lysine methyltransferases involved in methylating lysine 79 of histone H3; and (3) arginine

methyltransferases involved in methylating arginine 2, 17, and 26 of histone H3 as well as arginine 3 of histone H4 (Kouzarides, 2007).

a) Histone H3 lysine 4 methylation enzyme complex

The past decade of biochemical and cellular studies have revealed that HMTs are the key component in regulation of gene transcription (Shilatifard, 2008). After the function of Su(var)3-9 (Suppressor of variegation 3-9), a SET (Suppressor of variegation-Enhancer of zeste-Trithorax) domain HMTase was identified, several other SET domain-containing proteins were discovered as HMTases (Rea et al., 2000). Methylation of H3K4 is extensively associated with gene transcriptional activation (Kouzarides, 2007; Shilatifard, 2006; Sims et al., 2006). COMPASS (Complex Proteins Associated with Set1) is a multiple complex that contains the *Saccharomyces cerevisiae* SET domain-containing protein Set1 and another yeast protein related to the human thioredoxin (trx) protein ASH (Abundant Src homology**)**. The first identified H3K4 methylase was COMPASS composed of Set1/KMT2 (SET domain-containing protein 1/Histone-lysine N-methyltransferase 2) and seven other polypeptides referred to as Cps60-Cps15 (Miller et al., 2001). Set1/KMT2 is only capable of mono-, di- and tri-methylating H3K4 within COMPASS (Krogan et al., 2002; Miller et al., 2001; Nagy et al., 2002; Roguev et al., 2001; Schneider et al., 2005; Shilatifard, 2006; Shilatifard, 2008; Wood et al., 2007). Recently, mammalian homologs of MLL (human mixed lineage leukemia) proteins including MLL1-4, hSet1A and B were found as COMPASS-like complex, and function to methylate H3K4 (Hughes et al., 2004; Shilatifard, 2006; Tenney and Shilatifard, 2005). MLL is a SET domain-containing protein that is largely associated with the pathogenesis of hematological malignancies including acute myeloid leukemia (Hess, 2004; Rowley, 1998; Tenney and Shilatifard, 2005; Ziemin-van der Poel et al., 1991).

Mixed lineage leukemia (MLLs) are primarily recognized as playing critical roles in gene activation via H3K4 methylation of promoters. H3K4 trimethylation is thought to recruit various transcriptional coregulators during transcription activation (Ansari and Mandal, 2010). The maintenance of the newly trimethylated H3K4me3 is largely accomplished by

phosphorylation of histone 3 at threonine 6 (H3T6) (Garske et al., 2010; Metzger et al., 2010) Phosphorylation eliminates the ability of lysine specific demethylase (LSD1) to demethylate H3K4me2/1 and prevents lysine (K)-specific demethylase 5B (JARID1B) from demethylating H3K4me3/2 (Xiang et al., 2007). Trimethylation of H3K4 recruits the basal transcription factor II D (TFIID) (Vermeulen et al., 2007), which results in an enhanced recruitment or stability of the RNA polymerase II preinitiation complex (Vermeulen et al., 2007). This provides the basis for its role as a transcriptional coactivator (Ansari and Mandal, 2010).

b) Histone H3 lysine 27 methylation

Drosophila polycomb group (PcG) proteins maintain transcriptional silencing of many genes through epigenetic mechanisms in a wide range of developmental processes (Grimaud et al., 2006; Kwong et al., 2008; Pietersen et al., 2008; Ringrose, 2007; Schwartz and Pirrotta, 2008). Recent molecular and genetic studies have shown that the PcG protein subunits are HMTases, and part of their silencing function is mediated by the HMTase activity. PcG family combine three different PcG complexes referred to as polycomb repressive complexes 1 (PRC1), PRC2, and Pho-repressive complex (PhoRC) (Klymenko et al., 2006; Ringrose and Paro, 2004). PRC1 is composed of four subunits: polyhomeotic (Ph), posterior sex combs (PSC), dRING (*Drosophila* Really Interesting New Gene), and Polycomb (Pc) (Francis et al., 2001; Lavigne et al., 2004; Levine et al., 2002; Saurin et al., 2001; Shao et al., 1999). PRC2 includes Eed (Embryonic ectoderm development), Ezh2 (Enhancer of Zeste) and Suz12 (Suppressor of zeste 12 homolog) proteins. Studies from several laboratories have showed that following the binding of PRC2 to chromatin, Ezh2 (which contain the SET domain within PRC2 complex) catalyzes H3 trimethylation on lysine 27 within nucleosomes (Cao et al., 2002; Muller et al., 2002), which is then recognized by Pc, one of components of PRC1, through its chromodomain (Fischle et al., 2003; Min et al., 2003). Hence, PRC1 facilitates PcG-mediated repression by forming a heterochromatin structure that interferes with the transcription machinery (Francis et al., 2004; Ringrose and Paro, 2004; Sarma et al., 2008). In this case Ezh2 is a critical factor as further investigation revealed that without Ezh2 activity,

PRC1 cannot be recruited to chromatin and PcG-associated repression does not occur (Cao et al., 2002; Rastelli et al., 1993). More recently, it has been proposed that H3K27me3 signals for PRC1 recruitment at target promoters. PRC1 subsequently mediates ubiquitylation of core histone 2A at 119 (H2A119ub). This ubiquitylation represses transcription by interfering with polymerase elongation (Ernst et al., 2010). PRC1 components can promote compaction of nucleosomal arrays *in vitro* (Nikoloski et al., 2010) and mediate long-range interactions *in vivo*, suggesting a role for polycomb proteins in establishing repressive higher-order chromatin structure (Karanikolas et al., 2010; Pasini et al., 2007). In *Drosophila* embryos, the four major components of PRC2 complex include the ESC (Extra sex combs), E(Z) (Enhancer of Zeste in *Drosophila*), SU(Z)12 (Suppressor of zeste 12), and NURF-55 (Nucleosome remodeling factor 55). Methyltransferase activity on histone H3 lysine 27 associated with this complex can be reconstituted from these four subunits, and mutations in the E(Z) SET domain led to disruption of the methyltransferase activity (Muller et al., 2002). The human homologue of this complex, the EED-EZH2 (human homologue of Eed and Ezh2) complex, is also capable of methylating histone H3 on lysine 27 (Cao et al., 2002).

2.6.2.5 Histone methylation and transcriptional memory

Epigenetic marks that are stable to DNA synthesis and mitosis have been proposed as a mechanism for the maintenance of epigenetic memory (Beck et al., 2010).

Effect of histone methylation has implicated a functional memory mark of modification during gene transcription process (Bernstein et al., 2002; Santos-Rosa et al., 2002; Tenney and Shilatifard, 2005). A close relationship between transcriptional activity of RNA polymerase II (RNAPII) and methylated levels of histone H3 lysine 4 has been observed (Gerber and Shilatifard, 2003; Guenther et al., 2005; Krogan et al., 2003; Ng et al., 2003). An experiment was carried out on *GAL10* (encoding H. jecorina UDP-glucose 4-epimerase 10) gene which showed that the occupancy of Set1/COMPASS and levels of H3 lysine 4 methylation at the 5' coding region of *GAL10* went up significantly during and after activation; however, Set1/COMPASS levels fall rapidly when the gene is ‘turned off’. The

changes in methylated levels of H3K4 and the occupancy of catalytic enzymes are similar to the dynamic transcriptional process of RNAPII (Krogan et al., 2003). In contrast to Set1/COMPASS, the levels of histone H3 lysine 4 di- and trimethylation dropped relatively slowly (Guenther et al., 2005; Krogan et al., 2003). Additional analysis of RNA polymerase associated factor (*Paf1)* gene expression also demonstrated that trimethylation of histone H3 lysine 4 is lost by a slow process. This phenomenon can be considered as a "short-term memory" model for histone H3 lysine 4 methylation. In this model, the transcriptional status of a given gene can be distinguished by the level of H3K4 methylation (Gerber and Shilatifard, 2003; Guenther et al., 2005; Krogan et al., 2003).

2.6.2.6 Crosstalk between epigenetic modifications

Chromatin cross-talks allow an accurate co-ordination between these modifications (Verrier et al., 2011). Recent reports indicate that the mutual exclusion between H3K4 and H3K9 is an active process. This cross-talk can be mediated by various mechanisms and is clearly representative of how such mechanisms can be integrated to specify a mutual exclusion between two distinct chromatin modifications (Verrier et al., 2011).

2.6.2.6.1 DNA methyltransferases and histone modifying enzymes

DNA methylation patterns can directly affect chromatin modification, where for example, methylated DNA binding protein MeCP2 can interact with SUV3-9 histone methyltransferase (Fuks et al., 2003). Histone modifying enzymes such as HDAC1 and HDAC2 can also interact with DNA methyltransferases such as DNMT1 and DNMT3b, and histone methyltransferases, SUV3-9 and EZH2 (Fuks et al., 2000; Fuks et al., 2003; Rountree et al., 2000; Vire et al., 2006). Recruitment of HDACs to heterochromatin protein 1 that binds to methylated H3K9 would induce a stable heterochromatin structure (Smallwood et al., 2007). One of the most important associations between chromatin and DNA methylation was found in tumor suppressor genes which exhibit a relationship between EZH2 and DNA methylation (Rauch et al., 2007). On these tumor suppressor genes in lung cancers, methylated CpG

islands were also the binding sites for EZH2 histone methyltransferase. As a result, sites that are bound by EZH2 are poised to become methylated (Rauch et al., 2007).

Similar to DNA methylation, DNA demethylation during transcription is also accompanied by chromatin modification changes. In the case of gene transcriptional activation, transcription factors recruit KATs to bind to promoter regions of genes, triggering gene-specific acetylation and recruitment of RNAPII, a process that is followed by DNA demethylation (D'Alessio et al., 2007).

‘‘Crosstalk’’ between modifications appears to be due to the accumulated modification abundance on histone tails. Many different types of histone modifications can occur on single or multiple histone residues, hence, interactions can be found in the same type of lysine residue modifications, or adjacent different type of modifications. For instance, phosphorylation of histone 3 serine 10 (H3S10) can change the binding of HP1 to methylated H3K9 (Fischle et al., 2005). Additionally, the enzyme catalytic activity can be compromised resulting from modification at its substrate recognition site (Kouzarides, 2007). One example is that the isomerization of histone 3 proline 38 (H3P38) subsequently affects methylation of H3K36 by Set2 (Nelson et al., 2006). A study of GCN5 acetyltransferase activity shows that the enzyme activity becomes more effective with a second modification (when H3 is phosphorylated at S10) (Clements et al., 2003). Finally, interactions can also occur when the modifications are on different histone tails. The best studied example is ubiquitination of H2B which is required for the methylation of H3K4me3 (Kouzarides, 2007).

2.6.2.6.2 DNA methylation and methylation of H3K4 and H3K9

Genome-wide DNA methylation screen suggests that DNA methylation is better correlated with histone methylation patterns than to the underlying genome organization and arrangements (Meissner et al., 2008). Methylation of H3K4 has been demonstrated (Shilatifard, 2008) to protect promoters from *de novo* DNA methylation in somatic cells (Appanah et al., 2007; Weber et al., 2007). There is an inverse relationship existing between H3K4 methylation and allele-specific DNA methylation (Delaval et al., 2007; Fournier et al.,

2002; Meissner et al., 2008; Vu et al., 2004; Yamasaki et al., 2005). A recent genome-scale analysis has further confirmed this inverse correlation between DNA methylation and H3K4 methylation. DNA methylation is associated with the absence of H3K4 methylation (Laurent et al., 2010). In contrast, DNA methylation is positively correlated with the presence of H3K9 methylation (Dindot et al., 2009). One study has shown inhibiting DNA methylation with the methyltransferase inhibitor 5azaC leads to a loss of H3K9 methylation (Nguyen et al., 2002).

De novo DNA methyltransferases and associated factors bind to unmethylated H3K4 (Ooi et al., 2007), whereas the H3K4 methyltransferase MLL preferentially binds to unmethylated DNA (Birke et al., 2002), providing a molecular correlation between H3K4me and DNA methylation levels (Meissner et al., 2008). This interplay suggests that when DNA methylation is present, it may serve as a reinforcing signal for preexisting but less stable epigenetic signatures such as histone modifications (Bonasio et al., 2010) .

2.7. Epigenetics and development

2.7.1. DNA methylation during development

DNA methylation patterns in mammals are dynamic and essential for development (Bird, 2002; Jackson-Grusby et al., 2001; Li et al., 1992; Okano et al., 1999) where patterns of DNA methylation are established early in development. In mammals, the paternal genome undergoes rapid demethylation within a few hours of fertilization (Mayer et al., 2000; Nonchev and Tsanev, 1990; Oswald et al., 2000), although the mechanism(s) of how this occurs is not known. The maternal genome is passively demethylated during subsequent mitotic divisions (Li, 2002; Reik et al., 2001; Santos et al., 2002). The overall effect of genome-wide DNA demethylation in pluripotent cells is to produce cells in which all genes are transcriptionally active (Burdge and Lillycrop, 2010). At the time of blastocyst formation, the genome of the blastocyst undergoes *de novo* methylation at distinct levels in order to establish cell differential patterns between the inner cell mass of blastocyst (ICM) and those of trophectoderm (Jaenisch and Bird, 2003). For example, *Oct4* gene is associated with cellular pluripotency and is permanently silenced by hypermethylation around E6.5 in mice

(Gidekel and Bergman, 2002). *Hoxa5* and *Hoxb5* are involved in early embryonic development pattern and are not silent until early postnatal life (Hershko et al., 2003). Other genes, however, undergo graded changes in the level of DNA methylation and transcription during development (Burdge and Lillycrop, 2010). Ultimately, loss of pluripotency and cell differentiation and the establishment of adult tissue function are dependent on the changes in the methylation status of individual genes at different times in development (Burdge and Lillycrop, 2010). In addition to the normal coordinated DNA methylation status during development, DNA methylome undergoing aberrant characteristic changes can induce cancer (Jones and Baylin, 2002).

a) CpG islands in genome

CpGs tend to cluster in specific regions of the genome. The clustered CpGs are termed CpG islands, and they are featured by high G+C content (Bird, 2002). Genomic studies indicate that 0.7% of the human genome contains CpG islands, and these regions contain 70% of the genome CG dinucleotides (Fazzari and Greally, 2004; Lander et al., 2001). CpG islands are associated with DNA methylation relating to gene regulation. In humans, about 60% of gene promoters are characterized by CpG islands. In normal cells most CpG islands are found unmethylated. However, a small subset of CpG islands may be subject to gene and tissue specific methylation during development (Bernstein et al., 2007; Bird, 2002; Strichman-Almashanu et al., 2002).

2.7.2 Oxidative stress and DNA methylation

Recent studies have suggested interactions between oxidative stress and DNA methylation (Andreazza et al., 2012). Oxidative stress induces glutathione S-transferase (GST) production to prevent oxidative damage. The production of GST requires the utilization of homocysteine which subsequently decrease the availability of a methyl donor, S-adenosylmethionine (SAM), leading to hypomethylation of DNA (Lertratanangkoon et al., 2007).

ROS also induce the hydroxylation of 5-methylcytosine (5mc) in a catalyzed reaction by ten-eleven-translocation (TET) oxygenase to 5-hydroxymethylcytosine (5hmc) (Matarese et al., 2011). The TET proteins were newly identified oxoglutarate- and iron-dependent dioxygenases in this enzyme superfamily (cupin superfamily) (Lyer et al., 2008; Lyer et al., 2009). Activation of TET correlates to the high oxygen concentration and requires alpha-ketoglutarate – a product of both the citric acid cycle and urea cycle (Chia et al., 2011).

Hydroxylation of 5mC to 5hmC could induce passive demethylation by preventing DNMT1 binding at hydroxymethylated CpGs during DNA replication (Reik et al., 2012). Also, the presence of 5hmC may attenuate the silencing effect of 5mc by preventing binding of methyl-binding proteins at 5mC (Valinluck et al., 2004).

However, whether there is a correlation between promoter 5hmC and gene transcription is not consistent among studies. Some analyses have found 5hmC and 5mC often co-exist in the genome (Ficz et al., 2011; William et al., 2011), and that 5mC within promoter regions causes transcriptional repression. In TET1 knockdown ESCs with a potential reduced activating role of 5hmC, several genes are downregulated; however, surprisingly a large number of genes are repressed (William et al., 2011, Wu et al., 2011; Xu et al., 2011). Many of these repressed genes are polycomb repressive complex (PRC2) target genes (Wu et al., 2011). In ESCs, such genes are often associated with histone bivalent domains with the active mark of trimethylation at histone H3 lysine 4 (H3K4me3) and the repressive mark (H3K27me3). Genes enriched with bivalent domains are generally transcriptionally ‘poised’ so that they can be rapidly activated or silenced depending on the specific differentiation pathway (Reik et al., 2012).

2.7.3 Epigenetic regulation of Hox genes during development

2.7.3.1 PcG and trxG proteins

The discovery of polycomb group (PcG) and trithorax (trxG) group is an important milestone in developmental biology. Over the last 60 years, studies of their role in epigenetic

regulation of *Drosophila* homeotic genes have provided invaluable information for exploring their functions (Schuettengruber et al., 2007) .

PcG proteins involve three different complexes (reviewed previously in 5.2.4.1b). The SET domain-containing E(z) subunit trimethylates lysine 27 of histone H3 (H3K27me3)(Cao and Zhang, 2004). This histone mark can be specifically recognized by the chromodomain of Pc (Cao and Zhang, 2004), a subunit of PRC1 type complex. Recently, a third complex, PhoRC, has been identified and is also involved in homeotic gene silencing (Klymenko et al., 2006). The dRing subunit of PRC1 and the mammalian homologs Ring1A and Ring1B, are E3 ubiquitin ligases that ubiquitinate H2AK119, a modification that is essential for silencing of *Hox* genes (Wang et al., 2004a). In mammals there is evidence that Yin Yang-1 (YY1) recruits PRC2, as knockdown of YY1 with RNA interference (RNAi) leads to loss of E(Z)H2 and H3K27 trimethylation (Caretti et al., 2004).

TrxG proteins are heterogeneous protein group. One class of trxG members is composed of SET domain factors like *Drosophila* Trx and Ash1 and vertebrate MLL, as well as their associated proteins. A second class of trxG factors consists of components from ATP-dependent chromatin remodeling complexes such as the SWI/SNF or the NURF complexes (Schuettengruber et al., 2007).

PcG and trxG proteins also bind near transcription start sites, suggesting a role in regulation of transcription. The trxG proteins are crucial for more than one phase of transcription. H3K4 methylation is highest near promoters and is required for transcriptional initiation and promoter clearance, as well as early transcriptional elongation (Petruk et al., 2006; Smith et al., 2004). However, promoter clearance, marked by the synthesis of a short strand of RNA and melting of the DNA ahead of RNA Pol II, did not occur, suggesting the PcG proteins prevent it (Beck et al., 2010).

Disruption of DNMT1 causes improper recruitment of polycomb ring finger oncogene B lymphoma Mo-MLV insertion region 1 homolog (Bmi1) and RING finger protein member of Polycomb group (Ring1B) to PcG bodies (Hernandez-Munoz et al., 2005). During *in vitro* ES

cell differentiation, 21% of genes that lose H3K4me2 and maintain H3K27me3 are de novo DNA methylated and PRC2 targets are more likely nonPRC2 targets to be de novo methylated (Mohn et al., 2008). An acceptable hypothesis is that PRC1 together with the maintenance DNA methyltransferase at the replication fork promote transcriptional silencing of newly synthesized daughter strands. Thus, DNA methylation may serve as a memory mark and simply stabilize gene silencing in which other mechanisms are involved. (Bird, 2002).

It is yet to be determined what regulates whether PcG or trxG proteins are recruited to a particular locus by sequence specific factors (Beck et al., 2010).

2.7.3.2 *Hox* and *Hoxa2* genes

Homeobox genes encode transcription factors which act as regulators of downstream gene activity and are characterized by the presence of a highly conserved 180-base pair sequence known as the homeobox. The homeobox encodes a 60-amino acid helix-turn-helix DNA binding motif within the transcription factor. *Hox* genes are homologous to homeobox genes of *Drosophila,* which map to the Antennapedia and Bithorax complex (Akin and Nazarali, 2005). They are organized into a single chromosomal cluster in invertebrates, in contrast to higher vertebrates such as the mouse which have 39 *Hox* genes, organized into four distinct chromosomal clusters (*Hoxa-Hoxd*) (McGinnis and Krumlauf, 1992) (Fig.2.5). The most significant feature of the organized expression of *Hox* gene family members is the spatial and temporal colinearity, which confers positional information along the body axis (Dolle et al., 1989; Donaldson et al., 2011; Duboule and Dolle, 1989; Kessel and Gruss, 1991; McGinnis and Krumlauf, 1992;Durston, 2012). *Hox* gene collinearity is crucial in embryogenesis and features the important interrelated properties -- functional collinearity and spatial and temporal collinearity. Functional collinearity describes the order in which *Hox* genes act along a body axis; spatial and temporal collinearity refers to the spatial order and the time sequence in which the *Hox* genes are expressed (Durston, 2012). *Hox* genes located nearer to the 3' end of the chromosomal cluster are expressed earlier during development and more anteriorly than those located nearer the 5' end, such that *Hox* genes exhibit nested domains of

expression along the anterior-posterior (A-P) axis along the neural tube and, each gene has a characteristic segmental limit of expression at its anterior boundary (Hunt et al., 1991; Durston et al., 2011;Pick and Heffer, 2012). *Hox* genes are key controllers of rostrocaudal patterning in the head, including hindbrain segmentation and rhombomere identity (Cordes, 2001; Lumsden, 2004; Durston et al., 2011; Pick and Heffer, 2012). *Hox* genes are expressed in neural crest cells, which migrate predominantly from even-numbered rhombomeres into the branchial arches, generating skeletal tissues and cranial ganglia (Graham et al., 1991; Kontges and Lumsden, 1996; Durston et al., 2011; Pick and Heffer, 2012).

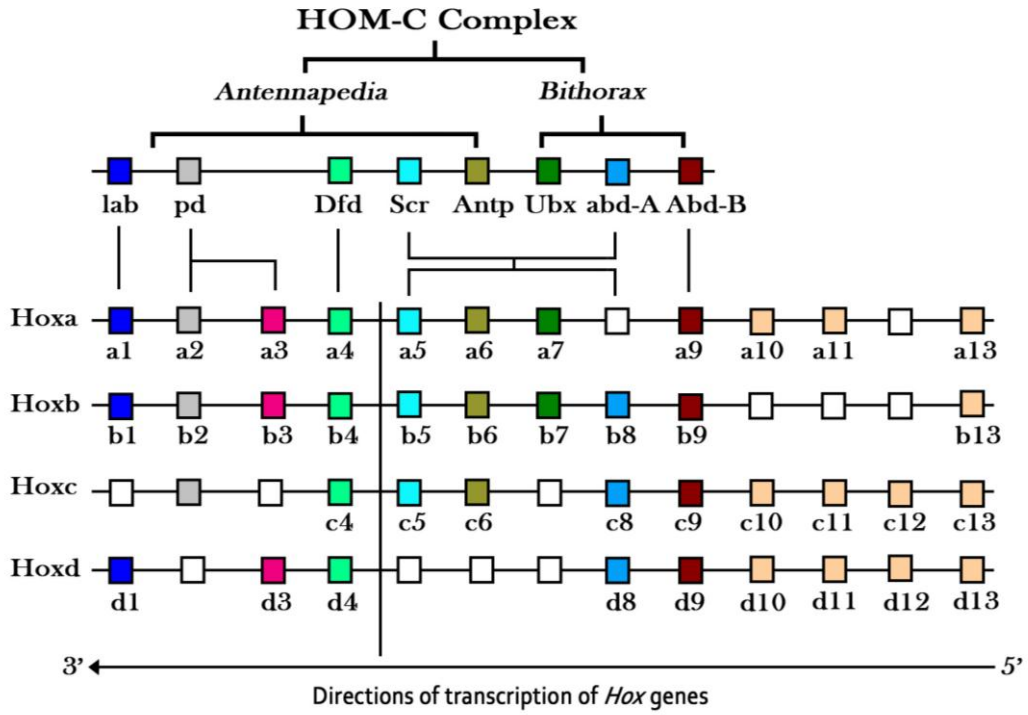

Fig. 2.5 The 39 mouse *Hox* genes are organized in four clusters on four separate chromosomes. They are derived from a single ancestral cluster from which the single *HOM-C* complex in *Drosophila* is also derived. *HOM-C* consists of two regions: *Antennapedia* and *Bithorax*. Cluster duplication during evolution has led to the concept of paralogous groups of *Hox* genes. Groups of up to four genes derived from a common ancestral gene can be identified based upon sequence homology. The paralogues show similar expression domains along the anterior-posterior axis of the embryo leading to the concept of functional redundancy between genes [Adapted from Cobourne, 2000].

Hoxa2 belongs to the HoxA cluster of the *Hox* gene family and is the most anteriorly expressed *Hox* gene. *Hoxa2* shows a rostral limit of expression at the border between rhombomere 1 (r1) and r2 in the E8 mouse hindbrain. During development *Hoxa2* is expressed in several tissues, including the neural tube and the neural crest-derived mesenchyme of the branchial area (Gavalas et al., 1997; Krumlauf, 1993; Prince and Lumsden, 1994;Donaldson et al., 2011). In mouse, disruption of the *Hoxa2* gene affects second branchial arch development. Second arch skeletal elements (stapes, styloid process, lesser horn of the hyoid bone) are transformed into first arch-specific skeletal elements (incus, malleus and tympanic ring). They are arranged in a mirror image disposition to their first arch counterparts. (Barrow and Capecchi, 1999; Gendron-Maguire et al., 1993; Rijli et al., 1993). A recent study from our lab was the first to demonstrate a direct role of *Hoxa2* in palate development (Smith et al., 2009). *Hoxa2* mRNA and protein were detected in the developing palate in mice between E12.5 and E15.5. *Hoxa2* plays intrinsic roles in regulating both cell proliferation and gene expression during palatogenesis (Smith et al., 2009). More recent studies using *Hoxa2* ChIP-sequencing reveals that *Hoxa2* has large genome coverage and potentially regulates thousands of genes in developmental stage (E11.5). In this study, a significant amount of genes involved in the Wnt-signaling pathway associated with Hoxa2-bound regions were identified. The tissue- and stage-specific activation of the Wnt–β-catenin pathway in the second branchial arch was observed, which is undetectable in *Hoxa2* mutant embryos. These data describe where *Hoxa2* localizes in the genome while functioning to direct embryonic development. This study presents one of the first global maps of the *in vivo* interactions between a *Hox* gene and chromatin during embryogenesis (Donaldson et al., 2011).

2.7.3.3 Genome-wide histone methylation of *Hox* genes

Hox genes play key roles in embryonic spatial segmental identity along the AP axis during development (Ringrose, 2007). The activation of *Hox* genes is referred to as spatial collinearity. Genes at anterior extremity of the cluster are activated in anterior parts of the

developing embryo, whereas genes located at the posterior end are transcribed in more posterior areas (Schwartz and Pirrotta, 2007). *Hox* gene promoters therefore demonstrate an organized AP polarity. The role of PcG and TrxG is to preserve appropriate *Hox* expression domains during development (Schwartz and Pirrotta, 2007). The PcG proteins act on *Hox* genes as silencers, maintaining previously established states of gene expression over cell generations; while the TrxG genes act to conteract PcG silencing and maintain *Hox* genes active wherever necessary (Klymenko and Muller, 2004; Muller and Kassis, 2006; Schuettengruber et al., 2007; Schwartz and Pirrotta, 2007; Simon et al., 1992). Both groups act through the same DNA elements – the Polycomb/Trithorax response elements (or PRE/TREs) (Ringrose, 2007). These are known as 'memory' elements of genes as the elements preserve gene transcriptional activity - active or silent. Regulation of PcG and TrxG proteins on *Hox* genes are conserved from flies to vertebrates, although PRE/TRE elements have only been identified in *Drosophila* (Pires-daSilva and Sommer, 2003; Ringrose and Paro, 2004; Schubert et al., 2005).

Major progress has recently been made in understanding mechanisms of epigenetic regulation of *Hox* genes during embryonic development. Faithful expression patterns of *Hox* genes are critical for the normal homeostasis of adult tissues and organs. Mis-regulation of *Hox* genes can readily lead to diseases such as cancer (Maroulakou and Spyropoulos, 2003; McGonigle et al., 2008).

To mediate long-term repression of *Hox* genes, Ezh2 of PRC2 tri-methylates H3 on K27 (Rea et al., 2000), and recruitment of PRC1 members to H3K27me3 and subsequently forms a heterochromatin structure (Fischle et al., 2003). Ubiquitination of H2A at K119, a modification that interferes with RNA polymerase II activity (Nakagawa et al., 2008; Stock et al., 2007; Zhou et al., 2008), is essential in this process and facilitates PRC1 member binding to H3K27me3 (Cao et al., 2005; de Napoles et al., 2004; Wang et al., 2004a).

Genome-wide studies in ES cells recently revealed the components of PRC1 and PRC2 are associated with promoters of many transcription factors (Boyer et al., 2006; Bracken et al.,

2006; Lee et al., 2006b; Ringrose et al., 2003; Schwartz et al., 2006; Tolhuis et al., 2006). The PRC2 and trimethylation of H3K27 were distributed along approx. 100 kb domains within all four *Hox* gene clusters (Lee et al., 2006b; Schwartz et al., 2006). Mutations in PcG genes can lead to ectopic *Hox* gene expression and posterior homeotic transformations in both *Drosophila* and vertebrates (van der Lugt et al., 1994). Analyses of PRC2 mutants have further demonstrated that PRC2-dependent methylation of H3K27 is required for silencing *Hox* genes in ES cells (Lee et al., 2006b). TrxG/MLL proteins complexes catalyze the trimethylation of H3K4, which is generally related to active transcription (Schuettengruber et al., 2007; Schwartz and Pirrotta, 2007). H3K4me3-modified nucleosomes are specifically enriched at the promoter region of active genes (Barski et al., 2007; Bernstein et al., 2002; Bernstein et al., 2005; Bernstein et al., 2006; Schubeler et al., 2004; Barski et al., 2007; Beck et al., 2010; Bernstein et al., 2002; Bernstein et al., 2005; Bernstein et al., 2006; Schubeler et al., 2004). In *Drosophila trx* or *Mll* mutants, *Hox* genes are properly expressed but cannot be faithfully maintained (Glaser et al., 2006; Schwartz and Pirrotta, 2007; Terranova et al., 2006). Further analysis of *Drosophila trxG/PcG* double mutants indicates that the activity of TrxG/MLL complexes is required to prevent PcG-mediated silencing of transcribed *Hox* genes (Klymenko and Muller, 2004). Interestingly, in ES cells, *Hox* gene promoters often display both H3K4me3 and H3K27me3 marks, which are referred to as 'bivalent domains'. Bivalent marks are mostly enriched at GC-rich promoters (Mikkelsen et al., 2007) where they may prevent DNA methylation and silencing, at least in stem cells (Mohn et al., 2008). The function of bivalent domains remains elusive, and this equilibrium between active and repressive marks may maintain genes in a poised state, ready for rapid activation during cell differentiation (Azuara et al., 2006; Bernstein et al., 2006).

Presently, the most popular explanation for temporal and spatial collinearity suggests that these phenomena are rate-limited transcription via a progressive opening of the chromatin at *Hox* complexes from 3′ ends towards 5′ ends (Duboule, 1994; Spitz et al., 2003; Duboule, 1994; Kmita and Duboule, 2003). During early mouse development, temporally collinear expression of the *Hoxd* complex correlates with the progressive 3′–5′ modification of its

chromatin from a repressing to an activating state (Soshnikova and Duboule, 2009b). Furthermore, elegant experiments showed that transposing a 3′ *Hox* gene to a 5′ position in the *Hoxd* complex caused later and more posterior expression (Kmita et al., 2000; van der Hoeven et al., 1996). In ES cells when retinoic acid is used to induce temporally collinear *Hoxb* gene expression, looping out of genes from their chromosome territory (a correlate of chromatin activation) occurs from 3′ to 5′ in coordination with *Hox* gene expression (Bickmore et al., 2004).

Hox genes are activated in a time dependent sequence. This is referred to as "temporal collinearity". In some species, the activation of *Hox* genes in a time dependent sequence reflects their position in the gene cluster (Kmita and Duboule, 2003). More recently, the sequential epigenetic activation of *Hoxd* cluster in developing murine tail buds was investigated by ChIP combined with hybridization on tiling array (ChIP-on-chip). A highly dynamic equilibrium was identified where demethylation of H3K27 paralleled an increase in trimethylation of H3K4, along with progressive gene activation. The region of transition between these two chromatin states corresponds to the areas where *Hoxd* genes become transcriptionally active, and this expression region of *Hoxd* genes shifts from one end of the cluster to the other during gastrulation (Soshnikova and Duboule, 2009a). For example, at E8.5, H3K4me3 marks drastically increased and covered the telomeric part of the cluster up to both *Hoxd10* and *Hoxd11*, which remain silenced at this time point. However, at E9.5, elevated levels of H3K4 trimethylation over the *Hoxd11* and *Hoxd12* loci was observed to correspond to their robust transcriptional activation. The results suggest that temporal collinearity of *Hoxd* gene cluster in tail buds corresponds to chromatin dynamics, which involves the removal of H3K27me3 marks, enrichment of the methylation of H3K4, and the acetylation of H3, a distance of about 100 kilobases over less than two days (Soshnikova and Duboule, 2009a). The observation also indicates the transcriptional activation occurs along gene cluster with transition between H3K27me3 and H3K4me3 during mouse tail bud development (Soshnikova and Duboule, 2009b).

Specific analysis of *HOXA* cluster in human embryonal carcinoma (EC) cells showed the presence of H3K4 trimethylation and dimethylation associated with cell differentiation. H3K4 trimethylation and dimethylation span the region from *HOXA4* to *HOXA11* with enrichment at the 3' end of *HOXA4* and *HOXA9*, and the 5' end of *HOXA10* during pluripotent cell differentiation (Atkinson et al., 2008). At the same time, acetylation of histones H3 and H4 is restricted to the same region from *HOXA4* to *HOXA11*. In undifferentiated EC cells, trimethylation of H3K9 is enriched at *HOXA3* and the intergenic region between *HOXA6* and *HOXA7*. These differential locations of epigenetic modifications in EC cells demonstrate that epigenetic modifications not only regulate the expression of *HOXA* genes in pluripotent cells, but also maintain the collinear activation of these genes during cell differentiation (Atkinson et al., 2008; Snowden et al., 2002).

Epigenetic modifications are also associated with *Hox* genes in cancer cell development. CpG methylation of *Hox* genes is sporadically observed during breast tumorigenesis, including methylation of *HOXB13* gene (Rodriguez et al., 2008), and members of the *HOXA* cluster genes (Novak et al., 2006; Raman et al., 2000). Hypermethylation of the *HOXB13* gene is a late-stage event in breast tumorigenesis (Rodriguez et al., 2008). Inappropriate silencing of *HOXA* gene cluster in breast tumors is widely seen both *in vivo* and *in vitro*, and is closely connected to the presence of hypoacetylation of H3 and H4 at CpG islands in *HOXA* gene cluster (Novak et al., 2006; Tommasi et al., 2009). A large number of homeobox genes were found methylated in lung tumors including adenocarcinomas and squamous cell carcinomas (Rauch et al., 2007). Therefore, it seems that all four *HOX* gene clusters are preferential targets for DNA methylation in cancer cell lines and the early stage lung tumors (Ohm et al., 2007; Pfeifer and Rauch, 2009).

Methylation profile of extrahepatic cholangiocarcinoma (CCA) was identified with MeDIP (Methylated DNA immunoprecipitation) microarray with respect to different gene functions and signaling pathways. The results showed that 97 genes with hypermethylated CpG islands in the promoter region were homeobox genes. The top 5 hypermethylated homeobox genes validated by BSP were *HOXA2* (94.29%), *HOXA5* (95.38%), *HOXA11*

(91.67%), *HOXB4* (90.56%) and *HOXD13* (94.38%). Expression of these genes was reactivated with 5'-aza-2'-deoxycytidine. Significant expression differences were found between normal bile duct cancer and extrahepatic CCA tissues (Shu et al., 2011). However, currently no other information exists on epigenetic regulation of *Hoxa2* gene. Hence the subject of my investigations described in this thesis was to identify if epigenetic regulation (DNA methylation and histone methylation) played a role in transcriptional control of *Hoxa2* in the developing embryo and whether VPA impacted *Hoxa2* gene expression through epigenetic modulation.

CHAPTER 3: MATERIALS AND METHODS

3.1 Chemicals

Valproic acid (2-propylpentanoic acid, P6273, ≥ 98% pure), L-ascorbic acid (sodium salt, A4034, ≥ 98% pure), L-buthionine-S, R-sulfoximine (BSO) and penicillin-streptomycin solutions (50 ×, Cat.# P4458) were obtained from Sigma (St. Louis, MO, USA). 2-vinylpyridine (Cat.# 132292, 97% pure), metaphosphoric acid (M 6288, ≥ 33.5% pure) and triethanolamine (T1377, ≥ 98% pure) were obtained from Sigma-Aldrich Inc., (St. Louis, MO, USA). Isoflurane (100% v/v) was purchased from Baxter Corporation (CA2L9107, 100% pure, Toronto, ON, CAN). Minimal essential medium (MEM) with Earle's salt was purchased from GIBCO (Cat.# 11095-080, NY, USA).

3.2 Animals and preparation of culture serum

The University Committee on Animal Care and Supply at the University of Saskatchewan approved all animal protocols. Timed-pregnant CD-1 mice at gestation day (GD) 8 were obtained from the Animal Resources Center at the University of Saskatchewan. Female CD-1 mice were mated overnight; mating was confirmed the following morning by the presence of a vaginal plug; this was considered gestation day GD 0. On GD 8.5, the pregnant dams were anesthetized with isoflurane and euthanized by cervical dislocation; uteri were then removed to prepare embryos for culture.

Retired male Sprague Dawley breeder rats weighing 400-450 g were used for serum preparation. The rats were anesthetized with isoflurane, and the serum was prepared from blood collected from the dorsal aorta of the animal. After collection, the blood was centrifuged immediately at 2,000 rpm for 5 min to separate the cells from the plasma. A fibrin clot was formed during centrifugation, and serum was obtained by squeezing the clot, followed by a second round of centrifugation at 3,000 rpm for 10 min. The supernatant plasma was then isolated. The serum was filtered using a 0.45 um filter, aliquoted and stored at -20 °C and used within two weeks. On the day of culturing, the serum was heat-inactivated at 56 °C for 30 min immediately prior to use (Zhang et al, 2010).

3.3 Mouse whole embryo culture and experimental design

Embryos were explanted and cultured as previously described (Freeman and Steele, 1986; New, 1978). After removal of deciduas and Reichert's membrane, embryos with 6 to 8 somites [E8.5], an intact visceral yolk sac and ectoplacental cone were placed randomly in sealed culture bottles (3 embryos/bottle) containing 4 mL culture medium (MEM culture media ratio to rat serum [1:3]). The culture media was supplemented at the initiation of culture with penicillin and streptomycin with final concentrations of 100 IU/mL and 100 μg/mL, respectively. Cultures were incubated at 37 °C in rolling culture bottles (rotation speed at 23 rpm) for 48 h. Culture bottles were saturated for 3 min on 3 occasions: initially with a gas mixture of 5% O_2:5% CO_2:90% N_2; after 18 h with a gas mixture of 20% O_2:5% CO_2:75% N_2; and after 25 h with a gas mixture of 40% O_2:5% CO_2:55% N_2. Embryos were taken from different pregnant dams**.**

3.4 VPA, L-Buthionine-sulfoximine (BSO) and antioxidant treatment in the mouse whole embryo culture

The culture media was supplemented at the initiation of culture with VPA completely dissolved in Hanks solution with final concentrations of 0, 50 μg/mL [0.35 mM], 100 μg/mL [0.7mM], 200 μg/mL [1.4mM], or 400 μg/mL [2.8mM]; and embryos (E8.5) were examined and evaluated after 48 h at E10.5 (Fig. 3.1).

In this earlier study on the toxicity-concentration relationship it was found that 400 μg/mL VPA produced maximal toxicity. Therefore, for the subsequent culture treatment of VPA in the presence of antioxidant, VPA was added at a concentration of 400 μg/mL 1 h after starting the embryo cultures. In order to determine the effects of an antioxidant, 1000 μg/mL [5mM] L-ascorbic acid (St. Louis, MO, USA) was added to the media just prior to addition of VPA and embryos harvested at 48 h. Control for this experiment was treated with L-ascorbic acid without VPA.

To examine the effect of a decrease in GSH content on *Hoxa2* gene expression in embryos, cultures were treated with BSO to block GSH synthesis. BSO dissolved in HBSS solution

was added to the culture media at a concentration of 225 μg/mL [1 mM] from time 0, and embryos were collected after 48 h to measure the total GSH level.

3.5 Morphological assessment

After 48 h of incubation, mouse embryos were harvested and examined under a dissecting microscope (Model 312684-122, Bausch & Lomb, Rochester, NY) for the presence of yolk sac circulation and heart beat (viability). The magnifications used to carry out morphological assessments were in the range of 2.5 × to 3.0 ×. Only live embryos were further evaluated according to the morphologic scoring system of Van Maele-Fabry et al. (1990). Diameters of the yolk sac, crown-rump length and head length of each viable embryo were determined by ocular micrometer. Seventeen morphological items were assessed including yolk sac circulation, allantois, embryonic flexion, heart, neural tube, cerebral vesicles (forebrain, midbrain and hindbrain), otic, optic and olfactory vesicle, branchial arch, maxillary, mandible, limb buds (forelimb bud and hind limb bud), and somites. Morphological assessments were made by the observer who was blinded to each VPA treatment group.

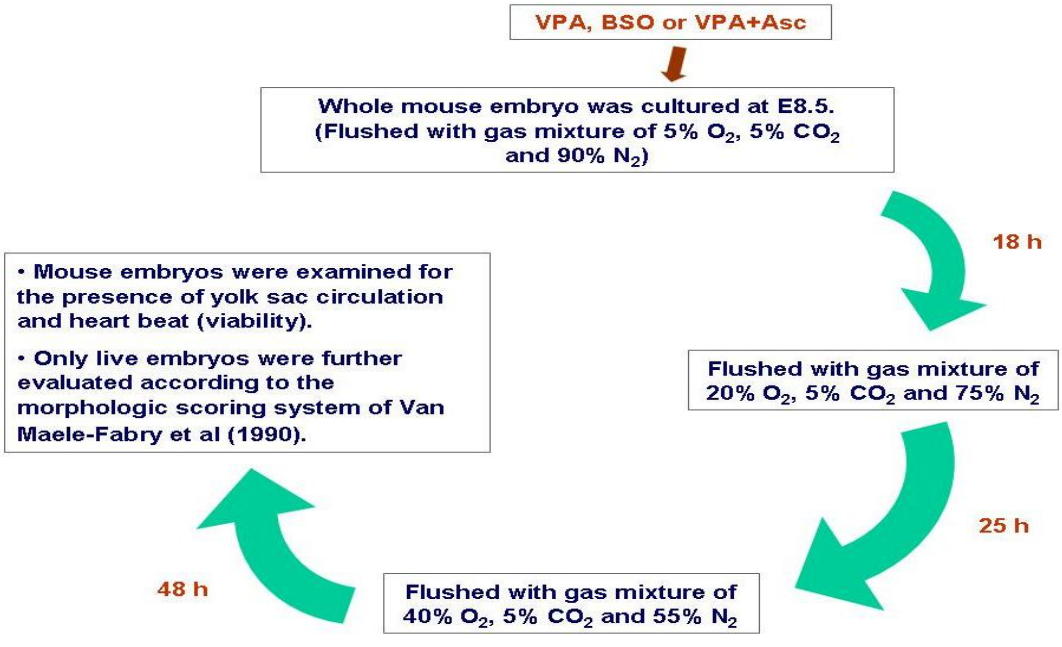

Fig. 3.1 Schematic diagram of procedures used in whole mouse embryo culture

3.6 Drug administration for animal *in vivo* study

Time pregnant CD-1 mice at E8 (30 – 40g) received a subcutaneous (s.c) injection of VPA at the dose of 400 mg/kg/day (Nau et al., 1981) or intraperitoneal (i.p) injection of ascorbic acid (vitamin C) at the dose of 250 mg/kg/day (Stojiljkovic, et al., 2010) followed by s.c injection of VPA. VPA and ascorbic acid were dissolved in saline and mice were administered VPA and/or ascorbic acid once daily in the morning (at 10 a.m.) at E8, E9 and E10, respectively. After 5-6 h following the last injection of VPA and/or ascorbic acid, E10.5 embryos were dissected from the uteri for DNA, RNA and protein isolation or chromatin immunoprecipitation assay. N=5-6 for each assay.

3.7 Cell lines and culture conditions

The mouse embryonic fibroblast cell line NIH3T3 and mouse T lymphocyte cell line EG7 were used for *in vitro* studies (**NIH3T3 cell line (ATCC)**: A hypertriploid mouse cell line. The modal chromosome number was 68 occurring in 30% of cells. The rate of cells with higher ploidies was 2.4%; **EG7 cell line (ATCC)**: E.G7-OVA derivative of EL4. The EL4 cells were transfected by electroporation with the plasmid pAc-neo-OVA which carries a complete copy of chicken ovalbumin (OVA) mRNA and the neomycin (G418) resistance gene). NIH3T3 cells were cultured in Dulbecco's Modified Eagle's Medium (DMEM, Invitrogen) with 10% (v/v) bovine calf serum (BCS, Invitrogen). EG7 cells were cultured in DMEM containing 110 mg/L sodium pyruvate supplemented with 10% (v/v) fetal bovine serum (FBS, Invitrogen). All cultures contained 1% antibiotic-antimycotic solution (Ab/Am, Sigma) and were maintained at 37° C, 5% CO_2 and 100% relative humidity. Cells were incubated with VPA for 24 h. EG7 cells were incubated with 5 -Aza for 48 h. NIH3T3 cell line was treated with VPA at the concentration of 0, 6.25 µg/mL [0.04 mM], 12.5 µg/mL [0.09 mM], 25 µg/mL [0.18 mM], 50 µg/mL [0.35 mM] or 100 µg/mL [0.70 mM], or BSO of 10 µM. EG7 cells were treated with VPA at doses of 0, 20 µg/mL [0.14 mM], 40 µg/mL [0.28 mM], 80 µg/mL [0.56 mM], 100 µg/mL [0.70 mM] or 200 µg/mL [1.4 mM]. NIH3T3 cells were treated with VPA (same doses as indicated above) or BSO (same doses as indicated above) in the presence of ascorbic acid at a concentration of 5 µg/mL [25 µM]. A

pre-trial with three ascorbic acid concentrations (5 µM, 25 µM and 100 µM) was used to treat NIH3T3 cells and 25 µM was identified as the highest dose that exhibited no cell death. EG7 cells were incubated with 5-Aza at the concentration of 0, 0.23 µg/mL [1 µM], 0.46 µg/mL [2 µM], 0.92 µg/mL [4 µM], 1.84 µg/mL [8 µM] or 2.3 µg/mL [10 µM], N=3-4.

3.8 Glutathione assay

Embryos isolated were stored immediately on dry ice and kept at -80 °C for analysis at a later time. Each individual embryo was analyzed. Embryos and NIH3T3 cells were homogenized respectively, in 200 µL of cold PBS buffer (50 mM phosphate, 1 mM EDTA, pH 6.3); 20 µL of the homogenized sample was removed for protein measurement using the Bio-Rad Protein Assay Kit (Bio-Rad Laboratories, Hercules, CA). The remainder of the sample was divided into two aliquots and immediately stored at -80 °C; one aliquot was used to measure total glutathione (GSSG+GSH) and the other for GSSG. Total glutathione and GSSG contents in embryos were measured spectrophotometrically by a Glutathione Assay Kit (Cayman Chemical Company, Ann Arbor, MI, USA). This kit utilized a carefully optimized enzymatic-recycling assay for the quantification of GSH based on glutathione reductase (Baker et al., 1990; Eyer and Podhradsky, 1986; Tietze, 1969). The sulfhydryl group of GSH reacts with DTNB (5,5'-dithiobis-2-nitrobenzoic acid) and produces a yellow-colour 5-thio-2-nitrobenzoic acid (TNB). Quantification of GSSG, exclusive of GSH, was accomplished by first derivatizing GSH with 2-vinylpyridine (Griffith, 1980). GSH content was estimated by subtracting the amount of GSSG from the total glutathione. A standard curve with concentrations of 0 to16 µM of GSH and 0 to 8.0 µM of GSSG was run simultaneously with each set of sample, respectively.

3.9 Isolation of DNA

Genomic DNA was isolated from cells and embryos using the PureLink genomic DNA kits (Invitrogen) according to manufacturer's instructions. It yielded approximately 15-20 µg of DNA per embryo at E10.5 or 5×10^6 starting cells. The samples were stored at -20 °C.

3.10 Isolation of total RNA

Total RNA was prepared with TRI Reagent (Sigma, St. Louis, MO) or RNeasy mini kit (Qiagen). For embryos using TRI Reagent extraction, 10-20 mg tissues were placed in 1.5 mL microcentrifuge tube with 250 μL of TRI Reagent and homogenized. The homogenate was stored for 15 min at room temperature, and extracted with 150 μL of 1-bromo-3-chloropropane (BCP) (Sigma, St. Louis, MO). The aqueous phase was combined with an equal volume (150 μL) of isopropanol (EMD, Gibbstown, NJ) to precipitate total RNA. The precipitate was centrifuged to form a pellet, subsequently washed with 75% ethanol and air-dried. The isolated total RNA was then re-dissolved in RNase free water (Sigma, St. Louis, MO).

Total RNA isolation from cells or embryos using RNeasy mini kit (Qiagen) followed the manufacturer's instruction. The kit yielded 10 μg of RNA per 1×10^6 starting cells, and ~ 20 μg of RNA per embryo between E8 to E10. The isolated total RNA was then dissolved in RNase free water. The purity of RNA was determined by the ratio of A260/A280 spectrophotometrical reading. Total RNA concentration was determined at OD260 using an Ultraspec 3100 *pro* Spectrophotometer (Biochrom Ltd. Cambridge, England). RNA samples were stored at -80°C. For quantitative real time PCR, total RNA solutions were diluted to concentrations of 50 ng/μL. An aliquot of 1.6 μL was taken for reverse transcription (RT) reaction.

3.11 Reverse transcription PCR (RT-PCR)

RT-PCR was used to measure gene expression in NIH3T3 cells, EG7 cells and developing embryos. Total RNA was used as a template for the synthesis of cDNA using SuperScript cDNA kit (Invitrogen, Carlsbad, CA) according to manufacturer's specification. Briefly, 80 ng of total RNA was mixed with 4.0 μl of 5 X first-strand reaction mix, 1.0 μl of dNTP (10 mM each), 2.0 μl of 0.1 M DTT, 1.0 μl of random primer (100 μM) and 1 μl of SuperScript II reverse transcriptase in a total volume of 20 μl. Synthesis of cDNA was completed by

incubation at 65°C for 5 min, 37 °C for 2 min, and 25°C for 10 min followed by 50 min at 37°C and 15 min at 85°C. Samples were stored at -20 °C or used immediately.

Polymerase chain reaction (PCR) was performed in a total volume of 50 µl containing 1-2 µl of cDNA, 1X PCR buffer, 1.5 mM $MgCl_2$, 0.2 mM dNTP, 0.5 µM of each primer and 2.5 units of Taq polymerase. The PCR program consisted of an initial step at 95°C for 2 min followed by 35 cycles of 95°C for 30 sec, annealing temperature (55°C-60°C depending on the primer), 72°C for 1 min and a final incubation of 72°C for 2 min.

3.12 Chromatin immunoprecipitation (ChIP)

Cells: ChIP experiments were carried out by using ChIP assay kit and protocol (Upstate). An aliquote of 135 µl of 37% formaldehyde (final 1% formaldehyde) was added to ~ 5×10^5 cells in a 100 mm culture dish containing 5 mL of growth media to crosslink protein and DNA at 37 °C for 15 min. After three washes in cold PBS containing protease inhibitor (1mM PMSF/1ug/ml aprotinin/1ug/ml pepstatin), the cells were resuspended in 200 µl of SDS lysis buffer. The lysates were sonicated (40% output) for 10s on ice and sonication repeated 4 times to obtain DNA in size range of 200 to 1000 bp. An aliquot (40 to 50 µl) of the sonicated lysate without the antibody was used as input DNA to quantitate the total amount of DNA present in different sample extracts before immunoprecipitation. The remaining sonicated lysate was diluted 10-fold in ChIP dilution buffer. The antibodies including anti-H3K27me3 (Abcam), anti-H3K4me3 (Abcam), anti-Ezh2 (Evx-1, Santa Cruz) and anti-Dnmt1 (Abcam) were used for immunoprecipitation at 4°C overnight. Immune complexes were then precipitated with protein A agarose provided in the kit, and washed sequentially with low salt, high salt immune complex wash, LiCl immune complex wash and TE buffer. The immune complex was then eluted from agarose beads with elution buffer (1% SDS, 0.1M $NaHCO_3$). At the end of the ChIP procedure, both the input DNA and the protein/DNA cross-linked chromatin complex immunoprecipitated with specific antibodies were reversed cross-linked with 5M NaCl at a final concentration of 200 mM at 65 °C for 8-12 h. Samples were then treated with proteinase K. Protein-free DNA was extracted in phenol/chloroform,

precipitated and washed in ethanol. The DNA extract was used for detection and quantification of regulator at *Hoxa2* gene promoter region with real-time PCR. N=3-4.

Tissue: About 10 mg of embryo tissue was used for this ChIP procedure. Tissue was first rinsed in cold PBS and cut into pieces. Tissue pieces were then incubated with 400 µl of PBS containing 1% formaldehyde at 37 °C for 15 min. After three washes with cold PBS containing protease inhibitors (1mM PMSF/1ug/ml aprotinin/1ug/ml pepstatin), tissue was homogenized in 200 to 400 µl of SDS lysis buffer. The ChIP procedure was then carried out by using the ChIP assay kit (Upstate) and protocol using the same procedures as described above for cells (Dong et al., 2008). N=3-4.

PCR primers for evaluating ChIP assays were designed to amplify 150-200 bp fragments from the region near the transcription start site at the *Hoxa2* gene promoter. For ChIP experiments, real-time PCR was performed in a final volume of 25 µl containing 50 ng of ChIP DNA or 50 ng of input DNA as template, 400 ng of each primer, and 12.5 µl of SYBR green PCR master mix (Applied Biosystems). The amplification consisted of 10 min at 95°C followed by 35 cycles of 95°C for 30 s, 60°C for 1min, and 72°C for 30 s in 7300 ABI detection system. The fold enrichment of each protein at the *Hoxa2* gene promoter was determined by the $2^{(-\Delta\Delta Ct)}$ method described in the Applied Biosystems User Bulletin (ABI PRISM 7700 Sequence Detection System, Applied Biosystems, 2001). Evaluations were determined from three independent ChIP assays, and each assay was evaluated in duplicate by real-time PCR (Fig. 3.2).

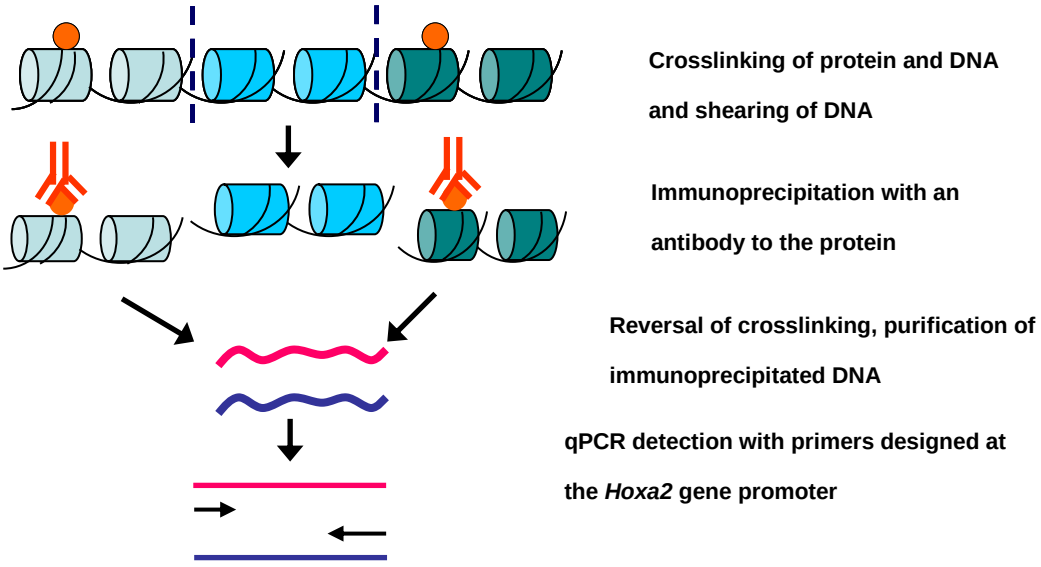

Fig. 3.2 Schematic diagram of ChIP assay

3.13 Quantitative real time PCR analysis

Quantitative Real-time PCR with TaqMan primers (Applied Biosystems, Foster City, CA) was used to quantify *Hoxa2*. For relative quantification, the amplification was performed in a Cepheid Smart Cycler® System (Roche Molecular System, Inc., Alameda, CA). Two µL of the RT reaction was amplified in a 20 µL PCR mixture, containing 1X Universal PCR master mix (Applied Biosystems, Foster City, CA) and 900 nM of PCR primers and probes designed by Applied Biosystems. The transcript of the *β-actin* housekeeping gene was amplified as an endogenous control. Four samples were analyzed at each dose treatment group. The real-time PCR conditions were 50°C/2 min (for optimal AmpErase uracil-N-glycosylase [UNG] activity), 95°C/12 min followed by 95°C/15 sec and 60°C/1 min for 45 cycles. The Smart Cycler® System established the threshold cycle (C_T) values needed to reveal the minimal amount of amplified material of the target transcript. The values of the total *Hoxa2* and *β-actin* transcript were calculated with the averaged C_T values of each sample, and extrapolated from standard curves. The normalized value of *Hoxa2* was established by dividing the average *Hoxa2* value with the average *β-actin* value for each sample. For comparative quantitation of gene expression, real time RT-PCR was employed using TaqMan® primers and labeled probe system and the ABI 7300 (Applied Biosystems). The reaction was

performed using the TaqMan® Universal Master Mix (2X), FAM-labeled TaqMan® Gene Expression assays for gene of interest (*Hoxa*2), VIC-labeled Taqman® Endogenous Control *β-actin*, and 36 ng of cDNA. All reactions were run in replicates of 4, and an n=3-4 was used for each group. Thermocycling parameters were as follows: 2 min. at 50°C, 10 min. at 95°C, 40 cycles of 15s at 95°C followed by 70s at 60°C.

3.14 Western blot analysis of Hoxa2 protein

Protein from the cultured mouse embryos was extracted with 10 µL of 1% SDS and 5 µL of 2X loading buffer. Individual embryos were analyzed. The protein samples were then denatured at 90 °C for 10 min. A 12% SDS-PAGE gel was used to separate proteins according to the manufacturer's protocol (Invitrogen, Carlsbad, CA) with 50 µg of total protein supernatant loaded onto the gel. The protein was transferred and immobilized onto a PVDF transfer membrane (PolyScreen, PerkinElmer, Boston, MA) using Xcell II Blot Module (Invitrogen, Carlsbad, CA) for wet transfer in 1 X transfer buffer containing 12 mM Tris, 96 mM glycine and 20% methanol, for 2 h at 30V/200 mAmp. Blocking of the membrane was carried out in 3% skim milk (in PBS) at 4 °C overnight. For detection of the Hoxa2 protein, the membrane was incubated for 2 h at 4 °C with the rabbit anti-Hoxa2 antiserum (Hao et al., 1999) at a dilution of 1:5000 in 3% skim milk. The membrane was then washed 3 x 20 min with 0.08% Tween-20 in PBS (Sigma, St. Louis, MO) and incubated for 2 h at room temperature with horse radish peroxidase (HRP) conjugated secondary goat anti-rabbit IgG (Bio-Rad, Hercules, CA), diluted 1:3000 in 3% skim milk. After visualization of Hoxa2 protein, the membrane was again blocked in 3% skim milk at 4 °C overnight for detection of the beta-actin protein. A 1:800 dilution of the mouse anti-actin (JLA20 monoclonal antibody, Developmental Studies Hybridoma Bank, Iowa City, IA) in 3% skim milk was used as the primary antibody. The membrane was incubated for 1 h at room temperature. After washing for 3 x 20 min with 0.08% Tween-20 in PBS, a 1:3000 dilution of HRP conjugated goat anti-mouse IgM was used as the secondary antibody, then the membrane washed 3 x 20 min in 0.08% Tween-20 in PBS. Visualization of proteins was performed by a Western Lightening Kit (PerkinElmer Life Sciences, Inc., Boston, MA) as per

manufacture's instructions, followed by exposure of the membrane to Kodak Scientific Imaging Film (X-OMAT Blue XB-1, Kodak, Rochester, NY) for 3 to 10 sec. Two replicates were run for each sample, and 8 samples were run in total for each dose of VPA.

3.15 DNA methylation analysis

3.15.1 Sodium bisulfite modification

Genomic DNA was modified with bisulfite reagent for DNA methylation analysis by using the EpiTect bisulfite kit (Qiagen) or EZ DNA methylation kit (Zymo Research, USA). Genomic DNA (2 μg) was modified per sample according to the manufacturer's instructions. The concentration and purity of bisulfite treated DNA samples were determined by NanoVue UV/visible Spectrophotometer (GE Healthcare Life Sciences). Bisulfite treated DNA samples were stored at -20°C.

3.15.2. Bisulfite specific PCR (BSP) and methylation specific PCR (MSP)

DNA methylation within promoter associated CpG islands was determined by BSP sequencing after sodium bisulfite modification of genomic DNA as described above (Fig. 3.3). BSP primers were designed using the online 'MethPrimer' (http://www.urogene.org//methprimer/) (Li and Dahiya, 2002). For BSP sequencing, three sets of primers were designed within 1688 bp region near the transcription start site at the *Hoxa2* gene promoter. PCR was carried out in a final volume of 50 μl containing 100-200 ng of bisulfite-modified DNA, 1 × HotStar Taq master mix, 2.5 mM $MgCl_2$, 200 μM of each dNTP, 500 nM of each primer, and 2.5 units of HotStar Taq DNA polymerase (Qiagen). The amplification consisted of a Taq activation step at 95°C for 15 min, 35 cycles of 94°C for 1min, 55°C for 1min, and 72°C for 2 min, and a final incubation at 72°C for 10 min. Mouse embryos were from E6.5, E8.5 and E10.5. E6.5 mouse embryos were taken with ectoplacental cone.

MSP primers also designed using online 'MethPrimer' software (Li and Dahiya, 2002). PCR amplification conditions were the same as described above for BSP.

3.15.3 Sub-cloning and sequencing

Bisulfite PCR products were subcloned into pGEM-T easy vector (Promega) according to manufacturer's protocol. Two clones were randomly selected on each plate. The clones were purified with PureLink HQ mini plasmid DNA purification kit (Invitrogen). The purified DNA was sent for sequencing using the vector primer M13F or M13R.

For sequencing DNA samples isolated from drug treated cells and embryos, the bisulfite primers near the transcription start site (Bsp_kx5 and kx6) were used to generate PCR products. The PCR products were confirmed by visualizing following agarose gel electrophoresis (1.5% agarose gel). Samples were then purified with PCR purification kit (Qiagen) and sent to National Research Council laboratories, Saskatoon, SK for DNA sequencing. Modified EG7 DNA served as the methylated positive control while modified NIH3T3 DNA served as the unmethylated positive control. (However, neither 5-mC nor 5-hmC undergo C-to-T transitions after bisulfite treatment) (Huang, et al., 2010).

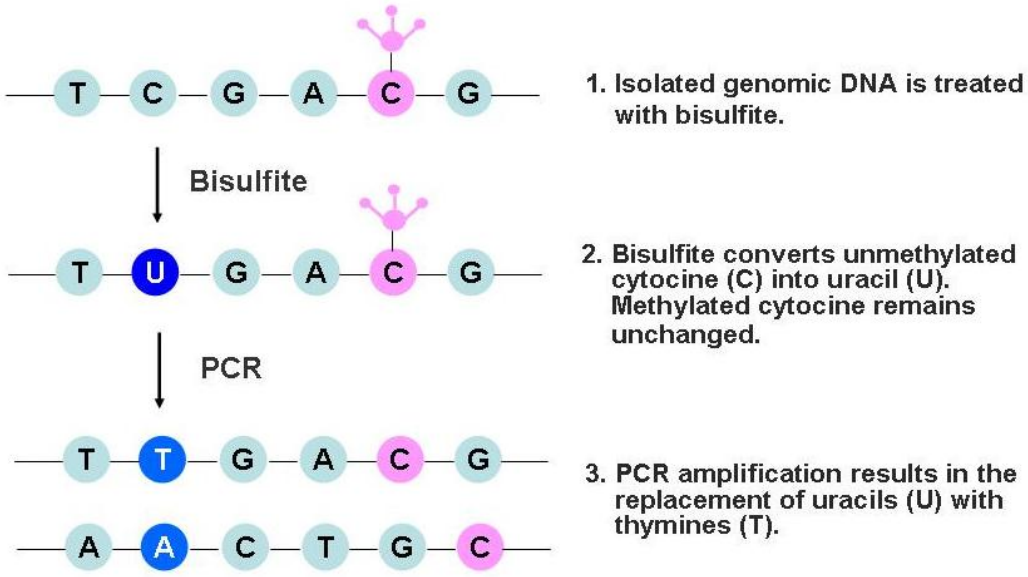

Fig. 3.3 Bisulfite determination of DNA methylation

3.16 Determining DNA methylation using Pyrosequencing assay

Pyrosequencing is a real-time sequencing that allows us to quantify methylation at multiple CpG sites individually (Colella et al., 2003; Rietschel et al., 2008; Ronaghi, 2003). Genomic DNA was extracted from NIH3T3 cells or mouse embryos using DNeasy Blood & Tissue Kit (Qiagen). DNA sample (200 ng to 2 µg) was bisulfite treated using Zymo DNA Methylation Kit (Zymo research, Orange, CA). The bisulfite treated DNA was eluted in 10 µl volume and used for PCR amplification with the primers designed and supplied by EpigenDx (Worcester, MA). The PCR was performed in a PCR reaction mix containing 1 µl of bisulfite-converted DNA sample or internal controls, 10 × PCR buffer, 3.0 mM $MgCl_2$, 200 µM of each dNTP, 0.2 µM forward primer, 0.02 µM reverse primer tailed, 0.18 µM universal primer, and 0.75 U of HotStar DNA polymerase (Qiagen Inc, Valencia, CA). The PCR conditions were as follows: 15 min at 95 °C, 35 cycles of 30s at 95 °C, 30s at 55 °C, and 30s at 72 °C, followed by a final extension step for 5 min at 72 °C. Samples subsequently were sent to EpigenDx for commercial pyrosequencing. The PCR products (each 10 µl) were sequenced by Pyrosequencing PSQ96 HS System (Qiagen Pyrosequencing) following the manufacturer's instructions (Qiagen Pyrosequencing). The methylation status of each locus was analyzed individually by EpigenDx as a T/C SNP using QCpG software (Qiagen Pyrosequencing). The extent of methylation at each CpG site was automatically calculated and is sensitive enough to detect 5% changes in methylation levels (EpigenDx) n=3.

3.17 Quantitative telomerase activity assay

The assay was performed using Quantitative Telomerase Detection Kit (Allied Biotech, Inc) which is determined through its ability to synthesize telomeric repeats onto an oligonucleotide substrate. The resultant extended product is subsequently amplified by SYBR real-time PCR. NIH3T3 cells (10^5-10^6 cells) or mouse embryos (40 to 100 mg) were homogenized and incubated in 200 µl 1 X lysis buffer (added with protease inhibitor) on ice for 30 min. The lysate were then centrifuged at 10,000 x g for 15 min at 4 °C. The supernatant was removed and stored at -80 °C until use. The protein concentration was

determined with Bio-Rad Protein Assay Kit (Bio-Rad Laboratories, Hercules, CA). For each assay the samples were diluted to 0.5 µg/uL. The PCR reaction mix contains 1 µl of diluted sample and 1x Quantitative Telomerase Premix. The telomerase reaction was carried out at 25 °C for 30 min. followed by PCR conditions: 10 min at 95 °C, 40 cycles of 30s at 95 °C, 35s at 60 °C and 30s at 72 °C. A standard curve was generated from dilutions of TSR control which is an oligonucleotide with a sequence similar to telomerase extended product (TSR is ratio of telomere repeat copy number to single gene copy number). The amount of the telomerase extended product of each sample was extrapolated from the standard curve. The relative value for each sample was established by dividing with the control value, representing the relative activity of telomerase of each sample.

3.18 Telomere length measurement by real-time PCR

Genomic DNA was extracted from NIH3T3 cells and mouse embryos using DNeasy Blood & Tissue Kit (Qiagen). Relative average telomere length was assessed by a modified version of real-time PCR-based method, in which the telomere repeat copy number to single gene copy number (β-globin) ratio (T/S) was determined (Cawthon, 2002; McGrath et al., 2007). Both telomere and β-globin PCR reaction mixture consisted of 1x SYBR green master mix (Qiagen) and 5 ng genomic DNA. For telomere PCR reaction contained 100 nM of telomere forward primer and 900 nM of telomere reverse primer. PCR reaction proceeded at 95 °C for 10 min, followed by 40 cycles at 95 °C for 15 s, and 54 °C for 1 min. β-globin PCR reaction contained 300 nM of globin forward primer and 700 nM of globin reverse primer. The reaction proceeded at 95 °C for 10 min, followed by 40 cycles at 95 °C for 15 s, 58 °C for 20 s, and 72 °C for 28 s. In addition to the samples, a standard curve from 0.0625 ng to 12.5 ng using genomic DNA was generated to assess the PCR efficiency. The slope of the standard curve for both the telomere and β -globin reactions ranged from -3.30 to -3.70. The T/S ratio (-dCt) for each sample was calculated by subtracting the β -globin Ct value from the telomere Ct value. The relative T/S ratio (-ddCt) was determined by subtracting the T/S ratio

of the 5 ng standard curve point from the T/S ratio previously calculated from each sample (Cawthon, 2002; McGrath et al., 2007).

3.19 Statistical analysis

All statistical analyses concerning morphologic scoring parameters, embryonic growth parameters, glutathione status, *Hoxa2* gene expression at mRNA level, ChIP real-time PCR results, pyrosequencing analysis of DNA methylation, telomere length and telomerase activity in treatment and control groups were compared using one-way ANOVA with Tukey's HSD (Honestly Significant Differences) as the post-hoc test, or were analyzed by independent-samples *t* test to compare. A probability of less than 0.05 was assumed to denote significant difference. The incidence of the embryonic malformation in treatment and control groups was compared using chi-square (x^2) test. The level of significance was $P \leq 0.05$.

Table 3.1 Sequences of primers used in this study

Name	Sequence
***Hoxa2* gene**	Forward: 5’ CTGGATGAAGGAGAAGAAGGC Reverse: 5’ CGGTTCTGAAACCACACTTTC
***GAPDH* gene**	Forward: 5’ ACCACAGTCCATGCCATCAC Reverse: 5’ TCCACCACCCTGTTGCTGTA
ChIP-PCR primers at *Hoxa2* gene promoter	**Fragment 1:** Forward: 5’ GTTGTCTTTTGAATCCTTCAGCC (A2-1) Reverse: 5’ GGCACTCTGGGTTTCATACC (A2-2) **Fragment 2:** Forward: 5’ TATGAATCGGTTCTGAGAACTG (A2-3) Reverse: 5’ GCCACTGTCTGTTTGATTGATCC (A2-4)
ChIP quantitative real-time PCR (both for H3K4me3 and H3K27me3)	Forward: 5’ CCAGGGAGCACACTAGATCC (Klx 3) Reverse: 5’ AGTCAGAAAGGAACGCCTCA (Klx 3-1)
Bisulfite specific PCR	Bsp_kx1: 5’ GGAAAGAGGGATTAAGAAATAAGAGTT Bsp_kx2: 5’ ACATATACCAAAAAAAACAACAACC Bsp_kx3: 5’ GGTTGTTGTTTTTTTTGGTATATGT Bsp_kx4: 5’ TCCAAAATCAATTCTCAAAAC Bsp_kx5: 5’ GTTAGGTTGAGGTGTTTAAAT Bsp_kx6: 5’ ACCACTATCTATTTAATTAATCC
Methylation specific PCR	Msp-kx1-MF: 5’ TTTTTGGAAGTCGGAAATATTTATC Msp-kx1-MR: 5’ AATCCCCGTAACCTAAACGAC Msp-kx1-UF: 5’ TTTTGGAAGTTGGAAATATTTATTGT Msp-kx1-UR: 5’ CAAATCCCCATAACCTAAACAAC Msp-kx2-MF: 5’ TAGTTATTTTTGAGAAGTTGATGGC Msp-kx2-MR: 5’ TATCCAACCCGAAACCTACG Msp-kx2-UF: 5’ GTTATTTTTGAGAAGTTGATGGTGA Msp-kx2-UR: 5’ TTAATATCCAACCCAAAACCTACAC Msp-kx3-MF: 5’ TTTTCGATAGTTTTAAATAATGCGC Msp-kx3-MR: 5’ TAAATAACAATACCCCGAAAATACG
	Sequence
	Msp-kx3-UF: 5’ TTTGATAGTTTTAAATAATGTGTGG Msp-kx3-UR: 5’ AATAACAATACCCCAAAAATACATA

CHAPTER 4: RESULTS

4.1 VPA-induced dysmorphogenesis in mouse embryo

4.1.1 Effect of VPA on embryonic differentiation and growth

To investigate the pattern of VPA-induced teratogenesis, E8.5 CD-1 mouse embryos with 6-8 somites were exposed to 0, 50, 100, 200, and 400 μg/mL VPA *in vitro* for 48 h. We observed a dose-dependent decrease in various parameters of embryonic growth (Table 4.1.1) and morphological score (Table 4.1.2), and an increase in the frequency of embryonic malformations (Table 4.1.3). Embryos exposed to 50 μg/mL VPA showed obvious inhibition of embryonic head development. At VPA concentrations ≥200 μg/mL, overall embryonic growth was affected, as represented by reduced yolk sac diameter, crown-rump length, head length, and decreased number of somites (Table 4.1.1).

As for embryonic differentiation, total morphological score (Table 4.1.2) decreased significantly at a VPA concentration of 50μg/mL, as did scoring parameters such as yolk sac circulation, allantois, caudal neural tube, hindbrain, forebrain, and branchial arch. At VPA concentrations ≥200 μg/mL, almost all scoring parameters except hind limb notably decreased (Table 4.1.2).

VPA concentrations of 50, 100, 200, and 400μg/mL increased the incidence of abnormal embryos by 11.8%, 35.3%, 47.1% and 88.2%, respectively (Table 4.1.3). VPA concentrations ≥200 μg/mL caused an obvious increase in the incidence of dead embryos. Embryo malformations included neural tube defects (NTDs), abnormal flexion, yolk sac circulation defects, somite defects, and craniofacial deformities such as fusion of maxillary and mandibular branchial arches (Fig. 4.1.1).

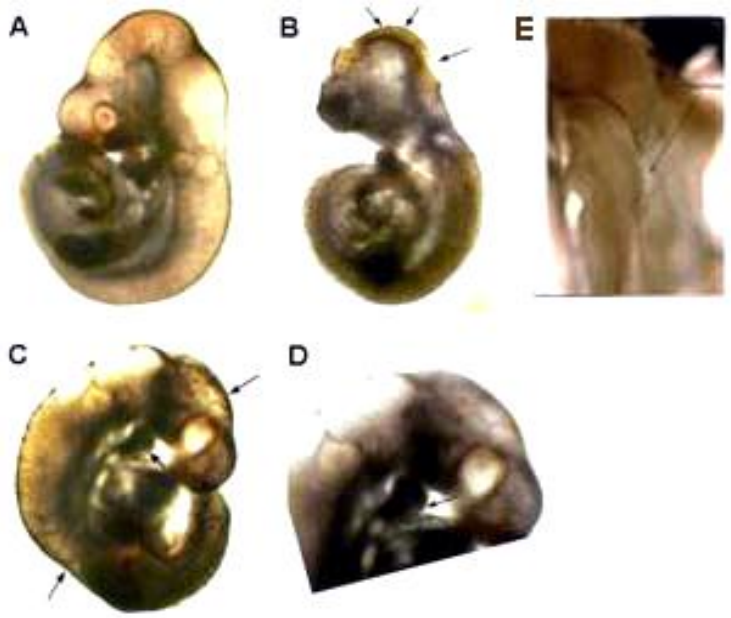

Fig. 4.1.1 Embryos treated with VPA. Control (**A**), 50 µg/mL (**B, E**), and 200 µg/mL (**C, D**). The types of malformations observed included open neural tube (**B, C** and **E**), somite defects (**C**), and craniofacial malformations such as fusion of first and second arch (**C**, **D**). **D** is the same embryo as **C** magnified to show the fusion of the first and second arches (arrow). **E**, Dorsal view of the embryo in (**B**), arrows exhibiting an open neural tube.

Table 4.1.1 Effect of VPA on mouse embryonic growth *in vitro* (Mean± SD)

Parameter	**Concentrations of VPA (µg/mL)**				
	0 (n=17)	**50.0 (n=17)**	**100.0 (n=17)**	**200.0 (n=15)**	**400.0 (n=15)**
Yolk sac diameter (mm)	4.70±0.37	4.26±0.20	4.15±0.36[a]	4.01±0.41[a]	3.83±0.37[b]
Crown-rump length (mm)	4.27±0.33	4.04±0.23	3.96±0.29	3.50±0.25[a]	2.56±0.15[b]
Head-length (mm)	2.53±0.57	2.17±0.12[a]	2.09±0.35[a]	1.70±0.27[b]	1.28±0.29[b]
Somite number	31.3±1.41	29.76±1.39	28.11±2.11	25.0±2.36[a]	22.5±2.77[a]

[a]: p ≤ 0.05 vs. control
[b:] p ≤ 0.01 vs. control

Table 4.1.2 Effect of VPA on mouse embryonic differentiation *in vitro* (Mean± SD)

Morphological score*	Concentrations of VPA (µg/mL)				
	0.0 (n=17)	**50.0 (n=17)**	**100.0 (n=17)**	**200.0 (n=15)**	**400.0 (n=15)**
Yolk sac circulation	4.58±0.50	3.76±0.43[a]	3.35±0.49[a]	2.67±0.62[b]	1.86±0.35[b]
Allantois	3.88±0.33	2.76±0.43[a]	2.59±0.50[a]	2.13±0.52[b]	2.06±0.26[b]
Flexion	5.00±0.00	4.76±0.42	4.44±0.78	3.06±0.95[a]	3.06±0.25[a]
Heart	4.35±0.60	3.94±0.42	3.64±0.60[a]	2.71±0.46[b]	2.13±0.35[b]
Candal neural tube	5.00±0.00	4.53±0.51[a]	3.73±1.25[b]	1.80±0.94[b]	1.33±0.48[b]
Hindbrain	4.88±0.33	4.29±0.58[a]	3.29±0.97[a]	2.00±0.77[b]	1.80±0.41[b]
Midbrain	5.00±0.00	4.53±0.51	3.29±0.77[b]	2.40±0.63[b]	1.80±0.41[b]
Forebrain	5.11±0.33	4.53±0.51[a]	3.29±0.84[b]	2.60±0.73[b]	1.20±0.56[b]
Otic system	5.23±0.43	4.71±0.46	4.00±0.50[a]	3.20±0.41[b]	1.53±0.51[b]
Optic system	4.59±0.51	4.47±0.51	4.05±0.42	2.47±0.63[a]	1.86±0.83[b]
Olfactory system	3.00±0.00	2.76±0.41	2.711±0.33	2.66±0.48[a]	2.07±0.26[b]
Branchial bar	3.54±0.62	2.82±0.39[a]	2.71±0.46[a]	2.60±0.50[b]	2.00±0.00[b]
Maxillary process	3.00±0.00	2.76±0.41	2.59±0.50	2.53±0.51[a]	2.06±0.26[a]
Mandibular process	3.35±0.49	3.23±0.43	3.14±0.78	2.27±0.45[b]	2.06±0.26[b]
Fore limb	3.00±0.00	2.71±0.46	2.62±0.39	2.33±0.48[a]	2.13±0.35[a]
Hind limb	1.06±0.24	0.76±0.43	0.64±0.49	0.60±0.50	0.33±0.48[a]
Somites (score)	5.00±0.00	5.00±0.00	4.88±0.33	4.33±0.48[a]	3.80±0.56[b]
Total score	68.29±2.51	62.53±1.81[a]	54.94±5.72[a]	42.00±4.09[b]	33.07±2.77[b]

***as per Van Maele-Fabry et al. (1990)**

[a]: p ≤ 0.05 vs. control

[b:] p ≤ 0.01 vs. control

Table 4.1.3 Incidence of dysmorphogenesis in mouse embryos *in vitro*

	Concentrations of VPA (µg/mL)				
	0.0	**50.0**	**100.0**	**200.0**	**400.0**
Embryos, n	17	17	17	17	17
Normal form, n	17	15	11	7	0
Malformations, n (%)	0	2 (11.76) [a]	6 (35.3) [a]	8 (47.1) [b]	15 (88.2) [b]
Death, n (%)	0	0	0	2 (11.76) [a]	2 (11.76) [a]

[a]: $p \leq 0.05$ vs. control; [b:] $p \leq 0.01$ vs. control

4.1.2 Effect of ascorbic acid on developing embryos treated with VPA

Mouse whole embryo cultures treated with VPA (100 µg/mL) exhibited abnormal differentiation in areas such as the hindbrain, midbrain, forebrain and the optic system (time-pregnant mice were administered a dose of VPA (100 µg/ml, s.c) at E8.5 and embryos harvested for culture after 48 h). There was a significant decrease in the morphological score (Van Maele-Fabry et al., 1990) of hindbrain, midbrain and forebrain in VPA treated embryos compared to untreated cultured embryos. Exposure to VPA (100 µg/mL) also induced embryonic malformations in 6 out 17 embryos with incidence rate of 35.3%. Exposure to ascorbic acid (5 mM, 1000 µg/mL) alone had no significant effect on embryonic growth whereas co-treatment with ascorbic acid significantly reduced the impact of VPA on the developing mouse brain (Table 4.1.4). Interestingly, treatment with ascorbic acid decreased the incidence of malformed embryos following VPA exposure (Table 4.1.5).

Table 4.1.4 Ascorbic acid protects embryos from abnormal brain differentiation

Morphological Score	VPA (µg/mL)		Ascorbic acid	VPA (100 µg/ml) + Ascorbic acid
	0 (n=17)	100 (n=17)	1000 µg/ml (n=17)	1000 µg/ml (n=15)
Hindbrain	4.88±0.33	3.29±0.97[a]	4.69±0.34	4.43±0.12
Midbrain	5.00±0.00	3.29±0.77[b]	4.92±0.10	4.67±0.29
Forebrain	5.11±0.33	3.29±0.84[b]	4.97±0.13	4.83±0.58
Optic system	4.59±0.51	4.05±0.42	4.72±0.10	4.67±0.29

([a], $p < 0.05$; [b], $p < 0.01$ compared to control)

Table 4.1.5 Ascorbic acid reduces the incidence of malformations induced by VPA

	VPA (µg/mL)		Ascorbic acid	VPA (100 µg/ml) + Ascorbic acid
	0 (n=17)	100 (n=17)	1000 µg/ml (n=4)	1000 µg/ml (n=15)
Embryos (n)	17	17	4	18
Normal form (n)	17	11	4	18
Malformations (n, %)	0	6 (35.3%)	0	0

4.1.3 Effect of VPA on mouse embryonic oxidative status

The oxidative status of cultured mice embryos was assessed by determining total glutathione and the GSSG/GSH ratio after exposure to 0, 50, 100, 200, and 400 μg/mL VPA. A significant decrease in total glutathione in embryos only occurred at a VPA dose of 400 μg/mL; a decreasing trend was evident as VPA doses increased from 0 to 400 μg/mL (Fig. 4.1.2a). The oxidative status of mice embryos using the GSSG/GSH ratio was also evaluated as this method accounts for possible compensatory increases in glutathione biosynthesis that may occur in response to redox changes (Ozolinš and Hales, 1997). A dose-dependent increase in embryonic GSSG/GSH ratio was observed; the GSSG/GSH ratio was significantly affected at VPA exposure doses ≥100 μg/mL (Fig. 4.1.2b).

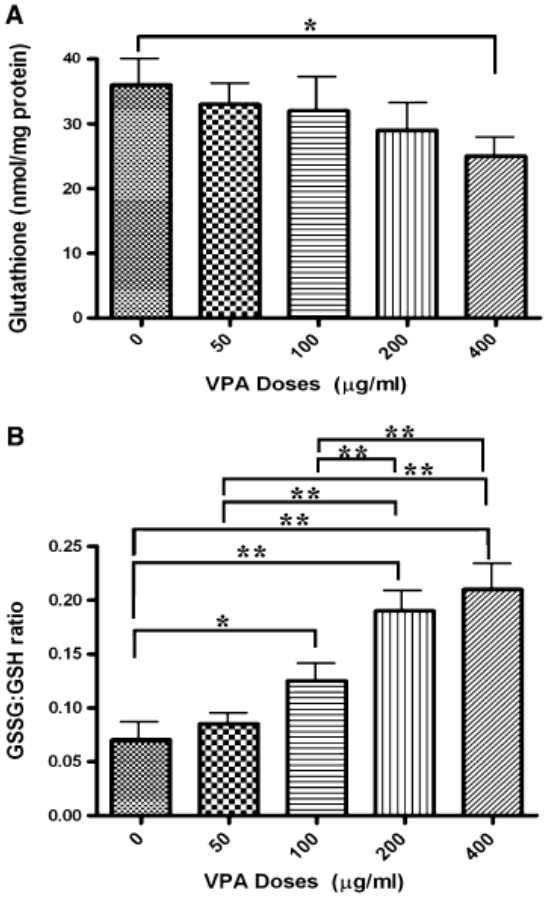

Fig. 4.1.2 Effect of VPA on total glutathione content (**A**) and on GSSG/GSH ratio (**B**) in mice embryos *in vitro* (n=8). GSSG glutathione disulfide, GSH reduced glutathione. * $p \leq 0.05$ and ** $p \leq 0.01$ between *bars* indicated by *brackets*

4.1.4 Effect of VPA on *Hoxa2* gene expression in mice embryos

The level of *Hoxa2* gene expression in embryos in culture was measured at the protein level by Western blot analysis (Fig. 4.1.3) and at the gene expression level by quantitative real-time RT-PCR (Table 4.1.6). Western blot results show that VPA causes a dose-dependent decrease in Hoxa2 protein expression in developing mice embryos in culture. A dose-dependent decrease in *Hoxa2* mRNA expression was also observed. Total *Hoxa2* mRNA content in embryos and *Hoxa2* gene expression normalized to *β*-actin decreased with increasing exposure to VPA. Significant decreases in *Hoxa2* gene expression occurred in every experimental group (VPA ≥ 50 µg/mL) after VPA exposure.

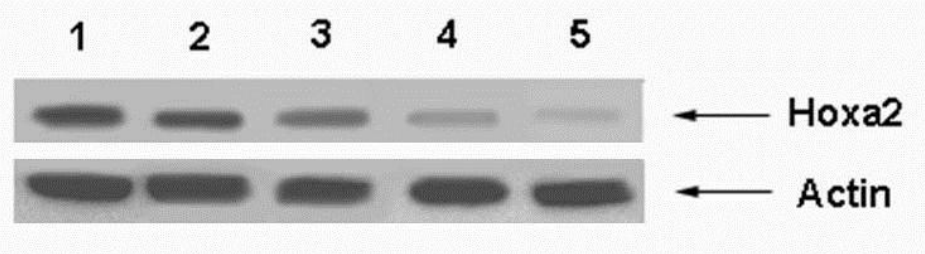

Fig. 4.1.3 Western blot analysis of Hoxa2 in embryos treated with VPA.

Lane 1: untreated control embryos; Lanes 2-5: embryos treated with dose of 50 µg/mL [0.35 mM], 100 µg/mL [0.7 mM], 200 µg/mL [1.4 mM] and 400 µg/mL [2.8 mM] VPA, respectively.

Table 4.1.6 Effect of VPA on *Hoxa2* gene expression in cultured mice embryos

(Mean ± SD), n=4

Concentrations of VPA (µg/mL)	*Hoxa2* ng Total RNA	*β*-actin ng Total RNA	*Hoxa2* normalized to β-actin
0	3.55±0.66	1.61±0.35	2.20±0.09
50	1.17±0.30[a]	1.37±0.79	0.85±0.14 [a]
100	1.11±0.78[a]	1.73±0.10	0.64±0.19 [b]
200	0.82±0.30[b]	1.79±0.29	0.46±0.04 [b]
400	0.04±0.02[b]	1.57±0.38	0.03±0.03 [b]

a: $p \leq 0.05$ vs. control
b: $p \leq 0.01$ vs. control

4.1.5 Antioxidant status of *Hoxa2*-/- embryos and wild-type embryos treated with BSO

To determine if a relationship exists between GSH content and *Hoxa2* gene expression, BSO (Buthionine sulphoximine) was added to mouse embryo cultures (starting at E8.5 for 48h to E10.5) to block the biosynthesis of glutathione. However, results indicate that BSO was unable to significantly reduce GSH content or to cause an increase in the GSSG/GSH ratio in cultured wild-type mice embryos (Fig.4.1.4). The antioxidant status of untreated *Hoxa2*-/- embryos at E10.5 was also investigated. Significant changes in GSH content or in GSSG/GSH ratio were not observed in the *Hoxa2*-/- mice embryos compared to matched control or BSO treated wild-type embryos (Fig. 4.1.4). Results indicate embryonic antioxidant status does not change with loss of *Hoxa2* gene function.

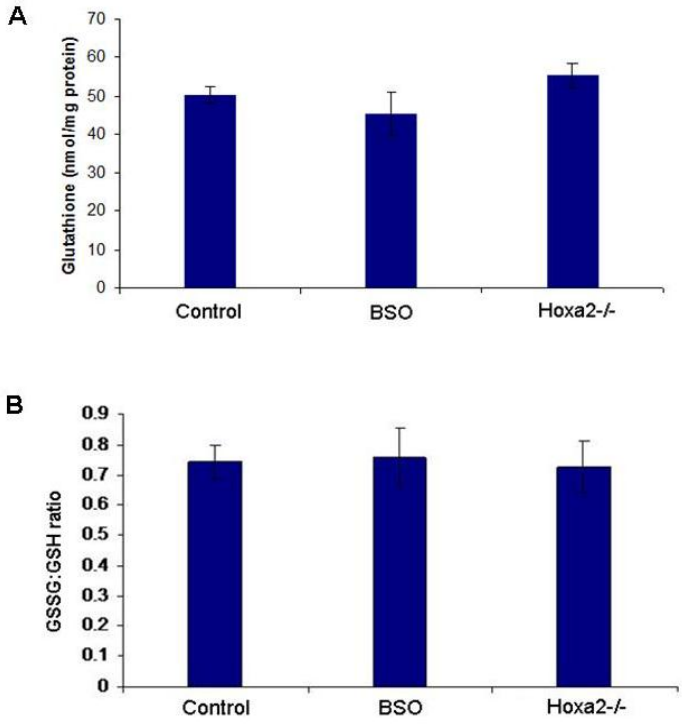

Fig. 4.1.4 GSH content **(A)** and GSSG:GSH ratio (**B**) in control untreated wild-type mice embryos in culture (control), wild-type embryos treated with BSO at a concentration of 225 μg/mL (1 mM) for 48 h in culture (BSO), and in *Hoxa2* -/- mice embryos (E10.5) (n=4-5 embryos). *Bars* represents mean ± SD.

4.1.6 Ascorbic acid maintains glutathione homeostasis in VPA-treated NIH3T3 cells and in VPA-treated embryos

To determine the effect of ascorbic acid (5μg/mL, 25 μM) on glutathione homeostasis, NIH3T3 fibroblast cells (1×10^5 cells/cm^2) were treated with VPA at doses of 6.25 μg/mL to 100 μg/mL for 24 h. The total glutathione content in VPA treated cultures at doses of 6.25 μg/mL to 50 μg/mL did not change from control untreated cells. However, a significant decrease in total glutathione occurred at VPA dose of 100 μg/mL; a decreasing trend was evident as VPA doses increased from 25 to 100 μg/mL (Fig. 4.1.5). The presence of 5 μg/mL [25 μM] ascorbic acid reversed the decline in total glutathione content (Fig. 4.1.5) in cells treated with VPA at 12.5 μg/mL and 25 μg/mL, however supplemental ascorbic acid had no effect at the highest VPA doses of 50 μg/mL and 100 μg/mL.

The effect of ascorbic acid on glutathione level and GSSG/GSH ratios in developing mice embryos in culture was also investigated. Embryos in culture were treated with L-ascorbic acid 1000 μg/mL [5 mM] just prior to exposure to the highest dose of VPA (400 μg/ml) and embryos harvested after 48 h. Pilot experiments with 400 μg/mL [2 mM] VPA and 1000 μg/ml [5 mM] ascorbic acid revealed 1000 μg/ml to be optimal for embryo protection. Results indicate that ascorbic acid was able to counter effects of VPA and reversed the depletion of total glutathione (Fig. 4.1.6a) and normalized the GSSG/GSH ratio in cultured embryos (Fig. 4.1.6b). Ascorbic acid alone had no significant effect on total glutathione levels in cultured embryos (Fig. 4.1.6a) but did have an inhibitory effect on the GSSG/GSH ratio (Fig. 4.1.6b) indicating its potent antioxidant property.

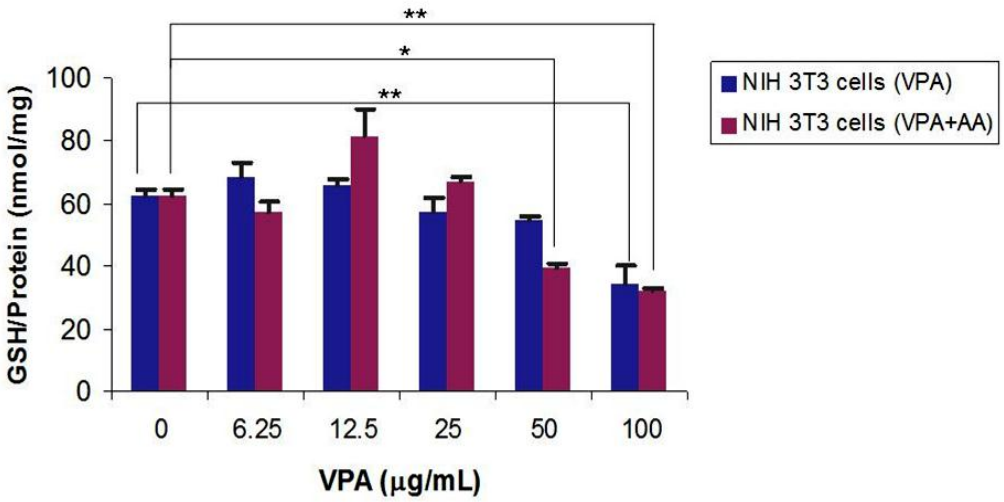

Fig. 4.1.5 Total glutathione in NIH3T3 cell cultures treated with VPA (6.25 to 100 μg/mL) [0.04 to 0.70 mM] and VPA in the presence of 5 μg/mL [25 μM] ascorbic acid for 24 h **(A)**. Cells were harvested at 5×10^5 cells/cm^2. *Bars* represents mean ± SD. * represents a significance $p \leq 0.05$ and ** represents a significance $p \leq 0.01$ between *bars* indicated by *brackets*. GSH: reduced glutathione. Statistical analysis: one-way ANOVA with Tukey's HSD as post-hoc analysis N=3-4.

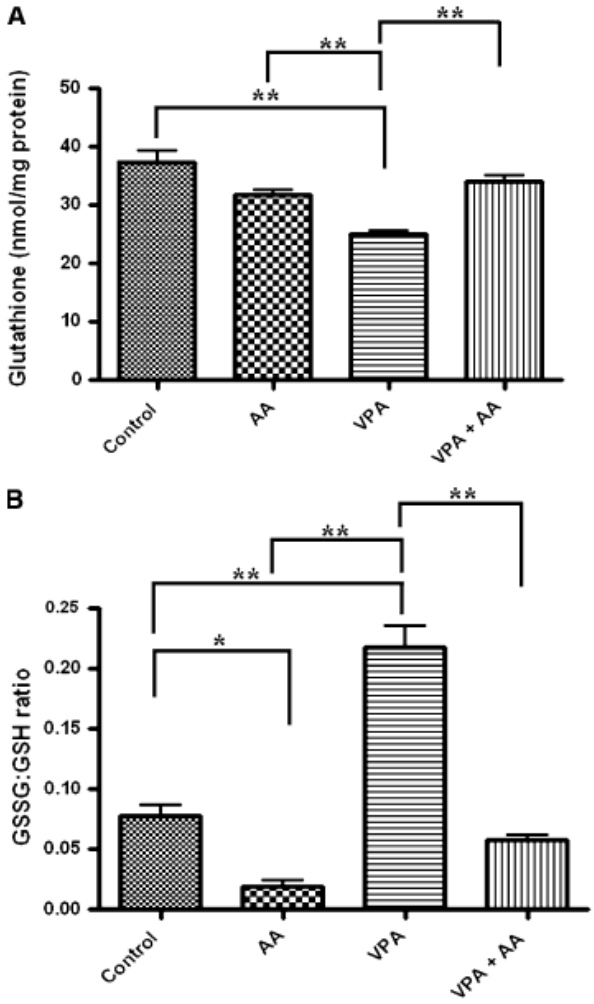

Fig. 4.1.6 Effect of ascorbic acid on total glutathione content (**A**) and on GSSG/GSH ratio (**B**) in cultured embryos treated with VPA. Control: AA, treated with 1000 µg/mL [5 mM] L-ascorbic acid; VPA, treated with 400 µg/mL [2.8 mM] of valproic acid; VPA+AA, treated with 1000 µg/mL L-ascorbic acid prior to addition of 400 µg/mL of valproic acid. Embryos were cultured for 48 h. *Bars* represents mean ± SD, n = 4-5. * represents a significance $p \leq 0.05$ and ** represents a significance $p \leq 0.01$ between *bars* indicated by *brackets*. GSSG: glutathione disulfide, GSH: reduced glutathione

4.1.7 Ascorbic acid prevents the VPA-induced inhibition of *Hoxa2*

In a separate set of mouse embryo cultures, the effect of ascorbic acid on VPA-induced inhibition of *Hoxa2* was measured using quantitative real-time RT-PCR. Mouse embryos in culture were pretreated with L-ascorbic acid 1000 µg/mL just prior to exposure to the highest dose of VPA (400 µg/ml) and embryos harvested 48 h later for analysis. Results indicate that

the relative quantity of *Hoxa2* gene expression was significantly decreased after VPA exposure but that this inhibition was prevented from occurring after pretreatment with ascorbic acid, with *Hoxa2* levels remaining higher than both control and VPA-treated embryos (Fig. 4.1.7a). Western blot analysis for protein expression also showed similar results (Fig. 4.1.7b). VPA-induced inhibition of *Hoxa2* is downstream from VPA-induced oxidative stress since *Hoxa2* null mice did not exhibit a change in total glutathione levels compared to wild-type embryos (Fig. 4.1.4a).

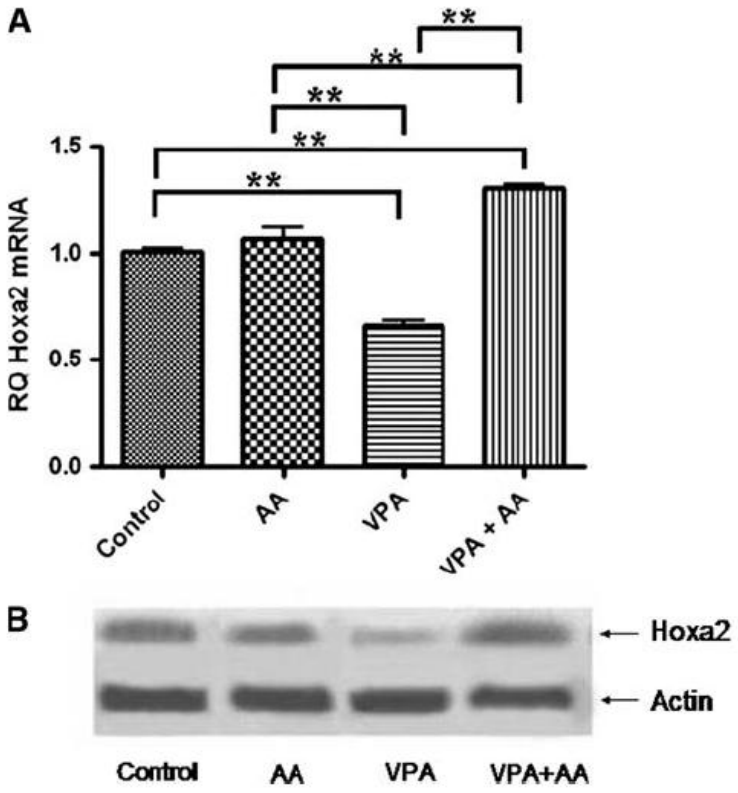

Fig. 4.1.7 Relative quantitative expression of *Hoxa2* in cultured mouse embryos as determined by quantitative real-time RT-PCR using TaqMan primers and probes (**A**). Western blot analysis of Hoxa2 protein in cultured embryos (**B**). Control; AA, treated with 1000 µg/mL [5 mM] L-ascorbic acid; VPA, treated with 400 µg/mL [2.8 mM] of valproic acid; VPA + AA, pretreated with 1000 µg/mL L-ascorbic acid prior to addition of 400 µg/ml of valproic acid. Embryos were cultured for 48 h. *Bars* represents mean ± SD, N = 3–4. ** Represents a significance $P < 0.01$ between bars indicated by *brackets*.

4.1.8 Effect of VPA on telomerase activity and telomere length *in vitro* and *in vivo*

Since it is known that telomerase activity is impacted by oxidative stress (Borras et al, 2004), we then determined the telomerase activity in VPA treated samples (NIH3T3 fibroblast cells and mouse embryos). A real-time PCR based quantitative telomerase detection kit (Allied Biotech, Inc.) was used to measure telomerase activity. Values for 1/Ct (Ct: real-time PCR cycle threshold) obtained are directly proportional to telomerase activity, hence an increase in 1/Ct corresponds to an increase in telomerase activity (Wege, 2003; Lanca, 2009). NIH3T3 cells (5×10^4 cells/cm^2) treated with VPA (6.25 to 100 µg/mL) for 24h showed no difference in telomerase activity compared to respective untreated control or to cells pre-treated with ascorbic acid (5µg/mL) (Fig. 4.1.8a).

In time-pregnant mice administered 400mg/Kg VPA, s.c once daily at E8, E9 and E10, and embryos harvested at E10.5 for analyses there was a significant decrease in 1/Ct value indicating a decrease in telomerase activity (Fig.4.1.8b). Time-pregnant mice pretreated with L-ascorbic acid 250mg/Kg, i.p. just prior to administration of VPA (400 mg/Kg, s.c. at E8, E9 and E10 and embryos harvested after E10.5) also exhibited a significant decrease in 1/Ct values indicating a significant decrease in telomerase activity. Thus, the inhibitory effect of VPA on telomerase activity appeared to be augmented by ascorbic acid.

Administration of ascorbic acid alone (i.p. injected with L-ascorbic acid 250 mg/kg/day) did not significantly change telomerase activity compared to untreated wild-type control embryos (Fig.4.1.8b).

A

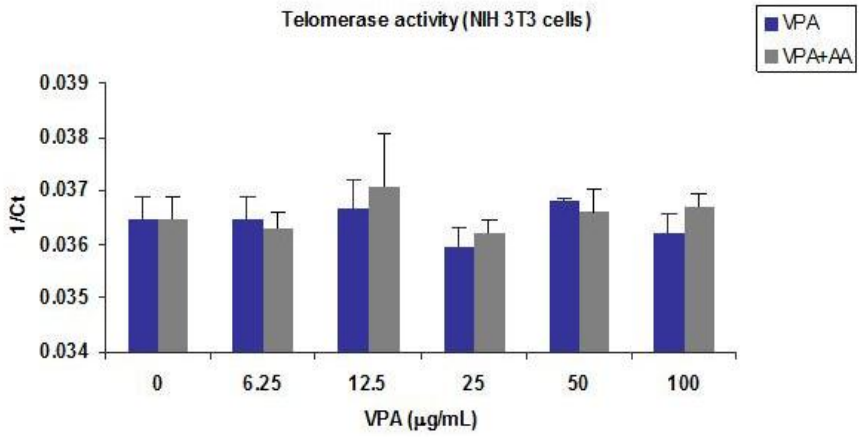

B

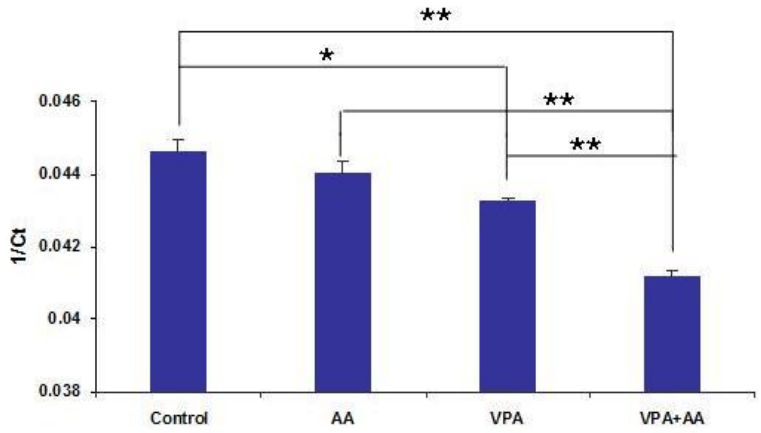

Fig.4.1.8 (a) Effect of VPA and ascorbic acid on telomerase activity (1/Ct) in protein extracts from NIH3T3 cells (1×10^5 cells/cm^2); **(b)** Effect of VPA and ascorbic acid on telomerase activity in developing embryos. NIH3T3 cells were treated with 0 to 100 µg/mL VPA alone, or pretreated with 5 µg/mL ascorbic acid followed by 0 to 100 µg/mL VPA for 24 h. Time-pregnant CD-1 mice (beginning at E8 till E10) received once daily s.c. dose of 400mg/Kg VPA, or i.p. dose of ascorbic acid (250 mg/Kg), or i.p. dose of ascorbic acid followed by the daily s.c dose of VPA at E8.0 to E10. After 6h following the last administration of VPA, E10.5 embryos were dissected from the uteri for further analyses. 1/Ct was used as Y-axis to represent telomerase activity. *Bars* represents mean ± SD. * represents a significance $p \leq 0.05$ and ** represents a significance $p \leq 0.01$ between *bars* indicated by *brackets*. Statistical analysis: one-way ANOVA with Tukey's HSD as post-hoc analysis (*, $p<0.05$, **, $p<0.01$ compared to untreated control cultures) N=3-4.

To assess the impact of VPA on telomere length in NIH3T3 cells and the developing embryos, quantitative real time PCR (SYBR green) was used. Telomere length is presented as relative telomere length, which is the ratio of number of telomere gene copies (quantity) to single copy gene (β-globin) quantity (Cawthon, 2002; McGrath et al., 2007).

Results showed no significant alteration in the mean telomere length in NIH3T3 cells treated with VPA at doses 6.25 to 100 µg/mL (Fig. 4.1.9a). NIH3T3 cells (5×10^4 cells/cm^2) treated with 5 µg/mL ascorbic acid prior to VPA treatment (doses12.5 to 100 µg/mL) for 24 h, however, exhibited a significant increase in telomere length compared to cells treated with VPA alone (Fig. 4.1.9a). Administration of VPA alone (s.c. injection of 400mg/Kg, (daily from E8.0 to E10) to time-pregnant mice decreased telomere length whereas administration of ascorbic acid alone (i.p. injection of 250mg/Kg daily from E8.0 to E10) exhibited an increase in telomere length. However, administration of ascorbic acid followed by VPA did not reverse the effect of VPA on telomere length (Fig.4.1.9b).

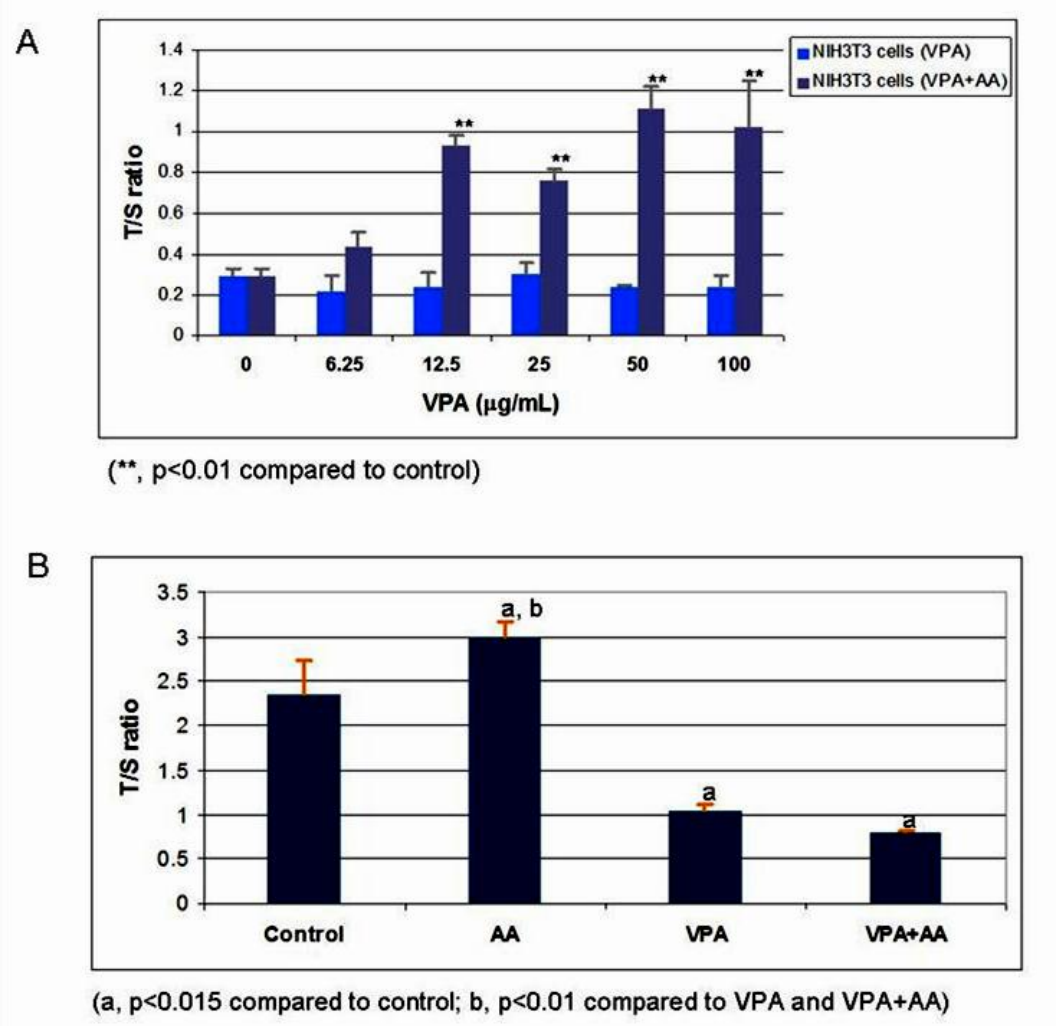

Fig.4.1.9 (a) Effect of VPA and ascorbic acid on telomere length in DNA extracts from NIH3T3 cell cultures; **(b)** Effect of VPA and ascorbic acid on telomere length in DNA extracts from developing embryos (T/S: the ratio of telomere repeat copy number to single gene β-globin copy number). NIH3T3 cells were treated with 0 to 100 µg/mL VPA alone, or treated with 5 µg/mL ascorbic acid followed by 100 µg/mL VPA for 24 h. Time pregnant CD-1 mice (beginning at E8 till E10) received once daily s.c. dose of 400mg/Kg VPA, or i.p. dose of ascorbic acid (250 mg/Kg), or i.p. dose of ascorbic acid followed by the s.c dose of VPA at E8.0 to E10. After 6h following the last administration of VPA, E10.5 embryos were dissected from the uteri for further analyses. Statistical analysis: one-way ANOVA with Tukey's HSD as post-hoc analysis (a, $p<0.05$ compared to untreated control; b, $p<0.01$ compared to VPA and VPA+AA), N=3-4.

4.1.9 Effect of VPA on telomerase gene expression in NIH3T3 cell cultures and in E10.5 mouse embryos

Telomerase gene expression in NIH3T3 cells and developing mouse embryos treated with VPA was quantified using qRT-PCR (Fig. 4.2.0a,b). Initially, NIH3T3 cell cultures incubated with VPA showed a significant decline in *telomerase* gene expression at the lower concentration of 6.25 µg/mL. However, this significance did not hold for VPA doses between 12.5 µg/mL and 50 µg/mL reaching significance only at 100 µg/mL where *telomerase* gene expression was higher than untreated NIH3T3 cells. Treatment with ascorbic acid (5 mM) followed by treatment with VPA (6.25 to 25 µg/mL), did not alter *telomerase* gene expression when compared with VPA treatment alone. However, at VPA doses of 50 and 100 µg/mL, pre-treatment with ascorbic acid significantly inhibited *telomerase* gene expression in NIH3T3 cells (Fig. 4.2.0a). For the *in vivo* study, time-pregnant CD-1 mice (E8 to E10) received once daily s.c. dose of 400mg/Kg VPA or pre-treatment with an i.p dose of ascorbic acid (250 mg/Kg) followed by the s.c dose of VPA (400mg/Kg once daily E8 to E10). After 6h following the last administration of VPA and/or ascorbic acid, E10.5 embryos were dissected from the uteri for qRT-PCR analyses of *telomerase* gene expression. Treatment with VPA alone increased *telomerase* gene expression in mouse embryos compared to saline treated control embryos (Fig. 4.2.0b). However, treatment with ascorbic acid followed by VPA administration, significantly reduced the *telomerase* gene expression (Fig. 4.2.0b).

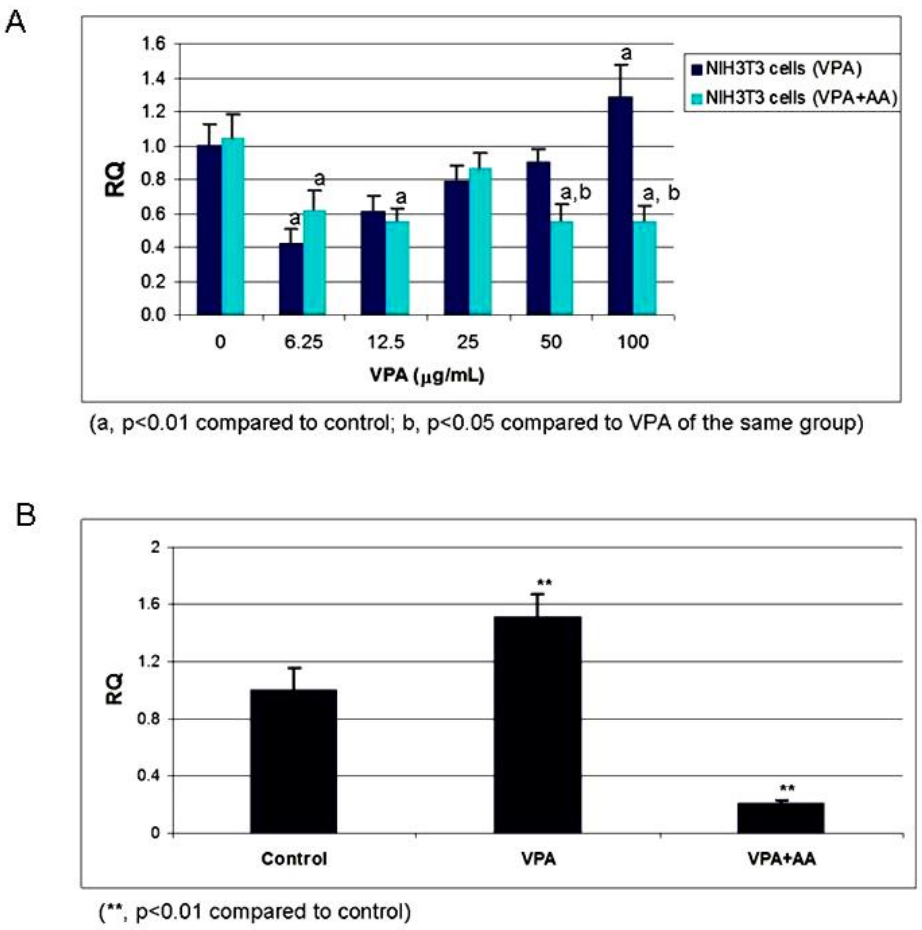

Fig.4.2.0 **(a)** Telomerase expression in control wild-type NIH3T3 cells or in NIH3T3 cells treated with VPA (6.25 to 100µg/mL); Telomerase expression in NIH3T3 cells treated with 5µg/mL [25 µM] ascorbic acid (AA), followed by VPA (6.25 to 100µg/mL). NIH3T3 cells were cultured for 24 h before harvesting for analyses (1×10^5 cells/cm^2). **(b)** Telomerase expression in developing embryos. Time-pregnant CD-1 mice (beginning at E8 till E10) received once daily s.c. dose of 400mg/Kg VPA or i.p dose of ascorbic acid (250 mg/Kg) followed by the s.c dose of VPA at E8.0 to E10, once daily. After 6h following the last administration of VPA and/or ascorbic acid, E10.5 embryos were dissected from the uteri for *telomerase* expression analysis. Statistical analysis: one-way ANOVA with Tukey's HSD as post-hoc analysis (a, $p<0.01$ compared to untreated control, b, $p<0.05$ compared to VPA treated in the same group; *, $p<0.05$, **, $p<0.01$ compared to untreated control cultures), n=3-6.

4.2 Effect of VPA on epigenetic regulation at the *Hoxa2* gene promoter

4.2.1 DNA methylation status at *Hoxa2* gene promoter in NIH3T3 and EG7 cells

Hoxa2 gene expression in NIH3T3 and EG7 cells was determined by RT-PCR (Fig.4.2.1). Results indicate presence of *Hoxa2* expression in NIH3T3 cells but not in in EG7 cells. Based on these finding, NIH3T3 cells with activated *Hoxa2* expression and EG7 cells with silenced *Hoxa2* expression were chosen as *in vitro* model cell lines in this epigenetic study.

To determine DNA methylation status at the *Hoxa2* promoter in NIH3T3 and EG7 cells, bisulfite specific PCR (BSP) sequencing and methylation specific PCR (MSP) were performed. For both assays, genomic DNA was isolated from the cells and subjected to bisulfite modification, which results in conversion of unmethylated cytosine to uracil, and subsequently to thymidine following PCR amplification (Fig. 3.3). BSP primers were designed outside CpG regions at the selected promoter region. Three pairs of primers were designed for the 3 CpG regions and sequences amplified from -1301 bp to -1176 bp, -1133 bp to -919 bp and -620 bp to -277 bp (Fig. 4.2.2a). Amplification using MSP was performed using two sets of primers, one set for unmethylated DNA and the other for methylated DNA. Results show that DNA at the three CpG islands (CpG islands 1 to 3) of *Hoxa2* promoter in EG7 cells is methylated, and same regions in NIH3T3 cells is primarily unmethylated (Fig. 4.2.2b). This was further confirmed by BSP sequencing (Fig. 4.2.3 and schematic Fig. 4.2.4). The highly unmethylated and methylated DNA at *Hoxa2* promoter correlates with the level of *Hoxa2* gene expression in the two cell lines. As shown in Fig. 4.2.1, *Hoxa2* gene is expressed in NIH3T3 cells, whereas *Hoxa2* mRNA transcript level is not detectable in EG7 cells.

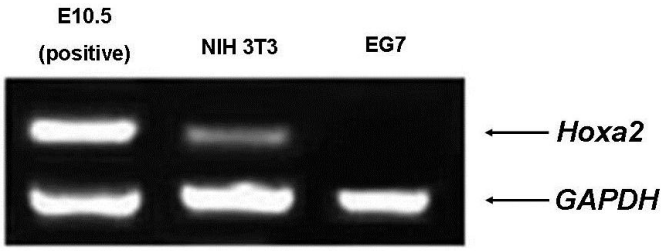

Fig.4.2.1. RT-PCR detection of *Hoxa2* gene expression in E10.5 embryo (positive control), NIH3T3 cells and EG7 cells. *Hoxa2* expression is not detectable in EG7 cells.

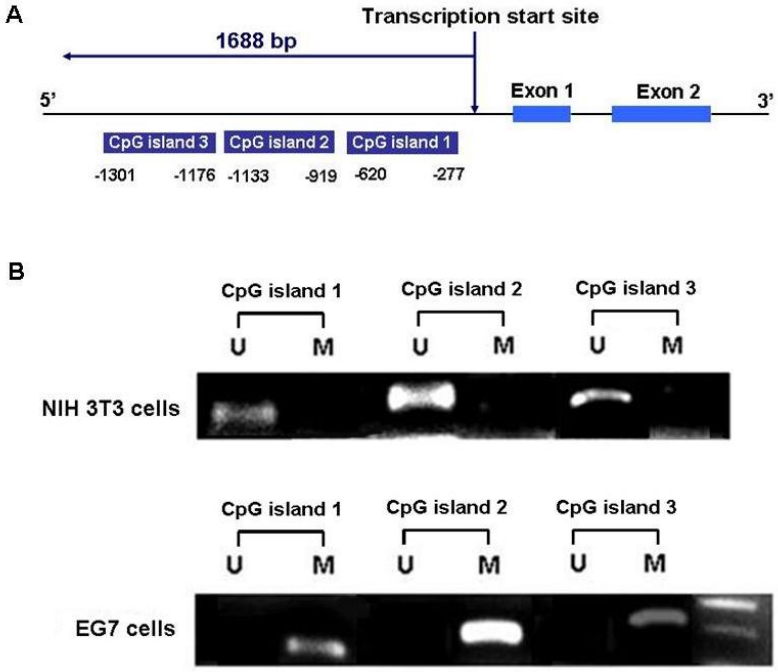

Fig.4.2.2 DNA methylation analysis at the *Hoxa2* gene promoter in NIH3T3 and EG7 cells (cells were harvested at 1×10^5 cells/cm^2). **(A)** Schematic diagram of CpG islands at *Hoxa2* gene promoter; **(B)** Methylation specific PCR at the *Hoxa2* gene promoter region (CpG islands 1-3) in NIH3T3 cells show unmethylated (U) DNA and in EG7 cells show methylated (M) DNA. Primers Msp-kx3-MF, Msp-kx3-MR, Msp-kx3-UF, Msp-kx3-UR were used for PCR amplification within CpG island 1; Primers Msp-kx2-MF, Msp-kx2-MR, Msp-kx2-UF, Msp-kx2-UR were used for PCR amplification within CpG island 2; Primers Msp-kx1-MF, Msp-kx1-MR, Msp-kx1-UF, Msp-kx1-UR were used for PCR amplification within CpG island 3 (see Methods section Table 5.1 for primer sequence).

(A) CpG island 1

NIH 3T3 cells

TGTTAGGTTGAGGTGTTTAAATGATTTG
TGAGGTGTGAGGTGTTTTTTTGATAGTT
TTAAATAATGTGTGGAGTGTGTGGGGGA
GGTAGAGGGTAGTTATTGGTGGGATGGT
AGTAGGGTTTATATGTATATACTTATAT
ATATACTTTAGGGAGTATATTAGATTTT
TGTAGATTAGGAGGTAAATAGGTATTTT
TGTTTTTTACGTATTTTTGGGGTATTGT
TATTTATATTTATATATATGTATTTTTG
TTTTGAAAAAAAGTGTAAATAAAGTTTT
GATGGTTTTTAATGAGGTG

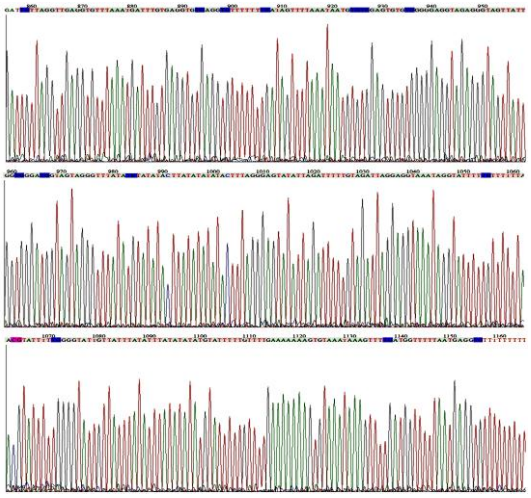

EG7 cells

TGTTAGGTTGAGGTGTTTAAATGATTTG
TGAGGTGCGAGGCGTTTTTTCGATAGTT
TTAAATAATGCGCGGAGTGTGCGGGGGA
GGTAGAGGGTAGTTATTGGCGGGACGGT
AGTAGGGTTTATACGTATATATTTATAT
ATATATTTTAGGGAGTATATTAGATTTT
TGTAGATTAGGAGGTAAATAGGTATTTT
CGTTTTTTACGTATTTTCGGGGTATTGT
TATTTATATTTATATATATGTATTTTTG
TTTTGAAAAAAAGTGTAAATAAAGTTTC
GATGGTTTTTAATGAGGCG

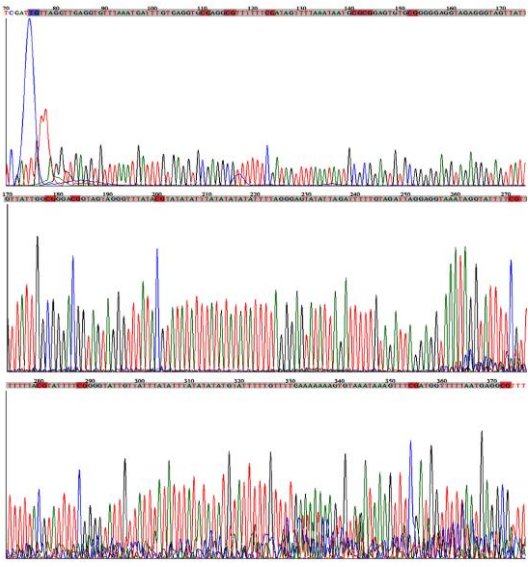

(B) CpG island 2

NIH 3T3 cells

TGAAGGAAGATTAGTAGGTTTTGAGAGT

TGTTTTTTGTTTTTTGTTGTTTGTAGGA

GTTAGATGTAAAGTTGTTGTGGAAAAGT

TGGTTAATAATGGGTTAGGGGTGTAGGT

TTTGGGTTGGATATTAAGAGGAGGTGAG

AGGTTGGGGGGGAGGAGAAGGGGATAGG

ATAGAGTGGGGTGGGGGAAGGAGAGAGG

AAAAAAGGAAAGGAGAATGGAAAGGAGA

GAGGGAGGGAGTG

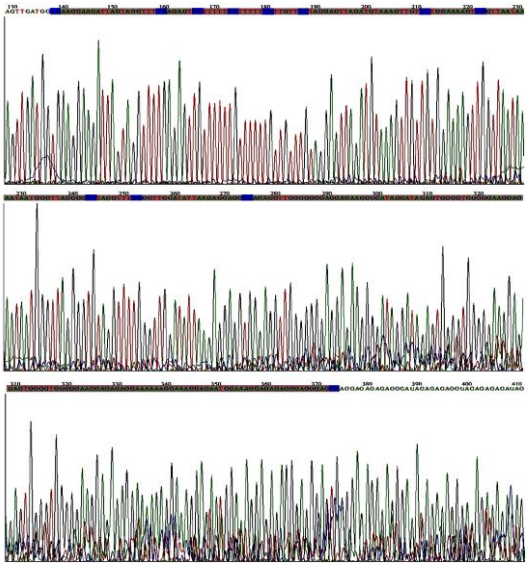

EG7 cells

CGAAGGAAGATTAGTAGGTTTCGAGAGT

CGTTTTTCGTTTTTCGTTGTTCGTAGGA

GTTAGATGTAAAGTTGTCGTGGAAAAGT

CGGTTAATAATGGGTTAGGGGCGTAGGT

TTCGGGTTGGATATTAAGAGGAGGCGAG

AGGTTGGGGGGGAGGAGAAGGGGATAGG

ATAGAGTGGGGTGGGGGAAGGAGAGAGG

AAAAAAGGAAAGGAGAAAGGAGAGGAGA

GAGGGAGGGAGCG

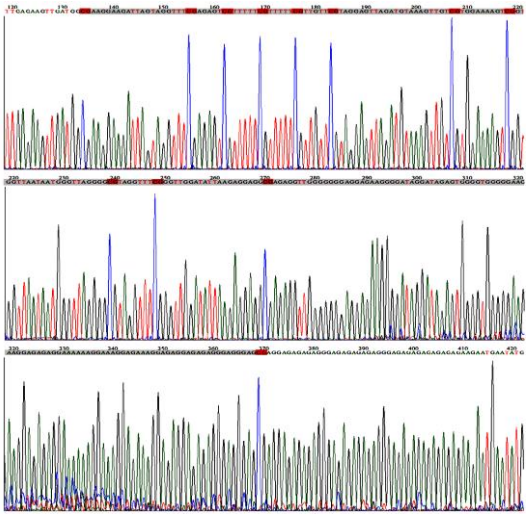

(C) CpG island 3

NIH 3T3 cells

TGGAAATATTTATTGTATTTGAGTTTTA

TGGGTATGAAATTTAGAGTGTTAGGAGT

TGTATGAGTTTGTTTGGGATGGTATTGT

TTTGGTTGGTTGTTGTTTAGGTTATG

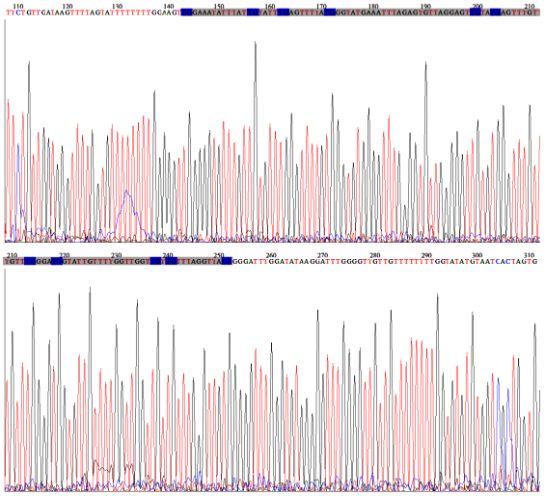

EG7 cells

CGGAAATATTTATCGTATTCGAGTTTTA

CGGGTATGAAATTTAGAGTGTTAGGAGT

TGTACGAGTTTGTTCGGGACGGTATTGT

TTTGGTTGGTCGTCGTTTAGGTTACG

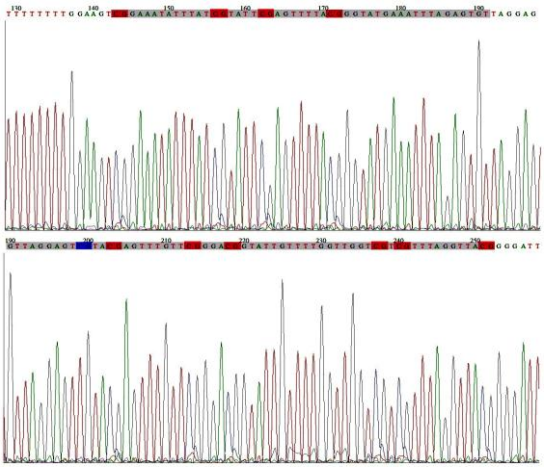

Fig. 4.2.3 DNA sequencing following bisulfite specific PCR at the *Hoxa2* gene promoter region in NIH3T3 cells and EG7 cells (see Appendix for original DNA sequencing chromatograms). Cells were harvested at 1×10^5 cells/cm^2. **(A)** CpG island 1, **(B)** CpG island 2, and **(C)** CpG island 3. Primers Bsp_kx5 and Bsp_kx6 were used for PCR amplification within CpG island 1; Primers Bsp_kx3 and Bsp_kx4 were used for PCR amplification within CpG island 2; Primers Bsp_kx1 and Bsp_kx2 were used for PCR amplification within CpG island 3 (see Methods Section, Table 5.1 for primer sequence).

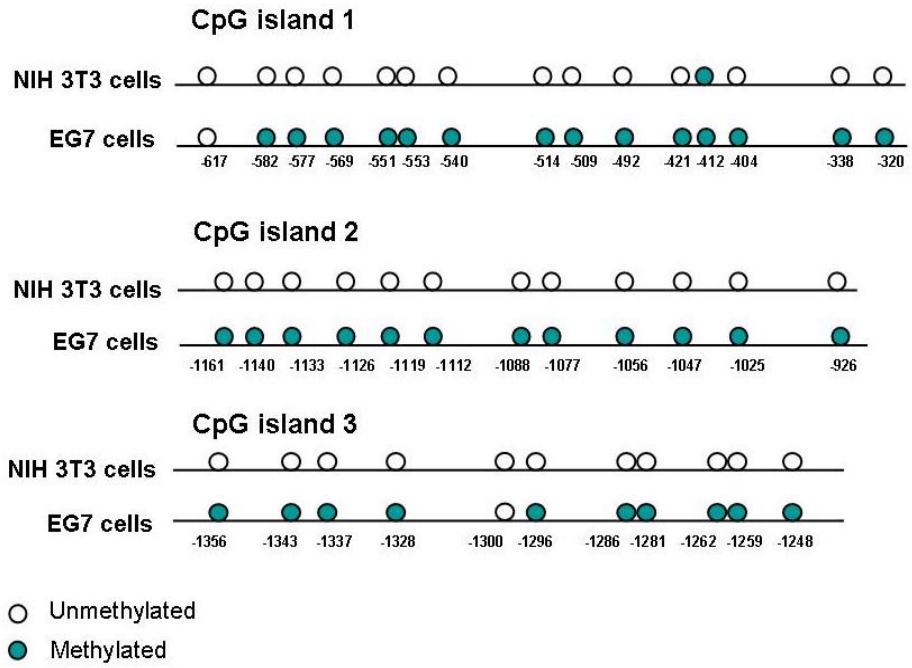

Fig.4.2.4 Schematic diagram of DNA methylation status at the three CpG islands of the *Hoxa2* gene promoter in NIH3T3 and EG7 cells after BSP sequencing (see DNA sequence above in Fig. 4.2.3)

4.2.2 Effect of VPA on *Hoxa2* gene expression and DNA methylation status at the *Hoxa2* promoter in NIH3T3 cells

Real-time RT-PCR was used to determine the effect of VPA on *Hoxa2* gene expression in NIH3T3 cells (Fig. 4.2.5). *Hoxa2* expression was measured at VPA doses (6.25, 12.5, 25, 50 and 100 µg/mL) in NIH3T3 cell cultures and were within VPA's therapeutic range (50-100 µg/mL) [0.35-0.70 mM] (Duenas-Gonzalez et al., 2008). *Hoxa2* expression decreased in a dose dependent manner in NIH3T3 cells with increasing doses of VPA. A significant decrease in *Hoxa2* gene expression was observed starting at VPA concentration of 12.5 µg/mL.

Exposure to VPA in NIH3T3 cells induced an increasing number of CpG sites to be methylated at *Hoxa2* promoter on CpG island 1, a region closest to the transcription start site (Fig. 4.2.6a). Differential DNA methylation level was subsequently measured at all ten CpG sites within CpG island 1 at *Hoxa2* gene promoter: CpG^{-617}, CpG^{-582}, CpG^{-577}, CpG^{-569}, CpG^{-551}, CpG^{-553}, CpG^{-540}, CpG^{-514}, CpG^{-509} and CpG^{-492}. Pyrosequencing data (Fig. 4.2.7) showed

VPA increased the percent of DNA methylation at CpG^{-551}, CpG^{-553}, CpG^{-540}, CpG^{-509} and CpG^{-492} (see Fig. 4.2.14 for comparison of pyrosequencing data in embryos).

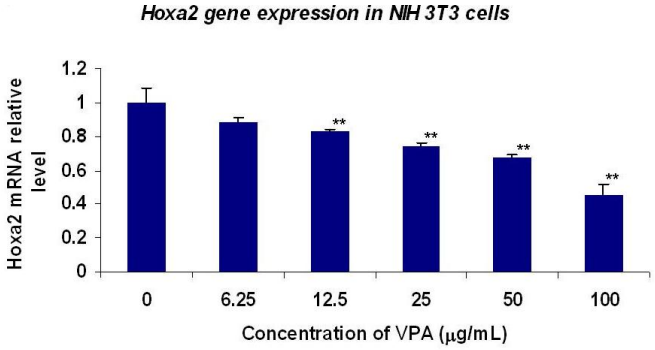

Fig. 4.2.5 Real-time RT-PCR of *Hoxa2* gene expression in NIH3T3 cells treated with VPA (6.25 μg/mL to 100 μg/mL) for 24 h. Cells were harvested at 1×10^5 cells/cm^2 (*, $p<0.05$; **, $p<0.01$ compared to control).

(A) CpG island 1 of *Hoxa2* promoter

NIH 3T3 cells (wild-type control)

TGTTAGGTTGAGGTGTTTAAATGATTTGTGA
GGTGTGAGGTGTTTTTTTGATAGTTTTAAAT
AATGTGTGGAGTGTGTGGGGGAGGTAGAGGG
TAGTTATTGGTGGGATGGTAGTAGGGTTTAT
ATG

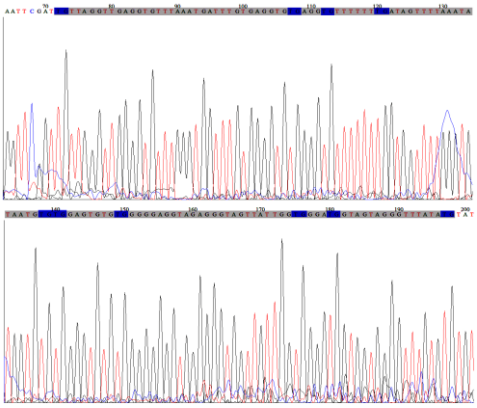

NIH 3T3 cells (treated with 100 μg/mL VPA)

GGTTAGGTTGAGGTGTTTAAATGATTTGTGA
GGTGTGAGGTGTTTTTTTGATAGTTTTAAAT
AATGCGCGGAGTGTGCGGGGGAGGTAGAGGG
TAGTTATTGGTGGGACGGTAGTAGGGTTTAT
ACG

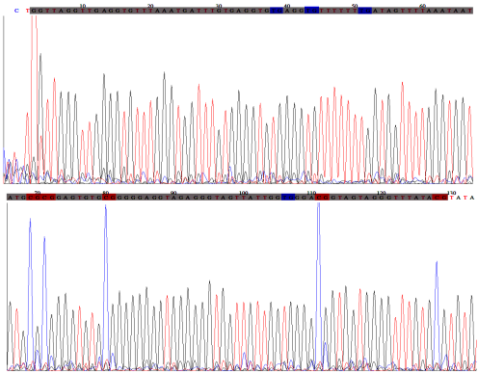

(B)

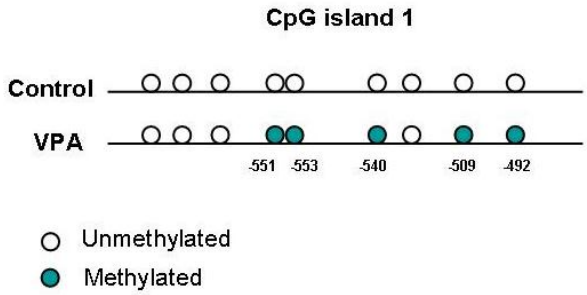

Fig. 4.2.6 (A) DNA sequence of CpG island 1 of *Hoxa2* promoter in wild-type NIH 3T3 cells and in NIH3T3 cells treated with VPA (100μg/mL) for 24 h. Cells were harvested at 1×10^5 cells/cm^2. **(B)** A schematic diagram of DNA methylation sites on CpG island 1 at the *Hoxa2* gene promoter in wild-type control NIH 3T3 cells and in cells treated with VPA following BSP sequencing (see Appendix for original DNA sequencing chromatograms).

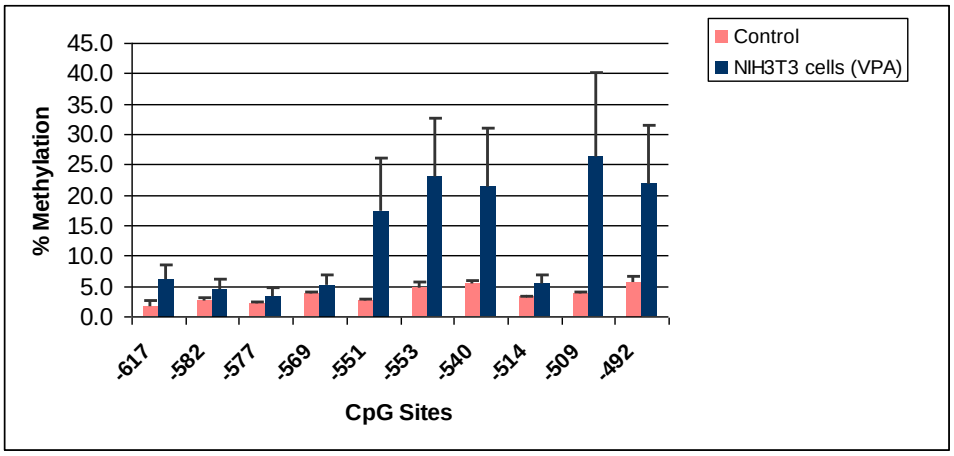

NIH3T3 cells (control)

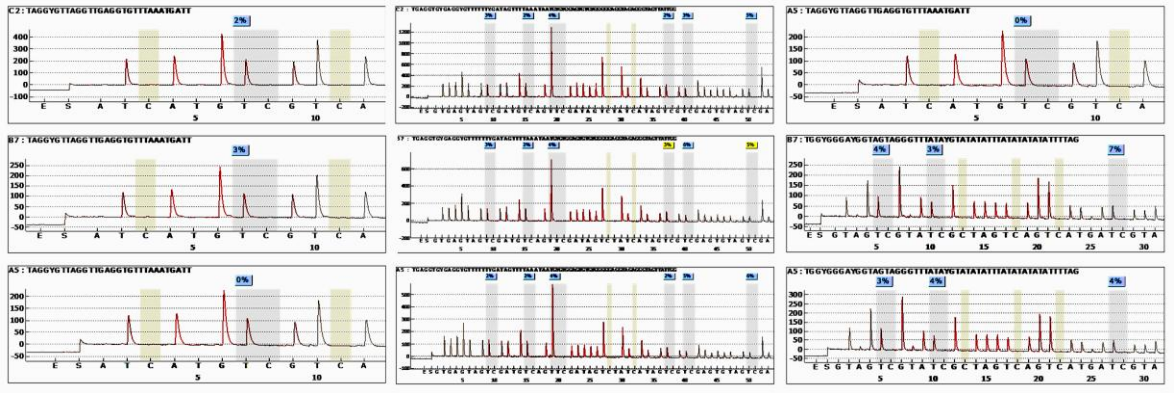

NIH3T3 cells (VPA)

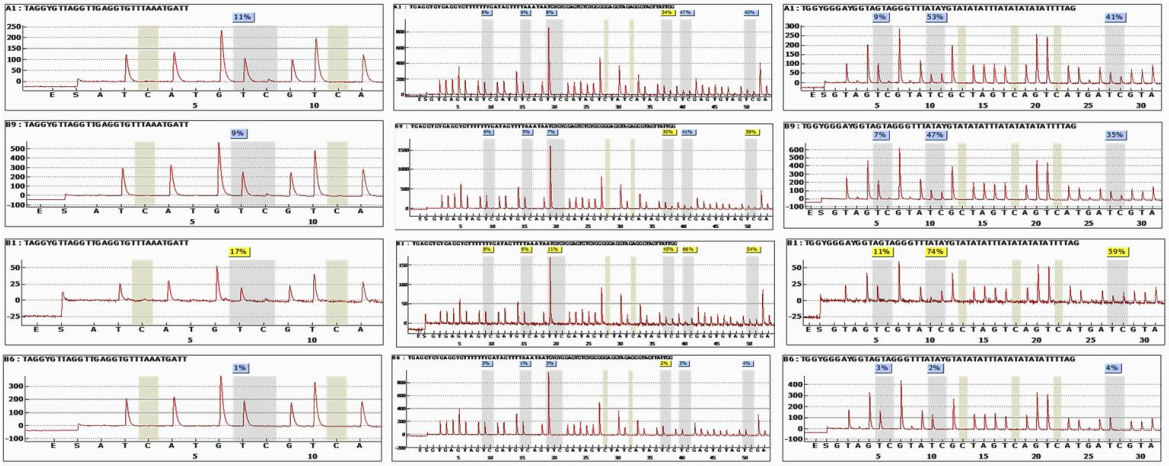

Fig. 4.2.7 Pyrosequencing analysis of DNA methylation on CpG island 1 of the *Hoxa2* promoter in wild-type control NIH3T3 cells and in NIH3T3 cells treated with VPA (100 µg/mL) for 24 h. Cell were harvested at 1×10^5 cells/cm^2. Statistical analysis: one-way ANOVA with Tukey's HSD as post-hoc analysis, n=3-4. Gray shaded boxes show CpG sites. Within the gray shaded boxes C denotes signal from methylated cytosines and T denotes signal from unmethylated cytosines.

4.2.3 Treatment of EG7 cells with VPA or 5-Aza did not induce *Hoxa2* gene expression

To determine if VPA or 5-Aza (5-Aza-2'-deoxycytidine), will inhibit DNA methylation (Christman, 2002) and have an effect on *Hoxa2* gene expression in EG7 cells, VPA at doses of 80 µg/mL and 200 µg/mL, and 5-Aza at doses of 0.23 µg/mL [1 µM], 0.46 µg/mL [2 µM], 0.92 µg/mL [4 µM], 1.84 µg/mL [8 µM] and 2.3 µg/mL [10 µM] were added to EG7 cells. *Hoxa2* gene expression was not detectable in treated cells using RT-PCR (Fig. 4.2.8a). In addition, pyrosequencing analysis of the *Hoxa2* gene promoter (CpG island 1) of EG7 cells treated with VPA or 5-Aza showed no change in DNA methylation status compared to control wild-type EG7 cells (Fig. 4.2.8b).

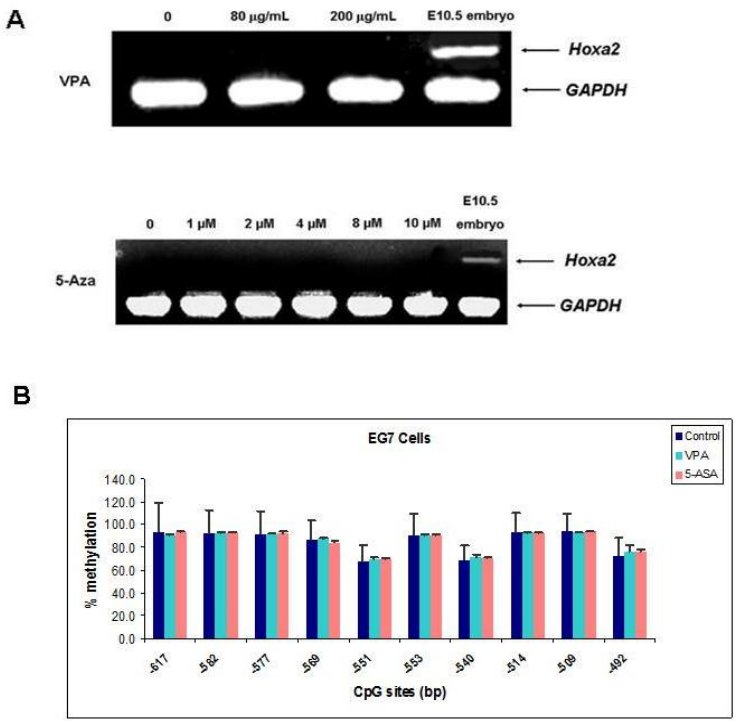

EG7 cells (control)

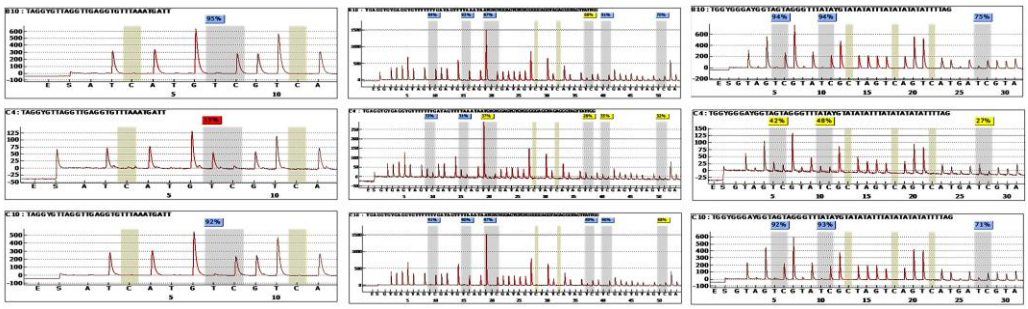

EG7 cells (VPA)

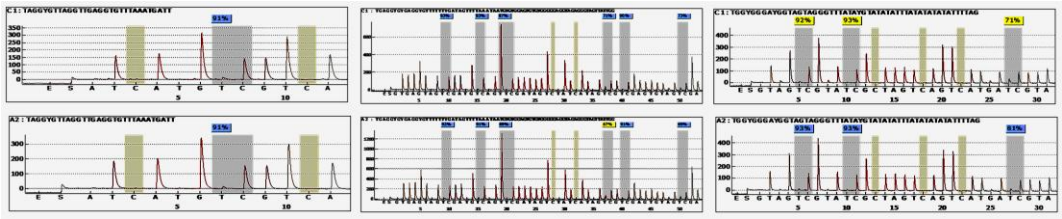

EG7 cells (5-AZA)

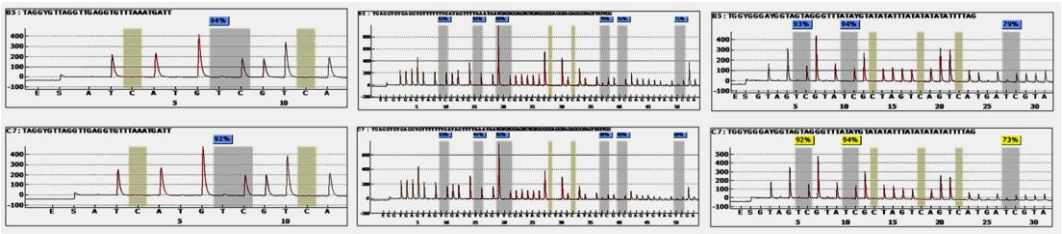

Fig. 4.2.8 (A) *Hoxa2* gene expression was not detected following RT-PCR in EG7 cells treated with VPA (80 and 200 µg/mL for 24 h) and 5-Aza (dose, 0.23 µg/mL [1 µM] to 2.3 µg/mL [10 µM] for 48 h). **(B)** Pyrosequence analysis of DNA methylation status at *Hoxa2* gene promoter (CpG island 1) in control wild-type EG7 cells and in EG7 cells treated with 200 µg/mL VPA and 2.3 µg/mL [10 µM] 5-Aza, respectively. Cells were harvested at $1\times 10^5/cm^2$. Statistical analysis: one-way ANOVA with Tukey's HSD as post-hoc analysis, n=2-3.

4.2.4 DNA methylation status at *Hoxa2* gene promoter in developing mice embryos (E6.5-E10.5)

Hoxa2 gene expression was not detected in E6.5 embryos but was expressed in developing mice embryos at E8.5 and E10.5 (Fig. 4.2.9). This matches with the fact that during embryonic development *Hoxa2* gene is initially expressed in the hindbrain at E8.0 in mice (Prince and Lumsden, 1994b). Bisulfite sequencing of the 3 CpG islands in E6.5 and E8.5 mouse embryos was performed to characterize *Hoxa2* promoter DNA methylation status. Results indicate *Hoxa2* promoter (CpG islands 1-3) in E8.5 embryos remained primarily unmethylated (Fig. 4.2.10), as did CpG islands 2 and 3 in E6.5 embryos. Interestingly, in E6.5 embryos the CpG island 1 (-620 to -277 bp) closest to transcription start site on the *Hoxa2* gene promoter is only partially methylated DNA and primarily at CpG sites -551 bp, -553 bp, -540 bp, -509 bp and -492 bp (Fig. 4.2.11). Subsequent quantification of DNA methylation following pyrosequencing indicated that percent of DNA methylation at the CpG island 1 at all ten CpG sites (-617 bp to -492 bp) in E6.5 and E8.5 embryos are higher than those in E10.5 embryo (Fig. 4.2.12). Since *Hoxa2* gene expression is not detected at E6.5, and is only initially expressed at E8.5 (Fig. 4.2.9), the significantly higher level of DNA methylation of the *Hoxa2* promoter in E6.5 embryos may reflect repression of *Hoxa2* gene expression at this stage in the developing mouse embryo.

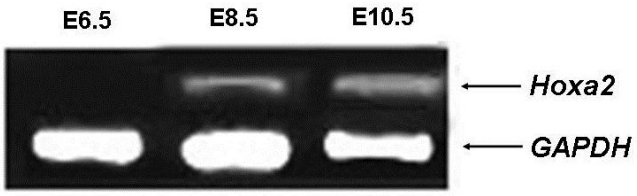

Fig.4.2.9 *Hoxa2* gene expression in developing embryos (E6.5 to E10.5).

(A) CpG island 1

E10.5

GGTTAGGTTGAGGTGTTTAAATGATTTG
TGAGGTGTGAGGTGTTTTTTTGATAGTT
TTAAATAATGTGTGGAGTGTGTGGGGGA
GGTAGAGGGTAGTTATTGGTGGGACGGT
AGTAGGGTTTATACGTATATATTTATAT
ATATATTTTAGGGAGTATATTAGATTTT
TGTAGATTAGGAGGTAAATAGGTATTTT
TGTTTTTTATGTATTTTTGGGGTATTGT
TATTTATATTTATATATATGTATTTTTG
TTTTGAAAAAAAGCCTGACAGAACTGTT
TACCCCAGGATG

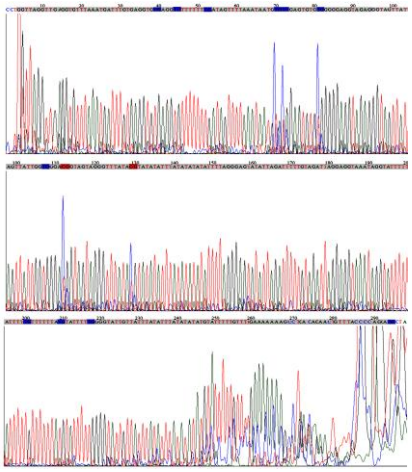

E8.5

TGTTAGGTTGAGGTGTTTAAATGATTTG
TGAGGTGTGAGGTGTTTTTTTGATAGTT
TTAAATAATGTGTGGAGTGTGTGGGGGA
GGTAGAGGGTAGTTATTGGTGGGATGGT
AGTAGGGTTTATATGTATATATTTATAT
ATATATTTTAGGGAGTATATTAGATTTT
TGTAGATTAGGAGGTAAATAGGTATTTT
TGTTTTTTATGTATTTTTGGGGTATTGT
TATTTATATTTATATATATGTATTTTTG
TTTTGAAAAAAAGTGTAAATAAAGTTTT
GATGGTTTTTAATGAGGTG

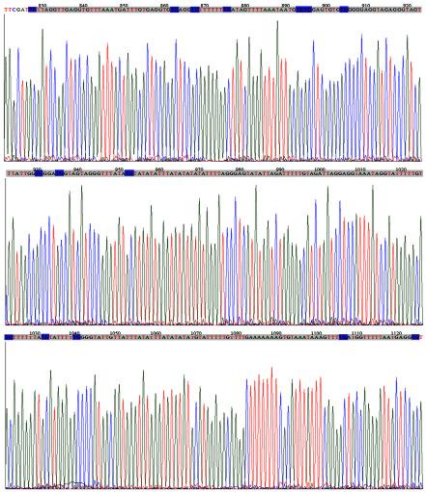

E6.5

TGTTAGGTTGAGGTGTTTAAATGATTTG
TGAGGTGTGAGGTGTTTTTTTGATAGTT
TTAAATAATGCGCGGAGTGTGCGGGGGA
GGTAGAGGGTAGTTATTGGTGGGACGGT
AGTAGGGTTTATACGTATATATTTATAT
ATATATTTTAGGGAGTATATTAGATTTT
TGTAGATTAGGAGGTAAATAGGTATTTT
TGTTTTTTATGTATTTTTGGGGTATTGT
TATTTATATTTATATATATGTATTTTTG
TTTTGAAAAAAAGTGTAAATAAAGTTTT
GATGGTTTTTAATGAGGTG

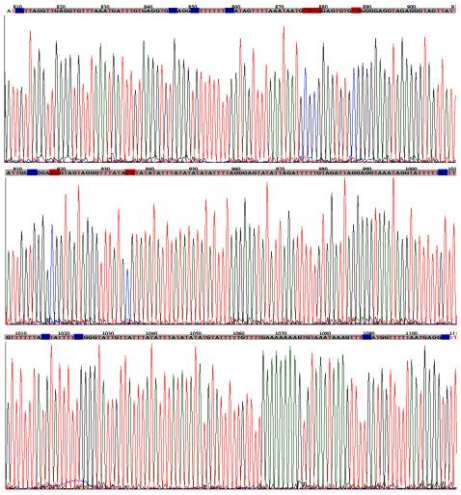

(B) CpG island 2

E8.5

TGAAGGAAGATTAGCAGGTTTTGAGA
GTTGTTTTTTGTTTTTTGTTGTTTGT
AGGAGTTAGATGTAAAGTTGTTGTGG
AAAAGTTGGTTAATAATGGGTTAGGG
GTGTAGGTTTTGGGTTGGATATTAAG
AGGAGGTGAGAGGTTGGGGGGGAGGA
GAAGGGGATAGGATAGAGTGGGGTGG
GGGAAGGAGAGAGGAAAAAAGGAAAG
GAGAAAGGAGAGGAGAGAGGGAGGGA
GTG

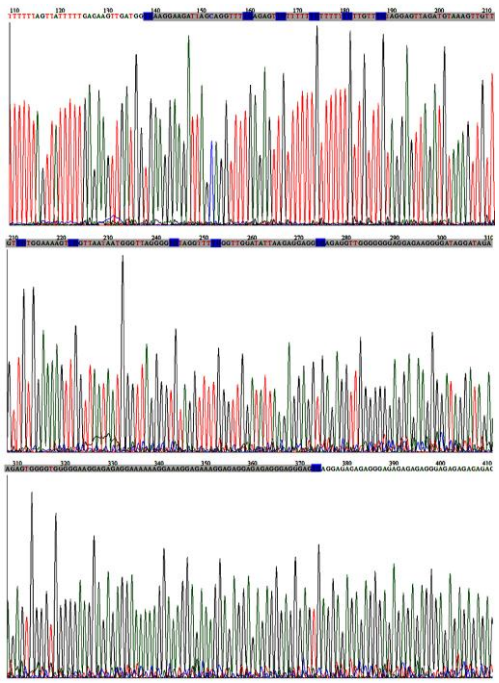

E6.5

TGAAGGAAGATTAGTAGGTTTTGAGA
GTTGTTTTTTGTTTTTTGTTGTTTGT
AGGAGTTAGATGTAAAGTTGTTGTGG
AAAAGTTGGTTAATAATGGGTTAGGG
GTGTAGGCTTTGGGTTGGATATTAAG
AGGAGGTGAGAGGTTGGGGGGGAGGA
GAAGGGGATAGGATAGAGTGGGGTGG
GGGAAGGAGAGAGGAAAAAAGGAAAG
GAGAAAGGAGAGGAGAGAGGGAGGGA
GTG

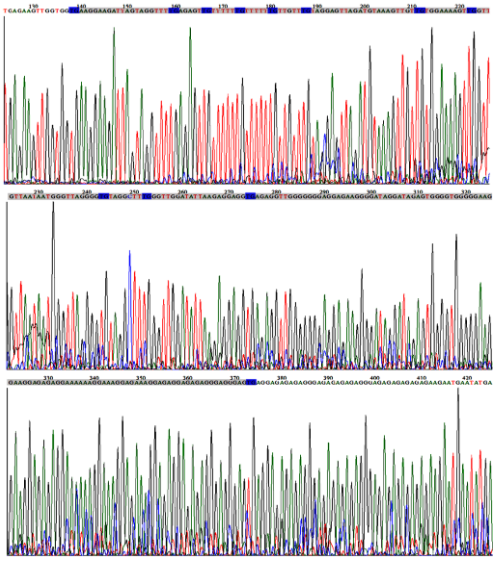

(C) CpG island 3

E8.5

TGGAAATATTTATTGTATTTGAGTTTTA
TGGGTATGAAATCTAGAGTGCCAGGAGT
TGTATGAGTTTGTTTGGGATGGTATTGT
TTTGGTTGGTTGTTGTTTAGGTTATG

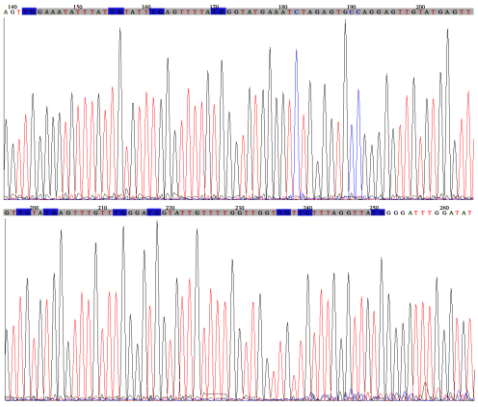

E6.5

TGGAAATATTTATTGTATTTGAGTTTTATT
GGGTATGAAATTTAGAGTGTTAGGAGTTG
TATTGAGTTTGTTTTGGGATTGGTATTGTTTT
GGTTGGTTTGTTTTGTTTAGGTTATTG

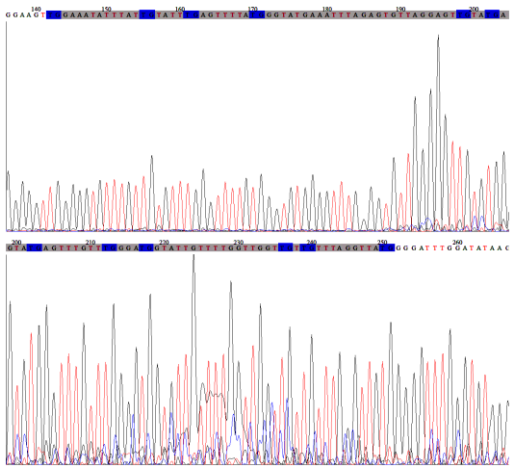

Fig. 4.2.10 DNA methylation status of *Hoxa2* gene promoter (CpG islands 1-3) in E6.5, E8.5 and E10.5 embryos. **(A)** CpG island 1, **(B)** CpG island 2, and **(C)** CpG island 3. The primers used in embryos were the same BSP primers used in NIH 3T3 cells (see Methods Section, Table 5.1 for primer sequence).

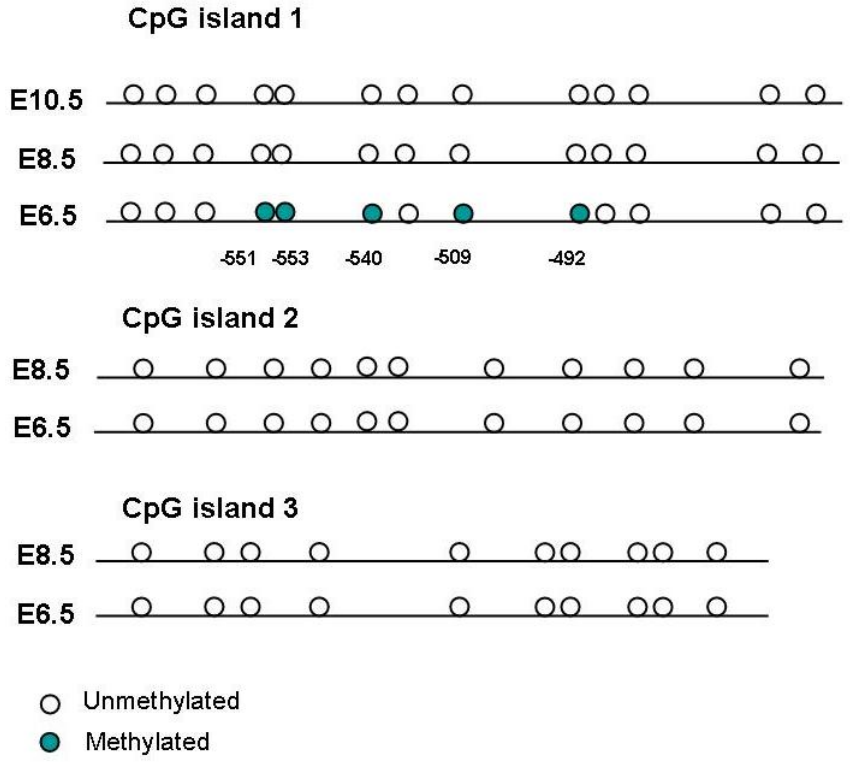

Fig. 4.2.11 Schematic diagram of DNA methylation status at *Hoxa2* gene promoter in embryos at E6.5, E8.5 and E10.5

E6.5

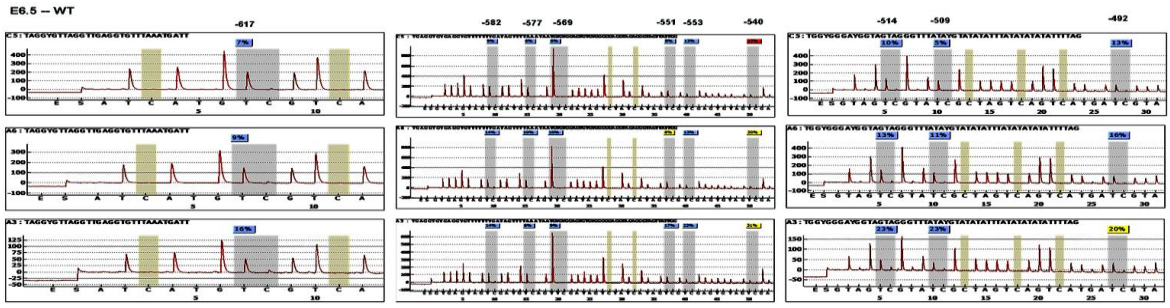
E6.5 – WT
-617
-582
-577
-569
-551
-553
-540
-514
-509
-492

E8.5

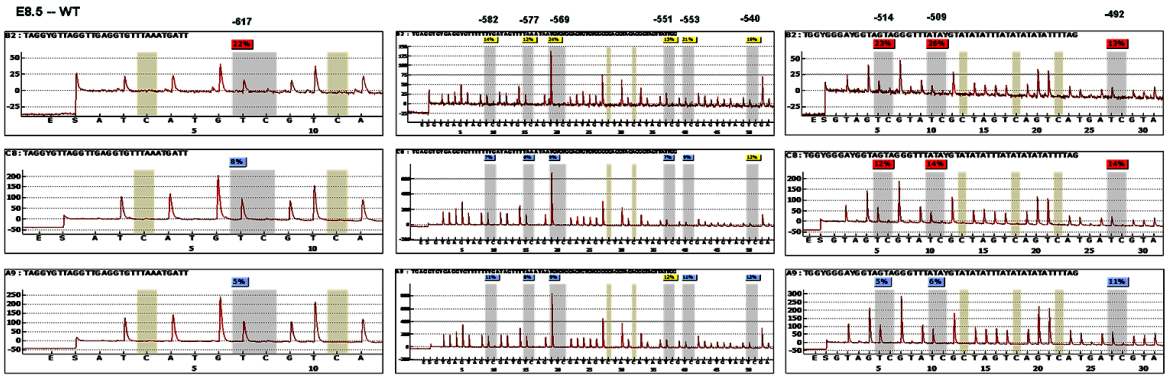
E8.5 – WT
-617
-582
-577
-569
-551
-553
-540
-514
-509
-492

E10.5

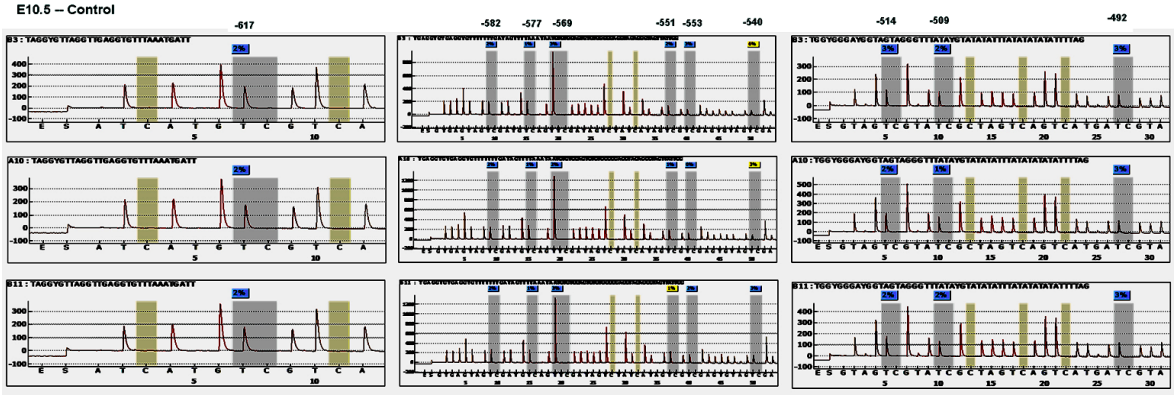
E10.5 – Control
-617
-582
-577
-569
-551
-553
-540
-514
-509
-492

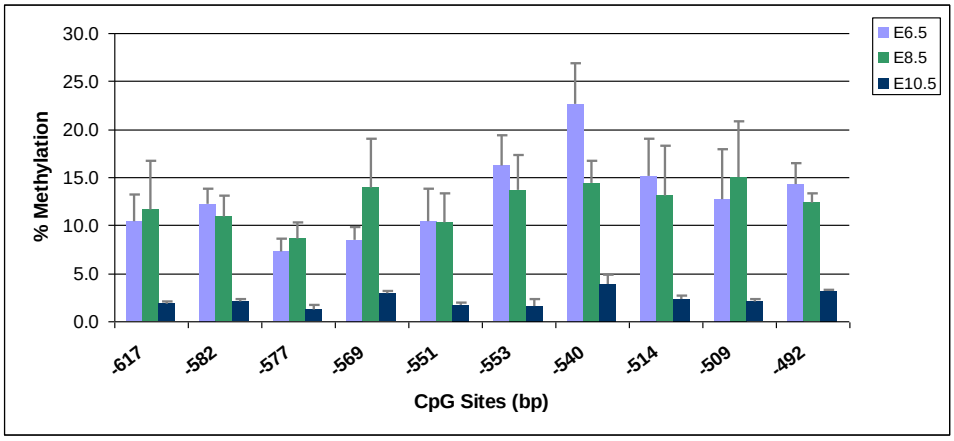

Fig.4.2.12 Pyrosequence analysis of DNA methylation on CpG island 1 of the *Hoxa2* gene promoter in developing embryos (E6.5, E8.5 and E10.5) (statistical analysis: one-way ANOVA with Tukey's HSD as post-hoc analysis, N=3)

4.2.5 Effect of VPA on DNA methylation at the *Hoxa2* promoter in E10.5 mouse embryos

Hoxa2 gene expression is down regulated in mouse embryos cultured *in vitro* after treatment with VPA (Table 4.1.4). Bisulfite specific PCR sequencing results reveal that in developing embryos treated with VPA, increased DNA methylation at the *Hoxa2* gene promoter within CpG island 1 was observed at some CpG sites (Fig. 4.2.13a). Interestingly, the VPA-induced methylation on CpG sites at CpG^{-551}, CpG^{-553}, and CpG^{-540} were among those found methylated in developing mouse embryos at E6.5 (Fig. 4.2.13b). These results demonstrate that the inhibition of *Hoxa2* gene expression in embryos treated with VPA could be due to increased DNA methylation at *Hoxa2* gene promoter. Similarly, pyrosequencing data also revealed an increase in percent of DNA methylation in embryos treated with VPA in all CpG sites within CpG island 1 (Fig. 4.2.14).

(A) CpG island 1 of *Hoxa2* promoter

E10.5 (control)

GGTTAGGTTGAGGTGTTTAAATGATTTGTGA
GGTGTGAGGTGTTTTTTTGATAGTTTTAAAT
AATGTGTGGAGTGTGTGGGGGAGGTAGAGGG
TAGTTATTGGTGGGACGGTAGTAGGGTTTAT
ACG

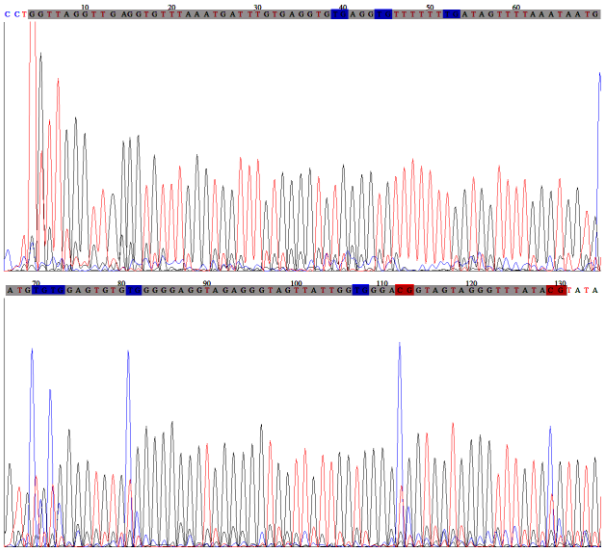

E10.5 (VPA treated)

GGTTTAAATGATTTGTGAGGTGTGAGGT
GTTTTTTTGATAGTTTTAAATAATGCGC
GGAGTGTGCGGGGGAGGTAGAGGGTAGT
TATTGGTGGGACGGTAGTAGGGTTTATA
CG

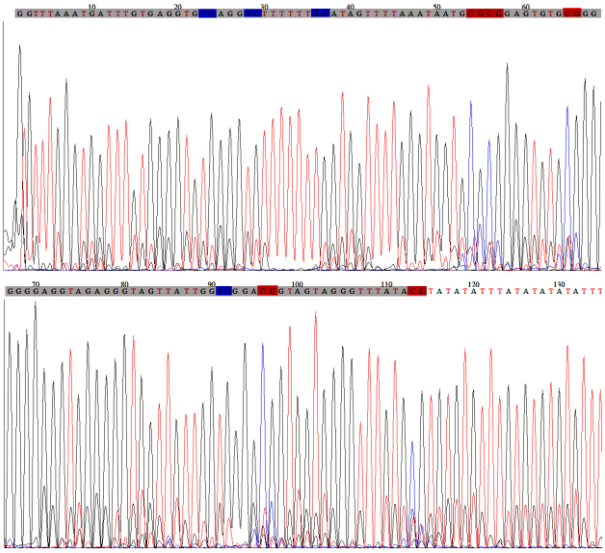

(B)

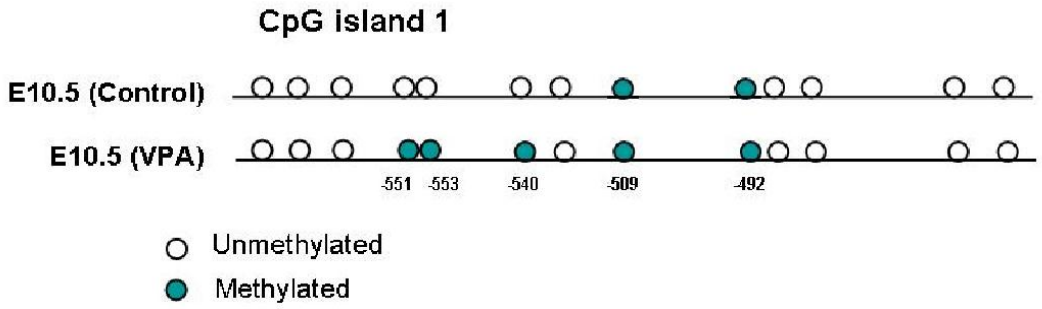

Fig. 4.2.13

(A) DNA sequence of CpG island 1 indicating the CpG sites in wild-type E10.5 embryo and in E10.5 embryos treated with VPA. Time-pregnant mice were administered s.c 400 mg/kg VPA once daily between E8 and E10 and embryos isolated for DNA sequence analysis at E10.5. **(B)** Schematic diagram of DNA methylation status at *Hoxa2* gene promoter (CpG island 1) in wild-type E10.5 developing embryo and in E10.5 embryo treated with VPA.

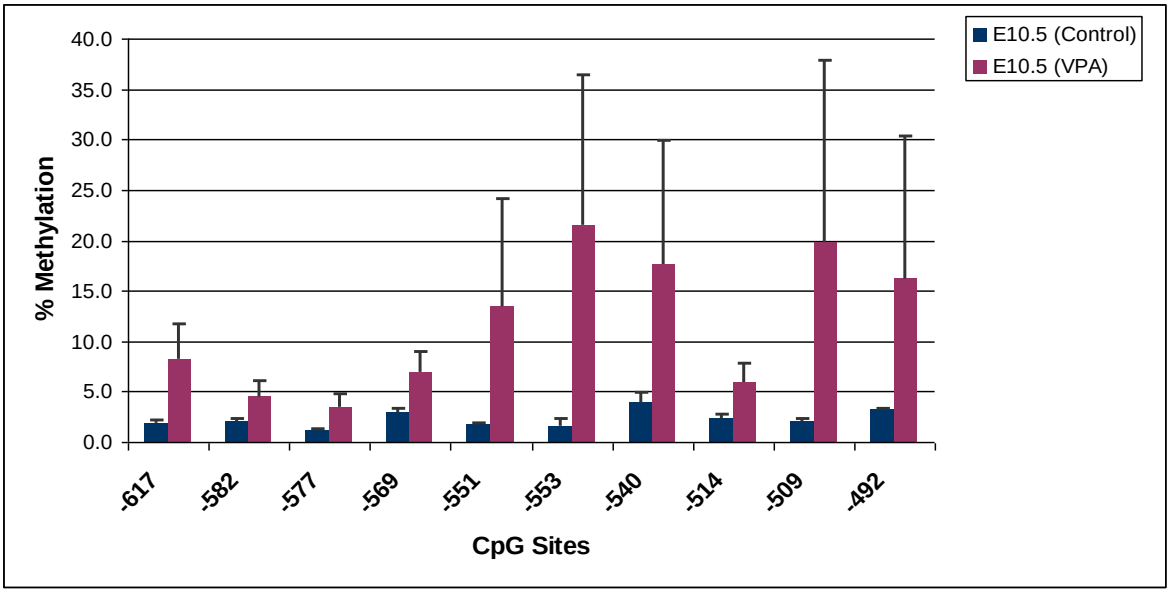
E10.5 (Control)
E10.5 (VPA)
% Methylation
40.0
35.0
30.0
25.0
20.0
15.0
10.0
5.0
0.0
-617
-582
-577
-569
-551
-553
-540
-514
-509
-492
CpG Sites

E10.5 (Control)

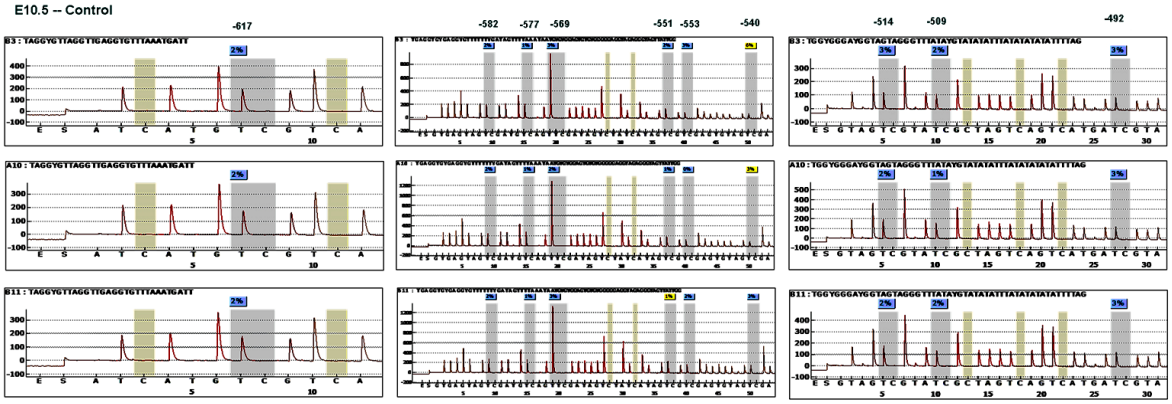

E10.5 (VPA)

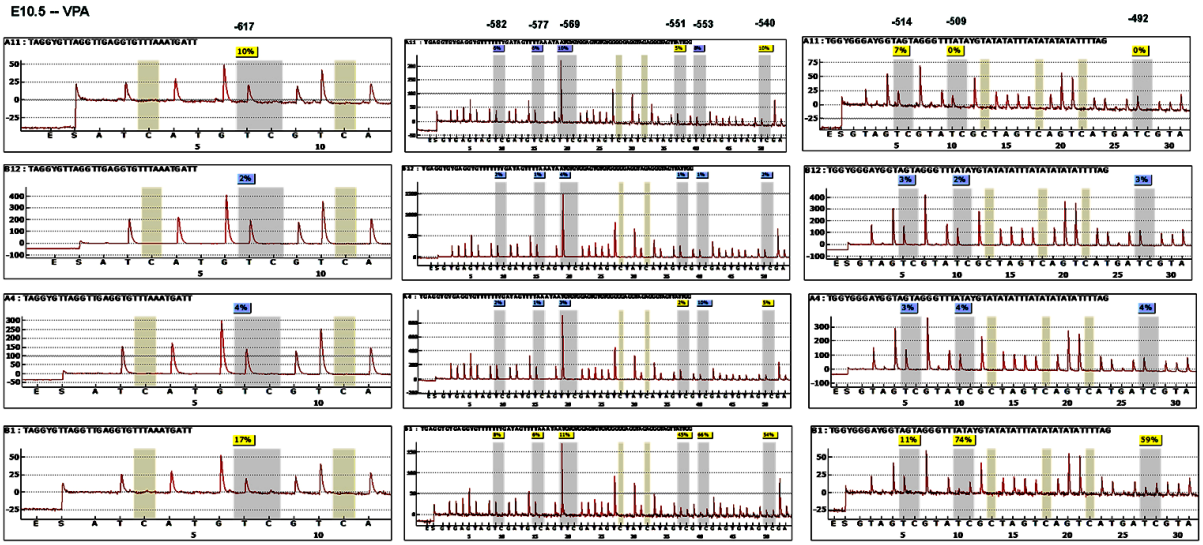

Fig. 4.2.14 Pyrosequence analysis of DNA methylation at *Hoxa2* gene promoter (CpG island 1) in a wild-type control E10.5 embryo and in a E10.5 embryo treated with VPA. Time-pregnant mice were administered s.c. 400 mg/kg VPA once daily between E8 and E10 and the embryos analyzed at E10.5 (Statistical analysis: one-way ANOVA with Tukey's HSD as post-hoc analysis, N=3-4).

4.2.6 Effect of VPA on DNA methyltransferase binding capacity at *Hoxa2* promoter in NIH3T3 cells and in E10.5 mouse embryos

DNA methyltransferase 1 (Dnmt1) binding on *Hoxa2* gene promoter (CpG island 1) was evaluated in NIH3T3 cells and in E10.5 embryos using Quantitative Chromatin Immunoprecipitation PCR (qChIP-PCR) (Fig. 4.2.15). Treatment with VPA (50 µg/mL and 100 µg/mL) resulted in higher level of Dnmt1 occupied at the *Hoxa2* gene promoter (CpG island 1) compared to wild-type untreated NIH3T3 cells (Fig. 4.2.15a). Results also reveal higher enrichment of Dnmt1 at the *Hoxa2* promoter (CpG island 1) in embryos treated with VPA at E10.5 (Fig. 4.2.15b). The increased binding capacity of Dnmt1 protein at the *Hoxa2* promoter region (CpG island 1) corresponds with increased DNA methylation at the *Hoxa2* gene promoter (Fig. 4.2.6 and Fig. 4.2.13).

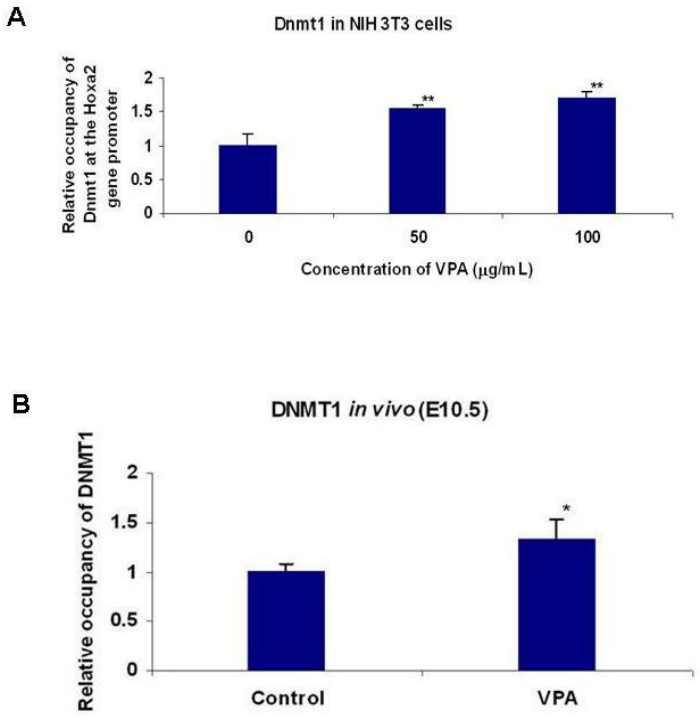

Fig. 4.2.15 qChIP-PCR assay of Dnmt1 binding at the *Hoxa2* gene promoter (CpG island 1) in NIH 3T3 cells and E10.5 mouse embryos treated with VPA. NIH 3T3 cells were exposed to VPA (50 and 100 µg/mL) for 24 h. Cells were harvested at 1×10^5 cells/cm^2. Time-pregnant mice were administered a daily of dose of VPA (s.c. 400 mg/kg) between E8 and E10 and the embryos were isolated for analyses at E10.5. Primers Klx 3 and Klx 3-1 (see Methods section, Table 5.1 for primer sequence) were used for qChIP-PCR of Dnmt1 within the CpG island 1 of the *Hoxa2* promoter (*, $p<0.05$; **, $p<0.01$).

4.2.7 Ascorbic acid decreased DNA methylation at *Hoxa2* gene promoter in NIH3T3 cells treated with VPA

Differential DNA methylation was measured at all ten CpG sites within the CpG island 1 close to transcription start site at the *Hoxa2* gene promoter: CpG^{-617}, CpG^{-582}, CpG^{-577}, CpG^{-569}, CpG^{-551}, CpG^{-553}, CpG^{-540}, CpG^{-514}, CpG^{-509}, CpG^{-492}. VPA significantly increased DNA methylation at CpG^{-551}, CpG^{-553}, CpG^{-540}, CpG^{-509}, CpG^{-492} in NIH 3T3 cells (Fig. 4.2.6). Pretreatment with ascorbic acid, however, reversed the higher level of DNA methylation status at these CpG sites induced by VPA (Fig. 4.2.16).

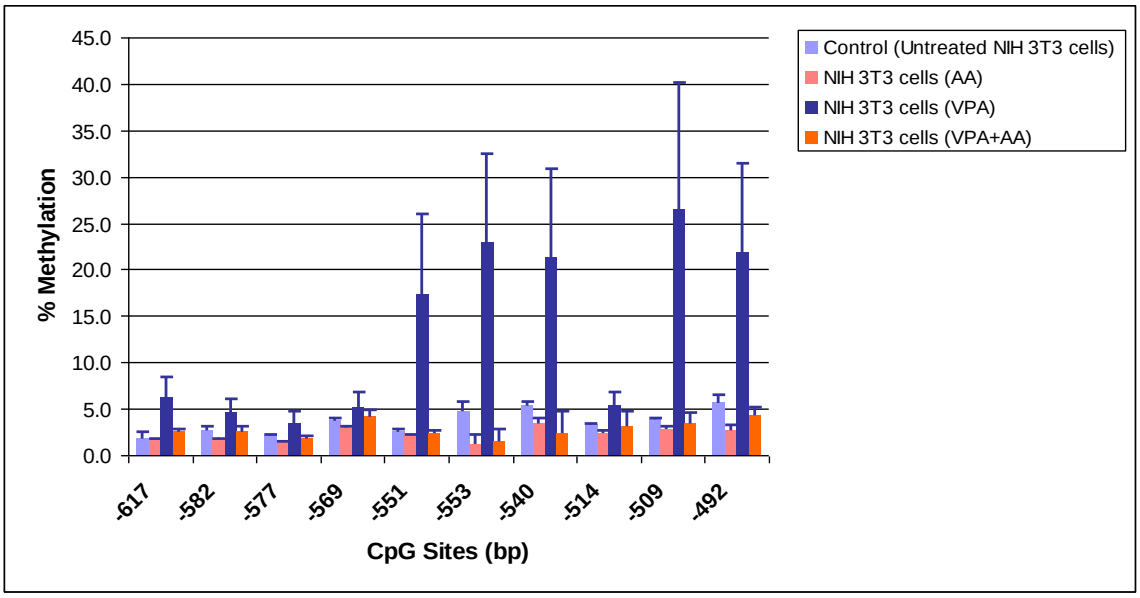

Fig. 4.2.16 Pyrosequence analysis of DNA methylation at *Hoxa2* gene promoter (CpG island 1) in wild-type untreated NIH3T3 cells, NIH3T3 cells treated with 100 µg/mL VPA alone, or 5 µg/mL [25 µM ascorbic acid alone or 5 µg/mL ascorbic acid followed by 100 µg/mL VPA for 24 h. Cells were harvested at $1\times 10^5/cm^2$. Statistical analysis: one-way ANOVA with Tukey's HSD as post-hoc analysis. N=2-4

Control (untreated NIH3T3 cells)

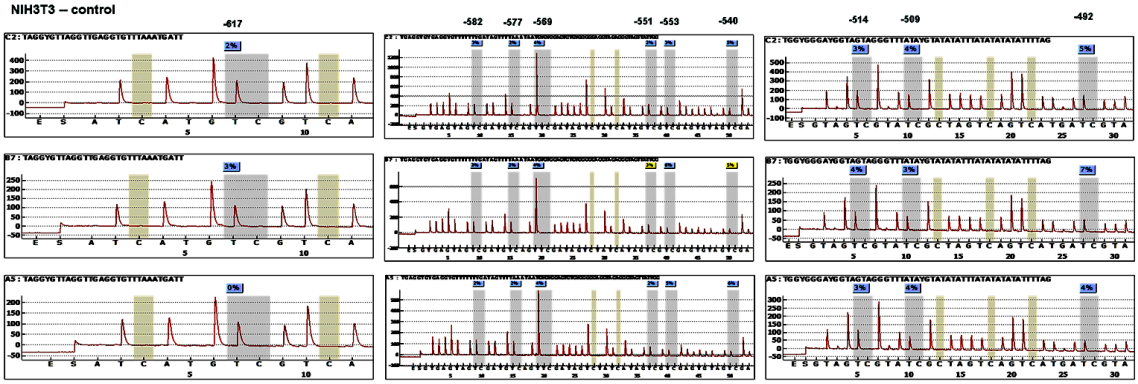

NIH3T3 cells (VPA)

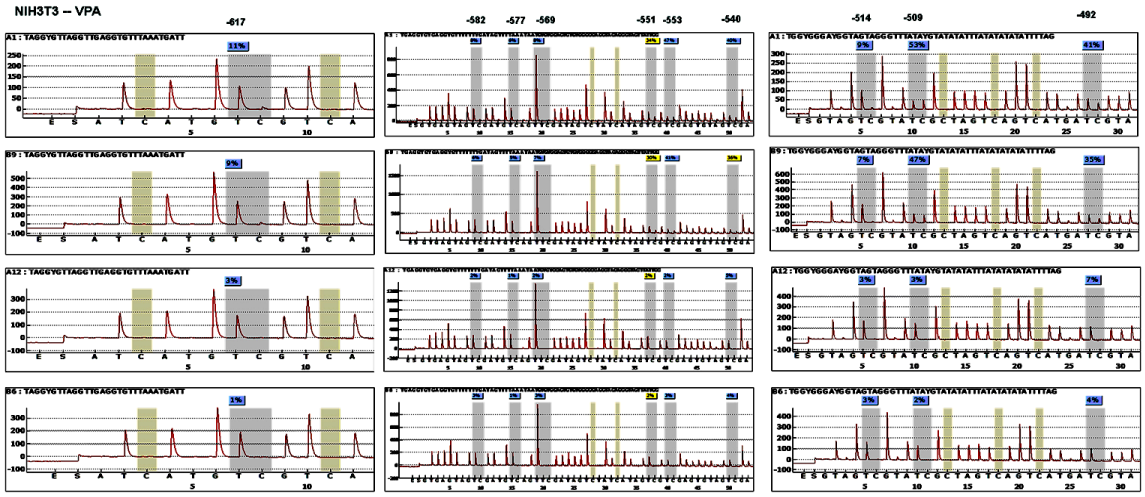

NIH3T3 cells (AA)

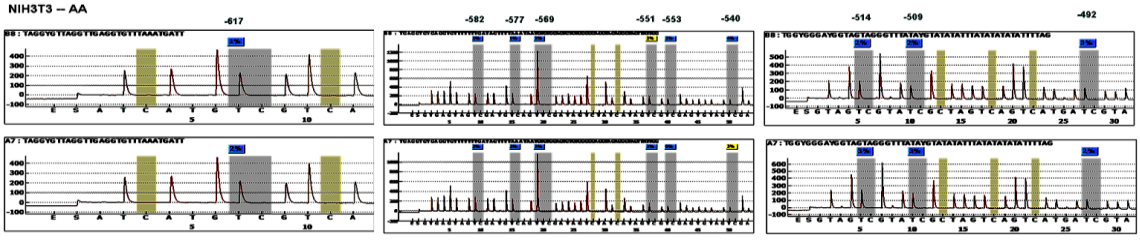

NIH3T3 cells (VPA+AA)

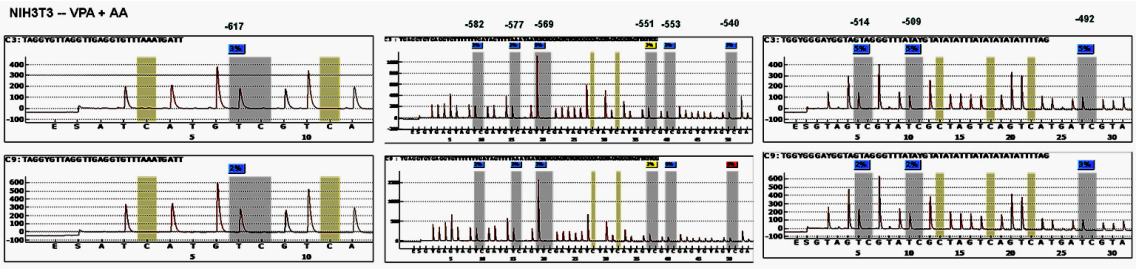

4.2.8 Effect of ascorbic acid on DNA methyltransferase binding capacity on *Hoxa2* promoter in NIH3T3 cells treated with VPA

DNA methyltransferase 1 (Dnmt1) binding on *Hoxa2* gene promoter (CpG island 1) was evaluated in NIH3T3 cells treated with VPA (50 µg/mL and 100 µg/mL) or with VPA (50 µg/mL and 100 µg/mL) following treatment with ascorbic acid (25 µM). VPA treatment resulted in higher level of Dnmt1 occupied at the *Hoxa2* gene promoter (CpG island 1) compared to wild-type untreated NIH3T3 cells (Fig. 4.2.17b). Cells treated with ascorbic acid alone, however decreased higher enrichment of Dnmt1 at *Hoxa2* promoter (Fig. 4.2.17a). As a result, when NIH 3T3 cells were treated with VPA in the presence of ascorbic acid (25 µM), the binding capacity of Dnmt1 protein at *Hoxa2* promoter region (CpG island 1) was significantly reduced (Fig. 4.2.17b). These results correspond with the decreased DNA methylation at the *Hoxa2* gene promoter (Fig. 4.2.16) in ascorbic acid treated NIH3T3 cells exposed to VPA.

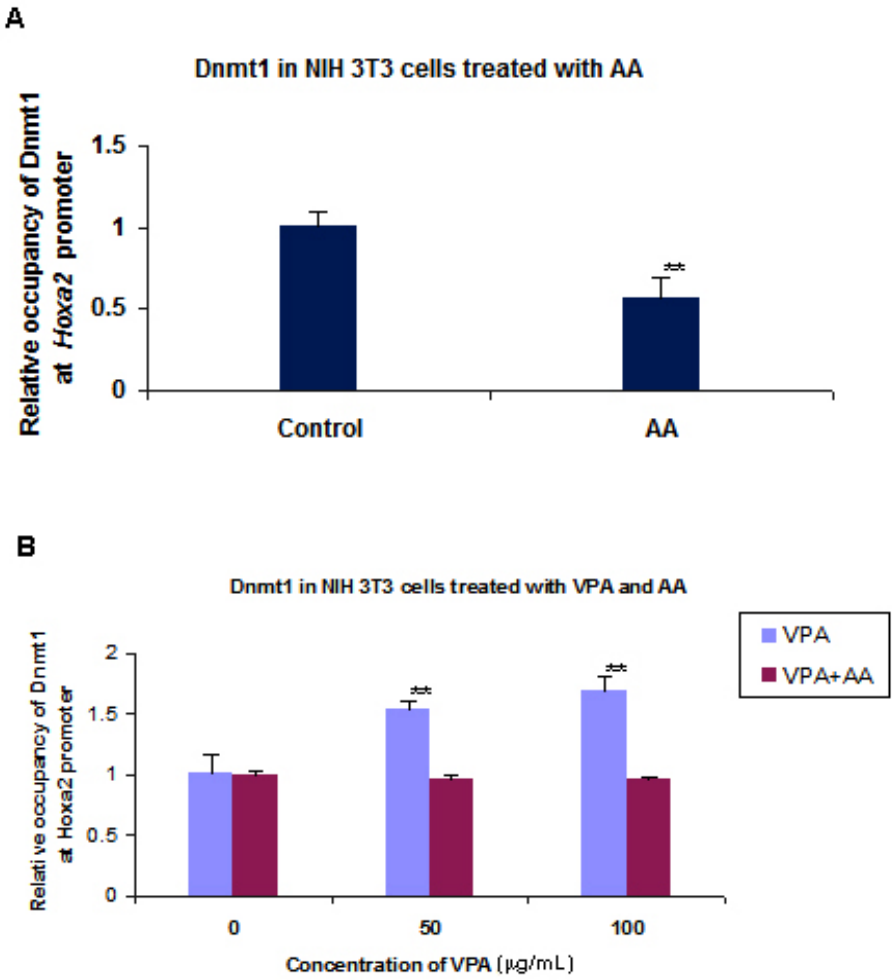

Fig. 4.2.17 qChIP-PCR assay of Dnmt1 binding at the *Hoxa2* gene promoter (CpG island 1) in NIH3T3 cells treated with ascorbic acid (5 µg/mL, 25 µM) (**A**), in NIH3T3 cells treated with ascorbic acid (25 µM) followed by VPA (50 and 100 µg/mL) for 24 h (**B**). Cells were harvested at 1×10^5 cells/cm^2. Primers Klx 3 and Klx 3-1 (see Methods section, Table 5.1 for primer sequence) were used for qChIP-PCR of Dnmt1 within the CpG island 1 of the *Hoxa2* promoter. Statistical analysis: one-way ANOVA with Tukey's HSD as post-hoc analysis (**, $p<0.01$), N=3.

4.2.9 Histone methylation is associated with *Hoxa2* gene promoter

To identify potential mechanisms that lead to transcriptional silencing of *Hoxa2* gene expression after VPA treatment, bivalent domains of active histone modification H3K4me3 and inactive histone modification H3K27me3 were characterized within 1688 bp of the *Hoxa2* gene promoter (Fig.6.2.18a). ChIP-PCR assay with the primers designed for the *Hoxa2* gene promoter showed that trimethylation of H3K27 and H3K4 were simultaneously associated at the *Hoxa2* promoter (Fig.6.2.18b). Results demonstrate that the two histone methylation marks (H3K27 and H3K4) are enriched near the transcription start site at the *Hoxa2* gene promoter, indicating the intermingled presence of active and inactive histone methylation marks (a bivalent domain) that is associated with *Hoxa2* gene activity.

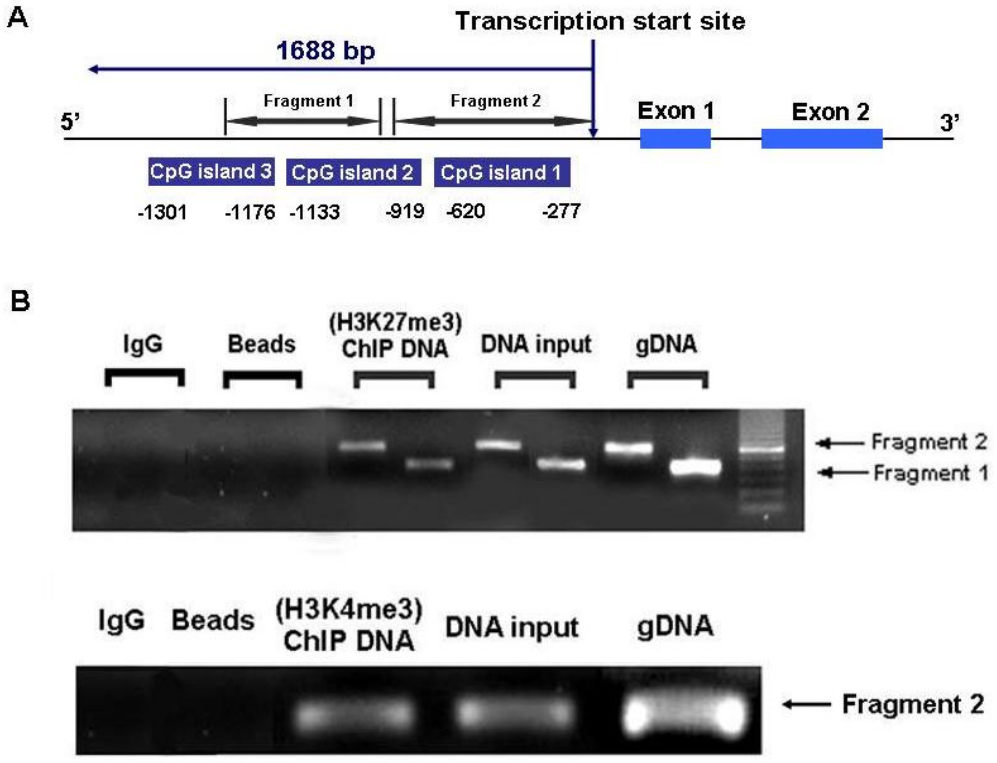

Fig. 4.2.18 (A) Schematic diagram of the *Hoxa2* gene showing the two regions (fragment 1 and fragment 2) of the promoter that were used for the ChIP-PCR assay using primers A2-1 and A2-2 for fragment 1 and primers A2-3 and A2-4 for fragment 2 (see Methods section, Table 5.1 for primer sequence). **(B)** PCR detection of H3K27me3 and H3K4me3 at *Hoxa2* gene promoter following chromatin immunoprecipitation (ChIP) in NIH3T3 cells. Enrichment of both H3K27me3 and H3K4me3 was only present in fragment 2 near the transcription start site of the *Hoxa2* gene. Cells were harvested at $1\times 10^5/cm^2$.

4.2.10 VPA increased H3K27me3 and decreased H3K4me3 enrichment at the *Hoxa2* gene promoter in NIH3T3 cells

To determine what effect VPA has on histone modification domain status, qChIP-PCR was used to quantify the enrichment of H3K27me3 and H3K4me3 at the *Hoxa2* gene promoter in NIH3T3 cells treated with VPA (Fig. 4.2.19). Results indicate that the enrichment of the repressive histone modification mark, H3K27me3, was enhanced at the *Hoxa2* gene promoter and was significant even at the lowest VPA concentration used (6.25 µg/mL) compared to control untreated group (Fig.4.2.19b). In contrast, the enrichment of the active histone modification mark, H3K4me3, was significantly reduced at all VPA doses relative to the control untreated group (Fig.4.2.19c). Generally, for chromatin domains over a gene promoter, an active domain mark (e.g H3K4me3) is defined by potential for high transcriptional rates, whereas a repressive chromatin domain mark (e.g. H3K27me3) is characterized by low transcriptional rates (Rodriguez et al., 2008b). The observed increased enrichment of H3K27me3 and a corresponding decreased enrichment of H3K4me4 in the same region of *Hoxa2* gene promoter near the transcription start site may explain lower *Hoxa2* expression in NIH3T3 cells treated with VPA.

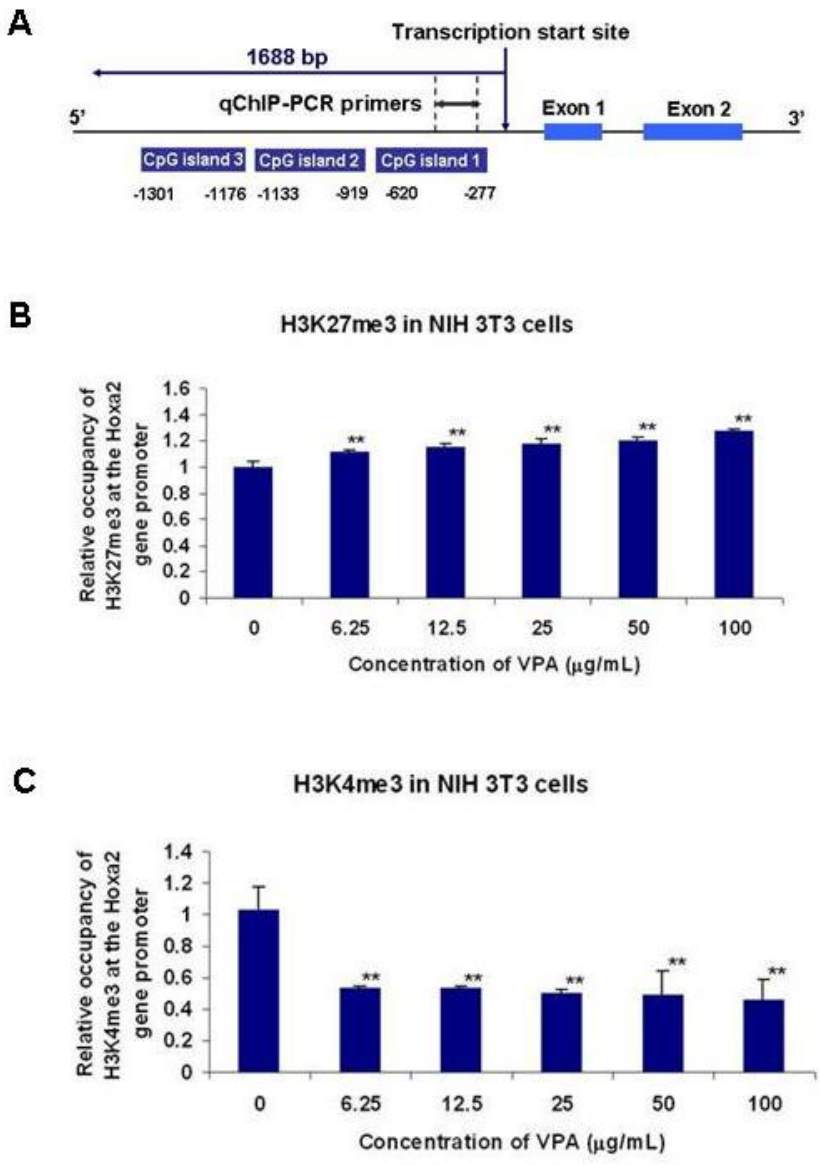

Fig. 4.2.19 Schematic diagram of the *Hoxa2* gene promoter (**A**). Primers Klx 3 and Klx 3-1 (see Methods section, Table 5.1 for sequence) were used for qChIP-PCR of both H3K27me3 and H3K4me3 within the CpG island 1 close to the transcription start site. VPA induced increased enrichment of H3K27me3 (**B**) and a decreased enrichment of H3K4me3 (**C**) at the *Hoxa2* gene promoter in NIH3T3 cells treated with VPA (dose, 6.25-100 µg/mL) for 24 h (*, $p<0.05$; **, $p<0.01$ compared to control). Cells were harvested at $1\times 10^5/cm^2$. Statistical analysis: one-way ANOVA with Tukey's HSD as post-hoc analysis (**, $p<0.01$), N=3.

4.2.11 Dynamic change in bivalent domain status induced by VPA is only associated with active *Hoxa2* gene expression when *Hoxa2* promoter is unmethylated

Hoxa2 gene is silenced in EG7 cells where the promoter region is highly methylated (Figs. 4.2.3 and Fig. 4.2.4). To determine if the methylation status of the *Hoxa2* gene promoter influenced the dynamic change in the histone bivalent domain, qChIP-PCR assays for the two histone modification marks, H3K27me3 and H3K4me3, were carried out in control untreated and VPA treated (200 µg/mL) EG7 cells (Fig. 4.2.20). VPA treatment did not significantly change enrichment of H3K27me3 or of H3K4me3 (Fig. 4.2.20) at *Hoxa2* gene promoter in EG7 cells. These findings indicate that significant dynamic change of these bivalent domains (H3K27me3 and H3K4me3) is specific to NIH 3T3 cells where the *Hoxa2* gene promoter is primarily unmethylated DNA with an active *Hoxa2* gene expression.

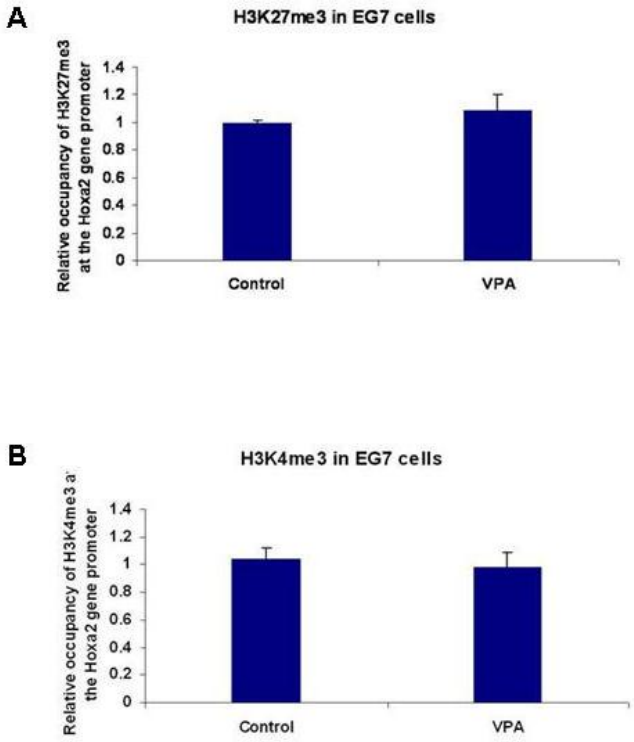

Fig. 4.2.20 Bivalent domains (H3K27me3 and H3K4me3) status at the *Hoxa2* gene promoter in wild-type untreated control EG7 cells and in EG7 cells treated with 200 µg/mL VPA for 24 h. No significant change in enrichment of H3K27me3 (**A**) or of H3K4me3 (**B**) at the *Hoxa2* gene promoter in wild-type control EG7 cells compared to EG7 cells treated with VPA was observed. Cells were harvested at $1\times 10^5/cm^2$. Statistical analysis: one-way ANOVA with Tukey's HSD as post-hoc analysis, N=3.

4.2.12 Ascorbic acid decreased H3K27me3 and increased H3K4me3 enrichment at *Hoxa2* gene promoter in NIH 3T3 cells treated with VPA

Hoxa2 gene expression is down regulated in both NIH3T3 cells and in whole mouse embryo cultures treated with VPA (Fig. 4.1.3, Table 4.1.4, and Fig. 4.2.5). Treatment with ascorbic acid (1000 µg/mL in embryos or 5 µg/mL in NIH 3T3 cells) blocked the effects of VPA on *Hoxa2* gene expression in both whole mouse embryo cultures (Fig. 4.1.7) and in NIH3T3 cells (Fig.4.2.21).

Indeed, treatment with ascorbic acid significantly decreased the enrichment of H3K27me3 at the *Hoxa2* promoter in VPA treated (25 µg/mL, 50 µg/mL or 100 µg/mL) NIH3T3 cells (Fig. 4.2.22a). In contrast, ascorbic acid induced higher enrichment of H3K4me3 at the *Hoxa2* promoter in VPA treated NIH3T3 cells compared to the untreated NIH3T3 cells. A significant enrichment of H3K4me3 was observed at VPA doses of 25 µg/mL and 100 µg/mL in NIH3T3 cells treated with ascorbic acid (Fig. 4.2.22b). Results demonstrate that ascorbic acid blocked the effect of VPA on the enrichment of bivalent domains, H3K27me3 and H3K4me3, at *Hoxa2* gene promoter.

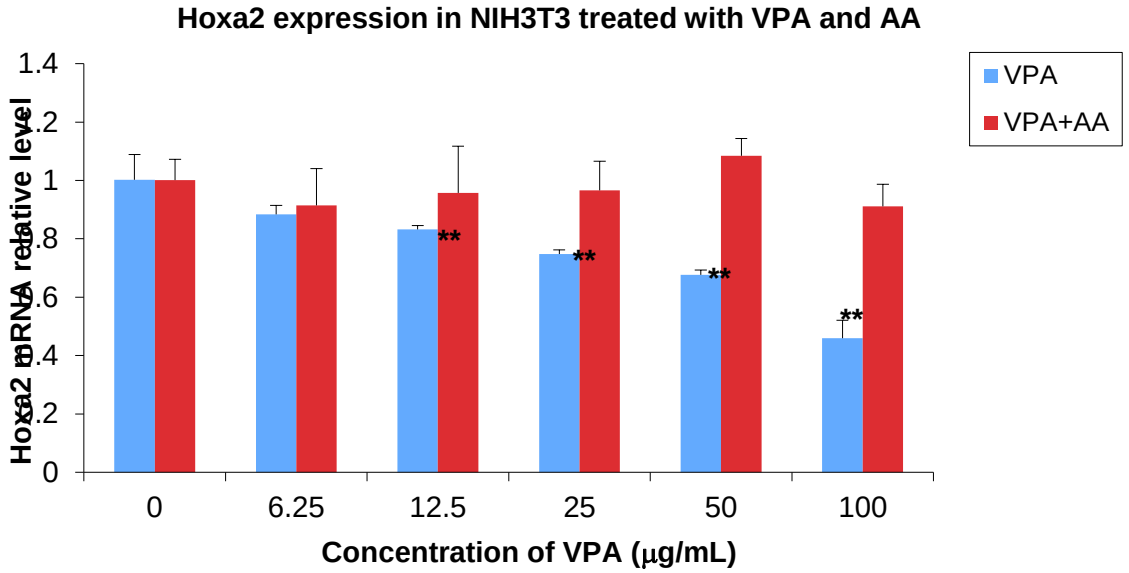

Fig. 4.2.21 *Hoxa2* gene expression in NIH3T3 cells treated with VPA (12.5 to 100 µg/mL) and VPA in the presence of 5µg/mL [25 µM] ascorbic acid for 24 h. Cells were harvested at $1\times 10^5/cm^2$. Statistical analysis: one-way ANOVA with Tukey's HSD as post-hoc analysis (**, $p < 0.01$ compared to control), N=3.

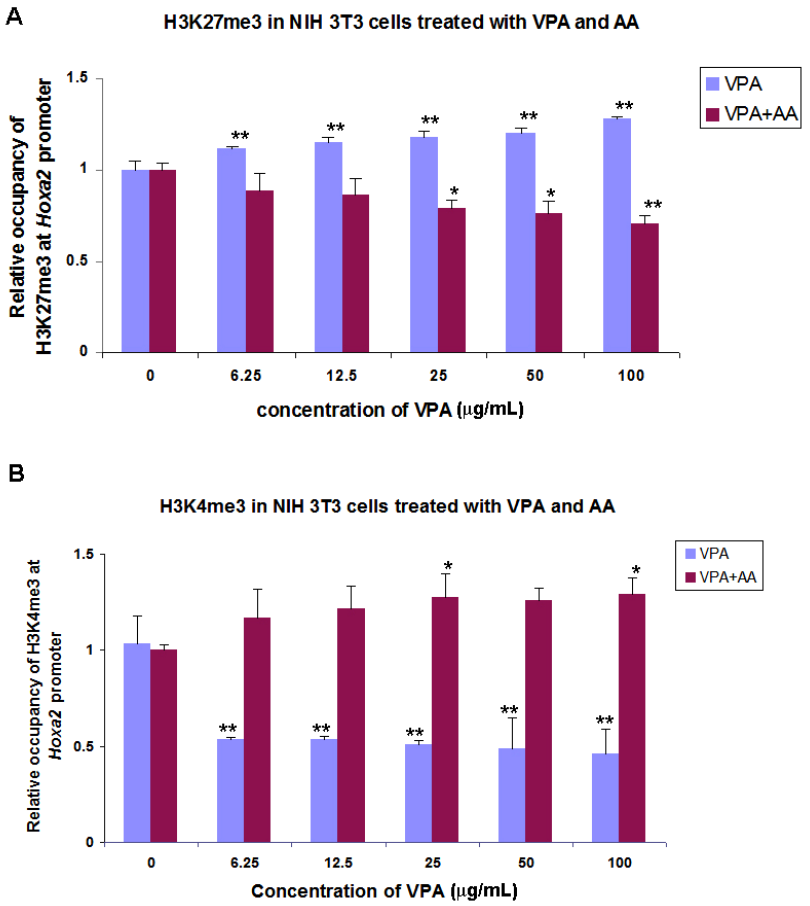

Fig. 4.2.22 H3K27me3 **(A)** and H3K4me3 **(B)** Binding capacity (at CpG island 1) in NIH3T3 cells treated with VPA (dose, 6.25 to 100 µg/mL) and VPA in the presence of 5 µg/mL [25 µM] ascorbic acid for 24 h (*, $p<0.05$; **, $p<0.01$ compared to control in each group). Cells were harvested at $1\times 10^5/cm^2$. Statistical analysis: one-way ANOVA with Tukey's HSD as post-hoc analysis , N=3.

4.2.13. Ascorbic acid decreased the enrichment of Ezh2 at *Hoxa2* gene promoter in NIH 3T3 cells treated with VPA

The histone methyltransferase Ezh2 was subsequently evaluated in NIH3T3 cells treated with ascorbic acid alone or following VPA treatment. Ascorbic acid alone reduced the association of Ezh2 at the *Hoxa2* promoter (Fig.4.2.23a). As a result, the total effect of ascorbic acid was to induce a decrease in enrichment of Ezh2 at the *Hoxa2* gene promoter in NIH3T3 cells treated with VPA (Fig.4.2.23b). These significant changes were observed at VPA concentrations of 12.5

to 100 µg/mL. A decline in enrichment of Ezh2 induced by ascorbic acid following VPA exposure is in concordance with the dissociation of H3K27me3 mark that was found at the *Hoxa2* gene promoter in NIH3T3 cells treated with VPA (Fig. 4.2.22a).

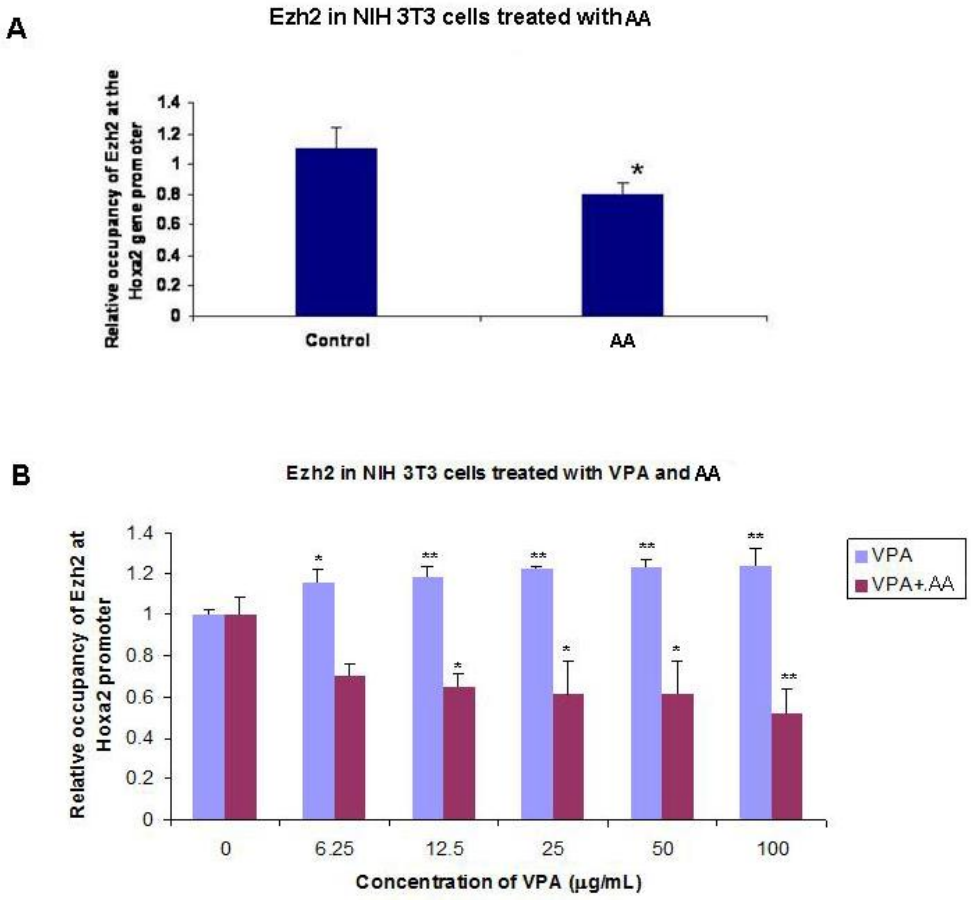

Fig. 4.2.23 Relative occupancy of Ezh2 in wild-type NIH3T3 cells or in NIH 3T3 cells treated with 5 µg/mL [25 µM] ascorbic acid **(A)** and in NIH3T3 cells treated with VPA (dose, 6.25 to 100 µg/mL) or VPA (dose, 6.25 to 100 µg/mL) following pretreatment with 5 µg/mL [25 µM] ascorbic acid **(B)** (all cell treatments were for 24 h) (*, $p<0.05$; **, $p<0.01$ compared to control of each group). Cells were harvested at $1\times 10^5/cm^2$. Primers of Klx 3 and Klx 3-1 were used for qChIP-PCR. Statistical analysis: one-way ANOVA with Tukey's HSD as post-hoc analysis, N=3

4.2.14 Dynamic changes of histone bivalent domains at the *Hoxa2* gene promoter in developing embryos (E6.5 – E10.5)

To gain further insight into the mechanism(s) that lead to transcriptional silencing of *Hoxa2* in mouse embryos treated with VPA, we first profiled active and inactive histone modification bivalent domains, H3K27me3 and H3K4me3, at the *Hoxa2* promoter region in the developing mouse embryo from E6.5 to E10.5 (Fig. 4.2.24). The chromatin profiling in the developing embryo revealed the coexistence of active H3K4me3 and inactive domains H3K27me3 at the *Hoxa2* gene promoter. Interestingly, the enrichment of H3K27me3 at the *Hoxa2* gene promoter in E8.5 and in E10.5 was significantly lower than in E6.5 embryos (Fig. 4.2.24a). In contrast, enrichment of H3K4me3 was significantly higher at same region of *Hoxa2* promoter in E8.5 and E10.5 compared to the E6.5 embryos (Fig. 4.2.24b). This enrichment trend of trimethylation of H3K27 and H3K4 at the *Hoxa2* gene promoter, together with DNA methylation status at the *Hoxa2* gene promoter (Fig. 4.2.10, Fig. 4.2.11), appears to be associated with the epigenetic regulation of *Hoxa2* gene in developing embryos.

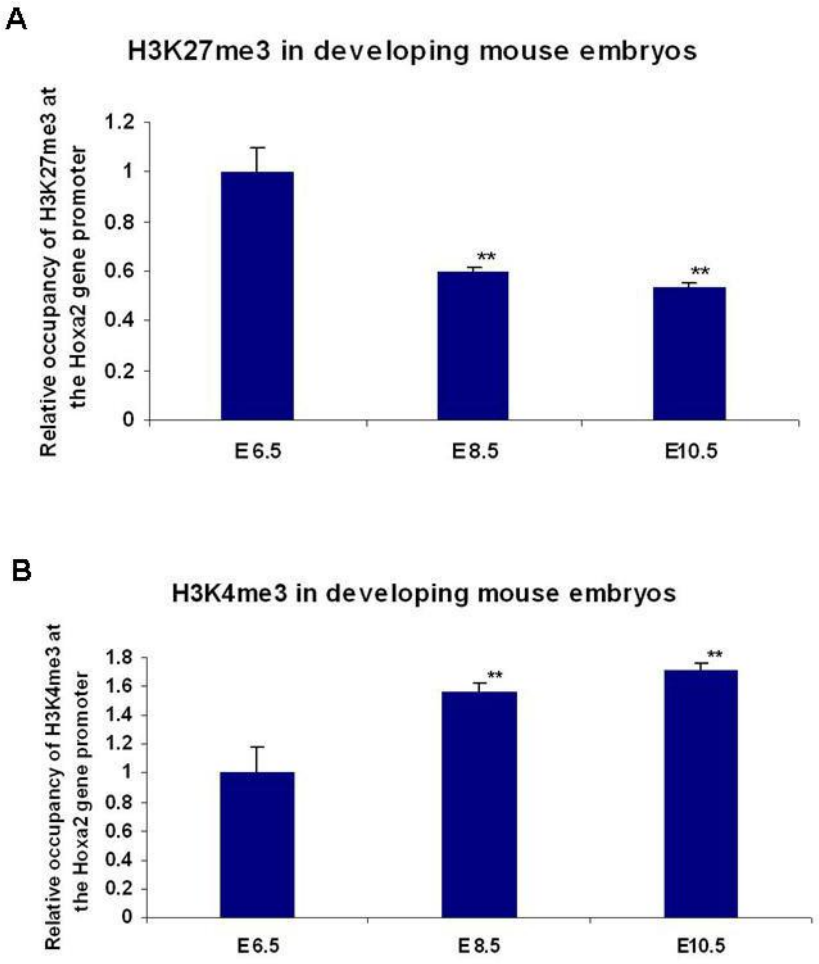

Fig. 4.2.24 Dynamic changes in H3K27me3 and H3K4me3 enrichment at the *Hoxa2* gene promoter in developing mouse embryos. There is a significant change in enrichment of H3K27me3 (**A**) and of H3K4me3 (**B**) at the *Hoxa2* gene promoter in E8.5 and E10.5 embryos compared to E6.5 embryos (**, $p<0.01$ compared to E6.5 embryos). Statistical analysis: one-way ANOVA with Tukey's HSD as post-hoc analysis, N=3.

4.2.15 VPA increases H3K27me3 and decreases H3K4me3 enrichment at the *Hoxa2* promoter in E10.5 mouse embryos

To determine VPA's effect on the bivalent domains at the *Hoxa2* gene promoter in developing mouse embryos, VPA was administered (s.c. 400 mg/kg, once daily) to time-

pregnant mice between E8 and E10. Mice receiving s.c. dose of 400 mg/kg VPA daily between gestational days 7 and 15 reportedly attain therapeutic plasma concentrations (50-100 µg/mL) after 3 to 4h of dosing (Nau et al., 1981). This is due to the short half-life and high plasma clearance rate of VPA in the mouse (Nau et al., 1981). In our study, VPA treatment induced a significant increase in enrichment of H3K27me3 (Fig. 4.2.25a) and a significant decrease in enrichment of H3K4me3 (Fig. 4.2.25b) at the *Hoxa2* gene promoter in E10.5 embryos which correlates with a switch in transcription from "on" to "off" as reduction in *Hoxa2* expression is evident (Fig. 4.1.3, Table 4.1.4). Similar change in the bivalent domains was also observed in VPA treated NIH 3T3 cells when *Hoxa2* mRNA is down-regulated (Fig. 4.2.19).

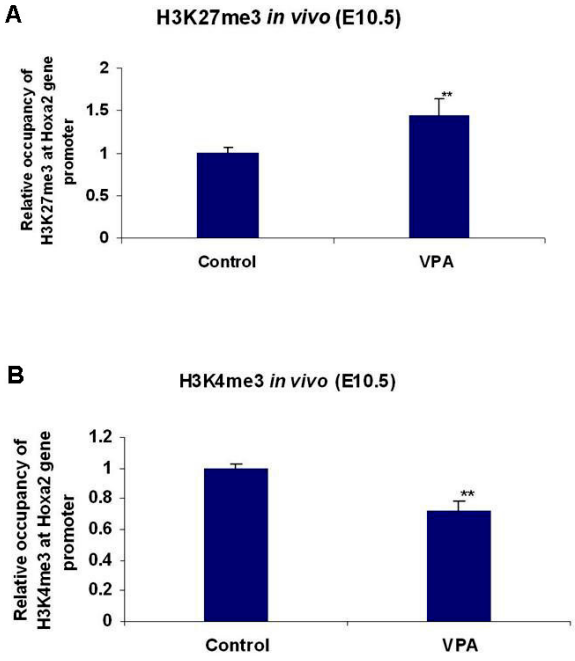

Fig. 4.2.25 VPA induced increased enrichment of H3K27me3 (**A**) and decreased enrichment of H3K4me3 (**B**) at the *Hoxa2* gene promoter in E10.5 embryos following once daily dose of s.c. 400 mg/kg VPA in timed-pregnant mice from E8 to E10 (**, $p<0.01$ compared to control saline treated mice). Statistical analysis: one-way ANOVA with Tukey's HSD as post-hoc analysis , N=3.

4.2.16 A component of the polycomb repressor complex is enriched at the *Hoxa2* promoter in NIH3T3 cells and in E10.5 mouse embryos after VPA treatment

An increased enrichment of H3K27me3 at the *Hoxa2* gene promoter suggested that components of the polycomb protein groups may be mediating, at least in part, the silencing of *Hoxa2* gene expression following VPA treatment. A polycomb repressor complex (PRC) protein, Enhancer of Zeste Homolog 2 (Ezh2), is known to be responsible for catalyzing the deposition of the H3K27me3 mark (Ringrose and Paro, 2004). To determine if Ezh2 is associated with *Hoxa2* gene promoter, qChIP-PCR assay for Ezh2 was performed in NIH 3T3 cells and in E10.5 embryos exposed to VPA (Fig. 4.2.26). Results show Ezh2 is enriched near the transcription start site at the *Hoxa2* gene promoter where high levels of the H3K27me3 mark is also detected (Fig.4.2.19b, Fig.4.2.25a). A significant increase in Ezh2 enrichment at *Hoxa2* gene promoter is observed in both NIH3T3 cells (Fig. 4.2.26a) and in E10.5 embryos (Fig. 4.2.26b) exposed to VPA.

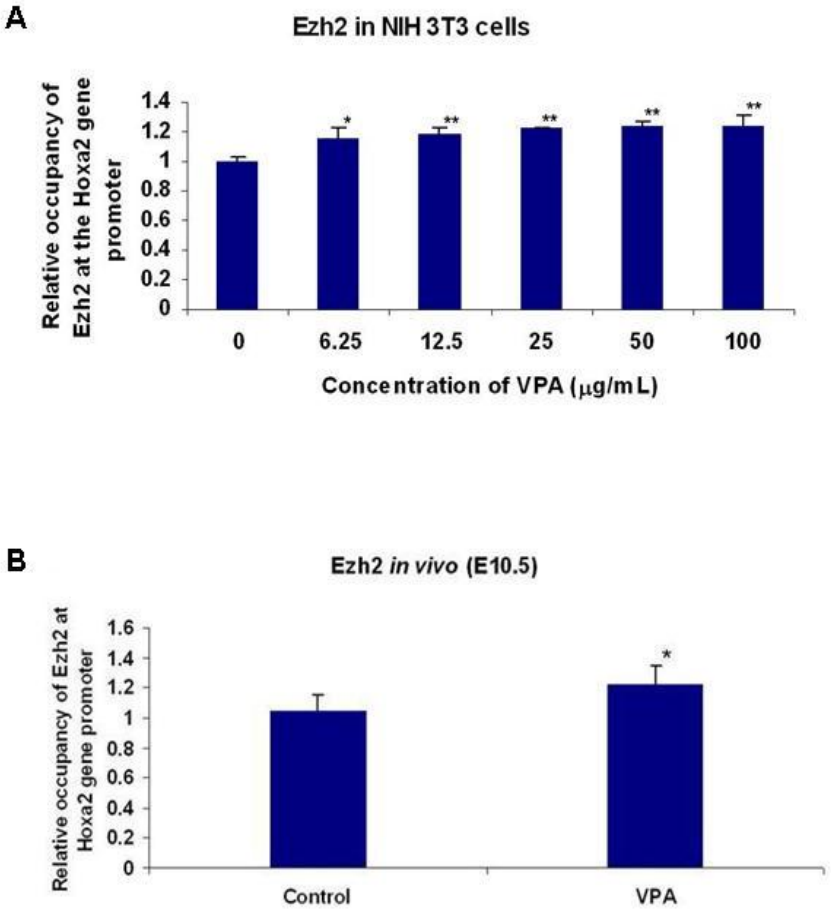

Fig. 4.2.26 Enrichment of Ezh2 at the *Hoxa2* gene promoter in VPA treated NIH3T3 cells (dose, 6.25 µg/mL to 100 µg/mL) for 24 h **(A)**; and in E10.5 embryos following once daily dose of s.c. 400 mg/kg VPA in timed-pregnant mice from E8 to E10 **(B).** Primers Klx 3 and Klx 3-1 (see Methods section, Table 5.1 for sequence) were used for qChIP-PCR of Ezh2 within the CpG island 1 (*$p<0.05$; ** $p<0.01$ compared to control saline treatment). Statistical analysis: one-way ANOVA with Tukey's HSD as post-hoc analysis, N=3.

CHAPTER 5: DISCUSSION

5.1 Effect of VPA on embryonic differentiation and growth

Results indicate that VPA can inhibit embryonic organ differentiation and development *in vitro*. Total morphological score decreases significantly at VPA concentrations as low as 50 μg/mL [0.35 mM]. Embryonic head development is also inhibited at this concentration. Scoring parameters such as yolk sac circulation, allantois, caudal neural tube, forebrain, and branchial arch also decrease, indicating these embryonic organs may be particularly sensitive to VPA insult. The reduced overall embryonic growth and increased incidence of abnormal embryos at higher VPA concentrations observed are in agreement with previous reports (Bruckner et al., 1983). Embryonic deformities such as fusion of the first and second branchial arches are of particular interest especially since these structures are implicated in the development of craniofacial skeletal components such as the mandibular bone, incus, and malleus, which originate from the first branchial arch, and the hyoid bone and stapes, which originate from the second branchial arch (Mahmood et al., 1996; Menegola et al., 2000). Fusion of the first and second arches probably produces a spectrum of mandibular, hyoid, ear, and cranial malformation. This result of the culture experiment correlates well with *in vivo* VPA-induced teratogenicity data in mice and humans where cranial abnormalities including small nose and mouth, low-set ears, craniosynostosis, and cleft palate are reported (Faiella et al., 2000; Polifka and Friedman, 2002).

5.2 Effect of VPA on embryonic antioxidant status

Glutathione (GSH), a major component of overall antioxidant defense, is synthesized within virtually every cell from glycine, cysteine, and glutamate in a series of reactions catalyzed by γ-glutamylcysteine synthetase and glutathione synthetase (Pallardo et al., 2009). During oxidative stress, GSH can neutralize free radicals through its oxidation into glutathione disulfide (GSSG); GSSG can then be reduced back to GSH enzymatically via glutathione disulfide reductase to regulate a normal cellular GSH/GSSG ratio (Bannai and Tateishi, 1986). During embryonic development, maintenance of proper redox status is essential, because these processes play important roles in cell proliferation, apoptosis, and differentiation. Redox changes can result in transcription factor activation or inhibition, depending on the type of redox potential shift

(Pallardo et al., 2009). Depletion of GSH or the generation of GSSG increases the GSSG/GSH ratio, reflecting an increase in oxidative stress, which can lead to abnormal proliferation, altered differentiation, and/or apoptosis resulting in teratogenesis (Allen, 1991; Hamza and Amin, 2007; Hutter et al., 1997; Ozolins and Hales, 1997; Sen and Packer, 1996). Our study demonstrated that total glutathione content in embryos only decreased significantly at the highest VPA dose (400 μg/mL). However, VPA altered the glutathione homeostasis of mice embryos by causing an increase in the embryonic GSSG/GSH ratio at doses ≥ 100 μg/mL (0.7 mM). The normal therapeutic dose of VPA in humans is in the range from 50 to 100 μg/mL (0.35 mM to 0.7 mM) plasma (Ornoy, 2006; Samaei et al., 2009). These results suggest alteration of the embryonic antioxidant status plays a very important role in VPA-induced teratogenesis. Interestingly, mouse embryos pretreated with 5 mM L-ascorbic acid had a protective effect and prevented the VPA-induced glutathione depletion at the highest VPA dose and normalized the GSSG/GSH ratio.

5.3 Effect of VPA on the *Hoxa2* gene expression in mouse embryos

Results of Western blot analysis and quantitative real-time RT-PCR show that VPA can inhibit *Hoxa2* expression in cultured mice embryos both at the protein and mRNA levels. *Hoxa2* gene is the only *Hox* gene expressed at the level of hindbrain in rhombomere 2 (r2) in the neuroectoderm, but not in neural crest cells that migrate from this region (Prince and Lumsden, 1994b). *Hoxa2* gene is also expressed in both r4 neuroectoderm and neural crest cells migrating into the second arch, and also in more posterior branchial arches (Maconochie et al., 1999; Prince and Lumsden, 1994b). *Hoxa2* plays a key role as a selector gene in determining second arch fate and imposes the unique identity of second arch structures (Santagati et al., 2005; Trainor and Krumlauf, 2001). *Hoxa2* knockout mice exhibit the defects in structures of neural crest origin, including the skeletal elements of the second branchial arch and the external ear pinna (Gendron-Maguire et al., 1993a; Rijli et al., 1993b). Exposure to VPA can induce a characteristic facial phenotype manifested as midfacial hypoplasia, epicanthal folds, down-slanting palpebral fissure, telecanthus, a broad low nasal bridge, and IUGR (Clayton-Smith and Donnai, 1995). The facial features of FVS are suggestive of neural crest involvement in the pathogenetic mechanism. Neural crest cell cultures exposed to VPA can substantially decrease the proportion of cells migrating individually, instead promoting migration as epithelial sheets (Fuller et al., 2002). Further, Padmanabhan and Ahmed (1996) reported a delay in the migration

of the neural crest and increased cell death in crest-derived craniofacial tissue, in the optic cup, otic vesicle, and trigeminal and otic ganglia in response to VPA treatment. Inhibition of *Hoxa2* gene expression likely affects pattern formation in the branchial region (Santagati et al., 2005). Our results suggest VPA-induced inhibition of *Hoxa2* expression may play an important role in its teratogenicity, especially in VPA-induced embryonic craniofacial malformations.

5.4 Ascorbic acid prevents VPA-induced inhibition of *Hoxa2* and maintains glutathione homeostasis in mouse embryos in culture

Treatment with ascorbic acid just prior to VPA exposure prevented VPA-induced downregulation of *Hoxa2* gene expression in concert with enhanced glutathione status, indicating a protective effect on embryos. Indeed, the incidence of dysmorphogenesis and death was substantially reduced in embryos treated with ascorbic acid prior to VPA exposure. To further delineate whether a relationship existed between VPA, oxidative stress and *Hoxa2*, total glutathione levels were measured in *Hoxa2* null mutant embryos. Findings demonstrate that glutathione levels are not altered in *Hoxa2*-/- embryos and indicate VPA specific depletion of glutathione. This prompted further investigations on whether VPA had a direct effect as an epigenetic modulator of *Hoxa2* gene promoter to regulate gene expression (Fig. 5.1).

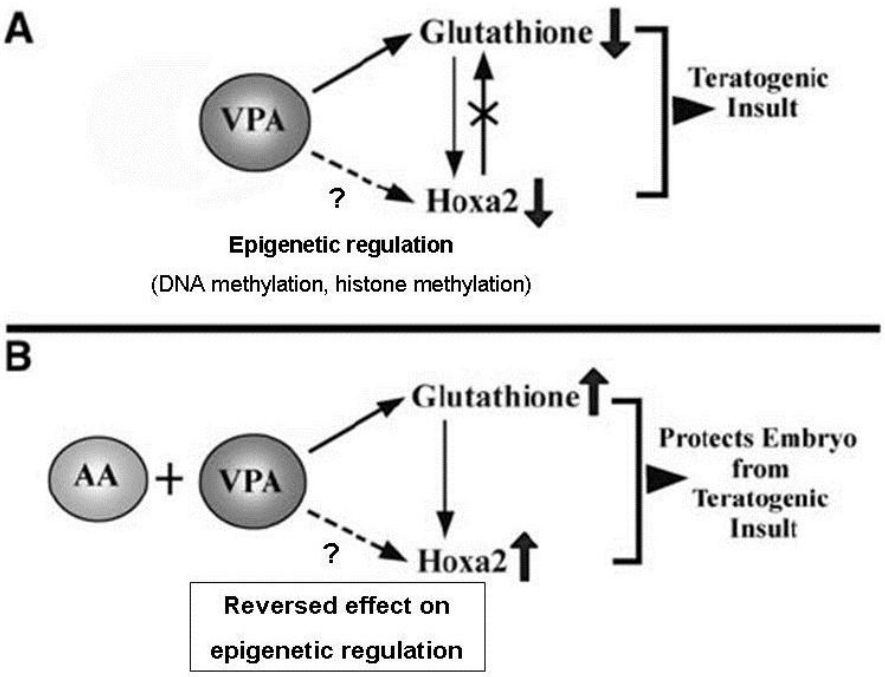

Fig. 5.1 Schematic diagram showing the relationship between VPA, glutathione, and *Hoxa2* gene expression. **A** VPA-induced oxidative stress leads to a decline in glutathione levels which in turn induces a downregulation of *Hoxa2* gene expression. VPA's inhibition of glutathione and glutathione's effect on *Hoxa2* may be direct or via several intermediary factors. The *arrow* with a *cross* indicates that the response is in one direction only since *Hoxa2*-/- mice do not display altered glutathione levels. The *broken arrow* indicates VPA could directly affect *Hoxa2*. A combination of reduced glutathione levels and downregulation of *Hoxa2* may trigger a teratogenic response. **B** Pretreatment with 5 mM L-ascorbic acid prior to VPA exposure prevents VPA-induced decline in glutathione and *Hoxa2* gene expression, protecting embryos from a teratogenic insult.

5.5 Protective effect of ascorbic acid on VPA-induced teratogenicity

Treatment with pro-vitamin C (tetra-isopalmitoyl ascorbic acid) is known to reduce levels of reactive oxygen species (ROS) (Yokoo et al., 2004). In addition, prolongation of life-span has been attributed to a decrease in ROS as a result of a caloric restricted diet (Dhahbi et al., 1998; Lipman et al., 1998) fed to mice, and *in vitro* cell lifespan increased in cell cultures after treatment with vitamin E (Yu et al., 1998), although this has not been conclusively proven. The ROS-induced DNA damage within a cell can also be prevented by ascorbic acid or its derivatives

(Kanatate et al., 1995). In this thesis, I report that cultured embryos treated with VPA (0.7mM) developed abnormal differentiation in brain areas such as hindbrain, midbrain, forebrain and optical system. A significant lower score was observed in the embryos of hindbrain, midbrain and forebrain compared to cultured embryos without drug treatment. The addition of ascorbic acid (5 mM) in cultured embryos reduced defects in VPA-target areas in the mouse developing brain. Additionally, the optic system of embryos after ascorbic acid treatment showed a better morphological score compared to VPA treatment alone. Ascorbic acid has a significant protective effect on embryos exposed to VPA (Fig. 5.2).

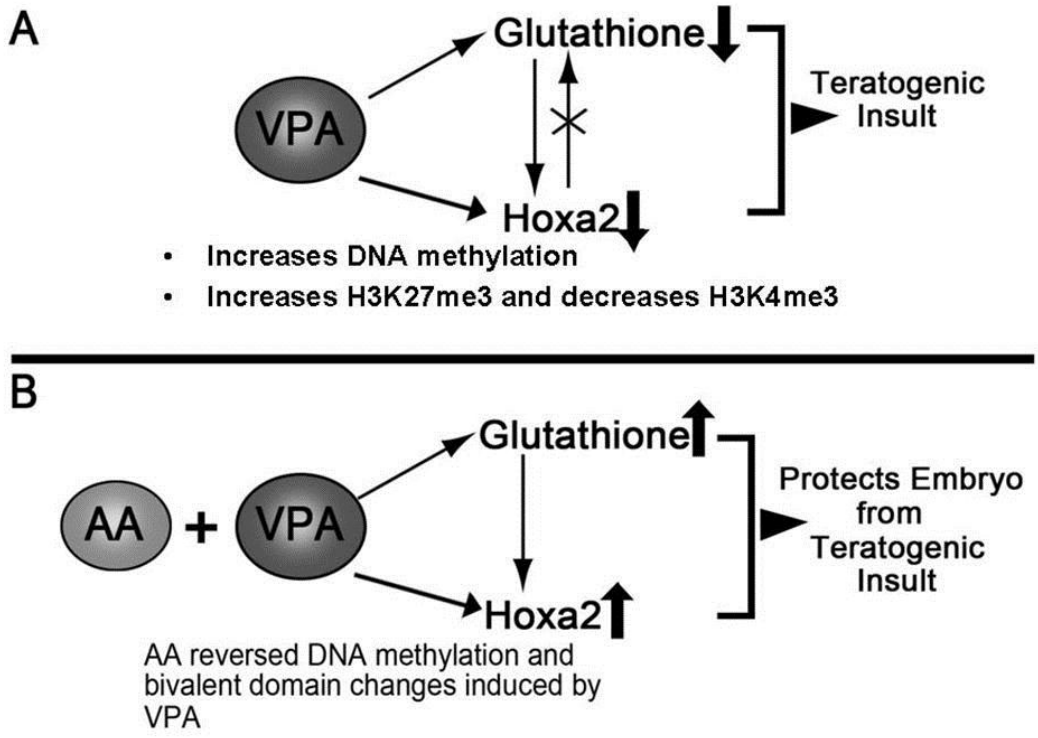

Fig. 5.2 Schematic diagram showing the relationship between VPA, glutathione, epigenetic changes and *Hoxa2* gene expression. **A** VPA increased DNA methylation and induced bivalent domain changes at *Hoxa2* promoter (increased enrichment of H3K27me3 and decreased enrichment of H3K4me3); **B** Ascorbic acid reversed DNA methylation and alteration of bivalent domain induced by VPA at the *Hoxa2* gene promoter.

HDAC inhibitors and generation of ROS

The mechanisms of how HDAC inhibitors induce oxidative stress are not well understood. Two prominent mechanisms have been suggested. One involves regulating antioxidants levels and the other implicates mitochondrial damage (Miller et al., 2011).

Cellular exposure to HDAC inhibitors leads to accumulation of ROS. This relates to the intracellular thioredoxin reduction-oxidation system (Duncan et al., 2011). Thioredoxin (Trx) is a hydrogen donor that is required for activation of many proteins, including ribonucleotide reductase that is essential for DNA synthesis (Lilig and Holmgren, 2007). Thioredoxin responds to the stressful stimuli that cause ROS to increase (Ungerstedt et al., 2005). Moreover, HDAC inhibitors upregulate the expression of Trx binding protein (TBP2) (Butler et al., 2002; Xu et al., 2006), which bind to and inhibit Trx activity in transformed cells (Butler et al., 2002; Nishiyama et al., 1999; Ungerstedt et al., 2005). Trx acts as an inhibitor of apoptosis signal regulating kinase 1 (ASK 1) (Saitoh et al., 1998). Inhibition of Trx by TBP2 activates ASK1. Furthermore, HDAC inhibitors increase the expression of ASK1. These effects act together to induce apoptosis. ROS accumulation may also be a consequence of apoptosis (Xu et al., 2007).

Vorinostat, the hydroxamic acid, has also been reported to be associated with ROS production (Chandra 2009). Vorinostat (SAHA) promotes expression of the proapoptotic B-cell lymphoma 2 (Bcl-2) family member, BH3 interacting-domain death agonist (Bid) (Ruefli et al., 2001). Bid induces ROS by translocation to mitochondria and subsequent disruption of mitochondria (Ruefli et al., 2001).

Oxidative stress in embryo vs. cell line

i) Sensitivity

An oxidation event early in G1 phase is a critical regulatory step in the progression to S phase, and this initiates the redox cycle within the cell cycle. The transient change of ROS could modify the redox state of cell regulatory proteins through critical cysteine residues (Markovic et al. 2009). The sensitivity to oxidative impacts may vary depending on cell types and experimental conditions (Guo et al., 2010). Embryonic stem cells (ESC) proliferation and viability show comparable sensitivity to hydrogen peroxide (H_2O_2) as do fibroblasts and vascular cells (Guo et al., 2010). The shifts in the redox potential determine the redox sensitive signaling and

regulatory pathways (Attene-Ramos et al., 2005; Imhoff and Hansen 2011; Jones et al., 2004; Nkabyo et al., 2002; Schafer and Buettner, 2001). The mechanisms are particularly important and relevant to developing embryos because the precise coordination of proliferation, differentiation, apoptosis, and necrosis are required for the temporal and spatial body formation and function (Harris and Hansen, 2012).

ii) Timing in cell cycle

Glutathione (GSH) is generally recruited into the nucleus in early phases of cell proliferation when cells are in an active division state (Markovic et al., 2010). It later redistributes uniformly between the nucleus and cytoplasm when cells reach confluence (Markovic, et al., 2007). In my studies, NIH3T3 cells were incubated with VPA for 24 h and the doubling time for NIH3T3 cells is 18 h (ATCC, Specifications for 3T3-Swiss albino). Within 24 h when NIH3T3 cells were proliferating, GSH is primarily accumulated in the nuclei, hence GSH was not significantly reduced in NIH3T3 cells treated with VPA at low concentration from 25 to 50 μg/mL. This finding demonstrated that short-term oxidative stress induced by VPA does not impact NIH3T3 cells. It has been suggested that the reduced intracellular environment as cells progress from quiescence to proliferation may protect genomic DNA from oxidative damage upon breakdown during mitosis (Conour et al., 2004).

iii) Function

Appropriate ROS levels generated within the cells may act as signaling molecules that trigger a wide range of cellular processes such as cellular defense (Yoon et al., 2002), and vascular functions (Rhee et al., 2005; Taniyama and Griendling 2003), differentiation, and proliferation (Kim et al., 2001; Sauer and Wartenberg 2005; Stouffs et al., 2006) depending on cell types. In normal embryonic development, energy production is generally achieved by a few metabolic pathways involved with O_2 utilization (Takahashi, 2012). ROS levels are highly related to cellular function and signal transduction. Therefore, the cellular redox balance is very important for providing suitable environments for metabolic pathways and gene expression in developing embryos (Takahashi, 2012).

However, in cells when the level of oxidative stress is beyond the capacity of cells to manage, apoptosis may be the best means to avoid transmission of mutation or other damages to the descendant cells (Guo et al., 2010). Oxidative status is usually used as a way to estimate the oxidative damage and associated dysfunctions in developing embryos (Takahashi, 2012).

Thiol-based biomolecules, as antioxidants, are one of the central and important cellular substances used to determine embryotoxicity (Harris and Hansen, 2012). It has been reported that the embryotoxicity caused by several classes of teratogens were altered significantly as a function of GSH status within cells and embryonic tissues (Harris 1993; Harris et al., 1995; Harris et al., 1988; Harris et al., 2004; McNutt and Harris 1994; Ozolins et al., 2002). Spatial and temporal patterns of GSH activity also show highly selective patterns of synthesis, turnover, and disposition of GSH, depending on the availability of amino acid precursors and cofactors, and gene expression (Harris and Hansen, 2012). In my experimental system, the developing mouse embryos appeared to be more vulnerable to VPA exposure compared to NIH3T3 cells. The changes of GSH in embryos were more significant and demonstrated tissue and organ malformations. Moreover, the impact of the antioxidant ascorbic acid on GSH status was also more significant in the embryos compared to NIH3T3 cells.

5.6 Epigenetic regulation of *Hoxa2* gene

5.6.1 CpG methylation status of the *Hoxa2* gene promoter in cell lines

A growing body of evidence has indicated that methylation of cytosines within CpG dinucleotides on genes is an important mechanism for differential regulation of gene transcription in mammalian cells (Frigola et al., 2006; Hitchins et al., 2007; Meissner et al., 2008; Mohn et al., 2008; Widschwendter et al., 2007). Three CpG islands on *Hoxa2* gene promoter were predicted using the following website (http://www.urogene.org//methprimer/)(Li and Dahiya, 2002) and manually identified using bisulfite specific PCR (BSP) sequencing. The three identified CpG islands on the *Hoxa2* gene promoter are: CpG island 1 (-277 to -620 bp), CpG island 2 (-919 to -1133 bp), and CpG island 3 (-1176 to -1301 bp) (Fig. 5.3). It is known that *de novo* methylation of CpG islands is associated with the transcriptional silencing of genes in many cancers (Esteller, 2007; Jones and Baylin, 2007). Data from my study indicates that methylation

status of specific CpG sites on the *Hoxa2* gene promoter in two different cell lines appears to correlate with the transcriptional activities of *Hoxa2*. Unmethylated CpG sites were found on the *Hoxa2* gene promoter in NIH 3T3 cells when *Hoxa2* gene is activated, whereas these same CpG sites were methylated in EG7 cells that do not express *Hoxa2*.

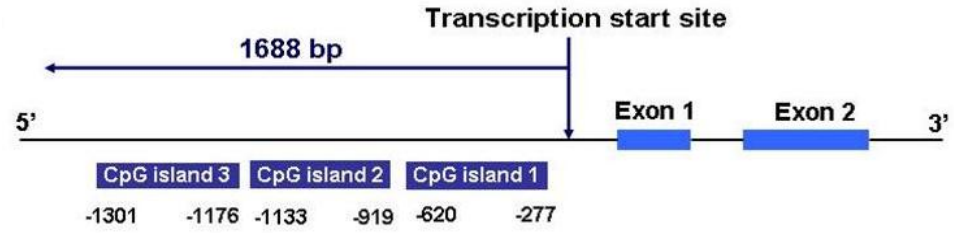

Fig. 5.3 Three CpG islands on *Hoxa2* gene promoter

5.6.2 Effect of VPA on CpG methylation status of *Hoxa2* gene promoter in cell lines

VPA inhibits *Hoxa2* gene expression in NIH3T3 cell lines (Fig. 4.2.5) and enhances the DNA methylation status of CpG island 1 closer to the *Hoxa2* transcription start site (Fig. 4.2.6). Cells treated with 100 µg/mL [0.7 mM] VPA increased methylation at CpG^{-617}, CpG^{-582}, CpG^{-577}, CpG^{-569}, CpG^{-514} sites by 3-9%, and enhanced methylation at CpG^{-551}, CpG^{-553}, CpG^{-540}, CpG^{-509} and CpG^{-492} sites by as much as 30-50%. The later five CpG sites that are closer to *Hoxa2* transcription start site may be critical regions for DNA methylation in silencing *Hoxa2* expression. Although it is not known how methylation status of the *Hoxa2* gene promoter affects the transcription of this gene, reduced *Hoxa2* gene expression could be due to direct blocking of the binding of transcription factors to methylated CpG sites (Mohn et al., 2008). Alternatively, binding of methyl-CpG-binding proteins to methylated CpG sites (Widschwendter et al., 2007) on the gene promoter may block expression of the *Hoxa2* gene.

To investigate if DNA methylation played a general role in *Hoxa2* regulation, EG7 cells were also tested. This cell line does not express *Hoxa2* (Fig.4.2.1) and is highly methylated at all of the CpG sites on the *Hoxa2* promoter (Fig. 4.2.2). It was reasoned that treatment with 5-Aza, a DNA demethylating agent (Lemaire et al., 2008), may block methylation on the *Hoxa2* promoter and induce the cells to start expressing *Hoxa2*. However, exposure to VPA (200 µg/mL) or to 5-

Aza (2.3 µg/mL [10 µM]) did not change the DNA methylation status in any of ten CpG sites (CpG^{-617}, CpG^{-582}, CpG^{-577}, CpG^{-569}, CpG^{-551}, CpG^{-553}, CpG^{-540}, CpG^{-514}, CpG^{-509}, and CpG^{-492}) of CpG 1 island in EG7 cells (Fig.4.2.8). Since these CpG sites are already highly methylated it was expected that VPA would have little or no effect on DNA methylation but it was expected that 5 Aza would demethylate the CpG sites. A higher concentration of 5 Aza were toxic to the EG7 cells and 2.3 µg/mL [10 µM] is highest dose that has been used (Lemaire et al., 2008). Not surprisingly, exposure to 5 Aza at doses 0.23 µg/mL [1 µM] to 2.3 µg/mL [10 µM] or to VPA 80 µg/mL (0.56 mM) and 200 µg/mL (1.4 mM) also did not induce *Hoxa2* expression (Fig.4.2.8). Unfortunately, since 5 Aza had no effect on the DNA methylation status of the CpG island and no effect on *Hoxa2* expression it was difficult to conclude whether DNA methylation in general played a role in regulating *Hoxa2* expression.

5.6.3 CpG methylation status of the *Hoxa2* gene promoter in developing embryos

Specific DNA methylation patterns are essential for early embryogenesis (Li et al., 1992). Since *Hoxa2* gene expression begins in mice at E8 to E8.5 stage of development (Prince and Lumsden, 1994b), I wanted to examine the DNA methylation profile of the *Hoxa2* gene promoter in mouse embryos at stages E6.5, E8.5 and E10.5. Interestingly, all of the CpG sites on the three CpG islands [CpG island 1 (-277 to -620 bp); CpG island 2 (-919 to -1133 bp), and CpG island 3 (-1176 to -1301 bp)] of the *Hoxa2* promoter remained unmethylated in E8.5 and E10.5 embryos when *Hoxa2* gene expression is evident (Fig. 4.2.10, 4.2.11, 4.2.12). However in E6.5 embryos, the CpG island 1 that is closer to transcription start site revealed partially methylated CpG sites (methylated at CpG^{-551}, CpG^{-553}, CpG^{-540}, CpG^{-509}, and CpG^{-492}) while the CpG sites on both CpG island 2 and 3 remained unmethylated. This finding implies that methylation of CpG sites on island 1 may play a more prominent role in *Hoxa2* gene regulation. Pyrosequencing revealed percent methylation of all 10 CpG sites (CpG^{-617}, CpG^{-582}, CpG^{-577}, CpG^{-569}, CpG^{-551}, CpG^{-553}, CpG^{-540}, CpG^{-514}, CpG^{-509}, and CpG^{-492}) on CpG island 1 in E6.5 embryos were higher than at E8.5 and E10.5. As CpG island 1 is closest to *Hoxa2* transcription start site and the most affected, differential DNA methylation status at this site between E6.5 and E8.5/E10.5 suggest a potential role for DNA methylation of CpG island 1 in regulating *Hoxa2* gene expression during the mouse embryonic development. The methylated status of several

CpG sites (methylated at CpG^{-551}, CpG^{-553}, CpG^{-540}, CpG^{-509}, and CpG^{-492}) on CpG island 1 in embryos at E6.5, may be one mechanism for transcriptional silencing of *Hoxa2* expression.

5.6.4 Effect of VPA on CpG methylation status of *Hoxa2* gene promoter in developing embryos

Bisulfite sequencing of *Hoxa2* gene promoter in E10.5 embryos exposed to VPA revealed methylation at CpG^{-551}, CpG^{-553}, CpG^{-540}, CpG^{-509}, and CpG^{-492} sites of CpG island 1 (Fig. 4.2.13). However, pyrosequencing data revealed increased percent DNA methylation at all 10 CpG sites of CpG island 1 (from CpG^{-492} to CpG^{-617}) although these only reached significance at CpG^{-617}, CpG^{-582}, CpG^{-577}, CpG^{-569}, CpG^{-551}, CpG^{-553}, CpG^{-540} sites when compared to untreated control embryos (Fig 4.2.14), ranging from 1-20%. VPA exposure also inhibits *Hoxa2* expression in these embryos (Fig.4.1.7), hence VPA induced methylation of the CpG sites on island 1 may be involved in the transcriptional silencing of *Hoxa2*. Interestingly, similar DNA methylation profile at CpG island 1 in E6.5 embryos when *Hoxa2* gene is not expressed does lend support to the suggestion that CpG island 1 may play a critical role in transcriptional silencing of *Hoxa2* expression. Although VPA is well known for its HDAC inhibitory properties (Phiel et al., 2001) this is the first time it has been demonstrated to induce DNA methylation. Hence, VPA appears to have dual role as a HDAC inhibitor and induction of DNA methylation in regulating gene expression.

5.6.5 Effect of VPA on enrichment of DNA methyltransferases in NIH3T3 cell line and in E10.5 mouse embryos

Since VPA induced methylation of specific CpG sites on the *Hoxa2* promoter, it was interesting to find enrichment of the enzyme DNA methyltransferase 1(Dnmt1) at the CpG island 1 of *Hoxa2* promoter in both NIH3T3 cells exposed to VPA (Fig. 4.2.15a) and in E10.5 embryos treated with VPA (Fig. 4.2.15b). These findings in NIH3T3 cells and in the embryo, indicates that VPA induces hypermethylation by either directly or indirectly increasing the relative occupancy of Dnmt1 at the *Hoxa2* gene promoter. Although VPA induced hypermethylation

appears to play an important role in suppressing *Hoxa2* expression, the role of other transcription factors or the essential role of histone modifications cannot be excluded.

5.6.6 Bivalent chromatin domains associated with *Hoxa2* promoter in cell lines

To investigate if histone modifications had a role in regulating *Hoxa2* gene expression, qChIP-PCR was used to determine whether histone bivalent domains (H3K4 and H3K27 trimethylation) were enriched at the *Hoxa2* gene promoter. H3K4 and H3K27 trimethylation possess both activating and repressive effects respectively, on developmental genes (Bernstein et al., 2005). H3K4 and H3K27 methylation are catalyzed, respectively, by trithorax- and polycomb-group proteins, which mediate mitotic inheritance of lineage-specific gene expression programs and have key developmental functions (Ringrose and Paro, 2004). The enrichment of bivalent domains is associated with low-level of gene expression (Bernstein et al., 2005). Previous study also suggests that the trithorax complexes that methylate histone 3 at Lys 4 are associated with CpG-rich DNA (Ayton et al., 2004; Lee and Skalnik, 2005). My data revealed the bivalent domains, H3K27me3 and H3K4me3, were simultaneously associated at the CpG-rich DNA region of the *Hoxa2* promoter (Fig. 4.2.18). H3K27me3 and H3K4me3 co-occupied at *Hoxa2* gene promoter may provide an epigenetic mechanism that maintains expression or repression of *Hoxa2*. Hence it is possible that these bivalent domains together with DNA methylation play a role in regulation of *Hoxa2* gene expression. This was further investigated in developing embryos and in cell lines treated with VPA (see below).

5.6.7. VPA increased H3K27me3 and decreased H3K4me3 enrichment at the *Hoxa2* gene promoter in the NIH3T3 cell lines

NIH3T3 cells exposed to VPA had a differential effect on the H3K27me3 and H3K4me3 bivalent domain marks. The histone modification mark, H3K27me3 which suppresses gene expression, is significantly enriched at the *Hoxa2* gene promoter even at the lowest VPA concentration (Fig.4.2.19b). In contrast, the enrichment of the active histone modification mark, H3K4me3, was significantly reduced at all VPA doses relative to the control untreated group (Fig.4.2.19c). Interestingly, this dynamic change in bivalent domain marks appears to be dependent on the methylation status of the *Hoxa2* promoter. In the EG7 cells where *Hoxa2*

promoter is highly methylated and *Hoxa2* gene is not expressed (Figs. 4.2.1 and Fig. 4.2.3) there was no change in the H3K27me3 and H3K4me3 bivalent domain marks in wild type or VPA treated cells (Fig. 4.2.20). Generally, for chromatin domains over a gene promoter, an active domain mark (e.g H3K4me3) is defined by high transcriptional rates, whereas a repressive chromatin domain mark (e.g. H3K27me3) is characterized by low transcriptional rates (Rodriguez et al., 2008b). The observed increased enrichment of H3K27me3 and a corresponding decreased enrichment of H3K4me4 in the same region of *Hoxa2* gene promoter near the transcription start site may explain lower *Hoxa2* expression in NIH 3T3 cells treated with VPA. Hence this differential effect on the histone bivalent domain marks over the CpG island 1 of the *Hoxa2* promoter could have a role in *Hoxa2* gene regulation.

5.6.8 A dynamic transition of bivalent domains is associated with *Hoxa2* gene expression during the mouse development (E6.5-E10.5)

To gain further insights into the mechanism(s) that lead to initiation of *Hoxa2* expression in the developing embryos or in the transcriptional silencing of *Hoxa2* gene in mouse embryos treated with VPA, I first characterized bivalent domains of H3K27me3 and H3K4me3 at the *Hoxa2* promoter between E6.5 and E10.5. The chromatin profiling revealed the coexistence of active H3K4me3 and inactive domains H3K27me3 at the *Hoxa2* promoter. These results raise intriguing facts about the establishment and function of chromatin structure on *Hoxa2* gene during development. The enrichment of H3K27me3 at the *Hoxa2* gene promoter is significantly reduced in embryos at E8.5 and E10.5 compared to embryos at E6.5. In contrast, H3K4me3 is the significantly enriched at the same region of *Hoxa2* promoter in E8.5 and E10.5 compared to embryos at E6.5. The data suggest the transcriptional activation of *Hoxa2* gene occurs with change in transition of enrichment from H3K27me3 to H3K4me3 during mouse development from E6.5 to E10.5. Interestingly, a reverse change in transition following VPA treatment with a significantly higher relative occupancy of H3K27me3 (Fig. 4.2.25a) and a significantly lower relative occupancy of H3K4me3 (Fig. 4.2.25b) at the *Hoxa2* gene promoter in E10.5 embryos is observed and correlates with a reduction in *Hoxa2* expression (Fig. 4.1.7, Table 4.1.4). Similar change in the bivalent domains was also observed in VPA treated NIH3T3 cells when *Hoxa2* mRNA is down-regulated (Fig. 4.2.19). Hence the increased relative occupancy of H3K4me3

and a parallel relative decrease in H3K27me3 occupancy appear to be required for subsequent gene activation during development (Orlando et al., 1998; Schmitt et al., 2005). A similar observation also was observed in a recent study of the sequential epigenetic activation of *Hoxd* cluster in developing murine tail buds (Soshnikova and Duboule, 2009b). In this study, a highly dynamic equilibrium was identified where demethylation of H3K27 paralleled an increase in trimethylation of H3K4, along with progressive gene activation. The region of transition between these two chromatin states corresponds to the areas where *Hoxd* genes become transcriptionally active, and this expression region of *Hoxd* genes shifts from one end of the cluster to the other during gastrulation (Soshnikova and Duboule, 2009a; Soshnikova and Duboule, 2009b) .

5.6.9 Changes in histone bivalent domain marks and DNA methylation status after exposure to VPA appear to be involved in transcriptional silencing of *Hoxa2* gene

The gene regulatory mechanism is a complicated process that involves discriminatory actions of transcriptional factors as well as epigenetic modifications including DNA and histone modifications (Wilson et al., 2005). The bivalent domains of H3K4me3 and H3K27me3 were characterized at *Hoxa2* gene promoter, indicating the intermingled presence of active and inactive histone methylation marks associated with *Hoxa2* gene transcriptional activity.

For transcription-related chromatin modifications that occur at specific gene promoters, an active domain is defined by high transcriptional rates, whereas the repressive chromatin domain is characterized by low transcriptional rates (Rodriguez et al., 2008a). The CpG island 1 is where the bivalent domains were identified and may play a crucial role in epigenetic regulation of *Hoxa2* gene expression. In the mouse embryos at E8.5 that have active *Hoxa2* gene expression, the CpG island 1 is very likely associated with active chromatin domains, which is featured by active transcription of *Hoxa2* mRNA, unmethylated CpG sites, high levels of transcriptional active histone modification H3K4me3 and low levels of transcriptional repressive histone modification H3K27me3. In contrast, the same region in embryos at E6.5 that has an inactive chromatin domain is defined by DNA hypermethylation, low enrichment of H3K4me3 and high levels of H3K27me3 enrichment leading to transcriptional silencing of *Hoxa2* gene.

The VPA-dose-dependent increased enrichment of H3K27me3 at the *Hoxa2* gene promoter suggested the components of the polycomb protein groups could be mediating, at least in part,

the silencing *Hoxa2* gene expression following VPA treatment. The reduction in enrichment of H3K4me3 at the *Hoxa2* gene was not as much affected in a VPA concentration dependent manner. Hence, transcriptional inhibition of *Hoxa2* gene expression after VPA treatment could be the result of changes in enrichment of bivalent domains and DNA hypermethylation at the gene promoter.

5.6.10 Enrichment of Ezh2 at the *Hoxa2* gene promoter

The PcG protein Ezh2 is a histone methyltransferase and catalyses the formation of H3K27 trimethylation (H3K27me3) (Cao et al., 2002; Czermin et al., 2002; Kuzmichev et al., 2002; Muller et al., 2002), resulting in the subsequent recruitment of additional PcG proteins contributing to the formation of a repressive chromatin state (Cao et al., 2002; Czermin et al., 2002; Kuzmichev et al., 2002). Treatment with VPA resulted in an increase in relative occupancy of Ezh2 at the *Hoxa2* gene promoter in E10.5 embryos *in vivo* and in NIH3T3 cells *in vitro*, which is in concordance with the higher enrichment of the H3K27me3 mark at this region when *Hoxa2* expression is downregulated.

In addition to Ezh2, DNMTs are also key epigenetic regulators involved in transcriptional repression by inducing promoter DNA methylation (Bachman et al., 2003; Fuks et al., 2000; Fuks et al., 2001). My data demonstrates that VPA induced increased binding capacity of Dnmt1, in agreement with the increased DNA methylation status at the *Hoxa2* gene promoter.

EZH2 is reported to associate with both the amino-terminal and carboxy-terminal regions of DNMTs (Vire et al., 2006). *In vivo* immunoprecipitation experiment (Vire et al., 2006) showed endogenous EZH2 precipitated with endogenous DNMT1, DNMT3A and DNMT3B. These results suggest that EZH2 associates with DNA methyltransferase activity, and interacts with DNMTs in components of PRC2/3 complexes (Vire et al., 2006). To test whether silencing of *Hoxa2* gene requires both Ezh2 and DNA methyltransferase, I performed chromatin immunoprecipitation assays. An increase in occupancy of Ezh2 and H3K27me3 at *Hoxa2* promoter after VPA coincided with a significant increase in DNMT1 binding to the *Hoxa2* promoter. Interestingly, VPA treatment in EG7 cells that have completely methylated CpG sites on the *Hoxa2* promoter did not impact binding of H3K27me3 at *Hoxa2* promoter. Taken together, it can be reasoned that the binding of Ezh2 may be necessary for binding of DNMT1 to the

unmethylated *Hoxa2* promoter. In contrast, in methylated *Hoxa2* promoter (e.g EG7 cells) Ezh2 or H3K27me3 binding is not required.

Next, I wanted to determine whether Ezh2 might influence DNA methylation status at the *Hoxa2* gene promoter. A number of CpG sites (CpG^{-551}, CpG^{-553}, CpG^{-540}, CpG^{-509}, and CpG^{-492}) located within the CpG island 1 were significantly methylated in VPA treated groups where higher level of Ezh2 was induced. These results may imply that Ezh2 is needed for CpG methylation of Ezh2-target *Hoxa2*. Our data suggest that PcG protein Ezh2 may be important in regulating CpG methylation through perhaps direct contact with DNMT1.

We can further speculate that the alteration of Ezh2-mediated H3K27 trimethylation and DNMT1 binding status induced by VPA may work together as part of an epigenetic program integrating *Hoxa2* gene-silencing. Other similar studies have also revealed that silencing of *MYT1* gene expression requires both EZH2 and DNA methyltransferases, and the association of EZH2 is necessary for binding of DNA methyltransferases to EZH2-target promoters (Vire et al., 2006). VPA enriched to a high level the inactive chromatin domain mark H3K27me3 and increased CpG methylation at *Hoxa2* promoter near transcription start site. This could inhibit the transcription regulator binding at the *Hoxa2* promoter, as a consequence, repressing *Hoxa2* gene transcription (Fig.5.4).

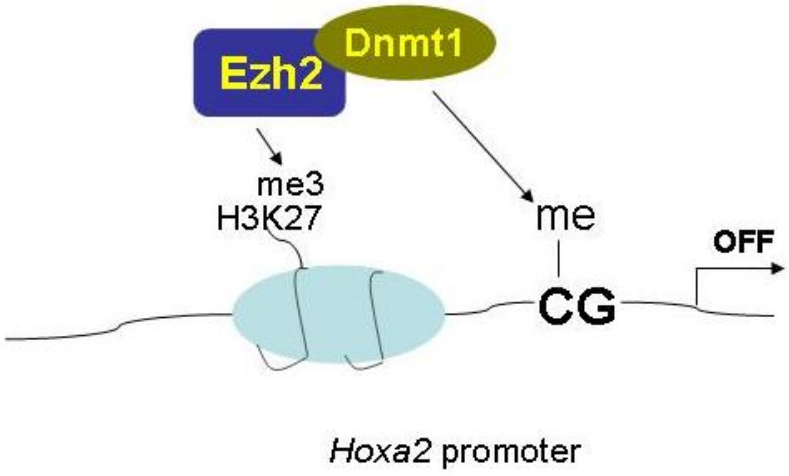

Fig.5.4 Ezh2 may be needed for binding of DNA methyltransferase (Dnmt1) and facilitates CpG methylation of Ezh2-target *Hoxa2* promoter through contact with Dnmt1

VPA acts to repress *Hoxa*2 expression

i) Histone acetylation plays an important role in chromatin modification and regulate gene transcription (Struhl, 1998). In general, histone acetylation by histone acetyltransferases loosens chromatin packaging and is associated with transcriptional activation, whereas histone deacetylation by HDACs is correlated with transcriptional repression (Struhl, 1998). Histone acetylation is a dynamic process and the acetylation level is determined by the balance of the activities between acetyltransferases and HDACs (Qiao et al., 2006). However, recent studies have indicated that histone deacetylation can also associate with transcriptional activation in certain genes (Nusinzon and Horvath 2005). VPA and other HDAC inhibitors generally increase histone acetylation by inhibiting HDAC activity. However, it has recently been reported that inhibition of HDAC activities also suppresses certain gene expression such as c-myc, interleukin-2 (IL-2), IL-8, and leucocyte-phosphotyrosine phosphatase (LC-pTP) (Gurvich and Klein 2002; Huang et al., 1997; Takahashi et al., 1996; Van Lint et al., 1996). HDAC inhibitors TSA or trapoxin could upregulate or downregulate gene expression (Van Lint et al., 1996). Therefore, HDAC inhibitors modulate gene transcription either positively or negatively in a gene-specific manner (Qiao et al., 2006).

VPA directly inhibits class I and II HDACs (Gottlicher et al., 2001; Gurvich et al., 2004; Phiel et al., 200;). Our study showed that VPA directly suppress *Hoxa2* expression. However, further studies need to be carried out to determine whether VPA increases in acetylation of both histones H3 and H4, and activities of HDAC1 and polymerase II at the *Hoxa2* locus change in response to VPA to investigate whether inhibition of HDAC activity is directly correlated with VPA-induced down-regulation of *Hoxa2* expression in cells and developing embryos.

ii) The general conclusion from our current study is that both active (H3K4me3) and repressive (H3k27me3) epigenetic marks together dictates the levels of *Hoxa2* mRNA expression in the developing embryo and cell line. DNA hypermethylation together with repressive histone modification (H3K27me3) dictate the silencing or extreme reduction in *Hoxa2* expression in mouse developing embryos and NIH3T3 fibroblast cells treated with VPA. When VPA was applied to embryos and NIH3T3 cells, it changed the bivalent chromatin pattern at the *Hoxa2* promoter. Our results are consistent with a recent study that showed global expression levels of the HOXA cluster genes during H9hESC differentiation where lower gene expression correlates

with the poorer enrichment of histone modification marks generally associated with active gene transcription (H3K4 trimethylation, dimethylation, and H3/H4 acetylation) (Atkinson et al., 2008).

The H3K27 trimethylation regulated by the PRC2 complex serves as a recruitment signal for the other polycomb complex, PRC1, whose core component (PC) recognizes H3K27me3 through its chromodomain (Min et al., 2003). Although the transcriptionally repressive role for PcG is well established, the precise molecular mechanisms by which silencing are achieved at PcG-target genes are not fully understood (reviewed by Sparmann and van Lohuizen, 2006). The *in vitro* interactions between EZH2 and DNA methyltransferases http://bloodjournal.hematologylibrary.org/content/112/9/3889.long - ref-20#ref-20 (Vire et al., 2006), and between EED (another core component of the PRC2 complex) and HDACs (van der Vlag and Otte 1999) suggests that both DNA methylation and histone deacetylases have been associated with polycomb-mediated silencing (Garrick et al., 2008). Recent work has also linked PRC2 to DNA methylation in neuronal development and differentiation in mice (Mohn et al., 2008; Schlesinger et al., 2007). In this study, I demonstrate that although the PRC2 complex (as indicated by Ezh2) and DNMT1 were increased in response to VPA in the developing embryos and NIH3T3 fibroblast cells, Ezh2 and DNMT1 proteins co-occupy the same promoter sites of *Hoxa2*, and transcription may be down-regulated via recruitments of both DNA methyltransferase and histone methyltransferase proteins. Moreover, this may indicate that epigenetic repressors (MBD and most likely others) form a large complex that cooperatively participates in regulation of *Hoxa2* gene expression. However, the mechanisms of recruitment and their precise interactions between Ezh2 and DNMT needs further characterization.

iii) Lastly, although the DNA sequence elements responsible for binding of PcG complex (Polycomb response elements, PREs) have not yet been identified in mammals (Garrick et al., 2008), the PRE elements are included within promoter CpG islands, and the associations between PREs and CpG islands have been reported by some studies (Roh et al., 2006; Tanay et al., 2007). Furthermore, bioinformatic analyses suggested that binding of PRC2 is partially influenced by the structural characteristics of the CpG islands (Garrick et al., 2008). It is more likely that genomic factors other than DNA sequence may also be associated with PcG

recruitment at *Hoxa2* gene. It can also be hypothesized that VPA treatment may also alter signal pathway(s) or transcription factor(s) and thereby inhibit *Hoxa2* gene transcription.

5.6.11 Ascorbic acid decreased DNA methylation at *Hoxa2* gene promoter in NIH 3T3 cells treated with VPA

It is possible that ascorbic acid may exert a protective effect through epigenetic modifications, particularly since treatment with ascorbic acid can restore *Hoxa2* gene expression following VPA exposure. To test this possibility, we investigated the effect of ascorbic acid on DNA methylation status at the *Hoxa2* gene promoter after treatment of NIH3T3 cell line with VPA. Interestingly, ascorbic acid significantly decreased DNA methylation by 30-47% at CpG^{-551}, CpG^{-553}, CpG^{-540}, CpG^{-509}, and CpG^{-492} that were hypermethylated following VPA treatment (Fig.4.2.7).

Fuso et al., (2005) analyzed levels of methylation of CpG islands on the promoter of the *APP* and the *PSEN1* genes in human cell lines, observing that in conditions of folate and vitamin B-12 deficiency, there was a variation in the methylation status of the PSEN1 promoter, with a subsequent deregulation of the production of PSEN1, BACE (the β-secretase) and APP proteins (Fuso et al., 2005). This study confirmed that some of the genes responsible for the production of Aβ fragments in Alzheimer's disease (AD) can be regulated through an epigenetic mechanism depending on the cellular availability of folate and vitamin B-12, and affected the production of S-adenosyl methionine (SAM) and the status of methylation of CpG islands in the DNA (Fuso et al., 2005).

Furthermore, prenatal or early life dietary and environmental exposures can have a profound effect on our epigenome, resulting in birth defects and diseases developed later in life (Reamon-Buettner and Borlak, 2007). Epigenetic changes in DNA methylation can impact both gene transcription and the ability to repair damaged DNA (Reamon-Buettner and Borlak, 2007). Similarly, my data demonstrate that VPA induces oxidative stress by reducing GSH content and increases DNA methylation at *Hoxa2* promoter. Ascorbic acid reversed oxidative stress, maintaining GSH homeostasis, hence normalizing DNA methylation at the *Hoxa2* gene promoter, preventing silencing of *Hoxa2* gene expression.

5.6.12 Ascorbic acid decreased H3K27me3 and increased H3K4me3 enrichment at *Hoxa2* gene promoter in NIH3T3 cells treated with VPA

We also examined the effect of ascorbic acid on histone bivalent domains. Ascorbic acid also reduced the enrichment of H3K27me3, whereas it increased the relative occupancy of H3K4me3 at the *Hoxa2* gene promoter. Recently, Hitchler et al., (2006) proposed a link between epigenetic regulation and transcriptional silencing of genes important in determining ROS levels such as *superoxide dismutase 2* (*SOD2*) (the antioxidant gene encoding manganese superoxide dismutase). An epigenetic perspective of the free radical theory of development was proposed (Hitchler and Domann, 2007) where increased GSH production influences epigenetic processes including DNA and histone methylation by limiting the availability of S-adenosylmethionine, an important cofactor utilized by DNA and histone methyltransferases during epigenetic control of gene expression (Hitchler and Domann, 2007).

VPA induces dysmorphogenesis and birth defects in mouse embryos possibly through altering the DNA methylation and the association of histone bivalent domains at the *Hoxa2* gene promoter, and ascorbic acid reverses this epigenetic alteration and protects the embryos from VPA induced toxicity (Fig.5.4).

5.7 Oxidative stress associated telomerase and telomere dysfunction

5.7.1 *Tert* expression is deregulated by VPA

Although knowledge of telomeres from cultured human cells has expanded, less is known about the biology of telomeres *in vivo*. We have used a mouse cell line and mouse embryos to investigate the effects of oxidative stress induced by VPA on telomere length and telomerase activity, and the effect of altered telomere length and telomerase activity on embryonic growth. In general, there is a close correlation between expression of the telomerase catalytic subunit (TERT) and telomerase activity (Liu, 1999). Most differentiated human somatic cells do not have *TERT* expression and telomerase activity, whereas germ cells, some stem cells, and a majority of cancers demonstrate both telomerase activity and *TERT* expression. In contrast, many tissues of adult rodents show abundant *Tert* expression and telomerase activity (Golubovskaya et al., 1997; Martin-Rivera et al., 1998; Miura et al., 1998; Yamaguchi et al., 1998). We first

examined *Tert* expression and observed a low level of telomerase activity in NIH3T3 cells and the mouse embryos. However, the reduced telomerase activity in VPA treated cells and embryos were accompanied by an increase in the abundance of *Tert* mRNA, indicating that posttranscriptional mechanisms could be involved in the VPA-regulated *Tert* expression as VPA is known as a histone deacetylase inhibitor. The upregulation of *Tert* expression by VPA may be through epigenetic mechanisms of histone or DNA modifications.

Santos et al., (Santos et al., 2004, 2006) have reported that ectopically expressed *TERT* in human fibroblasts under acute oxidative stress results in increased mitochondrial DNA damage. However, one study pointed out cells that overexpress *TERT* showed evidence for improved mitochondrial function, specifically less mitochondrial superoxide production and lower levels of cellular ROS, improved mitochondrial coupling and suppressed retrograde response (Ahmed et al., 2008). Our data showed that VPA caused overexpression of *Tert*, at the same time, induced oxidative stress as the result of reduced total glutathione and elevated GSSG/GSH ratio both *in vivo* and *in vitro*.

5.7.2 Oxidative stress-mediated telomerase and telomere dysfunction

It had been noted that increased oxidative stress accelerated telomere shortening even in telomerase-positive cells (Furumoto et al., 1998; von Zglinicki, 2002). Our results show that VPA induced oxidative stress interferes with telomere length and maintenance at two levels: 1) increases the rate of telomere shortening, and 2) prevents telomerase from counteracting telomere shortening by reducing telomerase activity.

Telomerase maintains a normal telomeric length after many cellular divisions and plays a key role in cellular homeostasis (Brown et al., 2007). We found VPA reduced telomerase activity, and also, depleted the total glutathione content and increased GSSG/GSH ratio. This decrease in telomerase activity could result from VPA-induced alterations in glutathione and thiol metabolism. Some studies (Brown et al., 1998; Brown et al., 2003; Brown et al., 2007) have demonstrated an increase in telomerase activity observed in the iron-loaded livers is accompanied by elevated levels of cysteine, γ-glutamyl cysteine, and glutathione as well as increased activity of rate-limiting enzyme glutamate cysteine ligase. (Brown et al., 2007)

Moreover, in cultured fibroblasts, telomerase activity is enhanced by a high ratio of GSH/GSSG, whereas activity is decreased after treatment with buthionine sulfoximine, an inhibitor of glutathione synthesis (Borras et al., 2004; Hayakawa et al., 1999). Consistent with these data, VPA may decrease the availability of reduced thiols, resulting in reduced telomerase activity. Although the data indicate telomerase activity in VPA treated cells and embryos is sensitive to modulatation by thiol redox state, this does not exclude the possibility that other mechanisms contribute to the reduction of telomerase activity exposed to VPA. Phosphorylation of human TERT by Akt/protein kinase B and protein kinase C has been implicated in nuclear translocation of TERT via interactions with NF-κB (Akiyama et al., 2002; Akiyama et al., 2003). It is likely that the glutathione redox potential may be important for maintaining the cysteine residue in a reduced state. Our results here indicate that telomerase is regulated by changes in glutathione redox potential following exposure to VPA (Borras et al., 2004).

We next measured telomere length in cells and embryos treated with VPA using quantitative real-time PCR. The relative average telomere length was assessed by a modified version of real-time PCR-based method, in which the telomere repeat copy number to single gene copy number (β-globin) ratio (T/S) was determined (Cawthon, 2002; McGrath et al., 2007). Treatment with VPA induced telomere length shortening in developing embryos compared to the untreated control. Moreover, the reduced telomerase activity can directly accelerate telomere shortening, which is a consequence of oxidative stress induced by VPA treatment.

Two major pathways have been proposed to lead to senescence, telomere shortening and oxidative stress-mediated cellular damage. Particularly, in fibroblast cells it has been reported that oxidative stress could cause telomere shortening due to 1) the high and very susceptible guanine content of the telomeres, and 2) the deficiency of telomeric DNA in repairing of single-stranded breaks (Erusalimsky and Kurz, 2005; Houben et al., 2008; Kawanishi and Oikawa, 2004; Passos and Von Zglinicki, 2006; von Zglinicki, 2002).

In summary, we have shown that histone methyltransferase Ezh2 is a novel target showing increased binding capacity at *Hoxa2* promoter induced by VPA, resulting in increased repression by histone mark H3K27me3 at *Hoxa2* promoter. Two groups of proteins (TrxG and PcG) have been implicated with histone bivalent domains (H3K4me3 and H3K27me3) in maintaining chromatin structure (Mahmoudi and Verrijzer, 2001; Simon and Tamkun, 2002). The PcG

protein, EZH2, is implicated in chromosome remodeling (Jones *et al.*, 1998; Sewalt *et al.*, 1998). Methylation of the histone H3 N-terminal tail causes stable changes in chromatin that define the status of gene expression (Strahl and Allis, 2000; Kouzarides, 2002). In the absence of telomerase activity, telomeres gradually shorten because of the inability of the DNA replication machinery to completely duplicate chromosome ends (Friedman, 2011). A novel VPA-induced mechanism for teratogenecity is proposed through epigenetic-mediated *Hoxa2* gene repression and VPA-induced oxidative stress. In addition, as telomerase activity is associated with senescence and oxidative stress, it can be speculated that decreased telomerase activity and telomere shortening may be involved in the regulation of VPA-induced developmental defects.

CHAPTER 6: CONCLUSION

Many anticonvulsant drugs are teratogenic to the embryo and fetus when exposed *in-utero* (Diav-Citrin et al., 2008; Kultima et al., 2004; Morrow et al., 2006; Ornoy, 2003). My results demonstrate that VPA, a clinically used anticonvulsant drug, inhibits embryonic organ differentiation and development in the whole mouse embryo culture system in the therapeutic dose range 50 to 100 μg/mL (0.35 mM to 0.7 mM). The scoring parameters measured in the assessment of embryonic development including yolk sac circulation, allantois, caudal neural tube, forebrain, and branchial arches have shown lower scores in the embryos treated with VPA, indicating these embryonic organs are particularly sensitive to VPA insult. Several mechanisms have been proposed for VPA induced teratogenicity including folic acid deficiency, oxidative stress, and inhibition of histone deacetylase (Tabatabaei and Abbott, 1999; Weber et al., 1991; Wegner and Nau, 1991, Wiltse, 2005). Our data from *in vitro* and *in vivo* studies suggests VPA induces depletion of GSH and increases the GSSG/GSH ratio, reflecting an increase in oxidative stress. In addition, a dose-dependent inhibition of *Hoxa2* gene expression after VPA treatment was also observed. *Hox* genes are embryonic developmental genes encoding transcription factors. They are key controllers of rostrocaudal patterning in early embryogenesis, particularly of hindbrain segmentation and rhombomere identity (Cordes, 2001; Lumsden, 2004). *Hoxa2* gene is the only *Hox* gene expressed at the level of hindbrain rhombomere 2 (r2) in the neuroectoderm. It plays a crucial role as a selector gene in determining second arch fates and imposes the unique identity of second arch structures (reviewed by Trainor and Krumlauf 2001; Santagati et al. 2005). Moreover, children affected by VPA develop a typical "fetal valproate syndrome" (FVS). Features include intrauterine growth restriction (IUGR) and facial dysmorphism such as mid-facial hypoplasia, short nose with a broad nasal bridge, cleft palate and cleft lips (Dean et al., 2000; DiLiberti et al., 1984). These facial features of FVS are suggestive of neural crest involvement in the pathogenetic mechanism (Fuller et al. 2002). Inhibition of *Hoxa2* gene likely affects pattern formation in the branchial arch region (Santagati et al. 2005). These evidences suggest that VPA-induced inhibition of *Hoxa2* gene expression may play an important role in its teratogenicity. To delineate a relationship between VPA, oxidative stress and *Hoxa2*, total glutathione levels were measured in *Hoxa2*-/- embryos. Results suggest that glutathione levels are not altered in *Hoxa2*-/- embryos. Interestingly, treatment with ascorbic acid just prior to VPA

exposure prevented VPA-induced downregulation of *Hoxa2* gene expression in concert with enhanced glutathione status, indicating VPA-induced inhibition of *Hoxa2* is downstream of the VPA-induced depletion of glutathione. Moreover, the telomerase activity and telomere length are both regulated by changes in glutathione redox potential induced by VPA. As a consequence of oxidative stress induced by VPA, the reduced telomerase activity can directly accelerate telomere shortening. Telomere and telomerase dysfunction can lead to cellular apoptosis and senescence. This could be one of the mechanisms of VPA induced developmental malformations in mouse embryos.

Next, to determine if VPA is a direct epigenetic modulator regulating *Hoxa2* gene expression, the effect of VPA on dynamic changes of transcription-associated histone trimethylation bivalent domains (H3K4me3 and H3K27me3) and DNA methylation status at *Hoxa2* gene promoter was investigated. It has been reported that in ES cells *Hox* gene promoters often display both H3K4me3 active and H3K27me3 repressive marks, which are referred to as 'bivalent domains'. Bivalent marks are mostly enriched at GC-rich promoters (Mikkelsen et al., 2007) where they may prevent DNA methylation and silencing in stem cells (Mohn et al., 2008). This equilibrium of active and repressive marks may maintain genes in a poised state, ready for rapid activation during cell differentiation (Azuara et al., 2006; Bernstein et al., 2006).

Characterization of the DNA methylation and bivalent domain status at *Hoxa2* gene promoter was undertaken in the developing mouse embryos at E6.5, E8.5 and E10.5. Results showed that the higher percentage of DNA methylation of *Hoxa2* gene promoter occurs at E6.5 and E8.5 compared to E10.5, which corresponds to the *Hoxa2* transcription level since *Hoxa2* gene expression initiates at E8.0 (Prince and Lumsden, 1994). The increased level of H3K27me3 and reduced H3K4me3 at *Hoxa2* promoter are also associated with the transcription of *Hoxa2* gene expression in the developing embryo between E6.5 and E10.5.

We next investigated whether VPA altered the status of these bivalent domains. I performed ChIP real-time PCR (qChIP-PCR) to quantitate the enrichment of H3K27me3 and H3K4me3 at the *Hoxa2* promoter. Treatment of NIH3T3 cell line and mouse embryos with VPA induced a significant increased enrichment of H3K27me3 and a significantly decreased enrichment of H3K4me3 at the *Hoxa2* promoter. The VPA-dose-dependent increased enrichment of H3K27me3 at the *Hoxa2* gene promoter suggested the components of the polycomb protein

groups could be mediating, at least in part, the silencing *Hoxa2* gene expression following VPA treatment. The reduction in enrichment of H3K4me3 at the *Hoxa2* gene was not as much affected in a VPA concentration dependent manner. Transcriptional inhibition of *Hoxa2* gene expression after VPA treatment could be the result of changes in enrichment of bivalent domains and DNA hypermethylation at the gene promoter.

My study also shows direct changes in chromatin status at CG-rich *Hoxa2* gene promoter both *in vivo* and *in vitro* after VPA treatment. Additionally, increased CpG methylation induced by VPA was found to be associated with dynamic changes of bivalent domains in the same *Hoxa2* promoter region. Thus, it appears that alteration of histone bivalent domains and increased DNA methylation cooperate with each other, serving important roles in VPA transcriptional silencing of *Hoxa2* gene. Interestingly, the presence of ascorbic acid prevented an increase in H3K27me3 and a decrease in H3K4me3 enrichment induced by VPA at *Hoxa2* gene promoter, and reduced higher level of DNA methylation induced by VPA both *in vivo* and *in vitro*. Taken together, this is the first study to assess the effects of VPA on oxidative stress as indicated by GSSG/GSH ratio, histone bivalent domains and DNA methylation status at *Hoxa2* gene promoter. Our results suggest that responses of ascorbic acid involving upregulation of glutathione level as well as blocking the epigenetic events occurring at *Hoxa2* gene promoter, normalizing *Hoxa2* gene expression in the presence of VPA, may represent an important protective mechanism against VPA-induced teratogenicity in the mouse embryos.

CHAPTER 7: FUTURE DIRECTIONS

Epigenetics provides stability and diversity to the cellular phenotype through chromatin marks that affect local transcriptional activity. Epigenetic marks are preserved or regenerated during cell division and embryonic development. The complex time/space patterns of gene expression necessary for normal development are likely to require multiple epigenetic signals (Bonasio et al., 2010).

We have demonstrated H3K27me3 and H3K4me3, the bivalent domain, were localized on *Hoxa2* gene promoter and affect the transcriptional level of *Hoxa2* gene. As H3K4me3 is associated with RNA Pol II, it is necessary to further investigate how H3K27me3 cooperates with H3K4me3 to regulate the initiation of gene transcription on *Hox* gene clusters. How are bivalent domains timely patterned on the gene promoter, and associated with RNA Pol II to exert the effect on gene expression during embryonic development?

H3K9 is a substrate for both acetylation and methylation. Acetylation of H3K9 correlates with activation of gene expression (Agalioti et al., 2002). In contrast, methylation of H3K9 can lead to the recruitment of silencing proteins (Bannister et al., 2001; Lachner et al., 2001) and is directly linked to DNA methylation in a number of human cell lines (Esteve et al., 2006). Since the acetylation of H3K9 precludes methylation, it would be interesting to investigate the effect of VPA on modification status of H3K9 associated with bivalent domains. In this case, the action of TrxG protein MLL1 in the *Hox* loci may generate and stabilize a pattern of chromatin modifications (H3K4me3) required for *Hox* gene expression.

Progress has been made in understanding the versatile role of PcG proteins, especially PRC2 protein. PRC is not only involved in the regulation of a broad array of biological processes, but it also establishes regulatory cues that are stable and propagated throughout embryonic development (Margueron and Reinberg, 2011). Previous studies have demonstrated PRC2 must be targeted to chromatin by a coordinated and intricate process to maintain the repression of different sets of genes dependent on cell types and developmental stages. These steps may require specific DNA sequences, non-coding RNA (nc RNA) and the chromatin structure proteins associated with its target genes (Margueron and Reinberg, 2011). Answering the questions such as: how ncRNA can recognize defined genomic locations? What is the exact

mechanism by which histone methyltransferase Ezh2 and histone demethylase JARID2 proteins contribute to PRC2 recruitment, will provide a future direction for pinpointing the aspects of PRC2-mediated processes on *Hoxa2* gene promoter.

Studies developed during the last two decades have also shown the importance of GSH during the process of mammalian chromatin sperm decondensation (Maeda et al., 1998; Perreault et al., 1984; Romanato et al., 2005). The alteration of nuclear redox conditions modulates chromatin conformation and stability (Markovic et al., 2010). Oxidants induce degradation of higher ordered chromatin structures (Bai and Konat, 2003). Oxidation of chromatin affects interaction between nucleosomes and the levels of reducing agents in the nucleus (Tas and Walford, 1982). However, the overall redox mechanisms that may regulate all these events remain unknown, although it has been speculated that ROS generation induced by a shift in the redox status of cells could affect gene expression by altering chromatin conformation (Hitchler and Domann, 2007).

Glutathione is closely connected with epigenetic mechanisms. Indeed, synthesis of S-adenosylmethionine (SAM) by SAM synthetases is a redox regulated process that depends on the GSH/GSSG ratio. When cells are depleted of glutathione by chemical means, methyl donors become deficient, leading to genome-wide DNA hypomethylation (Lertratanangkoon et al., 1996; Lertratanangkoon et al., 1997). However, we found VPA induced oxidative stress and also increased DNA methylation at *Hoxa2* gene. There could be other mechanisms related to VPA-induced hypermethylation at *Hoxa2* gene. Therefore, it will provide valuable insight to showing chromatin remodeling events occurring or directly linking histone modification with GSH depletion induced by oxidative stress.

Telomere attrition is modulated by oxidant-antioxidant balance (Saretzki, 2009). GSH is the most abundant non-protein thiol in most cells. The thiol moiety of GSH is important in antioxidant defense metabolism (Ketterer 1982; Meister 1983; Ziegler 1985). The response of a cell to an oxidative stress often involves changes in thiol content, and is then replaced through either enzymatic reduction of a disulfide, or by *de novo* synthesis. These changes in thiol content and metabolism can have effects on signaling pathways (Arrigo 1999; Dickinson and Forman 2002). We have shown the changes in telomerase activity by VPA associated with VPA-induced decreases in glutathione and thiol status (Fig.4.1.2, Fig. 4.1.5, Fig. 4.1.6, Fig. 4.1.8). Further

studies are needed to determine whether VPA-induced dysfunction in telomerase activity modulates apoptosis, and what is the enzyme machinery?

Telomerase regulation is complex and has prominent consequences not just for telomere length, but also for the development of many diseases (Koziel et al., 2011). Obtaining further insight into the role of telomerase gene regulation and therefore telomerase activity in disease development will assist in the generation of clinical therapies (Koziel et al., 2011). More recently, regulation of telomerase activity has been found not only to be controlled at the TERT transcriptional level, but also determined at the post-transcriptional level (Liu et al., 1999). Phosphorylation and nuclear translocation both play an important role in the post-transcriptional regulation of telomerase (Liu et al., 2001; Zhu et al., 2011). Therefore, understanding how telomerase is regulated at the epigenetic level will lead to improved targeting of telomerase as a therapy for genetic diseases and cancers.

CHAPTER 8: REFERENCES

Adab, N., Tudur, S. C., Vinten, J., Williamson, P., Winterbottom, J., 2004. Common antiepileptic drugs in pregnancy in women with epilepsy. Cochrane Database Syst Rev. CD004848.

Adimoolam, S., Sirisawad, M., Chen, J., Thiemann, P., Ford, J. M., Buggy, J. J., 2007. HDAC inhibitor PCI-24781 decreases RAD51 expression and inhibits homologous recombination. Proc Natl Acad Sci USA. 19482-7.

Agalioti, T., Chen, G., Thanos, D., 2002. Deciphering the transcriptional histone acetylation code for a human gene. Cell. 111**,** 381-92.

Ahmed, S., Passos, J. F., Birket, M. J., Beckmann, T., Brings, S., Peters, H., Birch-Machin, M. A., von Zglinicki, T., Saretzki, G., 2008. Telomerase does not counteract telomere shortening but protects mitochondrial function under oxidative stress. J Cell Sci. 121**,** 1046-53.

Akin, Z. N., Nazarali, A. J., 2005. Hox genes and their candidate downstream targets in the developing central nervous system. Cell Mol Neurobiol. 25**,** 697-741.

Akiyama, M., Hideshima, T., Hayashi, T., Tai, Y. T., Mitsiades, C. S., Mitsiades, N., Chauhan, D., Richardson, P., Munshi, N. C., Anderson, K. C., 2002. Cytokines modulate telomerase activity in a human multiple myeloma cell line. Cancer Res. 62**,** 3876-82.

Akiyama, M., Hideshima, T., Hayashi, T., Tai, Y. T., Mitsiades, C. S., Mitsiades, N., Chauhan, D., Richardson, P., Munshi, N. C., Anderson, K. C., 2003. Nuclear factor-kappaB p65 mediates tumor necrosis factor alpha-induced nuclear translocation of telomerase reverse transcriptase protein. Cancer Res. 63**,** 18-21.

Albani, F., Riva, R., Contin, M., Baruzzi, A., 1984. Valproic acid binding to human serum albumin and human plasma: effects of pH variation and buffer composition in equilibrium dialysis. Ther Drug Monit. 6**,** 31-3.

Allen, R. G., 1991. Oxygen-reactive species and antioxidant responses during development: the metabolic paradox of cellular differentiation. Proc Soc Exp Biol Med. 196**,** 117-29.

Allfrey, V. G., Faulkner, R., Mirsky, A. E., 1964. Acetylation and Methylation of Histones and Their Possible Role in the Regulation of Rna Synthesis. Proc Natl Acad Sci U S A. 51**,** 786-94.

Alonso-Aperte, E., Ubeda, N., Achon, M., Perez-Miguelsanz, J., Varela-Moreiras, G., 1999. Impaired methionine synthesis and hypomethylation in rats exposed to valproate during gestation. Neurology. 52**,** 750-6.

An, W., 2007. Histone acetylation and methylation: combinatorial players for transcriptional regulation. Subcell Biochem. 41**,** 351-69.

Ansari, K. I., Mandal, S. S., 2010. Mixed lineage leukemia: roles in gene expression, hormone signaling and mRNA processing. FEBS J. 277**,** 1790-804.

Aoki, F., Worrad, D. M., Schultz, R. M., 1997. Regulation of transcriptional activity during the first and second cell cycles in the preimplantation mouse embryo. Dev Biol. 181**,** 296-307.

Appanah, R., Dickerson, D. R., Goyal, P., Groudine, M., Lorincz, M. C., 2007. An unmethylated 3' promoter-proximal region is required for efficient transcription initiation. PLoS Genet. 3**,** e27.

Ardinger, H. H., Atkin, J. F., Blackston, R. D., Elsas, L. J., Clarren, S. K., Livingstone, S., Flannery, D. B., Pellock, J. M., Harrod, M. J., Lammer, E. J., et al., 1988. Verification of the fetal valproate syndrome phenotype. Am J Med Genet. 29**,** 171-85.

Armanios, M. Y., Chen, J. J., Cogan, J. D., Alder, J. K., Ingersoll, R. G., Markin, C., Lawson, W. E., Xie, M., Vulto, I., Phillips, J. A., 3rd, Lansdorp, P. M., Greider, C. W., Loyd, J. E., 2007. Telomerase mutations in families with idiopathic pulmonary fibrosis. N Engl J Med. 356**,** 1317-26.

Arndt, T. L., Stodgell, C. J., Rodier, P. M., 2005. The teratology of autism. Int J Dev Neurosci. 23**,** 189-99.

Artandi, S. E., Chang, S., Lee, S. L., Alson, S., Gottlieb, G. J., Chin, L., DePinho, R. A., 2000. Telomere dysfunction promotes non-reciprocal translocations and epithelial cancers in mice. Nature. 406**,** 641-5.

Artandi, S. E., DePinho, R. A., 2010. Telomeres and telomerase in cancer. Carcinogenesis. 31**,** 9-18.

Artlett, C. M., Black, C. M., Briggs, D. C., Stevens, C. O., Welsh, K. I., 1996. Telomere reduction in scleroderma patients: a possible cause for chromosomal instability. Br J Rheumatol. 35**,** 732-7.Atkinson, S. P., Koch, C. M., Clelland, G. K., Willcox, S., Fowler, J. C., Stewart, R., Lako, M., Dunham, I., Armstrong, L., 2008. Epigenetic marking prepares the human HOXA cluster for activation during differentiation of pluripotent cells. Stem Cells. 26**,** 1174-85.

Attene-Ramos, M.S., Kitiphongspattana, K., Ishii-Schrade, K., Gaskins, H.R., 2005. Temporal changes of multiple redox couples from proliferation to growth arrest in IEC-6 intestinal epithelial cells. Am J Physiol Cell Physiol. 289, C1220-8.

Aubert, G., Lansdorp, P. M., 2008. Telomeres and aging. Physiol Rev. 88**,** 557-79.

Augustine, K., Liu, E. T., Sadler, T. W., 1993. Antisense attenuation of Wnt-1 and Wnt-3a expression in whole embryo culture reveals roles for these genes in craniofacial, spinal cord, and cardiac morphogenesis. Dev Genet. 14**,** 500-20.

Autexier, C., Lue, N. F., 2006. The structure and function of telomerase reverse transcriptase. Annu Rev Biochem. 75**,** 493-517.

Ayton, P. M., Chen, E. H., Cleary, M. L., 2004. Binding to nonmethylated CpG DNA is essential for target recognition, transactivation, and myeloid transformation by an MLL oncoprotein. Mol Cell Biol. 24**,** 10470-8.

Azuara, V., Perry, P., Sauer, S., Spivakov, M., Jorgensen, H. F., John, R. M., Gouti, M., Casanova, M., Warnes, G., Merkenschlager, M., Fisher, A. G., 2006. Chromatin signatures of pluripotent cell lines. Nat Cell Biol. 8**,** 532-8.

Bachman, K. E., Park, B. H., Rhee, I., Rajagopalan, H., Herman, J. G., Baylin, S. B., Kinzler, K. W., Vogelstein, B., 2003. Histone modifications and silencing prior to DNA methylation of a tumor suppressor gene. Cancer Cell. 3**,** 89-95.

Bai, H., Konat, G. W., 2003. Hydrogen peroxide mediates higher order chromatin degradation. Neurochem Int. 42**,** 123-9.

Bannai, S., Tateishi, N., 1986. Role of membrane transport in metabolism and function of glutathione in mammals. J Membr Biol. 89**,** 1-8.

Bannister, A. J., Kouzarides, T., 1996. The CBP co-activator is a histone acetyltransferase. Nature. 384**,** 641-3.

Bannister, A. J., Kouzarides, T., 2005. Reversing histone methylation. Nature. 436**,** 1103-6.

Bannister, A. J., Zegerman, P., Partridge, J. F., Miska, E. A., Thomas, J. O., Allshire, R. C., Kouzarides, T., 2001. Selective recognition of methylated lysine 9 on histone H3 by the HP1 chromo domain. Nature. 410**,** 120-4.

Bantscheff, M., Hopf, C., Savitski, M. M., Dittmann, A., Grandi, P., Michon, A.M., Schlegl, J., Abraham, Y., Becher, I., Bergamini, G., Boesche, M., Delling, M., Dümpelfeld, B., Eberhard, D., Huthmacher, C., Mathieson, T., Poeckel, D., Reader, V., Strunk, K., Sweetman, G., Kruse, U., Neubauer, G., Ramsden, N. G., Drewes, G., 2011. Chemoproteomics profiling of HDAC inhibitors reveals selective targeting of HDAC complexes. Nat Biotechnol. 29, 255-65.

Barrow, J. R., Capecchi, M. R., 1999. Compensatory defects associated with mutations in Hoxa1 restore normal palatogenesis to Hoxa2 mutants. Development. 126**,** 5011-5026.

Barski, A., Cuddapah, S., Cui, K., Roh, T. Y., Schones, D. E., Wang, Z., Wei, G., Chepelev, I., Zhao, K., 2007. High-resolution profiling of histone methylations in the human genome. Cell. 129**,** 823-37.

Batty, N., Malouf, G. G., Issa, J. P., 2009. Histone deacetylase inhibitors as anti-neoplastic agents. Cancer Lett. 280**,** 192-200.

Bavik, C., Ward, S. J., Chambon, P., 1996. Developmental abnormalities in cultured mouse embryos deprived of retinoic by inhibition of yolk-sac retinol binding protein synthesis. Proc Natl Acad Sci U S A. 93**,** 3110-4.

Beck, S., Faradji, F., Brock, H., Peronnet, F., 2010. Maintenance of Hox gene expression patterns. Adv Exp Med Biol. 689**,** 41-62.

Becker, P. B., Horz, W., 2002. ATP-dependent nucleosome remodeling. Annu Rev Biochem. 71**,** 247-73.

Beddington, R. S., 1982. An autoradiographic analysis of tissue potency in different regions of the embryonic ectoderm during gastrulation in the mouse. J Embryol Exp Morphol. 69**,** 265-85.

Beddington, R. S. P., Lawson, K. A., Clonal analysis of cell lineages. In: A. J. Copp, D. L. Cockroft, Eds.), Postimplantation Mammalican Embryos. IRL Press, Oxford, 1990, pp. 267-292.

Beddington, S. P., 1981. An autoradiographic analysis of the potency of embryonic ectoderm in the 8th day postimplantation mouse embryo. J Embryol Exp Morphol. 64**,** 87-104.

Berger, S. L., 2002. Histone modifications in transcriptional regulation. Curr Opin Genet Dev. 12**,** 142-8.

Bernstein, B. E., Humphrey, E. L., Erlich, R. L., Schneider, R., Bouman, P., Liu, J. S., Kouzarides, T., Schreiber, S. L., 2002. Methylation of histone H3 Lys 4 in coding regions of active genes. Proc Natl Acad Sci U S A. 99**,** 8695-700.

Bernstein, B. E., Kamal, M., Lindblad-Toh, K., Bekiranov, S., Bailey, D. K., Huebert, D. J., McMahon, S., Karlsson, E. K., Kulbokas, E. J., 3rd, Gingeras, T. R., Schreiber, S. L., Lander, E. S., 2005. Genomic maps and comparative analysis of histone modifications in human and mouse. Cell. 120**,** 169-81.

Bernstein, B. E., Meissner, A., Lander, E. S., 2007. The mammalian epigenome. Cell. 128**,** 669-81.

Bernstein, B. E., Mikkelsen, T. S., Xie, X., Kamal, M., Huebert, D. J., Cuff, J., Fry, B., Meissner, A., Wernig, M., Plath, K., Jaenisch, R., Wagschal, A., Feil, R., Schreiber, S. L., Lander, E. S., 2006. A bivalent chromatin structure marks key developmental genes in embryonic stem cells. Cell. 125**,** 315-26.

Bernstein, E., Hake, S. B., 2006. The nucleosome: a little variation goes a long way. Biochem Cell Biol. 84**,** 505-17.

Betancur, J. G., Yoda, M., Tomari, Y., 2012. miRNA-like duplexes as RNAi triggers with improved specificity. Front Genet. 3**,** 127.

Bianchi, A., Shore, D., 2008. How telomerase reaches its end: mechanism of telomerase regulation by the telomeric complex. Mol Cell. 31**,** 153-65.

Bianchi, A., Smith, S., Chong, L., Elias, P., de Lange, T., 1997. TRF1 is a dimer and bends telomeric DNA. EMBO J. 16**,** 1785-94.

Bickmore, W. A., Mahy, N. L., Chambeyron, S., 2004. Do higher-order chromatin structure and nuclear reorganization play a role in regulating Hox gene expression during development? Cold Spring Harb Symp Quant Biol. 69**,** 251-7.

Binkerd, P. E., Rowland, J. M., Nau, H., Hendrickx, A. G., 1988. Evaluation of valproic acid (VPA) developmental toxicity and pharmacokinetics in Sprague-Dawley rats. Fundam Appl Toxicol. 11**,** 485-93.

Bird, A., 2002. DNA methylation patterns and epigenetic memory. Genes Dev. 16**,** 6-21.

Birke, M., Schreiner, S., Garcia-Cuellar, M. P., Mahr, K., Titgemeyer, F., Slany, R. K., 2002. The MT domain of the proto-oncoprotein MLL binds to CpG-containing DNA and discriminates against methylation. Nucleic Acids Res. 30**,** 958-65.

Bjerkedal, T., Czeizel, A., Goujard, J., Kallen, B., Mastroiacova, P., Nevin, N., Oakley, G., Jr., Robert, E., 1982. Valproic acid and spina bifida. Lancet. 2**,** 1096.

Blackledge, N. P., Klose, R., 2011. CpG island chromatin: a platform for gene regulation. Epigenetics. 6**,** 147-52.

Blanco, R., Munoz, P., Flores, J. M., Klatt, P., Blasco, M. A., 2007. Telomerase abrogation dramatically accelerates TRF2-induced epithelial carcinogenesis. Genes Dev. 21**,** 206-20.

Blasco, M. A., 2007. The epigenetic regulation of mammalian telomeres. Nat Rev Genet. 8**,** 299-309.

Blasco, M. A., Lee, H. W., Hande, M. P., Samper, E., Lansdorp, P. M., DePinho, R. A., Greider, C. W., 1997. Telomere shortening and tumor formation by mouse cells lacking telomerase RNA. Cell. 91**,** 25-34.

Bodnar, A. G., Ouellette, M., Frolkis, M., Holt, S. E., Chiu, C. P., Morin, G. B., Harley, C. B., Shay, J. W., Lichtsteiner, S., Wright, W. E., 1998. Extension of life-span by introduction of telomerase into normal human cells. Science. 279**,** 349-52.

Bolden, J. E., Peart, M. J., Johnstone, R. W., 2006. Anticancer activities of histone deacetylase inhibitors. Nat Rev Drug Discov. 5**,** 769-84.

Bonasio, R., Tu, S., Reinberg, D., 2010. Molecular signals of epigenetic states. Science. 330**,** 612-6.

Borras, C., Esteve, J. M., Vina, J. R., Sastre, J., Vina, J., Pallardo, F. V., 2004. Glutathione regulates telomerase activity in 3T3 fibroblasts. J Biol Chem. 279**,** 34332-5.

Bottomley, M. J., 2004. Structures of protein domains that create or recognize histone modifications. EMBO Rep. 5**,** 464-9.

Boyer, L. A., Plath, K., Zeitlinger, J., Brambrink, T., Medeiros, L. A., Lee, T. I., Levine, S. S., Wernig, M., Tajonar, A., Ray, M. K., Bell, G. W., Otte, A. P., Vidal, M., Gifford, D. K., Young, R. A., Jaenisch, R., 2006. Polycomb complexes repress developmental regulators in murine embryonic stem cells. Nature. 441**,** 349-53.

Bracken, A. P., Dietrich, N., Pasini, D., Hansen, K. H., Helin, K., 2006. Genome-wide mapping of Polycomb target genes unravels their roles in cell fate transitions. Genes Dev. 20**,** 1123-36.

Bradbury, C. A., Khanim, F. L., Hayden, R., Bunce, C. M., White, D. A., Drayson, M. T., Craddock, C., Turner, B. M., 2005. Histone deacetylases in acute myeloid leukaemia show a distinctive pattern of expression that changes selectively in response to deacetylase inhibitors. Leukemia. 19**,** 1751-9.

Brenner, C., Fuks, F., 2007. A methylation rendezvous: reader meets writers. Dev Cell. 12**,** 843-4.

Brown, K. E., Kinter, M. T., Oberley, T. D., Freeman, M. L., Frierson, H. F., Ridnour, L.A., Tao, Y., Oberley, L.W., Spitz, D.R., 1998. Enhanced γ-glutamyl transpeptidase expression and selective loss of CuZn superoxide dismutase in hepatic iron overload. Free Radic Biol Med. 24, 545–55.

Brown, K. E., Dennery, P. A., Ridnour, L.A., Fimmel, C. J., Kladney, R. D., Brunt, E. M., Spitz, D. R., 2003. Effect of iron overload and dietary fat on indices of oxidative stress and hepatic fibrogenesis in rats. Liver Int. 23, 232–42.

Brown, K. E., Meleah Mathahs, M., Broadhurst, K. A., Coleman, M. C., Ridnour, L. A., Schmidt, W. N., Spitz, D. R., 2007. Increased hepatic telomerase activity in a rat model of iron overload: a role for altered thiol redox state? Free Radic Biol Med. 42**,** 228-35.

Brownell, J. E., Allis, C. D., 1996. Special HATs for special occasions: linking histone acetylation to chromatin assembly and gene activation. Curr Opin Genet Dev. 6**,** 176-84.

Bruckner, A., Lee, Y. J., O'Shea, K. S., Henneberry, R. C., 1983. Teratogenic effects of valproic acid and diphenylhydantoin on mouse embryos in culture. Teratology. 27**,** 29-42.

Bryan, T. M., Englezou, A., Dalla-Pozza, L., Dunham, M. A., Reddel, R. R., 1997. Evidence for an alternative mechanism for maintaining telomere length in human tumors and tumor-derived cell lines. Nat Med. 3**,** 1271-4.

Bryan, T. M., Englezou, A., Gupta, J., Bacchetti, S., Reddel, R. R., 1995. Telomere elongation in immortal human cells without detectable telomerase activity. Embo J. 14**,** 4240-8.

Burdge, G. C., Lillycrop, K. A., 2010. Nutrition, Epigenetics, and Developmental Plasticity: Implications for Understanding Human Diseas. Annu Rev Nutr.

Butler, L.M., Zhou, X., Xu, W.S., Scher H.I., Rifkind, R.A., Marks, P.A., Richon, V.M., 2002.The histone deacetylase inhibitor SAHA arrests cancer cell growth, up-regulates thioredoxin-binding protein-2, and down-regulates thioredoxin. Proc Natl Acad Sci USA 99, 11700–11705.

Cairns, B. R., 2007. Chromatin remodeling: insights and intrigue from single-molecule studies. Nat Struct Mol Biol. 14**,** 989-96.

Calegari, F., Haubensak, W., Yang, D., Huttner, W. B., Buchholz, F., 2002. Tissue-specific RNA interference in postimplantation mouse embryos with endoribonuclease-prepared short interfering RNA. Proc Natl Acad Sci U S A. 99**,** 14236-40.

Calegari, F., Marzesco, A. M., Kittler, R., Buchholz, F., Huttner, W. B., 2004. Tissue-specific RNA interference in post-implantation mouse embryos using directional electroporation and whole embryo culture. Differentiation. 72**,** 92-102.

Campos, E. I., Reinberg, D., 2009. Histones: annotating chromatin. Annu Rev Genet. 43**,** 559-99.

Cao, R., Tsukada, Y., Zhang, Y., 2005. Role of Bmi-1 and Ring1A in H2A ubiquitylation and Hox gene silencing. Mol Cell. 20**,** 845-54.

Cao, R., Wang, L., Wang, H., Xia, L., Erdjument-Bromage, H., Tempst, P., Jones, R. S., Zhang, Y., 2002. Role of histone H3 lysine 27 methylation in Polycomb-group silencing. Science. 298**,** 1039-43.

Cao, R., Zhang, Y., 2004. SUZ12 is required for both the histone methyltransferase activity and the silencing function of the EED-EZH2 complex. Mol Cell. 15**,** 57-67.

Caravaca, J. M., Donahue, G., Becker, J. S., He, X., Vinson, C., Zaret, K. S., 2013. Bookmarking by specific and nonspecific binding of FoxA1 pioneer factor to mitotic chromosomes. Genes Dev. 27, 251-60.

Caretti, G., Di Padova, M., Micales, B., Lyons, G. E., Sartorelli, V., 2004. The Polycomb Ezh2 methyltransferase regulates muscle gene expression and skeletal muscle differentiation. Genes Dev. 18**,** 2627-38.

Cawthon, R. M., 2002. Telomere measurement by quantitative PCR. Nucleic Acids Res. 30**,** e47.

Cedar, H., Bergman, Y., 2009. Linking DNA methylation and histone modification: patterns and paradigms. Nat Rev Genet. 10**,** 295-304.

Cesare, A. J., Reddel, R. R., 2010. Alternative lengthening of telomeres: models, mechanisms and implications. Nat Rev Genet. 11**,** 319-30.

Chai, W., Du, Q., Shay, J. W., Wright, W. E., 2006. Human telomeres have different overhang sizes at leading versus lagging strands. Mol Cell. 21**,** 427-35.

Chandra J., 2009. Oxidative stress by targeted agents promotes cytotoxicity in hematologic malignancies. Antioxid Redox Signal. 11, 1123-37.

Chateauvieux, S., Morceau, F., Dicato, M., Diederich, M., 2010. Molecular and therapeutic potential and toxicity of valproic acid. J Biomed Biotechnol. 2010.

Chen, C. S., Wang, Y. C., Yang, H. C., Huang, P. H., Kulp, S. K., Yang, C. C., Lu, Y. S., Matsuyama, S., Chen, C. Y., Chen, C. S., 2007. Histone deacetylase inhibitors sensitize prostate cancer cells to agents that produce DNA double-strand breaks by targeting Ku70 acetylation. Cancer Res. 67, 5318-27.

Chen, P. S., Wang, C. C., Bortner, C. D., Peng, G. S., Wu, X., Pang, H., Lu, R. B., Gean, P. W., Chuang, D. M., Hong, J. S., 2007. Valproic acid and other histone deacetylase inhibitors induce microglial apoptosis and attenuate lipopolysaccharide-induced dopaminergic neurotoxicity. Neuroscience. 149**,** 203-12.

Chin, L., Artandi, S. E., Shen, Q., Tam, A., Lee, S. L., Gottlieb, G. J., Greider, C. W., DePinho, R. A., 1999. p53 deficiency rescues the adverse effects of telomere loss and cooperates with telomere dysfunction to accelerate carcinogenesis. Cell. 97**,** 527-38.

Choi, J., Fauce, S.R., Effros, R.B., 2008. Reduced telomerase activity in human T lymphocytes exposed to cortisol. Brain Behav Immun. 22, 600-5.

Christians, E., Rao, V. H., Renard, J. P., 1994. Sequential acquisition of transcriptional control during early embryonic development in the rabbit. Dev Biol. 164**,** 160-72.

Christianson, A. L., Chesler, N., Kromberg, J. G., 1994. Fetal valproate syndrome: clinical and neuro-developmental features in two sibling pairs. Dev Med Child Neurol. 36**,** 361-9.

Christman, J.K., 2002. 5-Azacytidine and 5-aza-2'-deoxycytidine as inhibitors of DNA methylation: mechanistic studies and their implications for cancer therapy. Oncogene. 21, 5483-95.

Ciusani, E., Balzarotti, M., Calatozzolo, C., de Grazia, U., Boiardi, A., Salmaggi, A., Croci, D., 2007. Valproic acid increases the in vitro effects of nitrosureas on human glioma cell lines. Oncol Res. 16**,** 453-63.

Clarkson, M. J., Wells, J. R., Gibson, F., Saint, R., Tremethick, D. J., 1999. Regions of variant histone His2AvD required for Drosophila development. Nature. 399**,** 694-7.

Clayton-Smith, J., Donnai, D., 1995. Fetal valproate syndrome. J Med Genet. 32**,** 724-7.

Clements, A., Poux, A. N., Lo, W. S., Pillus, L., Berger, S. L., Marmorstein, R., 2003. Structural basis for histone and phosphohistone binding by the GCN5 histone acetyltransferase. Mol Cell. 12**,** 461-73.

Cobourne, M., 2000. Construction for the modern head: current concepts in craniofacial development. Journal of Orthodontics. 27**,** 307-314.

Cockroft, D. L., 1980. Application of post-implantation embryo culture to problems in teratology. Acta Morphol Acad Sci Hung. 28**,** 117-24.

Cockroft, D. L., 1987. Growth and proliferation in mouse parietal yolk sac during whole embryo culture. J Reprod Fertil. 81**,** 575-81.

Collins, K., 2006. The biogenesis and regulation of telomerase holoenzymes. Nat Rev Mol Cell Biol. 7**,** 484-94.

Comb, M., Goodman, H. M., 1990. CpG methylation inhibits proenkephalin gene expression and binding of the transcription factor AP-2. Nucleic Acids Res. 18**,** 3975-82.

Conour, J.E., Graham, W.V., Gaskins, H.R., 2004. A combined in vitro/bioinformatic investigation of redox regulatory mechanisms governing cell cycle progression. Physiol Genomics.18, 196 – 205.

Cordes, S. P., 2001. Molecular genetics of cranial nerve development in mouse. Nat Rev Neurosci. 2**,** 611-23.

Cosgrove, M. S., 2007. Histone proteomics and the epigenetic regulation of nucleosome mobility. Expert Rev Proteomics. 4**,** 465-78.

Cotariu, D., Zaidman, J. L., Evans, S., 1990. Neurophysiological and biochemical changes evoked by valproic acid in the central nervous system. Prog Neurobiol. 34**,** 343-54.

Counter, C. M., Avilion, A. A., LeFeuvre, C. E., Stewart, N. G., Greider, C. W., Harley, C. B., Bacchetti, S., 1992. Telomere shortening associated with chromosome instability is arrested in immortal cells which express telomerase activity. Embo J. 11**,** 1921-9.

Cremer, T., Cremer, C., Schneider, T., Baumann, H., Hens, L., Kirsch-Volders, M., 1982. Analysis of chromosome positions in the interphase nucleus of Chinese hamster cells by laser-UV-microirradiation experiments. Hum Genet. 62**,** 201-9.

Cuthbert, G. L., Daujat, S., Snowden, A. W., Erdjument-Bromage, H., Hagiwara, T., Yamada, M., Schneider, R., Gregory, P. D., Tempst, P., Bannister, A. J., Kouzarides, T., 2004. Histone deimination antagonizes arginine methylation. Cell. 118**,** 545-53.

Czermin, B., Melfi, R., McCabe, D., Seitz, V., Imhof, A., Pirrotta, V., 2002. Drosophila enhancer of Zeste/ESC complexes have a histone H3 methyltransferase activity that marks chromosomal Polycomb sites. Cell. 111**,** 185-96.

d'Adda di Fagagna, F., Reaper, P. M., Clay-Farrace, L., Fiegler, H., Carr, P., Von Zglinicki, T., Saretzki, G., Carter, N. P., Jackson, S. P., 2003. A DNA damage checkpoint response in telomere-initiated senescence. Nature. 426**,** 194-8.

D'Alessio, A. C., Weaver, I. C., Szyf, M., 2007. Acetylation-induced transcription is required for active DNA demethylation in methylation-silenced genes. Mol Cell Biol. 27**,** 7462-74.

Dalens, B., Raynaud, E. J., Gaulme, J., 1980. Teratogenicity of valproic acid. J Pediatr. 97**,** 332-3.

Danielsson, B. R., Danielsson, C., Nilsson, M. F., 2007. Embryonic cardiac arrhythmia and generation of reactive oxygen species: common teratogenic mechanism for IKr blocking drugs. Reprod Toxicol. 24**,** 42-56.

Davis, R., Peters, D. H., McTavish, D., 1994. Valproic acid. A reappraisal of its pharmacological properties and clinical efficacy in epilepsy. Drugs. 47**,** 332-72.

Davis, W., Jr., De Sousa, P. A., Schultz, R. M., 1996. Transient expression of translation initiation factor eIF-4C during the 2-cell stage of the preimplantation mouse embryo: identification by mRNA differential display and the role of DNA replication in zygotic gene activation. Dev Biol. 174**,** 190-201.

de Napoles, M., Mermoud, J. E., Wakao, R., Tang, Y. A., Endoh, M., Appanah, R., Nesterova, T. B., Silva, J., Otte, A. P., Vidal, M., Koseki, H., Brockdorff, N., 2004. Polycomb group proteins Ring1A/B link ubiquitylation of histone H2A to heritable gene silencing and X inactivation. Dev Cell. 7**,** 663-76.

de Ruijter, A. J., van Gennip, A. H., Caron, H. N., Kemp, S., van Kuilenburg, A. B., 2003. Histone deacetylases (HDACs): characterization of the classical HDAC family. Biochem J. 370**,** 737-49.

Dean, J. C., Hailey, H., Moore, S. J., Lloyd, D. J., Turnpenny, P. D., Little, J., 2002. Long term health and neurodevelopment in children exposed to antiepileptic drugs before birth. J Med Genet. 39**,** 251-9.

Dean, J. C., Moore, S. J., Turnpenny, P. D., 2000. Developing diagnostic criteria for the fetal anticonvulsant syndromes. Seizure. 9**,** 233-4.

Delaval, K., Govin, J., Cerqueira, F., Rousseaux, S., Khochbin, S., Feil, R., 2007. Differential histone modifications mark mouse imprinting control regions during spermatogenesis. EMBO J. 26**,** 720-9.

Dhahbi, J. M., Tillman, J. B., Cao, S., Mote, P. L., Walford, R. L., Spindler, S. R., 1998. Caloric intake alters the efficiency of catalase mRNA translation in the liver of old female mice. J Gerontol A Biol Sci Med Sci. 53**,** B180-5.

Diav-Citrin, O., Shechtman, S., Bar-Oz, B., Cantrell, D., Arnon, J., Ornoy, A., 2008. Pregnancy outcome after in utero exposure to valproate : evidence of dose relationship in teratogenic effect. CNS Drugs. 22**,** 325-34.

DiLiberti, J. H., Farndon, P. A., Dennis, N. R., Curry, C. J., 1984. The fetal valproate syndrome. Am J Med Genet. 19**,** 473-81.

Dindot, S. V., Person, R., Strivens, M., Garcia, R., Beaudet, A. L., 2009. Epigenetic profiling at mouse imprinted gene clusters reveals novel epigenetic and genetic features at differentially methylated regions. Genome Res. 19**,** 1374-83.

Dixit, D., Sharma, V., Ghosh, S., Koul, N., Mishra, P. K., Sen, E., 2009. Manumycin inhibits STAT3, telomerase activity, and growth of glioma cells by elevating intracellular reactive oxygen species generation. Free Radic Biol Med. 47**,** 364-74.

Dolle, P., Izpisua-Belmonte, J. C., Falkenstein, H., Renucci, A., Duboule, D., 1989. Co-ordinate expression of the murine Hox-5 complex homeobox-containing genes during limb pattern formation. Nature. 342**,** 767-772.

Donaldson, I. J., Amin, S., Hensman, J. J., Kutejova, E., Rattray, M., Lawrence, N., Hayes, A., Ward, C. M., Bobola, N., 2011. Genome-wide occupancy links Hoxa2 to Wnt-beta-catenin signaling in mouse embryonic development. Nucleic Acids Res. 40**,** 3990-4001.

Donate, L. E., Blasco, M. A., 2011. Telomeres in cancer and ageing. Philos Trans R Soc Lond B Biol Sci. 366**,** 76-84.

Drake, C. J., Little, C. D., 1991. Integrins play an essential role in somite adhesion to the embryonic axis. Dev Biol. 143**,** 418-21.

Dravet, C., Julian, C., Legras, C., Magaudda, A., Guerrini, R., Genton, P., Soulayrol, S., Giraud, N., Mesdjian, E., Trentin, G., et al., 1992. Epilepsy, antiepileptic drugs, and malformations in children of women with epilepsy: a French prospective cohort study. Neurology. 42**,** 75-82.

Driscoll, R., Hudson, A., Jackson, S. P., 2007. Yeast Rtt109 promotes genome stability by acetylating histone H3 on lysine 56. Science. 315, 649-52.

Duboule, D., 1994. Temporal colinearity and the phylotypic progression: a basis for the stability of a vertebrate Bauplan and the evolution of morphologies through heterochrony. Dev Suppl. 135-42.

Duboule, D., Dolle, P., 1989. The structural and functional organization of the muring HOX gene family resembles that Drosophila homeotic genes. EMBO J. 8**,** 1497-1505.

Duncan, H.F., Smith, A.J., Fleming, G.J., Cooper, P.R., 2011. HDACi: cellular effects, opportunities for restorative dentistry**.** J Dent Res. 90, 1377-88.

Ehlers, K., Elmazar, M. M., Nau, H., 1996. Methionine reduces the valproic acid-induced spina bifida rate in mice without altering valproic acid kinetics. J Nutr. 126**,** 67-75.

Ehlers, K., Sturje, H., Merker, H. J., Nau, H., 1992. Valproic acid-induced spina bifida: a mouse model. Teratology. 45**,** 145-54.

Eikel, D., Hoffmann, K., Zoll, K., Lampen, A., Nau, H., 2006a. S-2-pentyl-4-pentynoic hydroxamic acid and its metabolite s-2-pentyl-4-pentynoic acid in the NMRI-exencephaly-mouse model: pharmacokinetic profiles, teratogenic effects, and histone deacetylase inhibition abilities of further valproic acid hydroxamates and amides. Drug Metab Dispos. 34**,** 612-20.

Eikel, D., Lampen, A., Nau, H., 2006b. Teratogenic effects mediated by inhibition of histone deacetylases: evidence from quantitative structure activity relationships of 20 valproic acid derivatives. Chem Res Toxicol. 19**,** 272-8.

Eisen, J. A., Sweder, K. S., Hanawalt, P. C., 1995. Evolution of the SNF2 family of proteins: subfamilies with distinct sequences and functions. Nucleic Acids Res. 23**,** 2715-23.

El Ouakfaoui, S., Schnell, J., Abdeen, A., Colville, A., Labbe, H., Han, S., Baum, B., Laberge, S., Miki, B., 2012. Control of somatic embryogenesis and embryo development by AP2 transcription factors. Plant Mol Biol. 74**,** 313-26.

Elbashir, S. M., Harborth, J., Lendeckel, W., Yalcin, A., Weber, K., Tuschl, T., 2001. Duplexes of 21-nucleotide RNAs mediate RNA interference in cultured mammalian cells. Nature. 411**,** 494-8.

Else, T., Trovato, A., Kim, A. C., Wu, Y., Ferguson, D. O., Kuick, R. D., Lucas, P. C., Hammer, G. D., 2009. Genetic p53 deficiency partially rescues the adrenocortical dysplasia phenotype at the expense of increased tumorigenesis. Cancer Cell. 15**,** 465-76.

Emmanouil-Nikoloussi, E. N., Foroglou, N. G., Kerameos-Foroglou, C. H., Thliveris, J. A., 2004. Effect of valproic acid on fetal and maternal organs in the mouse: a morphological study. Morphologie. 88**,** 41-5.

Engelhardt, M., Albanell, J., Drullinsky, P., Han, W., Guillem, J., Scher, H. I., Reuter, V., Moore, M. A., 1997a. Relative contribution of normal and neoplastic cells determines telomerase activity and telomere length in primary cancers of the prostate, colon, and sarcoma. Clin Cancer Res. 3**,** 1849-57.

Engelhardt, M., Drullinsky, P., Guillem, J., Moore, M. A., 1997b. Telomerase and telomere length in the development and progression of premalignant lesions to colorectal cancer. Clin Cancer Res. 3**,** 1931-41.

Eot-Houllier, G., Fulcrand, G., Magnaghi-Jaulin, L., Jaulin, C., 2008. Histone deacetylase inhibitors and genomic instability. Cancer Letters. 274, 169-76.

Eriksson, K., Viinikainen, K., Monkkonen, A., Aikia, M., Nieminen, P., Heinonen, S., Kalviainen, R., 2005. Children exposed to valproate in utero--population based evaluation of risks and confounding factors for long-term neurocognitive development. Epilepsy Res. 65**,** 189-200.

Ernst, T., Chase, A. J., Score, J., Hidalgo-Curtis, C. E., Bryant, C., Jones, A. V., Waghorn, K., Zoi, K., Ross, F. M., Reiter, A., Hochhaus, A., Drexler, H. G., Duncombe, A., Cervantes, F., Oscier, D., Boultwood, J., Grand, F. H., Cross, N. C., 2010. Inactivating mutations of the histone methyltransferase gene EZH2 in myeloid disorders. Nat Genet. 42**,** 722-6.

Erusalimsky, J. D., Kurz, D. J., 2005. Cellular senescence in vivo: its relevance in ageing and cardiovascular disease. Exp Gerontol. 40**,** 634-42.

Espejel, S., Franco, S., Rodriguez-Perales, S., Bouffler, S. D., Cigudosa, J. C., Blasco, M. A., 2002a. Mammalian Ku86 mediates chromosomal fusions and apoptosis caused by critically short telomeres. EMBO J. 21**,** 2207-19.

Espejel, S., Franco, S., Sgura, A., Gae, D., Bailey, S. M., Taccioli, G. E., Blasco, M. A., 2002b. Functional interaction between DNA-PKcs and telomerase in telomere length maintenance. EMBO J. 21**,** 6275-87.

Esteller, M., 2007. Cancer epigenomics: DNA methylomes and histone-modification maps. Nat Rev Genet. 8**,** 286-98.

Esteve, P. O., Chin, H. G., Smallwood, A., Feehery, G. R., Gangisetty, O., Karpf, A. R., Carey, M. F., Pradhan, S., 2006. Direct interaction between DNMT1 and G9a coordinates DNA and histone methylation during replication. Genes Dev. 20**,** 3089-103.

Faiella, A., Wernig, M., Consalez, G. G., Hostick, U., Hofmann, C., Hustert, E., Boncinelli, E., Balling, R., Nadeau, J. H., 2000. A mouse model for valproate teratogenicity: parental effects, homeotic transformations, and altered HOX expression. Hum Mol Genet. 9**,** 227-36.

Fakler, B., Herlitze, S., Amthor, B., Zenner, H. P., Ruppersberg, J. P., 1994. Short antisense oligonucleotide-mediated inhibition is strongly dependent on oligo length and concentration but almost independent of location of the target sequence. J Biol Chem. 269**,** 16187-94.

Fazzari, M. J., Greally, J. M., 2004. Epigenomics: beyond CpG islands. Nat Rev Genet. 5**,** 446-55.

Feng, J., Funk, W. D., Wang, S. S., Weinrich, S. L., Avilion, A. A., Chiu, C. P., Adams, R. R., Chang, E., Allsopp, R. C., Yu, J., et al., 1995. The RNA component of human telomerase. Science. 269**,** 1236-41.

Feng, S., Cokus, S. J., Zhang, X., Chen, P. Y., Bostick, M., Goll, M. G., Hetzel, J., Jain, J., Strauss, S. H., Halpern, M. E., Ukomadu, C., Sadler, K.C., Pradhan, S., Pellegrini, M.,

Jacobsen, S. E. 2010. Conservation and divergence of methylation patterning in plants and animals. Proc Natl Acad Sci U S A. 2010 107, 8689-94.

Ficz, G., Branco, M.R., Seisenberger, S., Santos, F., Krueger, F., Hore, T.A, Marques, C.J., Andrews, S., Reik, W., 2011. Dynamic regulation of 5-hydroxymethylcytosine in mouse ES cells and during differentiation. Nature. 473, 398-402.

Finnell, R. H., Junker, W. M., Wadman, L. K., Cabrera, R. M., 2002. Gene expression profiling within the developing neural tube. Neurochem Res. 27**,** 1165-80.

Fischle, W., Kiermer, V., Dequiedt, F., Verdin, E., 2001. The emerging role of class II histone deacetylases. Biochem Cell Biol. 79**,** 337-48.

Fischle, W., Tseng, B. S., Dormann, H. L., Ueberheide, B. M., Garcia, B. A., Shabanowitz, J., Hunt, D. F., Funabiki, H., Allis, C. D., 2005. Regulation of HP1-chromatin binding by histone H3 methylation and phosphorylation. Nature. 438**,** 1116-22.

Fischle, W., Wang, Y., Jacobs, S. A., Kim, Y., Allis, C. D., Khorasanizadeh, S., 2003. Molecular basis for the discrimination of repressive methyl-lysine marks in histone H3 by Polycomb and HP1 chromodomains. Genes Dev. 17**,** 1870-81.

Fisher, A. G., Merkenschlager, M., 2002. Gene silencing, cell fate and nuclear organisation. Curr Opin Genet Dev. 12**,** 193-7.

Flores, I., Benetti, R., Blasco, M. A., 2006. Telomerase regulation and stem cell behaviour. Curr Opin Cell Biol. 18**,** 254-60.

Fournier, C., Goto, Y., Ballestar, E., Delaval, K., Hever, A. M., Esteller, M., Feil, R., 2002. Allele-specific histone lysine methylation marks regulatory regions at imprinted mouse genes. EMBO J. 21**,** 6560-70.

Francastel, C., Schubeler, D., Martin, D. I., Groudine, M., 2000. Nuclear compartmentalization and gene activity. Nat Rev Mol Cell Biol. 1**,** 137-43.

Francis, N. J., Kingston, R. E., Woodcock, C. L., 2004. Chromatin compaction by a polycomb group protein complex. Science. 306**,** 1574-7.

Francis, N. J., Saurin, A. J., Shao, Z., Kingston, R. E., 2001. Reconstitution of a functional core polycomb repressive complex. Mol Cell. 8**,** 545-56.

Fried, S., Kozer, E., Nulman, I., Einarson, T. R., Koren, G., 2004. Malformation rates in children of women with untreated epilepsy: a meta-analysis. Drug Saf. 27**,** 197-202.

Frigola, J., Song, J., Stirzaker, C., Hinshelwood, R. A., Peinado, M. A., Clark, S. J., 2006. Epigenetic remodeling in colorectal cancer results in coordinate gene suppression across an entire chromosome band. Nat Genet. 38**,** 540-9.

Fritsch, R. D., Shen, X., Illei, G. G., Yarboro, C. H., Prussin, C., Hathcock, K. S., Hodes, R. J., Lipsky, P. E., 2006. Abnormal differentiation of memory T cells in systemic lupus erythematosus. Arthritis Rheum. 54**,** 2184-97.

Fu, J., Shao, C. J., Chen, F. R., Ng, H. K., Chen, Z. P., 2010. Autophagy induced by valproic acid is associated with oxidative stress in glioma cell lines. Neuro Oncol. 12**,** 328-40.

Fujita, N., Takebayashi, S., Okumura, K., Kudo, S., Chiba, T., Saya, H., Nakao, M., 1999. Methylation-mediated transcriptional silencing in euchromatin by methyl-CpG binding protein MBD1 isoforms. Mol Cell Biol. 19**,** 6415-26.

Fuks, F., 2005. DNA methylation and histone modifications: teaming up to silence genes. Curr Opin Genet Dev. 15**,** 490-5.

Fuks, F., Burgers, W. A., Brehm, A., Hughes-Davies, L., Kouzarides, T., 2000. DNA methyltransferase Dnmt1 associates with histone deacetylase activity. Nat Genet. 24**,** 88-91.

Fuks, F., Burgers, W. A., Godin, N., Kasai, M., Kouzarides, T., 2001. Dnmt3a binds deacetylases and is recruited by a sequence-specific repressor to silence transcription. EMBO J. 20**,** 2536-44.

Fuks, F., Hurd, P. J., Wolf, D., Nan, X., Bird, A. P., Kouzarides, T., 2003. The methyl-CpG-binding protein MeCP2 links DNA methylation to histone methylation. J Biol Chem. 278**,** 4035-40.

Fuller, L. C., Cornelius, S. K., Murphy, C. W., Wiens, D. J., 2002. Neural crest cell motility in valproic acid. Reprod Toxicol. 16**,** 825-39.

Furumoto, K., Inoue, E., Nagao, N., Hiyama, E., Miwa, N., 1998. Age-dependent telomere shortening is slowed down by enrichment of intracellular vitamin C via suppression of oxidative stress. Life Sci. 63**,** 935-48.

Fuso, A., Seminara, L., Cavallaro, R. A., D'Anselmi, F., Scarpa, S., 2005. S-adenosylmethionine/homocysteine cycle alterations modify DNA methylation status with consequent deregulation of PS1 and BACE and beta-amyloid production. Mol Cell Neurosci. 28**,** 195-204.

Fyhrquist, F., Tiitu, A., Saijonmaa, O., Forsblom, C., Groop, P. H., Telomere length and progression of diabetic nephropathy in patients with type 1 diabetes. J Intern Med. 267**,** 278-86.

Garcia-Manero, G., Kantarjian, H. M., Sanchez-Gonzalez, B., Yang, H., Rosner, G., Verstovsek, S., Rytting, M., Wierda, W. G., Ravandi, F., Koller, C., Xiao, L., Faderl, S., Estrov, Z., Cortes, J., O'Brien, S., Estey, E., Bueso-Ramos, C., Fiorentino, J., Jabbour, E., Issa, J. P., 2006. Phase 1/2 study of the combination of 5-aza-2'-deoxycytidine with valproic acid in patients with leukemia. Blood. 108**,** 3271-9.

Garrick, D., De Gobbi, M., Samara, V., Rugless, M., Holland, M., Ayyub, H., Lower, K., Sloane-Stanley, J., Gray, N., Koch, C., Dunham, I., Higgs, D.R., 2008. The role of the polycomb complex in silencing alpha-globin gene expression in nonerythroid cells. Blood. 112, 3889-99.

Garske, A. L., Oliver, S. S., Wagner, E. K., Musselman, C. A., LeRoy, G., Garcia, B. A., Kutateladze, T. G., Denu, J. M., 2010. Combinatorial profiling of chromatin binding modules reveals multisite discrimination. Nat Chem Biol. 6**,** 283-90.

Gasser, S. M., Cockell, M. M., 2001. The molecular biology of the SIR proteins. Gene. 279**,** 1-16.

Gavalas, A., Davenne, M., Lumsden, A., Chambon, P., Rijli, F. M., 1997. Role of Hoxa2 in axon pathfinding and rostral hindbrain patterning. Development. 124**,** 3693-3702.

Gendron-Maguire, M., Mallo, M. Z., Zhang, M., Gridley, T., 1993. Hoxa-2 mutant mice exhibit Homeoic transformation of skeletal elements derived from cranial neural crest. Cell. 75**,** 1317-1331.

Georgin-Lavialle, S., Aouba, A., Mouthon, L., Londono-Vallejo, J. A., Lepelletier, Y., Gabet, A. S., Hermine, O., 210 The telomere/telomerase system in autoimmune and systemic diseases. Autoimmun Rev. 10, 646-51.

Gerber, M., Shilatifard, A., 2003. Transcriptional elongation by RNA polymerase II and histone methylation. J Biol Chem. 278**,** 26303-6.

Geserick, C., Blasco, M. A., 2006. Novel roles for telomerase in aging. Mech Ageing Dev. 127**,** 579-83.

Gessert, S., Kuhl, M., 2010. The multiple phases and faces of wnt signaling during cardiac differentiation and development. Circ Res. 107**,** 186-99.

Ghibelli, L., Fanelli, C., Rotilio, G., Lafavia, E., Coppola, S., Colussi, C., Civitareale, P., Ciriolo, M. R., 1998. Rescue of cells from apoptosis by inhibition of active GSH extrusion. FASEB J. 12**,** 479-86.

Gidekel, S., Bergman, Y., 2002. A unique developmental pattern of Oct-3/4 DNA methylation is controlled by a cis-demodification element. J Biol Chem. 277**,** 34521-30.

Gilbert, N., Gilchrist, S., Bickmore, W. A., 2005. Chromatin organization in the mammalian nucleus. Int Rev Cytol. 242**,** 283-336.

Glaser, S., Schaft, J., Lubitz, S., Vintersten, K., van der Hoeven, F., Tufteland, K. R., Aasland, R., Anastassiadis, K., Ang, S. L., Stewart, A. F., 2006. Multiple epigenetic maintenance factors implicated by the loss of Mll2 in mouse development. Development. 133**,** 1423-32.

Goll, M. G., Kirpekar, F., Maggert, K. A., Yoder, J. A., Hsieh, C. L., Zhang, X., Golic, K. G., Jacobsen, S. E., Bestor, T. H., 2006. Methylation of tRNAAsp by the DNA methyltransferase homolog Dnmt2. Science. 311**,** 395-8.

Golubovskaya, V. M., Presnell, S. C., Hooth, M. J., Smith, G. J., Kaufmann, W. K., 1997. Expression of telomerase in normal and malignant rat hepatic epithelia. Oncogene. 15**,** 1233-40.

Gomez, M. R., 1981. Possible teratogenicity of valproic acid. J Pediatr. 98**,** 508-9.

Gommans, W. M., Haisma, H. J., Rots, M. G., 2005. Engineering zinc finger protein transcription factors: the therapeutic relevance of switching endogenous gene expression on or off at command. J Mol Biol. 354**,** 507-19.

Gottlicher, M., Minucci, S., Zhu, P., Kramer, O.H., Schimpf, A., Giavara, S., Sleeman, J.P., Lo Coco, F., Nervi, C., Pelicci, P.G., Heinzel, T., 2001. Valproic acid defines a novel class of HDAC inhibitors inducing differentiation of transformed cells. EMBO J. 20, 6969–78.

Graf, W. D., Oleinik, O. E., Glauser, T. A., Maertens, P., Eder, D. N., Pippenger, C. E., 1998. Altered antioxidant enzyme activities in children with a serious adverse experience related to valproic acid therapy. Neuropediatrics. 29**,** 195-201.

Graff, J., Kim, D., Dobbin, M. M., Tsai, L. H., 2011. Epigenetic regulation of gene expression in physiological and pathological brain processes. Physiol Rev. 91**,** 603-49.

Graham, A., Maden, M., Krumlauf, R., 1991. The murine Hox-2 genes display dynamic dorsoventral patterns of expression during central nervous system development. Development. 112**,** 255-64.

Gratsch, T. E., De Boer, L. S., O'Shea, K. S., 2003. RNA inhibition of BMP-4 gene expression in postimplantation mouse embryos. Genesis. 37**,** 12-7.

Gray, J., Ross, M. E., 2011. Neural tube closure in mouse whole embryo culture. J Vis Exp.

Gray, J. D., Nakouzi, G., Slowinska-Castaldo, B., Dazard, J. E., Rao, J. S., Nadeau, J. H., Ross, M. E., 2011. Functional interactions between the LRP6 WNT co-receptor and folate supplementation. Hum Mol Genet. 19**,** 4560-72.

Greider, C. W., Blackburn, E. H., 1985. Identification of a specific telomere terminal transferase activity in Tetrahymena extracts. Cell. 43**,** 405-13.

Greider, C. W., Blackburn, E. H., 1987. The telomere terminal transferase of Tetrahymena is a ribonucleoprotein enzyme with two kinds of primer specificity. Cell. 51**,** 887-98.

Greider, C. W., Blackburn, E. H., 1989. A telomeric sequence in the RNA of Tetrahymena telomerase required for telomere repeat synthesis. Nature. 337**,** 331-7.

Grewal, S. I., Jia, S., 2007. Heterochromatin revisited. Nat Rev Genet. 8**,** 35-46.

Griffith, J., Bianchi, A., de Lange, T., 1998. TRF1 promotes parallel pairing of telomeric tracts in vitro. J Mol Biol. 278**,** 79-88.

Griffith, J. D., Comeau, L., Rosenfield, S., Stansel, R. M., Bianchi, A., Moss, H., de Lange, T., 1999. Mammalian telomeres end in a large duplex loop. Cell. 97**,** 503-14.

Grimaud, C., Negre, N., Cavalli, G., 2006. From genetics to epigenetics: the tale of Polycomb group and trithorax group genes. Chromosome Res. 14**,** 363-75.

Grozinger, C. M., Schreiber, S. L., 2002. Deacetylase enzymes: biological functions and the use of small-molecule inhibitors. Chem Biol. 9**,** 3-16.

Grzenda, A., Ordog, T., Urrutia, R., 2011. Polycomb and the emerging epigenetics of pancreatic cancer. J Gastrointest Cancer. 42**,** 100-11.

Guan, J. Z., Maeda, T., Sugano, M., Oyama, J., Higuchi, Y., Suzuki, T., Makino, N., 2007. An analysis of telomere length in sarcoidosis. J Gerontol A Biol Sci Med Sci. 62**,** 1199-203.

Guarente, L., 2000. Sir2 links chromatin silencing, metabolism, and aging. Genes Dev. 14**,** 1021-6.

Guenther, M. G., Jenner, R. G., Chevalier, B., Nakamura, T., Croce, C. M., Canaani, E., Young, R. A., 2005. Global and Hox-specific roles for the MLL1 methyltransferase. Proc Natl Acad Sci U S A. 102**,** 8603-8.

Gulbins, E., Jekle, A., Ferlinz, K., Grassme, H., Lang, F., 2000. Physiology of apoptosis. Am J Physiol Renal Physiol. 279**,** F605-15.

Guo, Y-L., Chakraborty, S., Rajan, S.S., Wang, R., Huang, F., 2010. Effects of oxidative stress on mouse embryonic stem cell proliferation, apoptosis, senescence, and self-renewal. Stem Cells and Development. 19, 1321-31.

Gurvich, N., Klein, P.S., 2002. Lithium and valproic acid: parallels and contrasts in diverse signaling contexts. Pharmacol Ther. 96, 45–66.

Gurvich, N., Tsygankova, O.M., Meinkoth, J.L., Klein, P.S., 2004. Histone deacetylase is a target of valproic acid-mediated cellular differentiation. Cancer Res. 64, 1079–86.

Haendeler, J., Hoffmann, J., Diehl, J. F., Vasa, M., Spyridopoulos, I., Zeiher, A. M., Dimmeler, S., 2004. Antioxidants inhibit nuclear export of telomerase reverse transcriptase and delay replicative senescence of endothelial cells. Circ Res. 94**,** 768-75.

Halazonetis, T. D., Gorgoulis, V. G., Bartek, J., 2008. An oncogene-induced DNA damage model for cancer development. Science. 319**,** 1352-5.

Hamza, A. A., Amin, A., 2007. Apium graveolens modulates sodium valproate-induced reproductive toxicity in rats. J Exp Zool Part A Ecol Genet Physiol. 307**,** 199-206.

Hanahan, D., Weinberg, R. A., 2000. The hallmarks of cancer. Cell. 100**,** 57-70.

Hang, C. T., Chang, C. P., 2012. Use of whole embryo culture for studying heart development. Methods Mol Biol. 843**,** 3-9.

Harris, C., 1993. Glutathione biosynthesis in the postimplantation rat conceptus in vitro. Toxicol Appl Pharmacol. 120, 247–56.

Harris, C., Dixon, M., Hansen, J.M., 2004. Glutathione depletion modulates methanol, formaldehyde and formate toxicity in cultured rat conceptuses. Cell Biol Toxicol. 20, 133–145.

Harris, C., Hansen, J.M., 2012. Oxidative stress, thiols, and redox profiles. Methods Mol Biol. 889, 325-46.

Harris, C., Hiranruengchok, R., Lee, E., Berberian, R.M., Eurich, G.E., 1995, Glutathione status in chemical embryotoxicity: synthesis, turnoverand adduct formation. Toxicol In Vitro. 9, 623–31.

Harris, C, Stark, K.L., Juchau, M.R., 1988. Glutathione status and the incidence of neural tube defects elicited by direct acting teratogens in vitro. Teratology. 37, 577–90.

Harris, M. J., Juriloff, D. M., 2007. Mouse mutants with neural tube closure defects and their role in understanding human neural tube defects. Birth Defects Res A Clin Mol Teratol. 79**,** 187-210.

Harris, M. J., Juriloff, D. M., 2010. An update to the list of mouse mutants with neural tube closure defects and advances toward a complete genetic perspective of neural tube closure. Birth Defects Res A Clin Mol Teratol. 88**,** 653-69.

Hawkins, R. D., Hon, G. C., Lee, L. K., Ngo, Q., Lister, R., Pelizzola, M., Edsall, L. E., Kuan, S., Luu, Y., Klugman, S., Antosiewicz-Bourget, J., Ye, Z., Espinoza, C., Agarwahl, S., Shen, L., Ruotti, V., Wang, W., Stewart, R., Thomson, J. A., Ecker, J. R., Ren, B., 2010. Distinct epigenomic landscapes of pluripotent and lineage-committed human cells. Cell Stem Cell. 6**,** 479-91.

Hayakawa, N., Nozawa, K., Ogawa, A., Kato, N., Yoshida, K., Akamatsu, K., Tsuchiya, M., Nagasaka, A., Yoshida, S., 1999. Isothiazolone derivatives selectively inhibit telomerase from human and rat cancer cells in vitro. Biochemistry. 38**,** 11501-7.

Heiss, N. S., Knight, S. W., Vulliamy, T. J., Klauck, S. M., Wiemann, S., Mason, P. J., Poustka, A., Dokal, I., 1998. X-linked dyskeratosis congenita is caused by mutations in a highly conserved gene with putative nucleolar functions. Nat Genet. 19**,** 32-8.

Hendrich, B., Bird, A., 1998. Identification and characterization of a family of mammalian methyl-CpG binding proteins. Mol Cell Biol. 18**,** 6538-47.

Hendrickx, A. G., Nau, H., Binkerd, P., Rowland, J. M., Rowland, J. R., Cukierski, M. J., Cukierski, M. A., 1988. Valproic acid developmental toxicity and pharmacokinetics in the rhesus monkey: an interspecies comparison. Teratology. 38**,** 329-45.

Henery, C. C., Miranda, M., Wiekowski, M., Wilmut, I., DePamphilis, M. L., 1995. Repression of gene expression at the beginning of mouse development. Dev Biol. 169**,** 448-60.

Henikoff, S., Ahmad, K., 2005. Assembly of variant histones into chromatin. Annu Rev Cell Dev Biol. 21**,** 133-53.

Hernandez-Munoz, I., Lund, A. H., van der Stoop, P., Boutsma, E., Muijrers, I., Verhoeven, E., Nusinow, D. A., Panning, B., Marahrens, Y., van Lohuizen, M., 2005. Stable X chromosome inactivation involves the PRC1 Polycomb complex and requires histone MACROH2A1 and the CULLIN3/SPOP ubiquitin E3 ligase. Proc Natl Acad Sci U S A. 102**,** 7635-40.

Herrera, E., Samper, E., Martin-Caballero, J., Flores, J. M., Lee, H. W., Blasco, M. A., 1999. Disease states associated with telomerase deficiency appear earlier in mice with short telomeres. EMBO J. 18**,** 2950-60.

Hershko, A. Y., Kafri, T., Fainsod, A., Razin, A., 2003. Methylation of HoxA5 and HoxB5 and its relevance to expression during mouse development. Gene. 302**,** 65-72.

Hess, J. L., 2004. MLL: a histone methyltransferase disrupted in leukemia. Trends Mol Med. 10**,** 500-7.

Hitchins, M. P., Lin, V. A., Buckle, A., Cheong, K., Halani, N., Ku, S., Kwok, C. T., Packham, D., Suter, C. M., Meagher, A., Stirzaker, C., Clark, S., Hawkins, N. J., Ward, R. L., 2007. Epigenetic inactivation of a cluster of genes flanking MLH1 in microsatellite-unstable colorectal cancer. Cancer Res. 67**,** 9107-16.

Hitchler, M. J., Domann, F. E., 2007. An epigenetic perspective on the free radical theory of development. Free Radic Biol Med. 43**,** 1023-36.

Hitchler, M. J., Wikainapakul, K., Yu, L., Powers, K., Attatippaholkun, W., Domann, F. E., 2006. Epigenetic regulation of manganese superoxide dismutase expression in human breast cancer cells. Epigenetics. 1**,** 163-71.

Holmes, L. B., Coull, B. A., Dorfman, J., Rosenberger, P. B., 2005. The correlation of deficits in IQ with midface and digit hypoplasia in children exposed in utero to anticonvulsant drugs. J Pediatr. 146**,** 118-22.

Honda, M., Mengesha, E., Albano, S., Nichols, W. S., Wallace, D. J., Metzger, A., Klinenberg, J. R., Linker-Israeli, M., 2001. Telomere shortening and decreased replicative potential, contrasted by continued proliferation of telomerase-positive CD8+CD28(lo) T cells in patients with systemic lupus erythematosus. Clin Immunol. 99**,** 211-221.

Houben, J. M., Moonen, H. J., van Schooten, F. J., Hageman, G. J., 2008. Telomere length assessment: biomarker of chronic oxidative stress? Free Radic Biol Med. 44**,** 235-46.

Hsu, C. P., Hsu, N. Y., Lee, L. W., Ko, J. L., 2006. Ets2 binding site single nucleotide polymorphism at the hTERT gene promoter--effect on telomerase expression and telomere length maintenance in non-small cell lung cancer. Eur J Cancer. 42**,** 1466-74.

Huang, M., Cham, E. M., Eppes, C. S., Gerber, S. E., Reed, K. D., Ernst, L. M., 2012. Placental and fetal findings in intrauterine Candida lusitaniae infection following in vitro fertilization and embryo transfer. Pediatr Dev Pathol. 15**,** 127-31.

Huang, N., Katz, J.P., Martin, D.R., Wu, G.D., 1997. Inhibition of IL-8 gene expression in Caco-2 cells by compounds which induce histone hyperacetylation. Cytokine. 9, 27–36.

Huang Y., Pastor WA., Shen Y., Tahiliani M., Liu DR., Rao A., 2010. The Behaviour of 5-Hydroxymethylcytosine in Bisulfite Sequencing. PLoS ONE 5: e8888.

Hughes, C. M., Rozenblatt-Rosen, O., Milne, T. A., Copeland, T. D., Levine, S. S., Lee, J. C., Hayes, D. N., Shanmugam, K. S., Bhattacharjee, A., Biondi, C. A., Kay, G. F., Hayward, N. K., Hess, J. L., Meyerson, M., 2004. Menin associates with a trithorax family histone methyltransferase complex and with the hoxc8 locus. Mol Cell. 13**,** 587-97.

Hughes, T. R., Evans, S. K., Weilbaecher, R. G., Lundblad, V., 2000. The Est3 protein is a subunit of yeast telomerase. Curr Biol. 10**,** 809-12.

Hunt, P., Gulisano, M., Cook, M., Sham, M., Faiella, A., Wilkinson, D., Boncinelli, E., Krumlauf, R., 1991. A distinct Hox code for the branchial region of the vertebrate head. Nature. 353**,** 861-864.

Hurd, R. W., Van Rinsvelt, H. A., Wilder, B. J., Karas, B., Maenhaut, W., De Reu, L., 1984. Selenium, zinc, and copper changes with valproic acid: possible relation to drug side effects. Neurology. 34**,** 1393-5.

Hutter, D. E., Till, B. G., Greene, J. J., 1997. Redox state changes in density-dependent regulation of proliferation. Exp Cell Res. 232**,** 435-8.

Iizuka, M., Matsui, T., Takisawa, H., Smith, M. M., 2006. Regulation of replication licensing by acetyltransferase Hbo1. Mol Cell Biol. 26**,** 1098-108.

Ikura, T., Ogryzko, V. V., Grigoriev, M., Groisman, R., Wang, J., Horikoshi, M., Scully, R., Qin, J., Nakatani, Y., 2000. Involvement of the TIP60 histone acetylase complex in DNA repair and apoptosis. Cell. 102**,** 463-73.

Illingworth, R. S., Bird, A. P., 2009. CpG islands--'a rough guide'. FEBS Lett. 583**,** 1713-20.

Imai, S., Armstrong, C. M., Kaeberlein, M., Guarente, L., 2000. Transcriptional silencing and longevity protein Sir2 is an NAD-dependent histone deacetylase. Nature. 403**,** 795-800.

Imhoff, B.R., Hansen, J.M., 2011. Differential redox potential profiles during adipogenesis and osteogenesis. Cell Mol Biol Lett. 16, 149-61.

Inamdar, N. M., Ehrlich, K. C., Ehrlich, M., 1991. CpG methylation inhibits binding of several sequence-specific DNA-binding proteins from pea, wheat, soybean and cauliflower. Plant Mol Biol. 17**,** 111-23.

Indran, I. R., Hande, M. P., Pervaiz, S., 2009. Tumor cell redox state and mitochondria at the center of the non-canonical activity of telomerase reverse transcriptase. Mol Aspects Med.

Ingram, J. L., Peckham, S. M., Tisdale, B., Rodier, P. M., 2000. Prenatal exposure of rats to valproic acid reproduces the cerebellar anomalies associated with autism. Neurotoxicol Teratol. 22**,** 319-24.

Inoue, T., Krumlauf, R., 2001. An impulse to the brain--using in vivo electroporation. Nat Neurosci. 4 Suppl**,** 1156-8.

Inoue, T., Nakamura, S., Osumi, N., 2000. Fate mapping of the mouse prosencephalic neural plate. Dev Biol. 219**,** 373-83.

Jackson-Grusby, L., Beard, C., Possemato, R., Tudor, M., Fambrough, D., Csankovszki, G., Dausman, J., Lee, P., Wilson, C., Lander, E., Jaenisch, R., 2001. Loss of genomic methylation causes p53-dependent apoptosis and epigenetic deregulation. Nat Genet. 27**,** 31-9.

Jacobs, S. A., Khorasanizadeh, S., 2002. Structure of HP1 chromodomain bound to a lysine 9-methylated histone H3 tail. Science. 295**,** 2080-3.

Jaenisch, R., Bird, A., 2003. Epigenetic regulation of gene expression: how the genome integrates intrinsic and environmental signals. Nat Genet. 33 Suppl**,** 245-54.

Jeanclos, E., Krolewski, A., Skurnick, J., Kimura, M., Aviv, H., Warram, J. H., Aviv, A., 1998. Shortened telomere length in white blood cells of patients with IDDM. Diabetes. 47**,** 482-6.

Jenuwein, T., Allis, C. D., 2001. Translating the histone code. Science. 293**,** 1074-80.

Jergil, M., Forsberg, M., Salter, H., Stockling, K., Gustafson, A. L., Dencker, L., Stigson, M., 2011. Short-time gene expression response to valproic acid and valproic acid analogs in mouse embryonic stem cells. Toxicol Sci. 121**,** 328-42.

Jones, D.P., Go, Y.M., Anderson, C.L., Ziegler, T.R., Kinkade, J.M.Jr., Kirlin, W.G., 2004. Cysteine/cystine couple is a newly recognized node in the circuitry for biologic redox signaling and control. FASEB J. 18, 1246-68.

Jones, P. A., Baylin, S. B., 2002. The fundamental role of epigenetic events in cancer. Nat Rev Genet. 3**,** 415-28.

Jurima-Romet, M., Abbott, F. S., Tang, W., Huang, H. S., Whitehouse, L. W., 1996. Cytotoxicity of unsaturated metabolites of valproic acid and protection by vitamins C and E in glutathione-depleted rat hepatocytes. Toxicology. 112**,** 69-85.

Kachhap, S. K., Rosmus, N., Collis, S. J., Kortenhorst, M. S., Wissing, M. D., Hedayati, M., et al., 2010. Downregulation of homologous recombination DNA repair genes by HDAC inhibition in prostate cancer is mediated through the E2F1 transcription factor. PLoS One. 5: e11208.

Kageyama, S., Liu, H., Nagata, M., Aoki, F., 2006. Stage specific expression of histone deacetylase 4 (HDAC4) during oogenesis and early preimplantation development in mice. J Reprod Dev. 52**,** 99-106.

Kanatate, T., Nagao, N., Sugimoto, M., Kageyama, K., Fujimoto, T., Miwa, N., 1995. Differential susceptibility of epidermal keratinocytes and neuroblastoma cells to cytotoxicity of ultraviolet-B light irradiation prevented by the oxygen radical-scavenger ascorbate-2-phosphate but not by ascorbate. Cell Mol Biol Res. 41**,** 561-7.

Kaneko, S., Battino, D., Andermann, E., Wada, K., Kan, R., Takeda, A., Nakane, Y., Ogawa, Y., Avanzini, G., Fumarola, C., Granata, T., Molteni, F., Pardi, G., Minotti, L., Canger, R., Dansky, L., Oguni, M., Lopes-Cendas, I., Sherwin, A., Andermann, F., Seni, M. H., Okada, M., Teranishi, T., 1999. Congenital malformations due to antiepileptic drugs. Epilepsy Res. 33**,** 145-58.

Kar, S., Deb, M., Sengupta, D., Shilpi, A., Parbin, S., Torrisani, J., Pradhan, S., Patra, S., 2012. An insight into the various regulatory mechanisms modulating human DNA methyltransferase 1 stability and function. Epigenetics. 7.

Karanikolas, B. D., Figueiredo, M. L., Wu, L., 2009. Polycomb group protein enhancer of zeste 2 is an oncogene that promotes the neoplastic transformation of a benign prostatic epithelial cell line. Mol Cancer Res. 7**,** 1456-65.

Karanikolas, B. D., Figueiredo, M. L., Wu, L., 2010. Comprehensive evaluation of the role of EZH2 in the growth, invasion, and aggression of a panel of prostate cancer cell lines. Prostate. 70**,** 675-88.

Karlseder, J., Broccoli, D., Dai, Y., Hardy, S., de Lange, T., 1999. p53- and ATM-dependent apoptosis induced by telomeres lacking TRF2. Science. 283**,** 1321-5.

Kataoka, S., Takuma, K., Hara, Y., Maeda, Y., Ago, Y., Matsuda, T., 2011. Autism-like behaviours with transient histone hyperacetylation in mice treated prenatally with valproic acid. Int J Neuropsychopharmacol. 1-13.

Kawanishi, S., Oikawa, S., 2004. Mechanism of telomere shortening by oxidative stress. Ann N Y Acad Sci. 1019**,** 278-84.

Keohane, A. M., O'Neill L, P., Belyaev, N. D., Lavender, J. S., Turner, B. M., 1996. X-Inactivation and histone H4 acetylation in embryonic stem cells. Dev Biol. 180**,** 618-30.

Kern, J. C., Kehrer, J. P., 2005. Free radicals and apoptosis: relationships with glutathione, thioredoxin, and the BCL family of proteins. Front Biosci. 10**,** 1727-38.

Kessel, M., Gruss, P., 1991. Homeotic transformations of murine prevertebrae and concommitant alteration of Hox codes induced by retinoic acid. Cell. 67**,** 89-104.

Kim, B.Y., Han, M.J., Chung, A.S., 2001. Effects of reactive oxygen species on proliferation of Chinese hamster lung fibroblast (V79) cells. Free Radic Biol Med. 30, 686-98.

Kim, S. H., Kaminker, P., Campisi, J., 1999. TIN2, a new regulator of telomere length in human cells. Nat Genet. 23**,** 405-12.

Kim, T. H., Abdullaev, Z. K., Smith, A. D., Ching, K. A., Loukinov, D. I., Green, R. D., Zhang, M. Q., Lobanenkov, V. V., Ren, B., 2007. Analysis of the vertebrate insulator protein CTCF-binding sites in the human genome. Cell. 128**,** 1231-45.

Kimura, H., Cook, P. R., 2001. Kinetics of core histones in living human cells: little exchange of H3 and H4 and some rapid exchange of H2B. J Cell Biol. 153**,** 1341-53.

Kini, U., Adab, N., Vinten, J., Fryer, A., Clayton-Smith, J., 2006. Dysmorphic features: an important clue to the diagnosis and severity of fetal anticonvulsant syndromes. Arch Dis Child Fetal Neonatal Ed. 91**,** F90-5.

Kleer, C. G., Cao, Q., Varambally, S., Shen, R., Ota, I., Tomlins, S. A., Ghosh, D., Sewalt, R. G., Otte, A. P., Hayes, D. F., Sabel, M. S., Livant, D., Weiss, S. J., Rubin, M. A., Chinnaiyan, A. M., 2003. EZH2 is a marker of aggressive breast cancer and promotes neoplastic transformation of breast epithelial cells. Proc Natl Acad Sci U S A. 100**,** 11606-11.

Klobutcher, L. A., Swanton, M. T., Donini, P., Prescott, D. M., 1981. All gene-sized DNA molecules in four species of hypotrichs have the same terminal sequence and an unusual 3' terminus. Proc Natl Acad Sci U S A. 78**,** 3015-9.

Klymenko, T., Muller, J., 2004. The histone methyltransferases Trithorax and Ash1 prevent transcriptional silencing by Polycomb group proteins. EMBO Rep. 5**,** 373-7.

Klymenko, T., Papp, B., Fischle, W., Kocher, T., Schelder, M., Fritsch, C., Wild, B., Wilm, M., Muller, J., 2006. A Polycomb group protein complex with sequence-specific DNA-binding and selective methyl-lysine-binding activities. Genes Dev. 20**,** 1110-22.

Kmita, M., Duboule, D., 2003. Organizing axes in time and space; 25 years of colinear tinkering. Science. 301**,** 331-3.

Kmita, M., van Der Hoeven, F., Zakany, J., Krumlauf, R., Duboule, D., 2000. Mechanisms of Hox gene colinearity: transposition of the anterior Hoxb1 gene into the posterior HoxD complex. Genes Dev. 14**,** 198-211.

Koch, S., Jager-Roman, E., Losche, G., Nau, H., Rating, D., Helge, H., 1996. Antiepileptic drug treatment in pregnancy: drug side effects in the neonate and neurological outcome. Acta Paediatr. 85**,** 739-46.

Koetz, K., Bryl, E., Spickschen, K., O'Fallon, W. M., Goronzy, J. J., Weyand, C. M., 2000. T cell homeostasis in patients with rheumatoid arthritis. Proc Natl Acad Sci U S A. 97**,** 9203-8.

Kontges, G., Lumsden, A., 1996. Rhombencephalic neural crest segmentation is preserved throughout craniofacial ontogeny. Development. 122**,** 3229-42.

Kouzarides, T., 2002. Histone methylation in transcriptional control. Curr Opin Genet Dev. 12**,** 198-209.

Kouzarides, T., 2007. Chromatin modifications and their function. Cell. 128**,** 693-705.

Koziel, J. E., Fox, M. J., Steding, C. E., Sprouse, A. A., Herbert, B. S., 2011. Medical genetics and epigenetics of telomerase. J Cell Mol Med. 15**,** 457-67.

Krämer, O. H., Zhu, P., Ostendorff , H. P., Golebiewski, M., Tiefenbach, J., Peters, M. A., Brill, B., Groner, B., Bach, I., Heinzel, T., Göttlicher, M., 2003. The histone deacetylase inhibitor valproic acid selectively induces proteasomal degradation of HDAC2. EMBO J. 22, 3411-20.

Krogan, N. J., Dover, J., Khorrami, S., Greenblatt, J. F., Schneider, J., Johnston, M., Shilatifard, A., 2002. COMPASS, a histone H3 (Lysine 4) methyltransferase required for telomeric silencing of gene expression. J Biol Chem. 277**,** 10753-5.

Krogan, N. J., Dover, J., Wood, A., Schneider, J., Heidt, J., Boateng, M. A., Dean, K., Ryan, O. W., Golshani, A., Johnston, M., Greenblatt, J. F., Shilatifard, A., 2003. The Paf1 complex is required for histone H3 methylation by COMPASS and Dot1p: linking transcriptional elongation to histone methylation. Mol Cell. 11**,** 721-9.

Krumlauf, R., 1993. Hox genes and pattern formation in the branchial region of the vertebrate head. Trends Genet. 9**,** 106-112.

Kuendgen, A., Knipp, S., Fox, F., Strupp, C., Hildebrandt, B., Steidl, C., Germing, U., Haas, R., Gattermann, N., 2005. Results of a phase 2 study of valproic acid alone or in combination with all-trans retinoic acid in 75 patients with myelodysplastic syndrome and relapsed or refractory acute myeloid leukemia. Ann Hematol. 84 Suppl 1**,** 61-6.

Kuendgen, A., Schmid, M., Schlenk, R., Knipp, S., Hildebrandt, B., Steidl, C., Germing, U., Haas, R., Dohner, H., Gattermann, N., 2006. The histone deacetylase (HDAC) inhibitor valproic acid as monotherapy or in combination with all-trans retinoic acid in patients with acute myeloid leukemia. Cancer. 106**,** 112-9.

Kultima, K., Nystrom, A. M., Scholz, B., Gustafson, A. L., Dencker, L., Stigson, M., 2004. Valproic acid teratogenicity: a toxicogenomics approach. Environ Health Perspect. 112**,** 1225-35.

Kumaran, R. I., Spector, D. L., 2008. A genetic locus targeted to the nuclear periphery in living cells maintains its transcriptional competence. J Cell Biol. 180**,** 51-65.

Kurosaka, D., Yasuda, J., Yoshida, K., Yokoyama, T., Ozawa, Y., Obayashi, Y., Kingetsu, I., Saito, S., Yamada, A., 2003. Telomerase activity and telomere length of peripheral blood mononuclear cells in SLE patients. Lupus. 12**,** 591-9.

Kurosaka, D., Yasuda, J., Yoshida, K., Yoneda, A., Yasuda, C., Kingetsu, I., Toyokawa, Y., Yokoyama, T., Saito, S., Yamada, A., 2006. Abnormal telomerase activity and telomere length in T and B cells from patients with systemic lupus erythematosus. J Rheumatol. 33**,** 1102-7.

Kuzmichev, A., Nishioka, K., Erdjument-Bromage, H., Tempst, P., Reinberg, D., 2002. Histone methyltransferase activity associated with a human multiprotein complex containing the Enhancer of Zeste protein. Genes Dev. 16**,** 2893-905.

Kwon, Y. W., Masutani, H., Nakamura, H., Ishii, Y., Yodoi, J., 2003. Redox regulation of cell growth and cell death. Biol Chem. 384**,** 991-6.

Kwong, C., Adryan, B., Bell, I., Meadows, L., Russell, S., Manak, J. R., White, R., 2008. Stability and dynamics of polycomb target sites in Drosophila development. PLoS Genet. 4**,** e1000178.

Lachner, M., O'Carroll, D., Rea, S., Mechtler, K., Jenuwein, T., 2001. Methylation of histone H3 lysine 9 creates a binding site for HP1 proteins. Nature. 410**,** 116-20.

Lamond, A. I., Earnshaw, W. C., 1998. Structure and function in the nucleus. Science. 280**,** 547-53.

Lanca, V., Zee, R.Y., Rivera, A., Romero, J.R., 2009. Quantitative telomerase activity in circulating human leukocytes: utility of real-time telomeric repeats amplification protocol (RQ-TRAP) in a clinical/epidemiological setting. Clin Chem Lab Med. 47, 870-3.

Lander, E. S., Linton, L. M., Birren, B., Nusbaum, C., Zody, M. C., Baldwin, J., Devon, K., Dewar, K., Doyle, M., FitzHugh, W., Funke, R., Gage, D., Harris, K., Heaford, A., Howland, J., Kann, L., Lehoczky, J., LeVine, R., McEwan, P., McKernan, K., Meldrim,

J., Mesirov, J. P., Miranda, C., Morris, W., Naylor, J., Raymond, C., Rosetti, M., Santos, R., Sheridan, A., Sougnez, C., Stange-Thomann, N., Stojanovic, N., Subramanian, A., Wyman, D., Rogers, J., Sulston, J., Ainscough, R., Beck, S., Bentley, D., Burton, J., Clee, C., Carter, N., Coulson, A., Deadman, R., Deloukas, P., Dunham, A., Dunham, I., Durbin, R., French, L., Grafham, D., Gregory, S., Hubbard, T., Humphray, S., Hunt, A., Jones, M., Lloyd, C., McMurray, A., Matthews, L., Mercer, S., Milne, S., Mullikin, J. C., Mungall, A., Plumb, R., Ross, M., Shownkeen, R., Sims, S., Waterston, R. H., Wilson, R. K., Hillier, L. W., McPherson, J. D., Marra, M. A., Mardis, E. R., Fulton, L. A., Chinwalla, A. T., Pepin, K. H., Gish, W. R., Chissoe, S. L., Wendl, M. C., Delehaunty, K. D., Miner, T. L., Delehaunty, A., Kramer, J. B., Cook, L. L., Fulton, R. S., Johnson, D. L., Minx, P. J., Clifton, S. W., Hawkins, T., Branscomb, E., Predki, P., Richardson, P., Wenning, S., Slezak, T., Doggett, N., Cheng, J. F., Olsen, A., Lucas, S., Elkin, C., Uberbacher, E., Frazier, M., Gibbs, R. A., Muzny, D. M., Scherer, S. E., Bouck, J. B., Sodergren, E. J., Worley, K. C., Rives, C. M., Gorrell, J. H., Metzker, M. L., Naylor, S. L., Kucherlapati, R. S., Nelson, D. L., Weinstock, G. M., Sakaki, Y., Fujiyama, A., Hattori, M., Yada, T., Toyoda, A., Itoh, T., Kawagoe, C., Watanabe, H., Totoki, Y., Taylor, T., Weissenbach, J., Heilig, R., Saurin, W., Artiguenave, F., Brottier, P., Bruls, T., Pelletier, E., Robert, C., Wincker, P., Smith, D. R., Doucette-Stamm, L., Rubenfield, M., Weinstock, K., Lee, H. M., Dubois, J., Rosenthal, A., Platzer, M., Nyakatura, G., Taudien, S., Rump, A., Yang, H., Yu, J., Wang, J., Huang, G., Gu, J., Hood, L., Rowen, L., Madan, A., Qin, S., Davis, R. W., Federspiel, N. A., Abola, A. P., Proctor, M. J., Myers, R. M., Schmutz, J., Dickson, M., Grimwood, J., Cox, D. R., Olson, M. V., Kaul, R., Shimizu, N., Kawasaki, K., Minoshima, S., Evans, G. A., Athanasiou, M., Schultz, R., Roe, B. A., Chen, F., Pan, H., Ramser, J., Lehrach, H., Reinhardt, R., McCombie, W. R., de la Bastide, M., Dedhia, N., Blocker, H., Hornischer, K., Nordsiek, G., Agarwala, R., Aravind, L., Bailey, J. A., Bateman, A., Batzoglou, S., Birney, E., Bork, P., Brown, D. G., Burge, C. B., Cerutti, L., Chen, H. C., Church, D., Clamp, M., Copley, R. R., Doerks, T., Eddy, S. R., Eichler, E. E., Furey, T. S., Galagan, J., Gilbert, J. G., Harmon, C., Hayashizaki, Y., Haussler, D., Hermjakob, H., Hokamp, K., Jang, W., Johnson, L. S., Jones, T. A., Kasif, S., Kaspryzk, A., Kennedy, S., Kent, W. J., Kitts, P., Koonin, E. V., Korf, I., Kulp, D., Lancet, D., Lowe, T. M., McLysaght, A., Mikkelsen, T., Moran, J. V., Mulder, N., Pollara, V. J.,

Ponting, C. P., Schuler, G., Schultz, J., Slater, G., Smit, A. F., Stupka, E., Szustakowski, J., Thierry-Mieg, D., Thierry-Mieg, J., Wagner, L., Wallis, J., Wheeler, R., Williams, A., Wolf, Y. I., Wolfe, K. H., Yang, S. P., Yeh, R. F., Collins, F., Guyer, M. S., Peterson, J., Felsenfeld, A., Wetterstrand, K. A., Patrinos, A., Morgan, M. J., de Jong, P., Catanese, J. J., Osoegawa, K., Shizuya, H., Choi, S., Chen, Y. J., 2001. Initial sequencing and analysis of the human genome. Nature. 409**,** 860-921.

Langer, B., Haddad, J., Gasser, B., Maubert, M., Schlaeder, G., 1994. Isolated fetal bilateral radial ray reduction associated with valproic acid usage. Fetal Diagn Ther. 9**,** 155-8.

Latham, J. A., Dent, S. Y., 2007. Cross-regulation of histone modifications. Nat Struct Mol Biol. 14**,** 1017-24.

Laurent, L., Wong, E., Li, G., Huynh, T., Tsirigos, A., Ong, C. T., Low, H. M., Kin Sung, K. W., Rigoutsos, I., Loring, J., Wei, C. L., 2010. Dynamic changes in the human methylome during differentiation. Genome Res. 20**,** 320-31.

Lavigne, M., Francis, N. J., King, I. F., Kingston, R. E., 2004. Propagation of silencing; recruitment and repression of naive chromatin in trans by polycomb repressed chromatin. Mol Cell. 13**,** 415-25.

Lawson, K. A., Meneses, J. J., Pedersen, R. A., 1986. Cell fate and cell lineage in the endoderm of the presomite mouse embryo, studied with an intracellular tracer. Dev Biol. 115**,** 325-39.

Lawson, K. A., Meneses, J. J., Pedersen, R. A., 1991. Clonal analysis of epiblast fate during germ layer formation in the mouse embryo. Development. 113**,** 891-911.

Lawson, K. A., Pedersen, R. A., 1987. Cell fate, morphogenetic movement and population kinetics of embryonic endoderm at the time of germ layer formation in the mouse. Development. 101**,** 627-52.

Lee, J., Bottje, W. G., Kong, B. W., 2012. Genome-wide host responses against infectious laryngotracheitis virus vaccine infection in chicken embryo lung cells. BMC Genomics. 13**,** 143.

Lee, M. G., Wynder, C., Bochar, D. A., Hakimi, M. A., Cooch, N., Shiekhattar, R., 2006a. Functional interplay between histone demethylase and deacetylase enzymes. Mol Cell Biol. 26**,** 6395-402.

Lee, T. I., Jenner, R. G., Boyer, L. A., Guenther, M. G., Levine, S. S., Kumar, R. M., Chevalier, B., Johnstone, S. E., Cole, M. F., Isono, K., Koseki, H., Fuchikami, T., Abe, K., Murray, H. L., Zucker, J. P., Yuan, B., Bell, G. W., Herbolsheimer, E., Hannett, N. M., Sun, K., Odom, D. T., Otte, A. P., Volkert, T. L., Bartel, D. P., Melton, D. A., Gifford, D. K., Jaenisch, R., Young, R. A., 2006b. Control of developmental regulators by Polycomb in human embryonic stem cells. Cell. 125**,** 301-13.

Leeb, M., Pasini, D., Novatchkova, M., Jaritz, M., Helin, K., Wutz, A., Polycomb complexes act redundantly to repress genomic repeats and genes. Genes Dev. 24**,** 265-76.

Leipe, D. D., Landsman, D., 1997. Histone deacetylases, acetoin utilization proteins and acetylpolyamine amidohydrolases are members of an ancient protein superfamily. Nucleic Acids Res. 25**,** 3693-7.

Lemaire, M., Chabot, G. G., Raynal, N. J., Momparler, L. F., Hurtubise, A., Bernstein, M. L., Momparler, R. L., 2008. Importance of dose-schedule of 5-aza-2'-deoxycytidine for epigenetic therapy of cancer. BMC Cancer. 8**,** 128.

Lengauer, C., Kinzler, K. W., Vogelstein, B., 1998. Genetic instabilities in human cancers. Nature. 396**,** 643-9.

Lertratanangkoon, K., Orkiszewski, R. S., Scimeca, J. M., 1996. Methyl-donor deficiency due to chemically induced glutathione depletion. Cancer Res. 56**,** 995-1005.

Lertratanangkoon, K., Savaraj, N., Scimeca, J. M., Thomas, M. L., 1997. Glutathione depletion-induced thymidylate insufficiency for DNA repair synthesis. Biochem Biophys Res Commun. 234**,** 470-5.

Levine, S. S., Weiss, A., Erdjument-Bromage, H., Shao, Z., Tempst, P., Kingston, R. E., 2002. The core of the polycomb repressive complex is compositionally and functionally conserved in flies and humans. Mol Cell Biol. 22**,** 6070-8.

Li, B., Carey, M., Workman, J. L., 2007. The role of chromatin during transcription. Cell. 128**,** 707-19.

Li, E., 2002. Chromatin modification and epigenetic reprogramming in mammalian development. Nat Rev Genet. 3**,** 662-73.

Li, E., Bestor, T. H., Jaenisch, R., 1992. Targeted mutation of the DNA methyltransferase gene results in embryonic lethality. Cell. 69**,** 915-26.

Li, H., Xu, D., Li, J., Berndt, M. C., Liu, J. P., 2006. Transforming growth factor beta suppresses human telomerase reverse transcriptase (hTERT) by Smad3 interactions with c-Myc and the hTERT gene. J Biol Chem. 281**,** 25588-600.

Li, L. C., Dahiya, R., 2002. MethPrimer: designing primers for methylation PCRs. Bioinformatics. 18**,** 1427-31.

Li, J., Stouffs, M., Serrander, L., Banfi, B., Bettiol, E., Charnay, Y., Steger, K., Krause, K.H., Jaconi, M.E., 2006. The NADPH oxidase NOX4 drives cardiac differentiation: Role in regulating cardiac transcription factors and MAP kinase activation. Mol Biol Cell. 17, 3978-88.

Lillig, C.H., Holmgren, A., 2007. Thioredoxin and related molecules-from biology to health and disease. Antioxid Redox Signal. 9, 25–47.

Lindhout, D., Meinardi, H., Meijer, J. W., Nau, H., 1992. Antiepileptic drugs and teratogenesis in two consecutive cohorts: changes in prescription policy paralleled by changes in pattern of malformations. Neurology. 42**,** 94-110.

Lingner, J., Cech, T. R., Hughes, T. R., Lundblad, V., 1997a. Three Ever Shorter Telomere (EST) genes are dispensable for in vitro yeast telomerase activity. Proc Natl Acad Sci U S A. 94**,** 11190-5.

Lingner, J., Hug, N., 2006. Telomere length homeostasis. Chromosoma. 115, 413-25.

Lingner, J., Hughes, T. R., Shevchenko, A., Mann, M., Lundblad, V., Cech, T. R., 1997b. Reverse transcriptase motifs in the catalytic subunit of telomerase. Science. 276**,** 561-7.

Lipman, R. D., Bronson, R. T., Wu, D., Smith, D. E., Prior, R., Cao, G., Han, S. N., Martin, K. R., Meydani, S. N., Meydani, M., 1998. Disease incidence and longevity are unaltered by dietary antioxidant supplementation initiated during middle age in C57BL/6 mice. Mech Ageing Dev. 103**,** 269-84.

Lister, R., Pelizzola, M., Dowen, R. H., Hawkins, R. D., Hon, G., Tonti-Filippini, J., Nery, J. R., Lee, L., Ye, Z., Ngo, Q. M., Edsall, L., Antosiewicz-Bourget, J., Stewart, R., Ruotti, V., Millar, A. H., Thomson, J. A., Ren, B., Ecker, J. R. 2009. Human DNA methylomes at base resolution show widespread epigenomic differences. Nature. 2009 Nov 19;462(7271):315-22.

Liu, C. L., Kaplan, T., Kim, M., Buratowski, S., Schreiber, S. L., Friedman, N., Rando, O. J., 2005. Single-nucleosome mapping of histone modifications in S. cerevisiae. PLoS Biol. 3**,** e328.

Liu, J. P., 1999. Studies of the molecular mechanisms in the regulation of telomerase activity. FASEB J. 13**,** 2091-104.

Liu, K., Hodes, R. J., Weng, N., 2001. Cutting edge: telomerase activation in human T lymphocytes does not require increase in telomerase reverse transcriptase (hTERT) protein but is associated with hTERT phosphorylation and nuclear translocation. J Immunol. 166**,** 4826-30.

Liu, K., Schoonmaker, M. M., Levine, B. L., June, C. H., Hodes, R. J., Weng, N. P., 1999. Constitutive and regulated expression of telomerase reverse transcriptase (hTERT) in human lymphocytes. Proc Natl Acad Sci U S A. 96**,** 5147-52.

Liu, Y., Kha, H., Ungrin, M., Robinson, M. O., Harrington, L., 2002. Preferential maintenance of critically short telomeres in mammalian cells heterozygous for mTert. Proc Natl Acad Sci U S A. 99**,** 3597-602.

Loden, M., van Steensel, B., 2005. Whole-genome views of chromatin structure. Chromosome Res. 13**,** 289-98.

Loke, S. L., Stein, C. A., Zhang, X. H., Mori, K., Nakanishi, M., Subasinghe, C., Cohen, J. S., Neckers, L. M., 1989. Characterization of oligonucleotide transport into living cells. Proc Natl Acad Sci U S A. 86**,** 3474-8.

Loscher, W., 1999. Valproate: a reappraisal of its pharmacodynamic properties and mechanisms of action. Prog Neurobiol. 58**,** 31-59.

Luberda, Z., 2005. The role of glutathione in mammalian gametes. Reprod Biol. 5**,** 5-17.

Luger, K., Rechsteiner, T. J., Flaus, A. J., Waye, M. M., Richmond, T. J., 1997. Characterization of nucleosome core particles containing histone proteins made in bacteria. J Mol Biol. 272**,** 301-11.

Lumsden, A., 2004. Segmentation and compartition in the early avian hindbrain. Mech Dev. 121**,** 1081-8.

Lundblad, V., 2003. Telomere replication: an Est fest. Curr Biol. 13**,** R439-41.

Lundblad, V., Szostak, J. W., 1989. A mutant with a defect in telomere elongation leads to senescence in yeast. Cell. 57**,** 633-43.

Luo, J., Nikolaev, A. Y., Imai, S., Chen, D., Su, F., Shiloh, A., Guarente, L., Gu, W., 2001. Negative control of p53 by Sir2alpha promotes cell survival under stress. Cell. 107**,** 137-48.

Lyer, L. M., Anantharaman, V., Wolf, M. Y., Aravind, L., 2008. Comparative genomics of transcription factors and chromatin proteins in parasitic protists and other eukaryotes. Int. J. Parasitol. 38, 1-31.

Lyer, L. M., Tahiliani, M., Rao, A., Aravind, L., 2009. Prediction of novel families of enzymes involved in oxidative and other complex modifications of bases in nucleic acids. Cell Cycle. 8, 1698-710.

Lyon, H. M., Holmes, L. B., Huang, T., 2003. Multiple congenital anomalies associated with in utero exposure of phenytoin: possible hypoxic ischemic mechanism? Birth Defects Res A Clin Mol Teratol. 67**,** 993-6.

Maconochie, M., Krishnamurthy, R., Nonchev, S., Meier, P., Manzanares, M., Mitchell, P. J., Krumlauf, R., 1999. Regulation of Hoxa2 in cranial neural crest cells involves members of the AP-2 family. Development. 126**,** 1483-94.

Maeda, Y., Yanagimachi, H., Tateno, H., Usui, N., Yanagimachi, R., 1998. Decondensation of the mouse sperm nucleus within the interphase nucleus. Zygote. 6**,** 39-45.

Mahmood, R., Mason, I. J., Morriss-Kay, G. M., 1996. Expression of Fgf-3 in relation to hindbrain segmentation, otic pit position and pharyngeal arch morphology in normal and retinoic acid-exposed mouse embryos. Anat Embryol (Berl). 194**,** 13-22.

Makarov, V. L., Hirose, Y., Langmore, J. P., 1997. Long G tails at both ends of human chromosomes suggest a C strand degradation mechanism for telomere shortening. Cell. 88**,** 657-66.

Makpol, S., Zainuddin, A., Rahim, N. A., Yusof, Y. A., Ngah, W. Z., Alpha-tocopherol modulates hydrogen peroxide-induced DNA damage and telomere shortening of human skin fibroblasts derived from differently aged individuals. Planta Med. 76**,** 869-75.

Margueron, R., Reinberg, D., 2011. The Polycomb complex PRC2 and its mark in life. Nature. 469**,** 343-9.

Markovic, J., Borras, C., Ortega, A., Sastre, J., Vina, J., Pallardo, F.V., 2007. Glutathione is recruited into the nucleus in early phases of cell. Proliferation. J Biol Chem. 282, 20416 – 24.

Markovic, J., Garcia-Gimenez, J. L., Gimeno, A., Vina, J., Pallardo, F. V., 2010. Role of glutathione in cell nucleus. Free Radic Res. 44**,** 721-33.

Markovic, J., Mora, N., Broseta, A.M., Gimeno, A., de-la-Concepcion, N., Vina, J., Pallarodo, F., 2009. The depletion of nuclear glutathione impair cell proliferation in 3t3 fibroblasts. PLoS ONE. 4, 2-14.

Maroulakou, I. G., Spyropoulos, D. D., 2003. The study of HOX gene function in hematopoietic, breast and lung carcinogenesis. Anticancer Res. 23**,** 2101-10.

Marshall, W. F., 2003. Gene expression and nuclear architecture during development and differentiation. Mech Dev. 120**,** 1217-30.

Martin-Rivera, L., Herrera, E., Albar, J. P., Blasco, M. A., 1998. Expression of mouse telomerase catalytic subunit in embryos and adult tissues. Proc Natl Acad Sci U S A. 95**,** 10471-6.

Martinez, P., Blasco, M. A., 2011. Telomeric and extra-telomeric roles for telomerase and the telomere-binding proteins. Nat Rev Cancer. 11**,** 161-76.

Martinez, P., Thanasoula, M., Munoz, P., Liao, C., Tejera, A., McNees, C., Flores, J. M., Fernandez-Capetillo, O., Tarsounas, M., Blasco, M. A., 2009. Increased telomere fragility and fusions resulting from TRF1 deficiency lead to degenerative pathologies and increased cancer in mice. Genes Dev. 23**,** 2060-75.

Maser, R. S., DePinho, R. A., 2002. Connecting chromosomes, crisis, and cancer. Science. 297**,** 565-9.

Masutomi, K., Possemato, R., Wong, J. M., Currier, J. L., Tothova, Z., Manola, J. B., Ganesan, S., Lansdorp, P. M., Collins, K., Hahn, W. C., 2005. The telomerase reverse transcriptase regulates chromatin state and DNA damage responses. Proc Natl Acad Sci U S A. 102**,** 8222-7.

Maunakea, A. K., Nagarajan, R. P., Bilenky, M., Ballinger, T. J., D'Souza, C., Fouse, S. D., Johnson, B. E., Hong, C., Nielsen, C., Zhao, Y., Turecki, G., Delaney, A., Varhol, R., Thiessen, N., Shchors, K., Heine, V. M., Rowitch, D. H., Xing, X., Fiore, C., Schillebeeckx, M., Jones, S. J., Haussler, D., Marra, M. A., Hirst, M., Wang, T., Costello, J. F,. 2010. Conserved role of intragenic DNA methylation in regulating alternative promoters. Nature. 466, 253-7

Mayer, W., Niveleau, A., Walter, J., Fundele, R., Haaf, T., 2000. Demethylation of the zygotic paternal genome. Nature. 403**,** 501-2.

McElligott, R., Wellinger, R. J., 1997. The terminal DNA structure of mammalian chromosomes. EMBO J. 16**,** 3705-14.

McGinnis, W., Krumlauf, R., 1992. Homeobox gene and axial patterning. Cell. 68**,** 283-302.

McGonigle, G. J., Lappin, T. R., Thompson, A., 2008. Grappling with the HOX network in hematopoiesis and leukemia. Front Biosci. 13**,** 4297-308.

McGrath, M., Wong, J. Y., Michaud, D., Hunter, D. J., De Vivo, I., 2007. Telomere length, cigarette smoking, and bladder cancer risk in men and women. Cancer Epidemiol Biomarkers Prev. 16**,** 815-9.

McNutt, T.L., Harris, C., 1994. Lindane embryotoxicity and differential alteration of cysteine and glutathione levels in rat embryos and visceral yolk sacs. Reprod Toxicol. 8, 351–62.

Meador, K. J., In utero antiepileptic drugs: differential cognitive outcomes in children of women with epilepsy. American Epilepsy Society 12, 2006.

Medvedeva, Y. A., Fridman, M. V., Oparina, N. J., Malko, D. B., Ermakova, E. O., Kulakovskiy, I. V., Heinzel, A., Makeev, V. J., Intergenic, gene terminal, and intragenic CpG islands in the human genome. BMC Genomics. 2010 Jan 19;11:48.

Meeker, A. K., Hicks, J. L., Gabrielson, E., Strauss, W. M., De Marzo, A. M., Argani, P., 2004a. Telomere shortening occurs in subsets of normal breast epithelium as well as in situ and invasive carcinoma. Am J Pathol. 164**,** 925-35.

Meeker, A. K., Hicks, J. L., Iacobuzio-Donahue, C. A., Montgomery, E. A., Westra, W. H., Chan, T. Y., Ronnett, B. M., De Marzo, A. M., 2004b. Telomere length abnormalities occur early in the initiation of epithelial carcinogenesis. Clin Cancer Res. 10**,** 3317-26.

Mehnert, J. M., Kelly, W. K., 2007. Histone deacetylase inhibitors: biology and mechanism of action. Cancer J. 13**,** 23-9.

Meissner, A., Mikkelsen, T. S., Gu, H., Wernig, M., Hanna, J., Sivachenko, A., Zhang, X., Bernstein, B. E., Nusbaum, C., Jaffe, D. B., Gnirke, A., Jaenisch, R., Lander, E. S., 2008. Genome-scale DNA methylation maps of pluripotent and differentiated cells. Nature. 454**,** 766-70.

Menegola, E., Broccia, M. L., Di Renzo, F., Prati, M., Giavini, E., 2000. In vitro teratogenic potential of two antifungal triazoles: triadimefon and triadimenol. In Vitro Cell Dev Biol Anim. 36**,** 88-95.

Menegola, E., Di Renzo, F., Broccia, M. L., Giavini, E., 2006. Inhibition of histone deacetylase as a new mechanism of teratogenesis. Birth Defects Res C Embryo Today. 78**,** 345-53.

Menegola, E., Di Renzo, F., Broccia, M. L., Prudenziati, M., Minucci, S., Massa, V., Giavini, E., 2005. Inhibition of histone deacetylase activity on specific embryonic tissues as a new mechanism for teratogenicity. Birth Defects Res B Dev Reprod Toxicol. 74**,** 392-8.

Meshorer, E., Misteli, T., 2006. Chromatin in pluripotent embryonic stem cells and differentiation. Nat Rev Mol Cell Biol. 7**,** 540-6.

Meshorer, E., Yellajoshula, D., George, E., Scambler, P. J., Brown, D. T., Misteli, T., 2006. Hyperdynamic plasticity of chromatin proteins in pluripotent embryonic stem cells. Dev Cell. 10**,** 105-16.

Metzger, E., Imhof, A., Patel, D., Kahl, P., Hoffmeyer, K., Friedrichs, N., Muller, J. M., Greschik, H., Kirfel, J., Ji, S., Kunowska, N., Beisenherz-Huss, C., Gunther, T., Buettner, R., Schule, R., 2010. Phosphorylation of histone H3T6 by PKCbeta(I) controls demethylation at histone H3K4. Nature. 464**,** 792-6.

Meyerson, M., Counter, C. M., Eaton, E. N., Ellisen, L. W., Steiner, P., Caddle, S. D., Ziaugra, L., Beijersbergen, R. L., Davidoff, M. J., Liu, Q., Bacchetti, S., Haber, D. A., Weinberg, R. A., 1997. hEST2, the putative human telomerase catalytic subunit gene, is up-regulated in tumor cells and during immortalization. Cell. 90**,** 785-95.

Mikkelsen, T. S., Ku, M., Jaffe, D. B., Issac, B., Lieberman, E., Giannoukos, G., Alvarez, P., Brockman, W., Kim, T. K., Koche, R. P., Lee, W., Mendenhall, E., O'Donovan, A., Presser, A., Russ, C., Xie, X., Meissner, A., Wernig, M., Jaenisch, R., Nusbaum, C., Lander, E. S., Bernstein, B. E., 2007. Genome-wide maps of chromatin state in pluripotent and lineage-committed cells. Nature. 448**,** 553-60.

Miller, C.P., Singh, M.M., Rivera-Del Valle, N., Manton, C.A., Chandra, J., 2011. Therapeutic strategies to enhance the anticancer efficacy of histone deacetylase inhibitors. J Biomed Biotechnol. ID: 514261

Miller, T., Krogan, N. J., Dover, J., Erdjument-Bromage, H., Tempst, P., Johnston, M., Greenblatt, J. F., Shilatifard, A., 2001. COMPASS: a complex of proteins associated with a trithorax-related SET domain protein. Proc Natl Acad Sci U S A. 98**,** 12902-7.

Min, J., Zhang, Y., Xu, R. M., 2003. Structural basis for specific binding of Polycomb chromodomain to histone H3 methylated at Lys 27. Genes Dev. 17**,** 1823-8.

Minamino, T., Mitsialis, S. A., Kourembanas, S., 2001. Hypoxia extends the life span of vascular smooth muscle cells through telomerase activation. Mol Cell Biol. 21**,** 3336-42.

Mitchell, J. R., Wood, E., Collins, K., 1999. A telomerase component is defective in the human disease dyskeratosis congenita. Nature. 402**,** 551-5.

Miura, M., Karasaki, Y., Abe, T., Higashi, K., Ikemura, K., Gotoh, S., 1998. Prompt activation of telomerase by chemical carcinogens in rats detected with a modified TRAP assay. Biochem Biophys Res Commun. 246**,** 13-9.

Mizzen, C. A., Yang, X. J., Kokubo, T., Brownell, J. E., Bannister, A. J., Owen-Hughes, T., Workman, J., Wang, L., Berger, S. L., Kouzarides, T., Nakatani, Y., Allis, C. D., 1996. The TAF(II)250 subunit of TFIID has histone acetyltransferase activity. Cell. 87**,** 1261-70.

Mohn, F., Weber, M., Rebhan, M., Roloff, T. C., Richter, J., Stadler, M. B., Bibel, M., Schubeler, D., 2008. Lineage-specific polycomb targets and de novo DNA methylation define restriction and potential of neuronal progenitors. Mol Cell. 30**,** 755-66.

Moore, S. J., Turnpenny, P., Quinn, A., Glover, S., Lloyd, D. J., Montgomery, T., Dean, J. C., 2000. A clinical study of 57 children with fetal anticonvulsant syndromes. J Med Genet. 37**,** 489-97.

Morrow, J., Russell, A., Guthrie, E., Parsons, L., Robertson, I., Waddell, R., Irwin, B., McGivern, R. C., Morrison, P. J., Craig, J., 2006. Malformation risks of antiepileptic drugs in

pregnancy: a prospective study from the UK Epilepsy and Pregnancy Register. J Neurol Neurosurg Psychiatry. 77**,** 193-8.

Muller, J., Hart, C. M., Francis, N. J., Vargas, M. L., Sengupta, A., Wild, B., Miller, E. L., O'Connor, M. B., Kingston, R. E., Simon, J. A., 2002. Histone methyltransferase activity of a Drosophila Polycomb group repressor complex. Cell. 111**,** 197-208.

Muller, J., Kassis, J. A., 2006. Polycomb response elements and targeting of Polycomb group proteins in Drosophila. Curr Opin Genet Dev. 16**,** 476-84.

Munoz, P., Blanco, R., Flores, J. M., Blasco, M. A., 2005. XPF nuclease-dependent telomere loss and increased DNA damage in mice overexpressing TRF2 result in premature aging and cancer. Nat Genet. 37**,** 1063-71.

Nagy, P. L., Griesenbeck, J., Kornberg, R. D., Cleary, M. L., 2002. A trithorax-group complex purified from Saccharomyces cerevisiae is required for methylation of histone H3. Proc Natl Acad Sci U S A. 99**,** 90-4.

Nakagawa, T., Kajitani, T., Togo, S., Masuko, N., Ohdan, H., Hishikawa, Y., Koji, T., Matsuyama, T., Ikura, T., Muramatsu, M., Ito, T., 2008. Deubiquitylation of histone H2A activates transcriptional initiation via trans-histone cross-talk with H3K4 di- and trimethylation. Genes Dev. 22**,** 37-49.

Nakamura, T. M., Morin, G. B., Chapman, K. B., Weinrich, S. L., Andrews, W. H., Lingner, J., Harley, C. B., Cech, T. R., 1997. Telomerase catalytic subunit homologs from fission yeast and human. Science. 277**,** 955-9.

Nakayama, J., Rice, J. C., Strahl, B. D., Allis, C. D., Grewal, S. I., 2001. Role of histone H3 lysine 9 methylation in epigenetic control of heterochromatin assembly. Science. 292**,** 110-3.

Nan, X., Campoy, F. J., Bird, A., 1997. MeCP2 is a transcriptional repressor with abundant binding sites in genomic chromatin. Cell. 88**,** 471-81.

Narotsky, M. G., Francis, E. Z., Kavlock, R. J., 1994. Developmental toxicity and structure-activity relationships of aliphatic acids, including dose-response assessment of valproic acid in mice and rats. Fundam Appl Toxicol. 22**,** 251-65.

Nau, H., Placental transfer and neonatal pharmacokinetics of valproic acid and some of its metabolites. In: D. e. a. Janz, (Ed.), Epilepsy, pregnancy, and the child. New York: Raven Press, 1982, pp. 367-372.

Ndlovu, M. N., Denis, H., Fuks, F., 2011. Exposing the DNA methylome iceberg. Trends Biochem Sci. 36**,** 381-7.

Nelson, C. J., Santos-Rosa, H., Kouzarides, T., 2006. Proline isomerization of histone H3 regulates lysine methylation and gene expression. Cell. 126**,** 905-16.

New, D. A., 1978. Whole-embryo culture and the study of mammalian embryos during organogenesis. Biol Rev Camb Philos Soc. 53**,** 81-122.

Ng, H. H., Robert, F., Young, R. A., Struhl, K., 2003. Targeted recruitment of Set1 histone methylase by elongating Pol II provides a localized mark and memory of recent transcriptional activity. Mol Cell. 11**,** 709-19.

Ng, H. H., Zhang, Y., Hendrich, B., Johnson, C. A., Turner, B. M., Erdjument-Bromage, H., Tempst, P., Reinberg, D., Bird, A., 1999. MBD2 is a transcriptional repressor belonging to the MeCP1 histone deacetylase complex. Nat Genet. 23**,** 58-61.

Nguyen, C. T., Weisenberger, D. J., Velicescu, M., Gonzales, F. A., Lin, J. C., Liang, G., Jones, P. A., 2002. Histone H3-lysine 9 methylation is associated with aberrant gene silencing in cancer cells and is rapidly reversed by 5-aza-2'-deoxycytidine. Cancer Res. 62**,** 6456-61.

Nikoloski, G., Langemeijer, S. M., Kuiper, R. P., Knops, R., Massop, M., Tonnissen, E. R., van der Heijden, A., Scheele, T. N., Vandenberghe, P., de Witte, T., van der Reijden, B. A., Jansen, J. H., 2010. Somatic mutations of the histone methyltransferase gene EZH2 in myelodysplastic syndromes. Nat Genet. 42**,** 665-7.

Nishiyama, A., Matsui, M., Iwata, S., Hirota, K., Masutani, H., Nakamura, H., Takagi, Y., Sono, H., Gon, Y., Yodoi, J., 1999. Identification of thioredoxinbinding protein-2/vitamin D(3)

up-regulated protein 1 as a negative regulator of thioredoxin function and expression. J Biol Chem 274, 21645–21650.

Nkabyo, Y.S., Ziegler, T.R., Gu, L.H., Watson, W.H., Jones, D.P., 2002. Glutathione and thioredoxin redox during differentiation in human colon epithelial (Caco-2) cells. Am J Physiol Gastrointest Liver Physiol. 283, G1352-9.

Nonchev, S., Tsanev, R., 1990. Protamine-histone replacement and DNA replication in the male mouse pronucleus. Mol Reprod Dev. 25**,** 72-6.

North, B. J., Verdin, E., 2004. Sirtuins: Sir2-related NAD-dependent protein deacetylases. Genome Biol. 5**,** 224.

Novak, P., Jensen, T., Oshiro, M. M., Wozniak, R. J., Nouzova, M., Watts, G. S., Klimecki, W. T., Kim, C., Futscher, B. W., 2006. Epigenetic inactivation of the HOXA gene cluster in breast cancer. Cancer Res. 66**,** 10664-70.

Nulman, I., Scolnik, D., Chitayat, D., Farkas, L. D., Koren, G., 1997. Findings in children exposed in utero to phenytoin and carbamazepine monotherapy: independent effects of epilepsy and medications. Am J Med Genet. 68**,** 18-24.

O'Sullivan, R. J., Karlseder, J., 2010. Telomeres: protecting chromosomes against genome instability. Nat Rev Mol Cell Biol. 11**,** 171-81.

Oback, B., Cid-Arregui, A., Huttner, W. B., Gene transfer into cultured postimplantation mouse embryos using herpes simplex amplicons. In: A. Cid-Arregui, A. Garcia-Carranca, Eds.), Viral vectors: basic science and gene therappy. Eaton Publishing, Natick, MA, 2000, pp. 277-293.

Odagiri, E., Kanada, N., Jibiki, K., Demura, R., Aikawa, E., Demura, H., 1994. Reduction of telomeric length and c-erbB-2 gene amplification in human breast cancer, fibroadenoma, and gynecomastia. Relationship to histologic grade and clinical parameters. Cancer. 73**,** 2978-84.

Ogryzko, V. V., Schiltz, R. L., Russanova, V., Howard, B. H., Nakatani, Y., 1996. The transcriptional coactivators p300 and CBP are histone acetyltransferases. Cell. 87**,** 953-9.

Ohm, J. E., McGarvey, K. M., Yu, X., Cheng, L., Schuebel, K. E., Cope, L., Mohammad, H. P., Chen, W., Daniel, V. C., Yu, W., Berman, D. M., Jenuwein, T., Pruitt, K., Sharkis, S. J., Watkins, D. N., Herman, J. G., Baylin, S. B., 2007. A stem cell-like chromatin pattern may predispose tumor suppressor genes to DNA hypermethylation and heritable silencing. Nat Genet. 39**,** 237-42.

Okada, A., Kurihara, H., Aoki, Y., Bialer, M., Fujiwara, M., 2004. Amidic modification of valproic acid reduces skeletal teratogenicity in mice. Birth Defects Res B Dev Reprod Toxicol. 71**,** 47-53.

Okano, M., Bell, D. W., Haber, D. A., Li, E., 1999. DNA methyltransferases Dnmt3a and Dnmt3b are essential for de novo methylation and mammalian development. Cell. 99**,** 247-57.

Okano, M., Xie, S., Li, E., 1998. Dnmt2 is not required for de novo and maintenance methylation of viral DNA in embryonic stem cells. Nucleic Acids Res. 26**,** 2536-40.

Oktyabrsky, O. N., Smirnova, G. V., 2007. Redox regulation of cellular functions. Biochemistry (Mosc). 72**,** 132-45.

Oliver, S. S., Denu, J. M., 2011. Dynamic interplay between histone H3 modifications and protein interpreters: emerging evidence for a "histone language". Chembiochem. 12**,** 299-307.

Olovnikov, A. M., 1973. A theory of marginotomy. The incomplete copying of template margin in enzymic synthesis of polynucleotides and biological significance of the phenomenon. J Theor Biol. 41**,** 181-90.

Omtzigt, J. G., Nau, H., Los, F. J., Pijpers, L., Lindhout, D., 1992. The disposition of valproate and its metabolites in the late first trimester and early second trimester of pregnancy in maternal serum, urine, and amniotic fluid: effect of dose, co-medication, and the presence of spina bifida. Eur J Clin Pharmacol. 43**,** 381-8.

Ooi, S. K., Qiu, C., Bernstein, E., Li, K., Jia, D., Yang, Z., Erdjument-Bromage, H., Tempst, P., Lin, S. P., Allis, C. D., Cheng, X., Bestor, T. H., 2007. DNMT3L connects unmethylated lysine 4 of histone H3 to de novo methylation of DNA. Nature. 448**,** 714-7.

Orlando, V., Jane, E. P., Chinwalla, V., Harte, P. J., Paro, R., 1998. Binding of trithorax and Polycomb proteins to the bithorax complex: dynamic changes during early Drosophila embryogenesis. EMBO J. 17**,** 5141-50.

Ornoy, A., 2003. The impact of intrauterine exposure versus postnatal environment in neurodevelopmental toxicity: long-term neurobehavioral studies in children at risk for developmental disorders. Toxicol Lett. 140-141**,** 171-81.

Ornoy, A., 2006. Neuroteratogens in man: an overview with special emphasis on the teratogenicity of antiepileptic drugs in pregnancy. Reprod Toxicol. 22**,** 214-26.

Ornoy, A., 2007. Embryonic oxidative stress as a mechanism of teratogenesis with special emphasis on diabetic embryopathy. Reprod Toxicol. 24**,** 31-41.

Ornoy, A., 2009. Valproic acid in pregnancy: how much are we endangering the embryo and fetus? Reprod Toxicol. 28**,** 1-10.

Osumi, N., Inoue, T., 2001. Gene transfer into cultured mammalian embryos by electroporation. Methods. 24**,** 35-42.

Oswald, J., Engemann, S., Lane, N., Mayer, W., Olek, A., Fundele, R., Dean, W., Reik, W., Walter, J., 2000. Active demethylation of the paternal genome in the mouse zygote. Curr Biol. 10**,** 475-8.

Ouellette, M. M., Liao, M., Herbert, B. S., Johnson, M., Holt, S. E., Liss, H. S., Shay, J. W., Wright, W. E., 2000. Subsenescent telomere lengths in fibroblasts immortalized by limiting amounts of telomerase. J Biol Chem. 275**,** 10072-6.

Owens, M. J., Nemeroff, C. B., 2003. Pharmacology of valproate. Psychopharmacol Bull. 37 Suppl 2**,** 17-24.

Ozolins, T. R., Hales, B. F., 1997. Oxidative stress regulates the expression and activity of transcription factor activator protein-1 in rat conceptus. J Pharmacol Exp Ther. 280**,** 1085-93.

Ozolins, T.R., Harrouk, W., Doerksen, T., Trasler, J.M., Hales, B.F., 2002. Buthionine sulfoximine embryotoxicity is associated with prolonged AP-1 activation. Teratology. 66,192–200.

Padmanabhan, R., Ahmed, I., 1996. Sodium valproate augments spontaneous neural tube defects and axial skeletal malformations in TO mouse fetuses [corrected]. Reprod Toxicol. 10**,** 345-63.

Pallardo, F. V., Markovic, J., Garcia, J. L., Vina, J., 2009. Role of nuclear glutathione as a key regulator of cell proliferation. Mol Aspects Med. 30**,** 77-85.

Palm, W., de Lange, T., 2008. How shelterin protects mammalian telomeres. Annu Rev Genet. 42**,** 301-34.

Pan, H., O'Brien M, J., Wigglesworth, K., Eppig, J. J., Schultz, R. M., 2005. Transcript profiling during mouse oocyte development and the effect of gonadotropin priming and development in vitro. Dev Biol. 286**,** 493-506.

Pan, W. W., Li, J. D., Huang, S., Papadimos, T. J., Pan, Z. K., Chen, L. Y., 2012. Synergistic activation of NF-{kappa}B by bacterial chemoattractant and TNF{alpha} is mediated by p38 MAPK-dependent RelA acetylation. J Biol Chem. 285**,** 34348-54.

Parada, L., Misteli, T., 2002. Chromosome positioning in the interphase nucleus. Trends Cell Biol. 12**,** 425-32.

Parada, L. A., McQueen, P. G., Misteli, T., 2004. Tissue-specific spatial organization of genomes. Genome Biol. 5**,** R44.

Parameswaran, M., Tam, P. P., 1995. Regionalisation of cell fate and morphogenetic movement of the mesoderm during mouse gastrulation. Dev Genet. 17**,** 16-28.

Park, J. I., Venteicher, A. S., Hong, J. Y., Choi, J., Jun, S., Shkreli, M., Chang, W., Meng, Z., Cheung, P., Ji, H., McLaughlin, M., Veenstra, T. D., Nusse, R., McCrea, P. D., Artandi, S. E., 2009. Telomerase modulates Wnt signalling by association with target gene chromatin. Nature. 460**,** 66-72.

Pasini, D., Bracken, A. P., Hansen, J. B., Capillo, M., Helin, K., 2007. The polycomb group protein Suz12 is required for embryonic stem cell differentiation. Mol Cell Biol. 27**,** 3769-79.

Passos, J. F., Saretzki, G., Ahmed, S., Nelson, G., Richter, T., Peters, H., Wappler, I., Birket, M. J., Harold, G., Schaeuble, K., Birch-Machin, M. A., Kirkwood, T. B., von Zglinicki, T., 2007. Mitochondrial dysfunction accounts for the stochastic heterogeneity in telomere-dependent senescence. PLoS Biol. 5**,** e110.

Passos, J. F., Von Zglinicki, T., 2006. Oxygen free radicals in cell senescence: are they signal transducers? Free Radic Res. 40**,** 1277-83.

Perreault, S. D., Wolff, R. A., Zirkin, B. R., 1984. The role of disulfide bond reduction during mammalian sperm nuclear decondensation in vivo. Dev Biol. 101**,** 160-7.

Perucca, E., 2002. Pharmacological and therapeutic properties of valproate: a summary after 35 years of clinical experience. CNS Drugs. 16**,** 695-714.

Perucca, E., 2005. Birth defects after prenatal exposure to antiepileptic drugs. Lancet Neurol. 4**,** 781-6.

Perucca, E., Tomson, T., 2006. Prenatal exposure to antiepileptic drugs. Lancet. 367**,** 1467-9.

Petruk, S., Sedkov, Y., Riley, K. M., Hodgson, J., Schweisguth, F., Hirose, S., Jaynes, J. B., Brock, H. W., Mazo, A., 2006. Transcription of bxd noncoding RNAs promoted by trithorax represses Ubx in cis by transcriptional interference. Cell. 127**,** 1209-21.

Pfeifer, G. P., Rauch, T. A., 2009. DNA methylation patterns in lung carcinomas. Semin Cancer Biol. 19**,** 181-7.

Phair, R. D., Scaffidi, P., Elbi, C., Vecerova, J., Dey, A., Ozato, K., Brown, D. T., Hager, G., Bustin, M., Misteli, T., 2004. Global nature of dynamic protein-chromatin interactions in vivo: three-dimensional genome scanning and dynamic interaction networks of chromatin proteins. Mol Cell Biol. 24**,** 6393-402.

Phiel, C. J., Zhang, F., Huang, E. Y., Guenther, M. G., Lazar, M. A., Klein, P. S., 2001. Histone deacetylase is a direct target of valproic acid, a potent anticonvulsant, mood stabilizer, and teratogen. J Biol Chem. 276**,** 36734-41.

Pidoux, A. L., Allshire, R. C., 2005. The role of heterochromatin in centromere function. Philos Trans R Soc Lond B Biol Sci. 360**,** 569-79.

Pietersen, A. M., Horlings, H. M., Hauptmann, M., Langerod, A., Ajouaou, A., Cornelissen-Steijger, P., Wessels, L. F., Jonkers, J., van de Vijver, M. J., van Lohuizen, M., 2008. EZH2 and BMI1 inversely correlate with prognosis and TP53 mutation in breast cancer. Breast Cancer Res. 10**,** R109.

Pires-daSilva, A., Sommer, R. J., 2003. Finally, worm polycomb-like genes meet Hox regulation. Dev Cell. 4**,** 770-2.

Polifka, J. E., Friedman, J. M., 2002. Medical genetics: 1. Clinical teratology in the age of genomics. CMAJ. 167**,** 265-73.

Porter, R. J., Meldrum, B. S., Antiseizure drugs. In: B. G. Katzung, (Ed.), Basic & Clinical Pharmacology. Lange Medical Books/McGraw-Hill, 2001, pp. 395-418.

Prince, V., Lumsden, A., 1994. Hoxa2 expression in normal and transposed rhombomeres: independent regulation in the neural tube and neural crest. Development. 120**,** 911-923.

Pryor, S. E., Massa, V., Savery, D., Greene, N. D., Copp, A. J., 2012. Convergent extension analysis in mouse whole embryo culture. Methods Mol Biol. 839**,** 133-46.

Quinlan, G. A., Williams, E. A., Tan, S. S., Tam, P. P., 1995. Neuroectodermal fate of epiblast cells in the distal region of the mouse egg cylinder: implication for body plan organization during early embryogenesis. Development. 121**,** 87-98.

Raman, V., Martensen, S. A., Reisman, D., Evron, E., Odenwald, W. F., Jaffee, E., Marks, J., Sukumar, S., 2000. Compromised HOXA5 function can limit p53 expression in human breast tumours. Nature. 405**,** 974-8.

Ramsahoye, B. H., Biniszkiewicz, D., Lyko, F., Clark, V., Bird, A. P., Jaenisch, R., 2000. Non-CpG methylation is prevalent in embryonic stem cells and may be mediated by DNA methyltransferase 3a. Proc Natl Acad Sci U S A. 97, 5237-42.

Rajendran, P., Ho, E., Williams, D. E., Dashwood, R. H., 2011. Dietary phytochemicals, HDAC inhibition, and DNA damage/repair defects in cancer cells. Clinical Epigenetics. 3: 4.

Rao, T. P., Kuhl, M., 2010. An updated overview on Wnt signaling pathways: a prelude for more. Circ Res. 106**,** 1798-806.

Rasalam, A. D., Hailey, H., Williams, J. H., Moore, S. J., Turnpenny, P. D., Lloyd, D. J., Dean, J. C., 2005. Characteristics of fetal anticonvulsant syndrome associated autistic disorder. Dev Med Child Neurol. 47**,** 551-5.

Rastelli, L., Chan, C. S., Pirrotta, V., 1993. Related chromosome binding sites for zeste, suppressors of zeste and Polycomb group proteins in Drosophila and their dependence on Enhancer of zeste function. EMBO J. 12**,** 1513-22.

Rauch, T., Wang, Z., Zhang, X., Zhong, X., Wu, X., Lau, S. K., Kernstine, K. H., Riggs, A. D., Pfeifer, G. P., 2007. Homeobox gene methylation in lung cancer studied by genome-wide analysis with a microarray-based methylated CpG island recovery assay. Proc Natl Acad Sci U S A. 104**,** 5527-32.

Razin, A., Cedar, H., 1977. Distribution of 5-methylcytosine in chromatin. Proc Natl Acad Sci U S A. 74**,** 2725-8.

Razin, A., Riggs, A. D., 1980. DNA methylation and gene function. Science. 210**,** 604-10.

Rea, S., Eisenhaber, F., O'Carroll, D., Strahl, B. D., Sun, Z. W., Schmid, M., Opravil, S., Mechtler, K., Ponting, C. P., Allis, C. D., Jenuwein, T., 2000. Regulation of chromatin structure by site-specific histone H3 methyltransferases. Nature. 406**,** 593-9.

Reamon-Buettner, S. M., Borlak, J., 2007. A new paradigm in toxicology and teratology: altering gene activity in the absence of DNA sequence variation. Reprod Toxicol. 24**,** 20-30.

Reichenbach, P., Hoss, M., Azzalin, C. M., Nabholz, M., Bucher, P., Lingner, J., 2003. A human homolog of yeast Est1 associates with telomerase and uncaps chromosome ends when overexpressed. Curr Biol. 13**,** 568-74.

Reik, W., Dean, W., Walter, J., 2001. Epigenetic reprogramming in mammalian development. Science. 293**,** 1089-93.

Ren, C., Zhang, L., Freitas, M. A., Ghoshal, K., Parthun, M. R., Jacob, S. T., 2005. Peptide mass mapping of acetylated isoforms of histone H4 from mouse lymphosarcoma cells treated with histone deacetylase (HDACs) inhibitors. J Am Soc Mass Spectrom. 16**,** 1641-53.

Rhee, S.G., Kang, S.W., Jeong, W., Chang, T.S., Yang, K.S., Woo, H.A., 2005. Intracellular messenger function of hydrogen peroxide and its regulation by peroxiredoxins. Curr Opin Cell Biol. 17, 183-9.

Rhodes, D., Giraldo, R., 1995. Telomere structure and function. Curr Opin Struct Biol. 5**,** 311-22.

Rijli, F. M., Mark, M., Lakkaraju, S., Dierich, A., Dolle, P., Chambon, P., 1993. A homeotic transformation is generated in the rostral branchial region of the head by disruption of Hoxa2, which acts as a selector gene. Cell. 75**,** 1333-1349.

Ringrose, L., 2007. Polycomb comes of age: genome-wide profiling of target sites. Curr Opin Cell Biol. 19**,** 290-7.

Ringrose, L., Paro, R., 2004. Epigenetic regulation of cellular memory by the Polycomb and Trithorax group proteins. Annu Rev Genet. 38**,** 413-43.

Ringrose, L., Rehmsmeier, M., Dura, J. M., Paro, R., 2003. Genome-wide prediction of Polycomb/Trithorax response elements in Drosophila melanogaster. Dev Cell. 5**,** 759-71.

Robert, E., Robert, J. M., Lapras, C., 1983. [Is valproic acid teratogenic?]. Rev Neurol (Paris). 139**,** 445-7.

Robert, T., Vanoli, F., Chiolo, I., Shubassi, G., Bernstein, K. A., Rothstein, R., Botrugno, O. A., et al., 2011. HDACs link the DNA damage response, processing of double-strand breaks and autophagy. Nature. 471, 74-9.

Rodier, P. M., Ingram, J. L., Tisdale, B., Nelson, S., Romano, J., 1996. Embryological origin for autism: developmental anomalies of the cranial nerve motor nuclei. J Comp Neurol. 370**,** 247-61.

Rodriguez, B. A., Cheng, A. S., Yan, P. S., Potter, D., Agosto-Perez, F. J., Shapiro, C. L., Huang, T. H., 2008. Epigenetic repression of the estrogen-regulated Homeobox B13 gene in breast cancer. Carcinogenesis. 29**,** 1459-65.

Rodriguez, J., Munoz, M., Vives, L., Frangou, C. G., Groudine, M., Peinado, M. A., 2008b. Bivalent domains enforce transcriptional memory of DNA methylated genes in cancer cells. Proc Natl Acad Sci U S A. 105**,** 19809-14.

Roguev, A., Schaft, D., Shevchenko, A., Pijnappel, W. W., Wilm, M., Aasland, R., Stewart, A. F., 2001. The Saccharomyces cerevisiae Set1 complex includes an Ash2 homologue and methylates histone 3 lysine 4. EMBO J. 20**,** 7137-48.

Roh, T.Y., Cuddapah, S., Cui, K., Zhao, K., 2006. The genomic landscape of histone modifications in human T cells. Proc Natl Acad Sci U S A. 103, 15782-7.

Romanato, M., Regueira, E., Cameo, M. S., Baldini, C., Calvo, L., Calvo, J. C., 2005. Further evidence on the role of heparan sulfate as protamine acceptor during the decondensation of human spermatozoa. Hum Reprod. 20**,** 2784-9.

Rosato, R. R., Almenara, J. A., Grant, S.,2003. The histone deacetylase inhibitor MS-275 promotes differentiation or apoptosis in human leukemia cells through a proces regulated by generation of reactive oxygen species and induction of p21CIP1/WAF11. Cancer Res. 63, 3637-45.

Rosato, R. R., Almenara, J. A., Maggio, S. C., Coe, S., Atadja, P., Dent, P., Grant, S., 2008. Role of histone deacetylase inhibitor-induced reactive oxygen species and DNA damage in LAQ-824/fludarabine antileukemic interactions. Mol Cancer Ther. 7, 3285-97.

Rosenfeld, J. A., Wang, Z., Schones, D. E., Zhao, K., DeSalle, R., Zhang, M. Q., 2009. Determination of enriched histone modifications in non-genic portions of the human genome. BMC Genomics. 10**,** 143.

Roth, S. Y., Denu, J. M., Allis, C. D., 2001. Histone acetyltransferases. Annu Rev Biochem. 70**,** 81-120.

Rountree, M. R., Bachman, K. E., Baylin, S. B., 2000. DNMT1 binds HDAC2 and a new co-repressor, DMAP1, to form a complex at replication foci. Nat Genet. 25**,** 269-77.

Rowley, J. D., 1998. The critical role of chromosome translocations in human leukemias. Annu Rev Genet. 32**,** 495-519.

Ruefli, A. A., Ausserlechner, M. J., Bernhard, D., Sutton, V. R., Tainton, K. M., Kofler, R., Smyth, M. J., Johnstone, R. W., 2001. The histone deacetylase inhibitor and chemotherapeutic agent suberoylanilide hydroxamic acid (SAHA) induces a cell-death pathway characterized by cleavage of Bid and production of reactive oxygen species. Proc. Natl. Acad. Sci. USA. 98, 10833-8.

Ruthenburg, A. J., Li, H., Patel, D. J., Allis, C. D., 2007. Multivalent engagement of chromatin modifications by linked binding modules. Nat Rev Mol Cell Biol. 8**,** 983-94.

Saitoh, M., Nishitoh, H., Fujii, M., Takeda, K., Tobiume, K., Sawada, Y., Kawabata, M., Miyazono, K., Ichijo, H., 1998.Mammalian thioredoxin is a direct inhibitor of apoptosis signal-regulating kinase (ASK) 1. EMBO J 17, 2596–606.

Salmon, M., Akbar, A. N., 2004. Telomere erosion: a new link between HLA DR4 and rheumatoid arthritis? Trends Immunol. 25**,** 339-41.

Sancar, A., Lindsey-Boltz, L. A., Unsal-Kacmaz, K., Linn, S., 2004. Molecular mechanisms of mammalian DNA repair and the DNA damage checkpoints. Annu. Rev. Biochem. 73, 39-85.

Sanda, T., Okamoto, T., Uchida, Y., Nakagawa, H., Lida, S., Kayukawa, S., Suzuki, T., Oshizawa, T., Suzuki, T., Miyata, N., Ueda, R., 2007. Proteome analyses of the growth

inhibitory effects of NCH-51, a novel histone deacetylase inhibitor, on lymphoid malignant cells. Leukemia. 21, 2344-53.

Santagati, F., Minoux, M., Ren, S. Y., Rijli, F. M., 2005. Temporal requirement of Hoxa2 in cranial neural crest skeletal morphogenesis. Development. 132**,** 4927-36.

Santini, V., Gozzini, A., Ferrari, G., 2007. Histone deacetylase inhibitors: molecular and biological activity as a premise to clinical application. Curr Drug Metab. 8**,** 383-93.

Santos-Rosa, H., Schneider, R., Bannister, A. J., Sherriff, J., Bernstein, B. E., Emre, N. C., Schreiber, S. L., Mellor, J., Kouzarides, T., 2002. Active genes are tri-methylated at K4 of histone H3. Nature. 419**,** 407-11.

Santos, F., Hendrich, B., Reik, W., Dean, W., 2002. Dynamic reprogramming of DNA methylation in the early mouse embryo. Dev Biol. 241**,** 172-82.

Santos, J. H., Meyer, J. N., Skorvaga, M., Annab, L. A., Van Houten, B., 2004. Mitochondrial hTERT exacerbates free-radical-mediated mtDNA damage. Aging Cell. 3**,** 399-411.

Santos, J. H., Meyer, J. N., Van Houten, B., 2006. Mitochondrial localization of telomerase as a determinant for hydrogen peroxide-induced mitochondrial DNA damage and apoptosis. Hum Mol Genet. 15**,** 1757-68.

Saretzki, G., 2009. Telomerase, mitochondria and oxidative stress. Exp Gerontol. 44**,** 485-92.

Sarma, K., Margueron, R., Ivanov, A., Pirrotta, V., Reinberg, D., 2008. Ezh2 requires PHF1 to efficiently catalyze H3 lysine 27 trimethylation in vivo. Mol Cell Biol. 28**,** 2718-31.

Sauer, H., Wartenber, M., 2005. Reactive oxygen species as signaling molecules in cardiovascular differentiation of embryonic stem cells and tumor-induced angiogenesis. Antioxid Redox Signal. 7, 1423-34.

Saurin, A. J., Shao, Z., Erdjument-Bromage, H., Tempst, P., Kingston, R. E., 2001. A Drosophila Polycomb group complex includes Zeste and dTAFII proteins. Nature. 412**,** 655-60.

Savage, S. A., Bertuch, A. A., 2010. The genetics and clinical manifestations of telomere biology disorders. Genet Med. 12**,** 753-64.

Scalera, F., Closs, E. I., Flick, E., Martens-Lobenhoffer, J., Boissel, J. P., Lendeckel, U., Heimburg, A., Bode-Boger, S. M., 2009. Paradoxical effect of L-arginine: acceleration of endothelial cell senescence. Biochem Biophys Res Commun. 386**,** 650-5.

Schafer, F.Q., Buettner, G.R., 2001. Redox environment of the cells as viewed through the redox state of the glutathione disulfide/glutathione couple. Free Radic Biol Med. 30, 1191-212.

Schlesinger, Y., Straussman, R., Keshet, I., Farkash, S., Hecht, M., Zimmerman, J., Eden, E., Yakhini, Z., Ben-Shushan, E., Reubinoff, B.E., Bergman, Y., Simon, I., Cedar, H., 2007. Polycomb-mediated methylation on Lys27 of histone H3 pre-marks genes for de novo methylation in cancer. Nat Genet. 39, 232–6.

Schmitt, S., Prestel, M., Paro, R., 2005. Intergenic transcription through a polycomb group response element counteracts silencing. Genes Dev. 19**,** 697-708.

Schneider, J., Wood, A., Lee, J. S., Schuster, R., Dueker, J., Maguire, C., Swanson, S. K., Florens, L., Washburn, M. P., Shilatifard, A., 2005. Molecular regulation of histone H3 trimethylation by COMPASS and the regulation of gene expression. Mol Cell. 19**,** 849-56.

Schonland, S. O., Lopez, C., Widmann, T., Zimmer, J., Bryl, E., Goronzy, J. J., Weyand, C. M., 2003. Premature telomeric loss in rheumatoid arthritis is genetically determined and involves both myeloid and lymphoid cell lineages. Proc Natl Acad Sci U S A. 100**,** 13471-6.

Schubeler, D., MacAlpine, D. M., Scalzo, D., Wirbelauer, C., Kooperberg, C., van Leeuwen, F., Gottschling, D. E., O'Neill, L. P., Turner, B. M., Delrow, J., Bell, S. P., Groudine, M., 2004. The histone modification pattern of active genes revealed through genome-wide chromatin analysis of a higher eukaryote. Genes Dev. 18**,** 1263-71.

Schubert, D., Clarenz, O., Goodrich, J., 2005. Epigenetic control of plant development by Polycomb-group proteins. Curr Opin Plant Biol. 8**,** 553-61.

Schuettengruber, B., Chourrout, D., Vervoort, M., Leblanc, B., Cavalli, G., 2007. Genome regulation by polycomb and trithorax proteins. Cell. 128**,** 735-45.

Schultz, R. M., 2002. The molecular foundations of the maternal to zygotic transition in the preimplantation embryo. Hum Reprod Update. 8**,** 323-31.

Schwartz, C., Palissot, V., Aouali, N., Wack, S., Brons, N. H., Leners, B., Bosseler, M., Berchem, G., 2007. Valproic acid induces non-apoptotic cell death mechanisms in multiple myeloma cell lines. Int J Oncol. 30**,** 573-82.

Schwartz, Y. B., Kahn, T. G., Nix, D. A., Li, X. Y., Bourgon, R., Biggin, M., Pirrotta, V., 2006. Genome-wide analysis of Polycomb targets in Drosophila melanogaster. Nat Genet. 38**,** 700-5.

Schwartz, Y. B., Pirrotta, V., 2007. Polycomb silencing mechanisms and the management of genomic programmes. Nat Rev Genet. 8**,** 9-22.

Schwartz, Y. B., Pirrotta, V., 2008. Polycomb complexes and epigenetic states. Curr Opin Cell Biol. 20**,** 266-73.

Seckin, S., Basaran-Kucukgergin, C., Uysal, M., 1999. Effect of acute and chronic administration of sodium valproate on lipid peroxidation and antioxidant system in rat liver. Pharmacol Toxicol. 85**,** 294-8.

Seet, B. T., Dikic, I., Zhou, M. M., Pawson, T., 2006. Reading protein modifications with interaction domains. Nat Rev Mol Cell Biol. 7**,** 473-83.

Sen, C. K., Packer, L., 1996. Antioxidant and redox regulation of gene transcription. FASEB J. 10**,** 709-20.

Sestili, P., Paolillo, M., Lenzi, M., Colombo, E., Vallorani, L., Casadei, L., Martinelli, C., Fimognari, C., 2010. Sulforaphane induces DNA single strand breaks in cultured human cells. Mutat Res. 689, 65-73.

Seuter, S., Heikkinen, S. and Carlberg, C. 2012. Chromatin acetylation at transcription start sites and vitamin D receptor binding regions relates to effects of 1alpha,25 dihydroxyvitamin D3 and histone deacetylase inhibitors on gene expression. Nucleic Acids Res. 41, 110–124.

Shan, Z., Feng-Nian, R., Jie, G. and Ting, Z. 2012. Effects of valproic acid on proliferation, apoptosis, angiogenesis and metastasis of ovarian cancer *in vitro* and *in vivo*. Asian Pac. J.

Cancer Prev. 13, 3977–82.

Shao, Z., Raible, F., Mollaaghababa, R., Guyon, J. R., Wu, C. T., Bender, W., Kingston, R. E., 1999. Stabilization of chromatin structure by PRC1, a Polycomb complex. Cell. 98**,** 37-46.

Shi, Y., Lan, F., Matson, C., Mulligan, P., Whetstine, J. R., Cole, P. A., Casero, R. A., 2004. Histone demethylation mediated by the nuclear amine oxidase homolog LSD1. Cell. 119**,** 941-53.

Shigetomi, H., Oonogi, A., Tsunemi, T., Tanase, Y., Yamada, Y., Kajihara, H., Yoshizawa, Y., Furukawa, N., Haruta, S., Yoshida, S., Sado, T., Oi, H., Kobayashi, H., 2011. The role of components of the chromatin modification machinery in carcinogenesis of clear cell carcinoma of the ovary (Review). Oncol Lett. 2**,** 591-597.

Shilatifard, A., 2006. Chromatin modifications by methylation and ubiquitination: implications in the regulation of gene expression. Annu Rev Biochem. 75**,** 243-69.

Shilatifard, A., 2008. Molecular implementation and physiological roles for histone H3 lysine 4 (H3K4) methylation. Curr Opin Cell Biol. 20**,** 341-8.

Shorvon, S. D., 1990. Epidemiology, classification, natural history, and genetics of epilepsy. Lancet. 336**,** 93-6.

Shu, Y., Wang, B., Wang, J., Wang, J. M., Zou, S. Q., 2011. Identification of methylation profile of HOX genes in extrahepatic cholangiocarcinoma. World J Gastroenterol. 17**,** 3407-19.

Simon, J., Chiang, A., Bender, W., 1992. Ten different Polycomb group genes are required for spatial control of the abdA and AbdB homeotic products. Development. 114**,** 493-505.

Sims, R. J., 3rd, Trojer, P., Li, G., Reinberg, D., 2006. Methods to identify and functionally analyze factors that specifically recognize histone lysine methylation. Methods. 40**,** 331-8.

Smallwood, A., Esteve, P. O., Pradhan, S., Carey, M., 2007. Functional cooperation between HP1 and DNMT1 mediates gene silencing. Genes Dev. 21**,** 1169-78.

Smith, S. T., Petruk, S., Sedkov, Y., Cho, E., Tillib, S., Canaani, E., Mazo, A., 2004. Modulation of heat shock gene expression by the TAC1 chromatin-modifying complex. Nat Cell Biol. 6**,** 162-7.

Smith, T. M., Wang, X., Zhang, W., Kulyk, W., Nazarali, A. J., 2009. Hoxa2 plays a direct role in murine palate development. Dev Dyn. 238**,** 2364-73.

Smogorzewska, A., de Lange, T., 2004. Regulation of telomerase by telomeric proteins. Annu Rev Biochem. 73**,** 177-208.

Smogorzewska, A., Karlseder, J., Holtgreve-Grez, H., Jauch, A., de Lange, T., 2002. DNA ligase IV-dependent NHEJ of deprotected mammalian telomeres in G1 and G2. Curr Biol. 12**,** 1635-44.

Snowden, A. W., Gregory, P. D., Case, C. C., Pabo, C. O., 2002. Gene-specific targeting of H3K9 methylation is sufficient for initiating repression in vivo. Curr Biol. 12**,** 2159-66.

Soriano, A. O., Yang, H., Faderl, S., Estrov, Z., Giles, F., Ravandi, F., Cortes, J., Wierda, W. G., Ouzounian, S., Quezada, A., Pierce, S., Estey, E. H., Issa, J. P., Kantarjian, H. M., Garcia-Manero, G., 2007. Safety and clinical activity of the combination of 5-azacytidine, valproic acid, and all-trans retinoic acid in acute myeloid leukemia and myelodysplastic syndrome. Blood. 110**,** 2302-8.

Soshnikova, N., Duboule, D., 2009a. Epigenetic regulation of vertebrate Hox genes: a dynamic equilibrium. Epigenetics. 4**,** 537-40.

Soshnikova, N., Duboule, D., 2009b. Epigenetic temporal control of mouse Hox genes in vivo. Science. 324**,** 1320-3.

Sparmann, A., van Lohuizen, M., 2006. Polycomb silencers control cell fate, development and cancer. Nat Rev Cancer. 6, 846-856.

Spitz, F., Gonzalez, F., Duboule, D., 2003. A global control region defines a chromosomal regulatory landscape containing the HoxD cluster. Cell. 113**,** 405-17.

Sproul, D., Gilbert, N., Bickmore, W. A., 2005. The role of chromatin structure in regulating the expression of clustered genes. Nat Rev Genet. 6**,** 775-81.

Steer, S. E., Williams, F. M., Kato, B., Gardner, J. P., Norman, P. J., Hall, M. A., Kimura, M., Vaughan, R., Aviv, A., Spector, T. D., 2007. Reduced telomere length in rheumatoid arthritis is independent of disease activity and duration. Ann Rheum Dis. 66**,** 476-80.

Stern, J. L., Bryan, T. M., 2008. Telomerase recruitment to telomeres. Cytogenet Genome Res. 122**,** 243-54.

Sterner, D. E., Berger, S. L., 2000. Acetylation of histones and transcription-related factors. Microbiol Mol Biol Rev. 64**,** 435-59.

Stock, J. K., Giadrossi, S., Casanova, M., Brookes, E., Vidal, M., Koseki, H., Brockdorff, N., Fisher, A. G., Pombo, A., 2007. Ring1-mediated ubiquitination of H2A restrains poised RNA polymerase II at bivalent genes in mouse ES cells. Nat Cell Biol. 9**,** 1428-35.

Stodgell, C. J., Ingram, J. L., O'Bara, M., Tisdale, B. K., Nau, H., Rodier, P. M., 2006. Induction of the homeotic gene Hoxa1 through valproic acid's teratogenic mechanism of action. Neurotoxicol Teratol. 28**,** 617-24.

Straussman, R., Nejman, D., Roberts, D., Steinfeld, I., Blum, B., Benvenisty, N., Simon, I., Yakhini, Z., Cedar, H., 2009. Developmental programming of CpG island methylation profiles in the human genome. Nat Struct Mol Biol. 16**,** 564-71.

Strichman-Almashanu, L. Z., Lee, R. S., Onyango, P. O., Perlman, E., Flam, F., Frieman, M. B., Feinberg, A. P., 2002. A genome-wide screen for normally methylated human CpG islands that can identify novel imprinted genes. Genome Res. 12**,** 543-54.

Struhl, K., 1998. Histone acetylation and transcriptional regulatory mechanisms. Genes Dev. 12, 599–606.

Suzuki, M. M., Bird, A., 2008. DNA methylation landscapes: provocative insights from epigenomics. Nat Rev Genet. 9**,** 465-76.

Sztajnkrycer, M. D., 2002. Valproic acid toxicity: overview and management. J Toxicol Clin Toxicol. 40**,** 789-801.

Szyf, M., 2009. Epigenetics, DNA methylation, and chromatin modifying drugs. Annu Rev Pharmacol Toxicol. 49**,** 243-63.

Tabatabaei, A. R., Abbott, F. S., 1999. LC/MS analysis of hydroxylation products of salicylate as an indicator of in vivo oxidative stress. Free Radic Biol Med. 26**,** 1054-8.

Taddei, A., Hediger, F., Neumann, F. R., Gasser, S. M., 2004. The function of nuclear architecture: a genetic approach. Annu Rev Genet. 38**,** 305-45.

Takahashi, I., Miyaji, H., Yoshida, T., Sato, S., Mizukami, T., 1996. Selective inhibition of IL-2 gene expression by trichostatin A, a potent inhibitor of mammalian histone deacetylase. J Antibiot (Tokyo). 49, 453–7.

Takahashi, M., Sato, K., Nomura, T., Osumi, N., 2002. Manipulating gene expressions by electroporation in the developing brain of mammalian embryos. Differentiation. 70**,** 155-62.

Takai, H., Smogorzewska, A., de Lange, T., 2003. DNA damage foci at dysfunctional telomeres. Curr Biol. 13**,** 1549-56.

Tam, P. P., 1989. Regionalisation of the mouse embryonic ectoderm: allocation of prospective ectodermal tissues during gastrulation. Development. 107**,** 55-67.

Tam, P. P., 1998. Postimplantation mouse development: whole embryo culture and micro-manipulation. Int J Dev Biol. 42**,** 895-902.

Tam, P. P., Behringer, R. R., 1997. Mouse gastrulation: the formation of a mammalian body plan. Mech Dev. 68**,** 3-25.

Tanay, A., O'Donnell, A.H., Damelin, M., Bestor, T.H., 2007. Hyperconserved CpG domains underlie Polycomb-binding sites. Proc Natl Acad Sci U S A. 104, 5521-6.

Tang, J., Yan, H., Zhuang, S., 2013. Histone deacetylases as targets for treatment of multiple diseases. Clin Sci (Lond). 124, 651-62.

Taniyama, Y., Griendling, K.K., 2003. Reactive oxygen species in the vasculature: molecular and cellular mechanisms. Hypertension. 42, 1075-81.

Tas, S., Walford, R. L., 1982. Influence of disulfide-reducing agents on fractionation of the chromatin complex by endogenous nucleases and deoxyribonuclease I in aging mice. J Gerontol. 37**,** 673-9.

Teixeira, M. T., Arneric, M., Sperisen, P., Lingner, J., 2004. Telomere length homeostasis is achieved via a switch between telomerase- extendible and -nonextendible states. Cell. 117**,** 323-35.

Tejera, A. M., Stagno d'Alcontres, M., Thanasoula, M., Marion, R. M., Martinez, P., Liao, C., Flores, J. M., Tarsounas, M., Blasco, M. A., 2010. TPP1 is required for TERT recruitment, telomere elongation during nuclear reprogramming, and normal skin development in mice. Dev Cell. 18**,** 775-89.

Tenney, K., Shilatifard, A., 2005. A COMPASS in the voyage of defining the role of trithorax/MLL-containing complexes: linking leukemogensis to covalent modifications of chromatin. J Cell Biochem. 95**,** 429-36.

Terranova, R., Agherbi, H., Boned, A., Meresse, S., Djabali, M., 2006. Histone and DNA methylation defects at Hox genes in mice expressing a SET domain-truncated form of Mll. Proc Natl Acad Sci U S A. 103**,** 6629-34.

Tolhuis, B., de Wit, E., Muijrers, I., Teunissen, H., Talhout, W., van Steensel, B., van Lohuizen, M., 2006. Genome-wide profiling of PRC1 and PRC2 Polycomb chromatin binding in Drosophila melanogaster. Nat Genet. 38**,** 694-9.

Tommasi, S., Karm, D. L., Wu, X., Yen, Y., Pfeifer, G. P., 2009. Methylation of homeobox genes is a frequent and early epigenetic event in breast cancer. Breast Cancer Res. 11**,** R14.

Trainor, P. A., Krumlauf, R., 2001. Hox genes, neural crest cells and branchial arch patterning. Curr Opin Cell Biol. 13**,** 698-705.

Tsakiri, K. D., Cronkhite, J. T., Kuan, P. J., Xing, C., Raghu, G., Weissler, J. C., Rosenblatt, R. L., Shay, J. W., Garcia, C. K., 2007. Adult-onset pulmonary fibrosis caused by mutations in telomerase. Proc Natl Acad Sci U S A. 104**,** 7552-7.

Tsantoulis, P. K., Kotsinas, A., Sfikakis, P. P., Evangelou, K., Sideridou, M., Levy, B., Mo, L., Kittas, C., Wu, X. R., Papavassiliou, A. G., Gorgoulis, V. G., 2008. Oncogene-induced replication stress preferentially targets common fragile sites in preneoplastic lesions. A genome-wide study. Oncogene. 27**,** 3256-64.

Tung, E. W., Winn, L. M., 2011. Valproic acid-induced DNA damage increases embryonic p27(KIP1) and caspase-3 expression: a mechanism for valproic-acid induced neural tube defects. Reprod Toxicol. 32**,** 255-60.

Turner, B. M., Fellows, G., 1989. Specific antibodies reveal ordered and cell-cycle-related use of histone-H4 acetylation sites in mammalian cells. Eur J Biochem. 179**,** 131-9.

Ubeda-Martin, N., Alonso-Aperte, E., Achon, M., Varela-Moreiras, G., Puerta, J., Perez de Miguelsanz, J., 1998. [Morphological changes induced by valproate and its administration concomitant with folinic acid or S-adenosylmethionine in pregnant rats]. Nutr Hosp. 13**,** 41-9.

Ungerstedt, J. S., Sowa, Y., Xu, W. S., Shao, Y., Dokmanovic, M., Perez, G., Ngo, L., Holmgren, A., Jiang, X., Marks, P. A., 2005. Role of thioredoxin in the response of normal and transformed cells to histone deacetylase inhibitors. Proc. Natl. Acad. Sci. USA. 102, 673-8.

Urnov, F. D., Wolffe, A. P., 2001. Chromatin remodeling and transcriptional activation: the cast (in order of appearance). Oncogene. 20**,** 2991-3006.

Utley, R. T., Cote, J., 2003. The MYST family of histone acetyltransferases. Curr Top Microbiol Immunol. 274**,** 203-36.

Vakoc, C. R., Mandat, S. A., Olenchock, B. A., Blobel, G. A., 2005. Histone H3 lysine 9 methylation and HP1gamma are associated with transcription elongation through mammalian chromatin. Mol Cell. 19**,** 381-91.

Valentini, A., Gravina, P., Federici, G., Bernardini, S., 2007. Valproic acid induces apoptosis, p16INK4A upregulation and sensitization to chemotherapy in human melanoma cells. Cancer Biol Ther. 6**,** 185-91.

Valinluck, V., Tsai, H.H., Rogstad, D.K., Burdzy, A., Bird, A., Sowers, L.C.,2004. Oxidative damage to methyl-CpG sequences inhibits the binding of the methyl-CpG binding domain (MBD) of methyl-CpG binding protein 2 (MeCP2). Nucleic Acids Res. 32, 4100-08.

van der Hoeven, F., Sordino, P., Fraudeau, N., Izpisua-Belmonte, J. C., Duboule, D., 1996. Teleost HoxD and HoxA genes: comparison with tetrapods and functional evolution of the HOXD complex. Mech Dev. 54**,** 9-21.

van der Lugt, N. M., Domen, J., Linders, K., van Roon, M., Robanus-Maandag, E., te Riele, H., van der Valk, M., Deschamps, J., Sofroniew, M., van Lohuizen, M., et al., 1994. Posterior transformation, neurological abnormalities, and severe hematopoietic defects in mice with a targeted deletion of the bmi-1 proto-oncogene. Genes Dev. 8**,** 757-69.

van der Vlag, J., Otte, A.P., 1999. Transcriptional repression mediated by the human polycomb-group protein EED involves histone deacetylation. Nat Genet. 23, 474-8.

van Heek, N. T., Meeker, A. K., Kern, S. E., Yeo, C. J., Lillemoe, K. D., Cameron, J. L., Offerhaus, G. J., Hicks, J. L., Wilentz, R. E., Goggins, M. G., De Marzo, A. M., Hruban, R. H., Maitra, A., 2002. Telomere shortening is nearly universal in pancreatic intraepithelial neoplasia. Am J Pathol. 161**,** 1541-7.

Van Lint, C., Emiliani, S., Verdin, E., 1996. The expression of a small fraction of cellular genes is changed in response to histone hyperacetylation. Gene Expr. 5, 245–53.

van Steensel, B., Smogorzewska, A., de Lange, T., 1998. TRF2 protects human telomeres from end-to-end fusions. Cell. 92**,** 401-13.

Vaquero, A., Scher, M. B., Lee, D. H., Sutton, A., Cheng, H. L., Alt, F. W., Serrano, L., Sternglanz, R., Reinberg, D., 2006. SirT2 is a histone deacetylase with preference for histone H4 Lys 16 during mitosis. Genes Dev. 20**,** 1256-61.

Varambally, S., Dhanasekaran, S. M., Zhou, M., Barrette, T. R., Kumar-Sinha, C., Sanda, M. G., Ghosh, D., Pienta, K. J., Sewalt, R. G., Otte, A. P., Rubin, M. A., Chinnaiyan, A. M., 2002. The polycomb group protein EZH2 is involved in progression of prostate cancer. Nature. 419**,** 624-9.

Venteicher, A. S., Abreu, E. B., Meng, Z., McCann, K. E., Terns, R. M., Veenstra, T. D., Terns, M. P., Artandi, S. E., 2009. A human telomerase holoenzyme protein required for Cajal body localization and telomere synthesis. Science. 323**,** 644-8.

Venteicher, A. S., Meng, Z., Mason, P. J., Veenstra, T. D., Artandi, S. E., 2008. Identification of ATPases pontin and reptin as telomerase components essential for holoenzyme assembly. Cell. 132**,** 945-57.

Verdel, A., Seigneurin-Berny, D., Faure, A. K., Eddahbi, M., Khochbin, S., Nonchev, S., 2003. HDAC6-induced premature chromatin compaction in mouse oocytes and fertilised eggs. Zygote. 11**,** 323-8.

Verdun, R. E., Karlseder, J., 2006. The DNA damage machinery and homologous recombination pathway act consecutively to protect human telomeres. Cell. 127**,** 709-20.

Vermeulen, M., Mulder, K. W., Denissov, S., Pijnappel, W. W., van Schaik, F. M., Varier, R. A., Baltissen, M. P., Stunnenberg, H. G., Mann, M., Timmers, H. T., 2007. Selective anchoring of TFIID to nucleosomes by trimethylation of histone H3 lysine 4. Cell. 131**,** 58-69.

Verrier, L., Vandromme, M., Trouche, D., 2011. Histone demethylases in chromatin cross-talks. Biol Cell. 103**,** 381-401.

Verrotti, A., Scardapane, A., Franzoni, E., Manco, R., Chiarelli, F., 2008. Increased oxidative stress in epileptic children treated with valproic acid. Epilepsy Res. 78**,** 171-7.

Verschure, P. J., van der Kraan, I., de Leeuw, W., van der Vlag, J., Carpenter, A. E., Belmont, A, S., van Driel, R., 2005. In vivo HP1 targeting causes large-scale chromatin condensation and enhanced histone lysine methylation. Mol Cell Biol. 25, 4552-64.

Viinikainen, K., Eriksson, K., Monkkonen, A., Aikia, M., Nieminen, P., Heinonen, S., Kalviainen, R., 2006. The effects of valproate exposure in utero on behavior and the need for educational support in school-aged children. Epilepsy Behav. 9**,** 636-40.

Vire, E., Brenner, C., Deplus, R., Blanchon, L., Fraga, M., Didelot, C., Morey, L., Van Eynde, A., Bernard, D., Vanderwinden, J. M., Bollen, M., Esteller, M., Di Croce, L., de Launoit, Y., Fuks, F., 2006. The Polycomb group protein EZH2 directly controls DNA methylation. Nature. 439**,** 871-4.

Vogt, S., Iking-Konert, C., Hug, F., Andrassy, K., Hansch, G. M., 2003. Shortening of telomeres: Evidence for replicative senescence of T cells derived from patients with Wegener's granulomatosis. Kidney Int. 63**,** 2144-51.

von Zglinicki, T., 2002. Oxidative stress shortens telomeres. Trends Biochem Sci. 27**,** 339-44.

von Zglinicki, T., Saretzki, G., Ladhoff, J., d'Adda di Fagagna, F., Jackson, S. P., 2005. Human cell senescence as a DNA damage response. Mech Ageing Dev. 126**,** 111-7.

Vu, T. H., Li, T., Hoffman, A. R., 2004. Promoter-restricted histone code, not the differentially methylated DNA regions or antisense transcripts, marks the imprinting status of IGF2R in human and mouse. Hum Mol Genet. 13**,** 2233-45.

Wagner, G. C., Reuhl, K. R., Cheh, M., McRae, P., Halladay, A. K., 2006. A new neurobehavioral model of autism in mice: pre- and postnatal exposure to sodium valproate. J Autism Dev Disord. 36**,** 779-93.

Wagner, E. J,, Carpenter, P. B.,2012 Understanding the language of Lys36 methylation at histone H3. *Nat Rev Mol Cell Biol*, 13, 115-126.

Wang, H., Wang, L., Erdjument-Bromage, H., Vidal, M., Tempst, P., Jones, R. S., Zhang, Y., 2004a. Role of histone H2A ubiquitination in Polycomb silencing. Nature. 431**,** 873-8.

Wang, Y., Wysocka, J., Sayegh, J., Lee, Y. H., Perlin, J. R., Leonelli, L., Sonbuchner, L. S., McDonald, C. H., Cook, R. G., Dou, Y., Roeder, R. G., Clarke, S., Stallcup, M. R., Allis, C. D., Coonrod, S. A., 2004b. Human PAD4 regulates histone arginine methylation levels via demethylimination. Science. 306**,** 279-83.

Watson, J. D., 1972. Origin of concatemeric T7 DNA. Nat New Biol. 239**,** 197-201.

Weber, G. F., Maertens, P., Meng, X. Z., Pippenger, C. E., 1991. Glutathione peroxidase deficiency and childhood seizures. Lancet. 337**,** 1443-4.

Weber, M., Hellmann, I., Stadler, M. B., Ramos, L., Paabo, S., Rebhan, M., Schubeler, D., 2007. Distribution, silencing potential and evolutionary impact of promoter DNA methylation in the human genome. Nat Genet. 39**,** 457-66.

Wege, H., Chui, M.S., Le, H.T., Tran, J.M., Zern, M.A., 2003. SYBR Green real-time telomeric repeat amplification protocol for the rapid quantification of telomerase activity. Nucleic Acids Res. 31, E3-3.

Wegner, C., Nau, H., 1991. Diurnal variation of folate concentrations in mouse embryo and plasma: the protective effect of folinic acid on valproic-acid-induced teratogenicity is time dependent. Reprod Toxicol. 5**,** 465-71.

Wegner, C., Nau, H., 1992. Alteration of embryonic folate metabolism by valproic acid during organogenesis: implications for mechanism of teratogenesis. Neurology. 42**,** 17-24.

Westin, E. R., Chavez, E., Lee, K. M., Gourronc, F. A., Riley, S., Lansdorp, P. M., Goldman, F. D., Klingelhutz, A. J., 2007. Telomere restoration and extension of proliferative lifespan in dyskeratosis congenita fibroblasts. Aging Cell. 6**,** 383-94.

Whetstine, J. R., Nottke, A., Lan, F., Huarte, M., Smolikov, S., Chen, Z., Spooner, E., Li, E., Zhang, G., Colaiacovo, M., Shi, Y., 2006. Reversal of histone lysine trimethylation by the JMJD2 family of histone demethylases. Cell. 125**,** 467-81.

Widschwendter, M., Fiegl, H., Egle, D., Mueller-Holzner, E., Spizzo, G., Marth, C., Weisenberger, D. J., Campan, M., Young, J., Jacobs, I., Laird, P. W., 2007. Epigenetic stem cell signature in cancer. Nat Genet. 39**,** 157-8.

Wiekowski, M., Miranda, M., DePamphilis, M. L., 1993. Requirements for promoter activity in mouse oocytes and embryos distinguish paternal pronuclei from maternal and zygotic nuclei. Dev Biol. 159**,** 366-78.

Williams, G., King, J., Cunningham, M., Stephan, M., Kerr, B., Hersh, J. H., 2001. Fetal valproate syndrome and autism: additional evidence of an association. Dev Med Child Neurol. 43**,** 202-6.

Williams, K., Christensen, J., Pedersen, M.T., Johansen, J.V., Cloos, P.A., Rappsilber, J., Helin, K., 2011. TET1 and hydroxymethylcytosine in transcription and DNA methylation fidelity. Nature. 473, 343-8.

Wilson, C. B., Makar, K. W., Shnyreva, M., Fitzpatrick, D. R., 2005. DNA methylation and the expanding epigenetics of T cell lineage commitment. Semin Immunol. 17**,** 105-19.

Wiltse, J., 2005. Mode of action: inhibition of histone deacetylase, altering WNT-dependent gene expression, and regulation of beta-catenin--developmental effects of valproic acid. Crit Rev Toxicol. 35**,** 727-38.

Wood, A., Shukla, A., Schneider, J., Lee, J. S., Stanton, J. D., Dzuiba, T., Swanson, S. K., Florens, L., Washburn, M. P., Wyrick, J., Bhaumik, S. R., Shilatifard, A., 2007. Ctk complex-mediated regulation of histone methylation by COMPASS. Mol Cell Biol. 27**,** 709-20.

Workman, J. L., Kingston, R. E., 1998. Alteration of nucleosome structure as a mechanism of transcriptional regulation. Annu Rev Biochem. 67**,** 545-79.

Wright, W. E., Shay, J. W., 2000. Telomere dynamics in cancer progression and prevention: fundamental differences in human and mouse telomere biology. Nat Med. 6**,** 849-51.

Wright, W. E., Tesmer, V. M., Huffman, K. E., Levene, S. D., Shay, J. W., 1997. Normal human chromosomes have long G-rich telomeric overhangs at one end. Genes Dev. 11**,** 2801-9.

Wu, C. H., Hsieh, S. C., Li, K. J., Lu, M. C., Yu, C. L., 2007. Premature telomere shortening in polymorphonuclear neutrophils from patients with systemic lupus erythematosus is related to the lupus disease activity. Lupus. 16**,** 265-72.

Wu, H., D'Alessio, A.C, Ito, S., Xia, K., Wang, Z., Cui, K., Zhao, K., Sun, Y.E., Zhang, Y., 2011. Dual functions of Tet1 in transcriptional regulation in mouse embrynic stem cells. Nature. 473, 389-93.

Xia, L., Wang, X. X., Hu, X. S., Guo, X. G., Shang, Y. P., Chen, H. J., Zeng, C. L., Zhang, F. R., Chen, J. Z., 2008. Resveratrol reduces endothelial progenitor cells senescence through augmentation of telomerase activity by Akt-dependent mechanisms. Br J Pharmacol. 155**,** 387-94.

Xiang, Y., Zhu, Z., Han, G., Ye, X., Xu, B., Peng, Z., Ma, Y., Yu, Y., Lin, H., Chen, A. P., Chen, C. D., 2007. JARID1B is a histone H3 lysine 4 demethylase up-regulated in prostate cancer. Proc Natl Acad Sci U S A. 104**,** 19226-31.

Xie, X., Mikkelsen, T. S., Gnirke, A., Lindblad-Toh, K., Kellis, M., Lander, E. S., 2007. Systematic discovery of regulatory motifs in conserved regions of the human genome, including thousands of CTCF insulator sites. Proc Natl Acad Sci U S A. 104**,** 7145-50.

Xu, W., Ngo, L., Perez, G., Dokmanovic, M., Marks, P. A., 2006. Intrinsic apoptotic and thioredoxin pathways in human prostate cancer cell response to histone deacetylase inhibitor. Proc. Natl. Acad. Sci. USA. 103, 15540-5.

Xu, W.S., Parmigiani, R.B., Marks, P.A., 2007. Histone deacetylase inhibitors: molecular mechanisms of action. Oncogene. 26, 5541-52.

Xu, Y., Wu., F., Tan, L., Kong, L., Xiong, L., Deng, J., Barbera, A.J., Zheng, L., Zhang, H., Huang, S., Min, J., Nicholson, T., Chen, T., Xu, G., Shi, Y., Zhang, K., Shi, Y.G. 2011. Genome-wide regulation of 5hmC, 5mC, and gene expression by Tet1 hydroxylase in mouse embryonic stem cells. Mol. Cell. 42, 451-64.

Yakubov, L. A., Deeva, E. A., Zarytova, V. F., Ivanova, E. M., Ryte, A. S., Yurchenko, L. V., Vlassov, V. V., 1989. Mechanism of oligonucleotide uptake by cells: involvement of specific receptors? Proc Natl Acad Sci U S A. 86**,** 6454-8.

Yamaguchi, Y., Nozawa, K., Savoysky, E., Hayakawa, N., Nimura, Y., Yoshida, S., 1998. Change in telomerase activity of rat organs during growth and aging. Exp Cell Res. 242**,** 120-7.

Yamane, K., Toumazou, C., Tsukada, Y., Erdjument-Bromage, H., Tempst, P., Wong, J., Zhang, Y., 2006. JHDM2A, a JmjC-containing H3K9 demethylase, facilitates transcription activation by androgen receptor. Cell. 125**,** 483-95.

Yamasaki, Y., Kayashima, T., Soejima, H., Kinoshita, A., Yoshiura, K., Matsumoto, N., Ohta, T., Urano, T., Masuzaki, H., Ishimaru, T., Mukai, T., Niikawa, N., Kishino, T., 2005. Neuron-specific relaxation of Igf2r imprinting is associated with neuron-specific histone modifications and lack of its antisense transcript Air. Hum Mol Genet. 14**,** 2511-20.

Yang, X. J., Seto, E., 2003. Collaborative spirit of histone deacetylases in regulating chromatin structure and gene expression. Curr Opin Genet Dev. 13**,** 143-53.

Yerby, M. S., 2003. Clinical care of pregnant women with epilepsy: neural tube defects and folic acid supplementation. Epilepsia. 44 Suppl 3**,** 33-40.

Yokoo, S., Furumoto, K., Hiyama, E., Miwa, N., 2004. Slow-down of age-dependent telomere shortening is executed in human skin keratinocytes by hormesis-like-effects of trace hydrogen peroxide or by anti-oxidative effects of pro-vitamin C in common concurrently with reduction of intracellular oxidative stress. J Cell Biochem. 93**,** 588-97.

Yoon, S.O., Yun, C.H., Chung, A.S., 2002. Dose effect of oxidative stress on signal transduction in aging. Mech Ageing Dev. 123, 1597-604.

Yu, B. P., Kang, C. M., Han, J. S., Kim, D. S., 1998. Can antioxidant supplementation slow the aging process? Biofactors. 7**,** 93-101.

Yuksel, A., Cengiz, M., Seven, M., Ulutin, T., 2001. Changes in the antioxidant system in epileptic children receiving antiepileptic drugs: two-year prospective studies. J Child Neurol. 16**,** 603-6.

Zeng, F., Baldwin, D. A., Schultz, R. M., 2004. Transcript profiling during preimplantation mouse development. Dev Biol. 272**,** 483-96.

Zeng, F., Schultz, R. M., 2005. RNA transcript profiling during zygotic gene activation in the preimplantation mouse embryo. Dev Biol. 283**,** 40-57.

Zhang, B., Wang, X., Nazarali, A. J., 2010. Ascorbic acid reverses valproic acid-induced inhibition of hoxa2 and maintains glutathione homeostasis in mouse embryos in culture. Cell Mol Neurobiol. 30**,** 137-48.

Zhang, Y., Carr, T., Dimtchev, A., Zaer, N., Dritschilo, A., Jung, M., 2007. Attenuated DNA damage repair by trichostatin A through BRCA1 suppression. Radiat Res. 168, 115-24.

Zhang, Y., Ng, H. H., Erdjument-Bromage, H., Tempst, P., Bird, A., Reinberg, D., 1999. Analysis of the NuRD subunits reveals a histone deacetylase core complex and a connection with DNA methylation. Genes Dev. 13**,** 1924-35.

Zhang, Y., Reinberg, D., 2001. Transcription regulation by histone methylation: interplay between different covalent modifications of the core histone tails. Genes Dev. 15**,** 2343-60.

Zhou, W., Zhu, P., Wang, J., Pascual, G., Ohgi, K. A., Lozach, J., Glass, C. K., Rosenfeld, M. G., 2008. Histone H2A monoubiquitination represses transcription by inhibiting RNA polymerase II transcriptional elongation. Mol Cell. 29**,** 69-80.

Zhu, H., Belcher, M., van der Harst, P., 2011. Healthy aging and disease: role for telomere biology? Clin Sci (Lond). 120**,** 427-40.

Ziemin-van der Poel, S., McCabe, N. R., Gill, H. J., Espinosa, R., 3rd, Patel, Y., Harden, A., Rubinelli, P., Smith, S. D., LeBeau, M. M., Rowley, J. D., et al., 1991. Identification of a gene, MLL, that spans the breakpoint in 11q23 translocations associated with human leukemias. Proc Natl Acad Sci U S A. 88**,** 10735-9.

Zuelke, K. A., Jeffay, S. C., Zucker, R. M., Perreault, S. D., 2003. Glutathione (GSH) concentrations vary with the cell cycle in maturing hamster oocytes, zygotes, and pre-implantation stage embryos. Mol Reprod Dev. 64**,** 106-12.

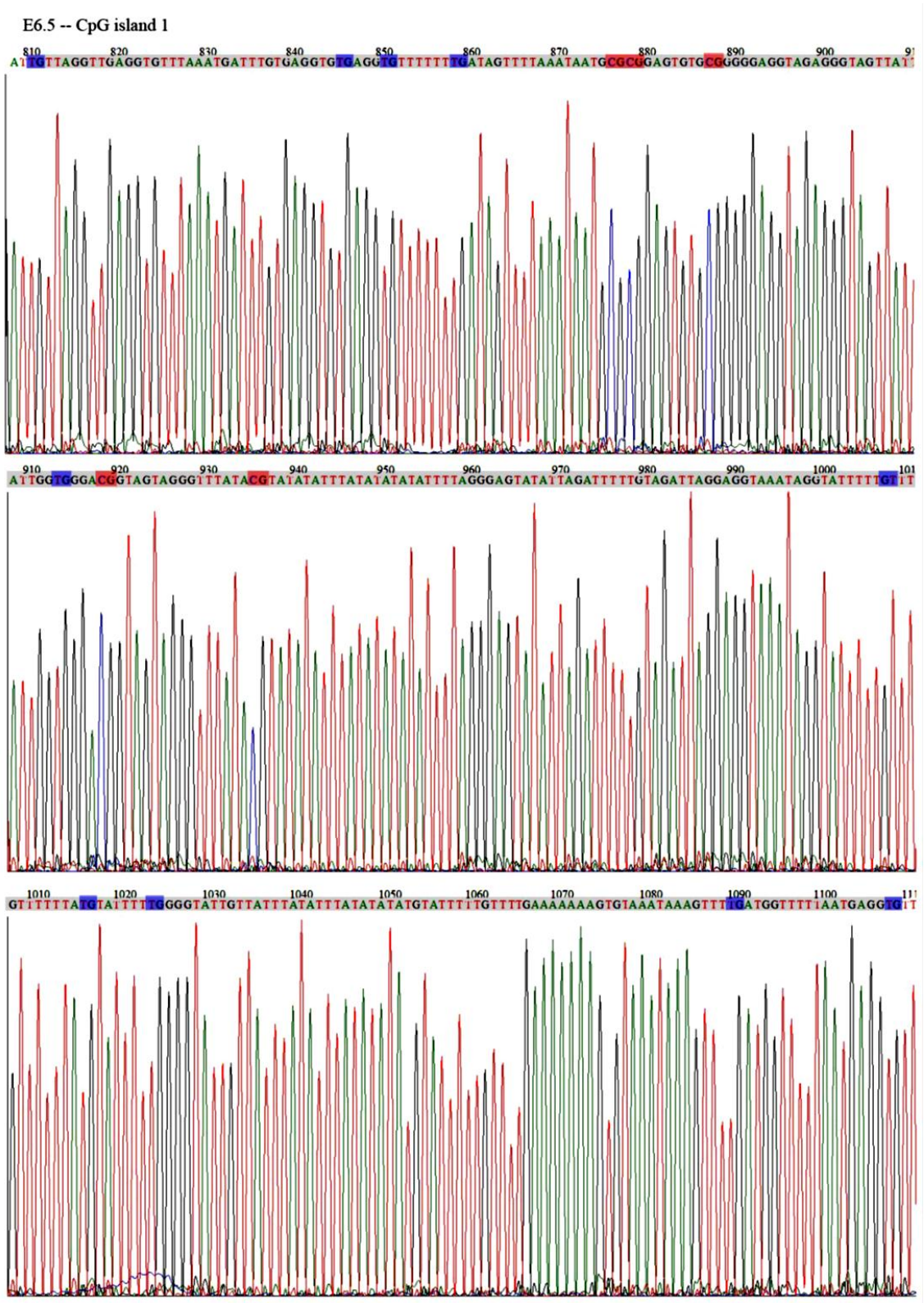

Appendix 1
DNA sequence chromatogram of *Hoxa2* promoter CpG island 1 from E6.5 mouse embryo genomic DNA

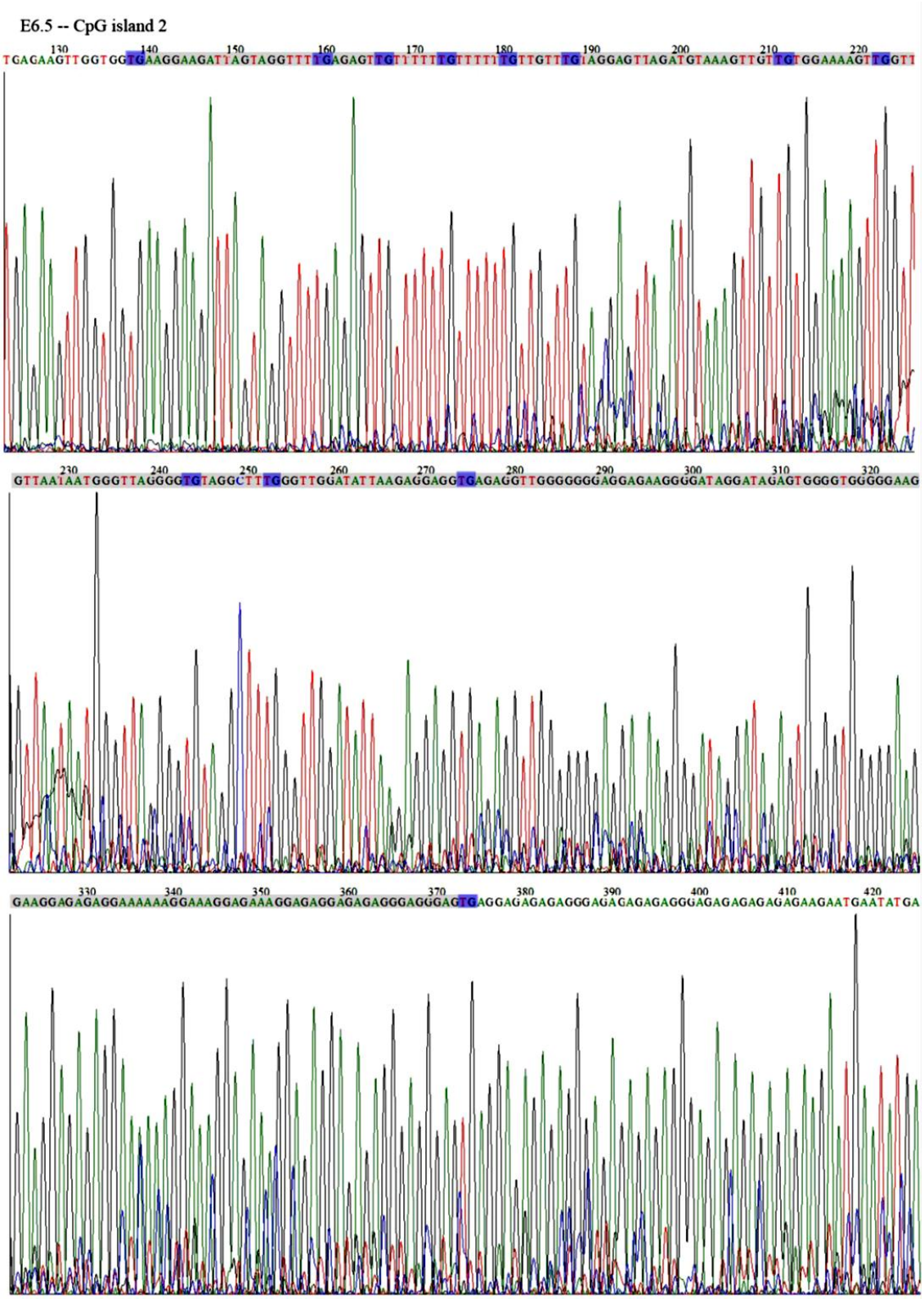

Appendix 2

DNA sequence chromatogram of *Hoxa2* promoter CpG island 2 from E6.5 mouse embryo genomic DNA

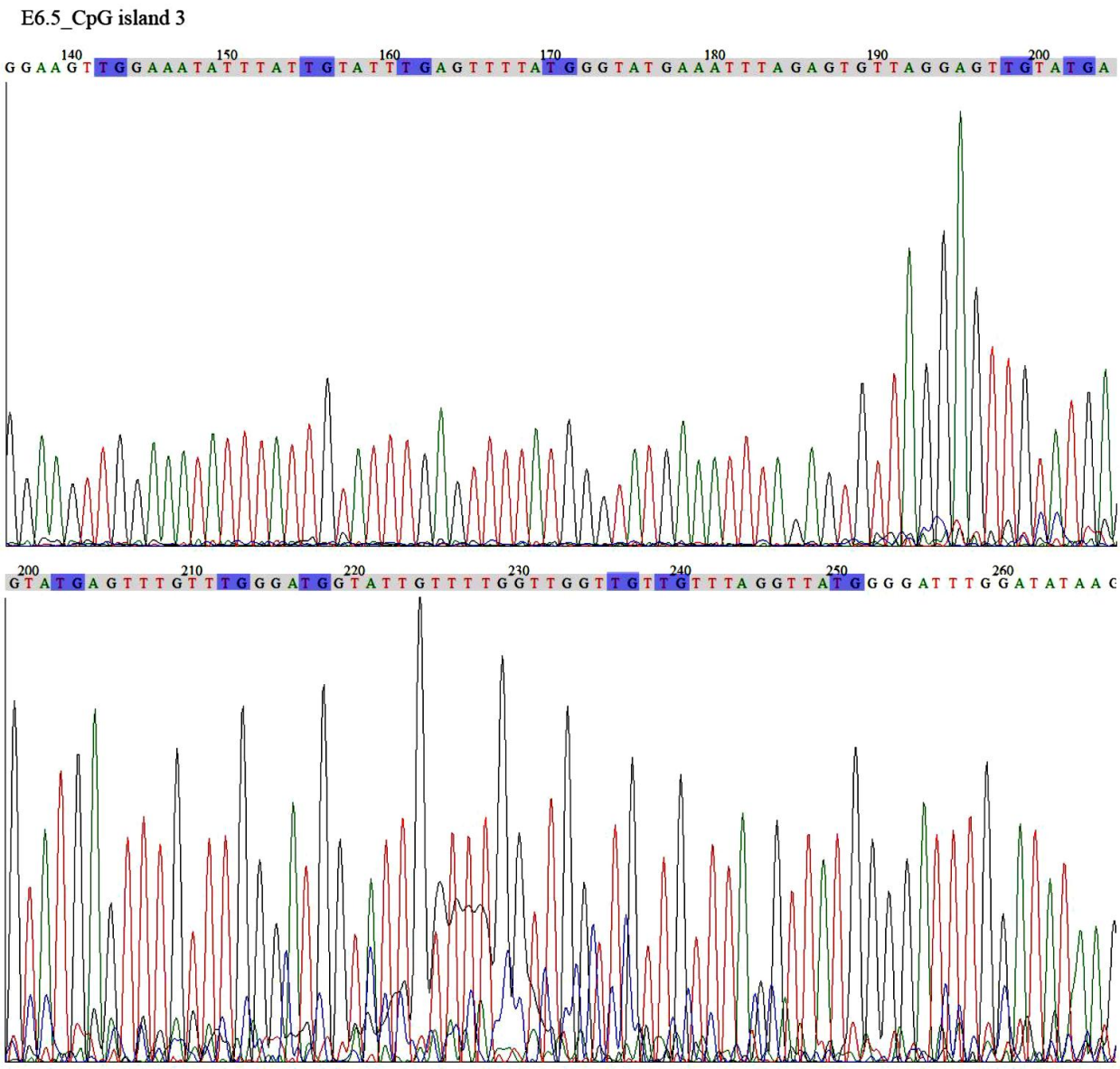

Appendix 3

DNA sequence chromatogram of *Hoxa2* promoter CpG island 3 from E6.5 mouse embryo genomic DNA

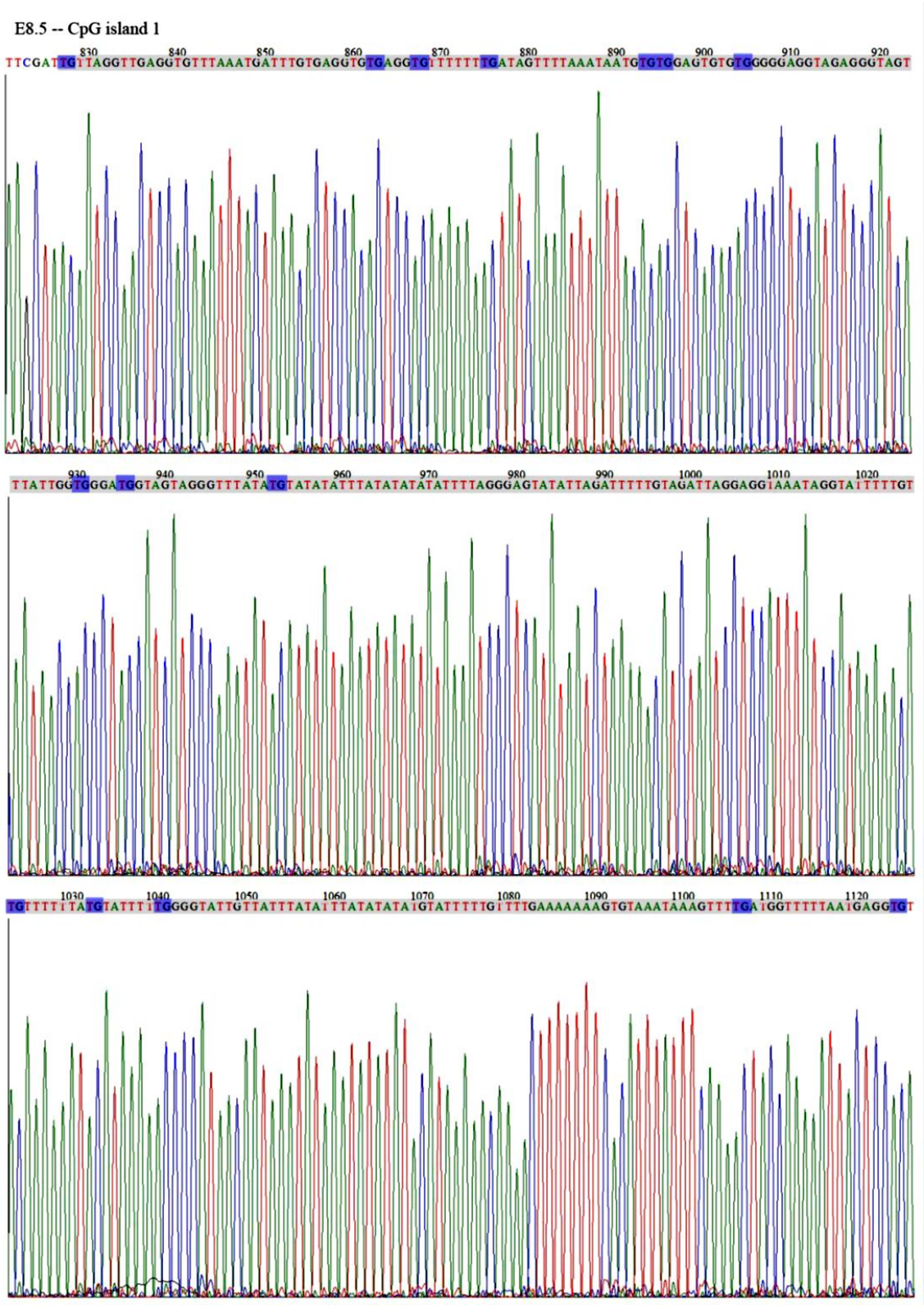

Appendix 4

DNA sequence chromatogram of *Hoxa2* promoter CpG island 1 from E8.5 mouse embryo genomic DNA

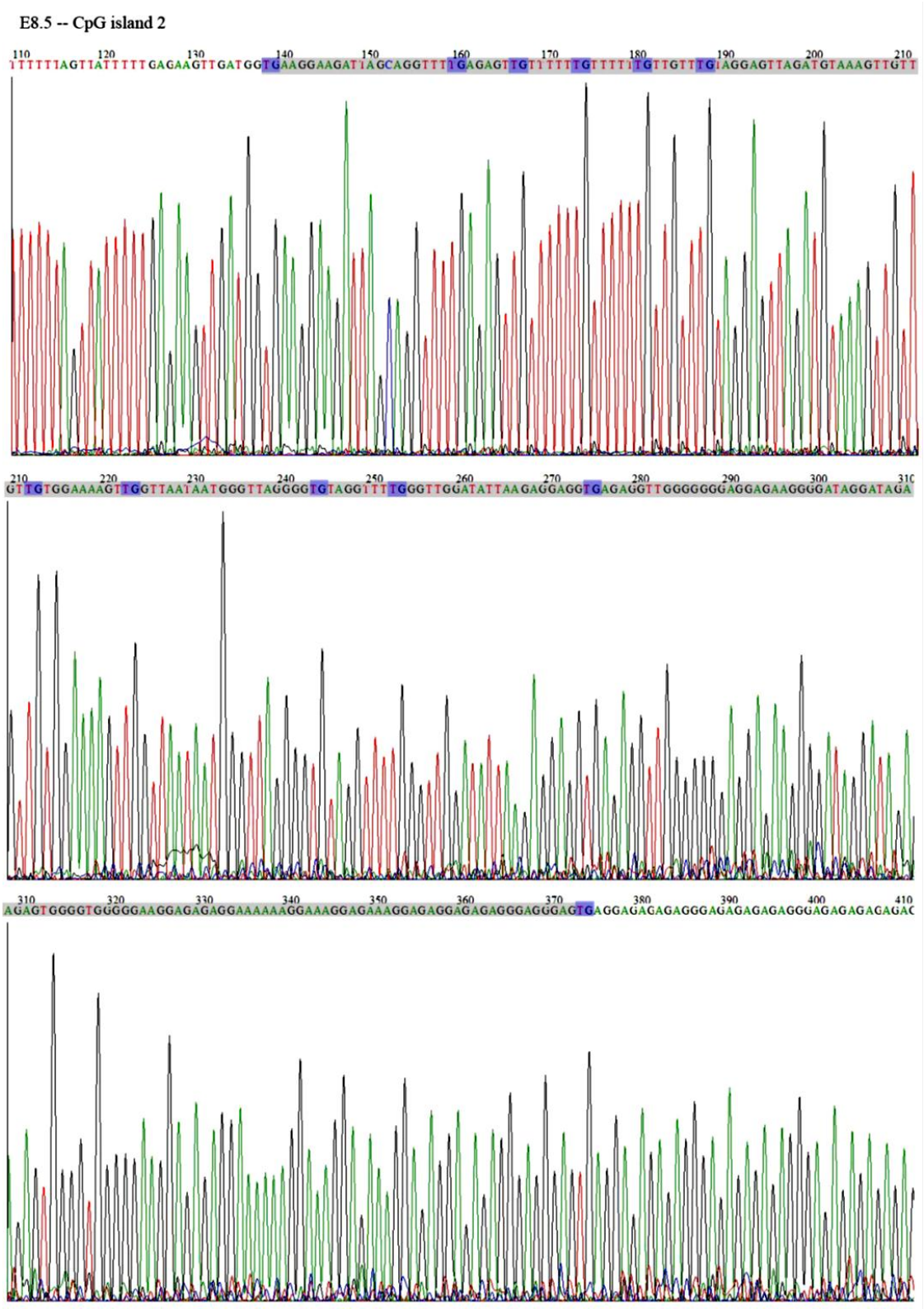

Appendix 5

DNA sequence chromatogram of *Hoxa2* promoter CpG island 2 from E8.5 mouse embryo genomic DNA

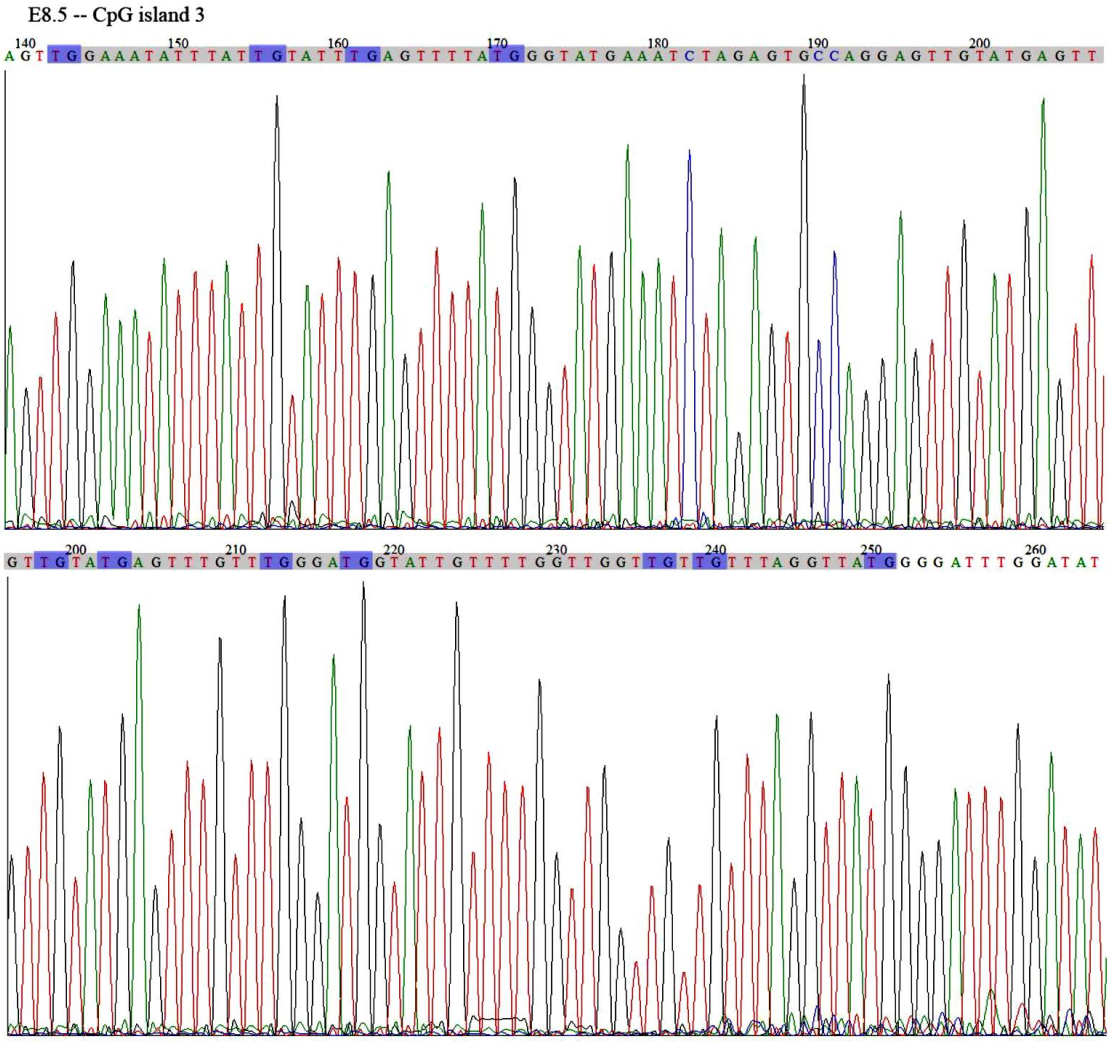

Appendix 6

DNA sequence chromatogram of *Hoxa2* promoter CpG island 3 from E8.5 mouse embryo genomic DNA

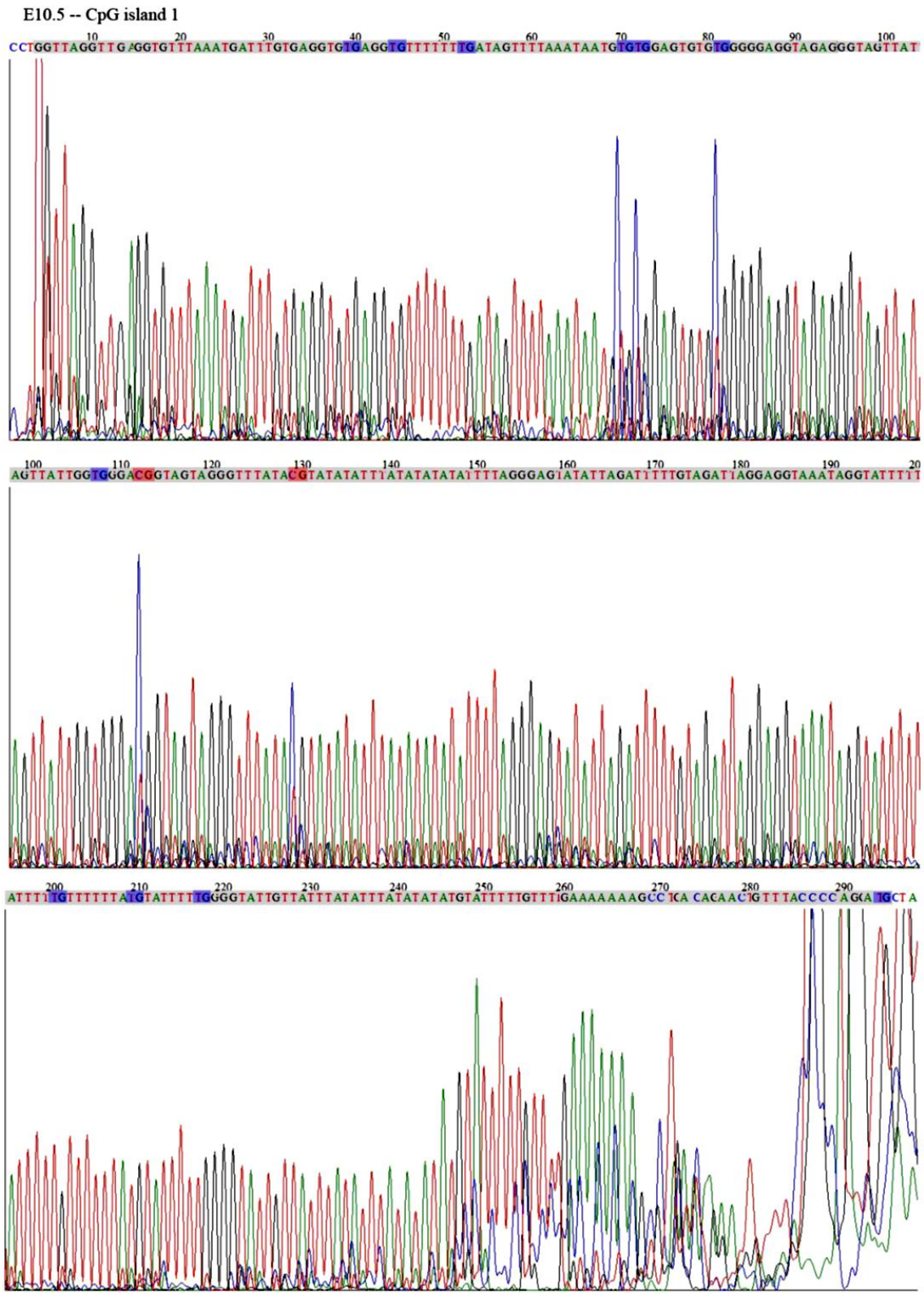

Appendix 7

DNA sequence chromatogram of *Hoxa2* promoter CpG island 1 from E10.5 mouse embryo genomic DNA

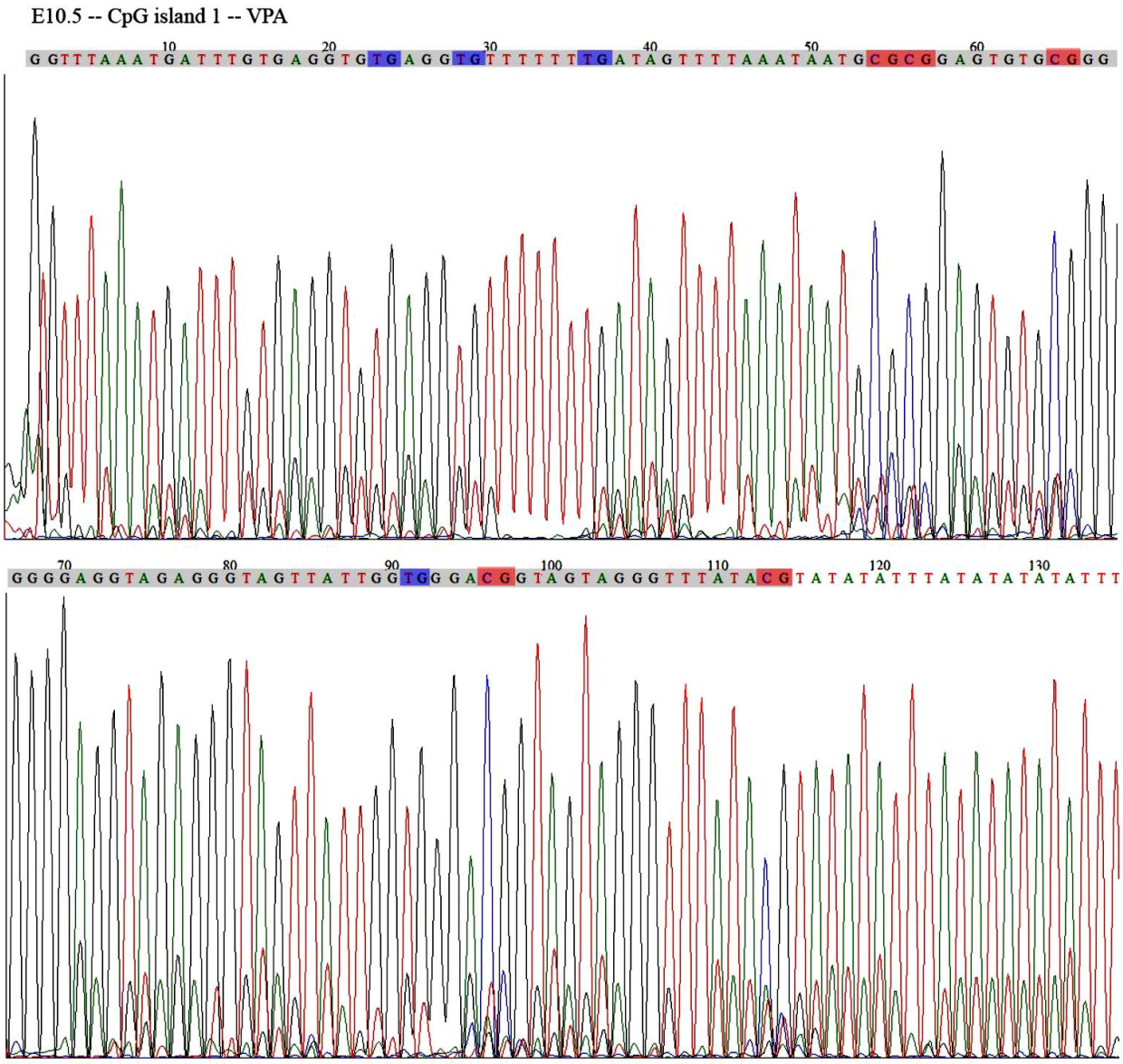

Appendix 8

DNA sequence chromatogram of *Hoxa2* promoter CpG island 1 from VPA treated E10.5 mouse embryo genomic DNA (Time-pregnant mice were administered s.c. 400 mg/kg VPA once daily between E8 and E10 and the embryos analyzed at E10.5).

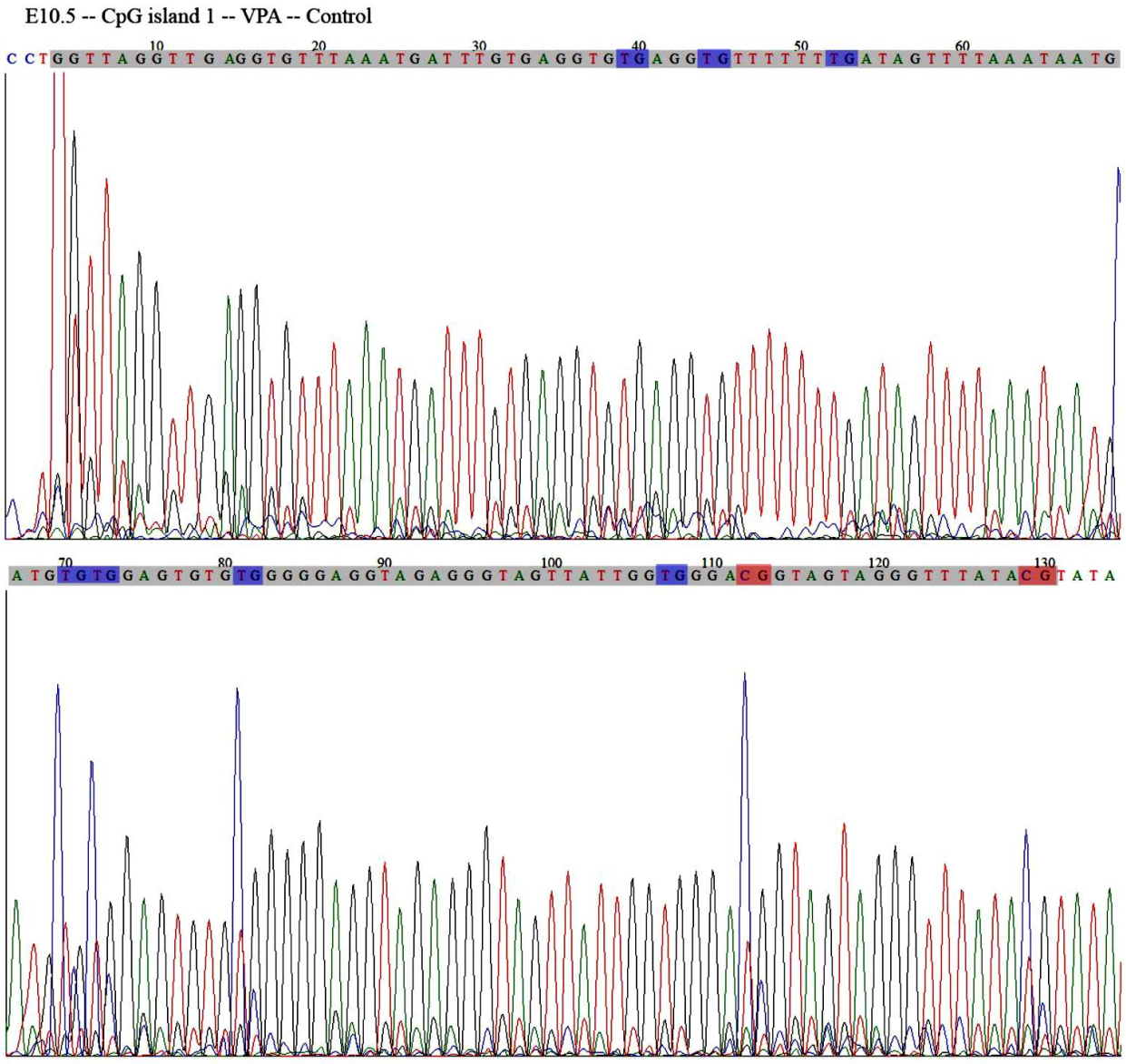

Appendix 9

DNA sequence chromatogram of *Hoxa2* promoter CpG island 1 from untreated control E10.5 mouse embryo genomic DNA

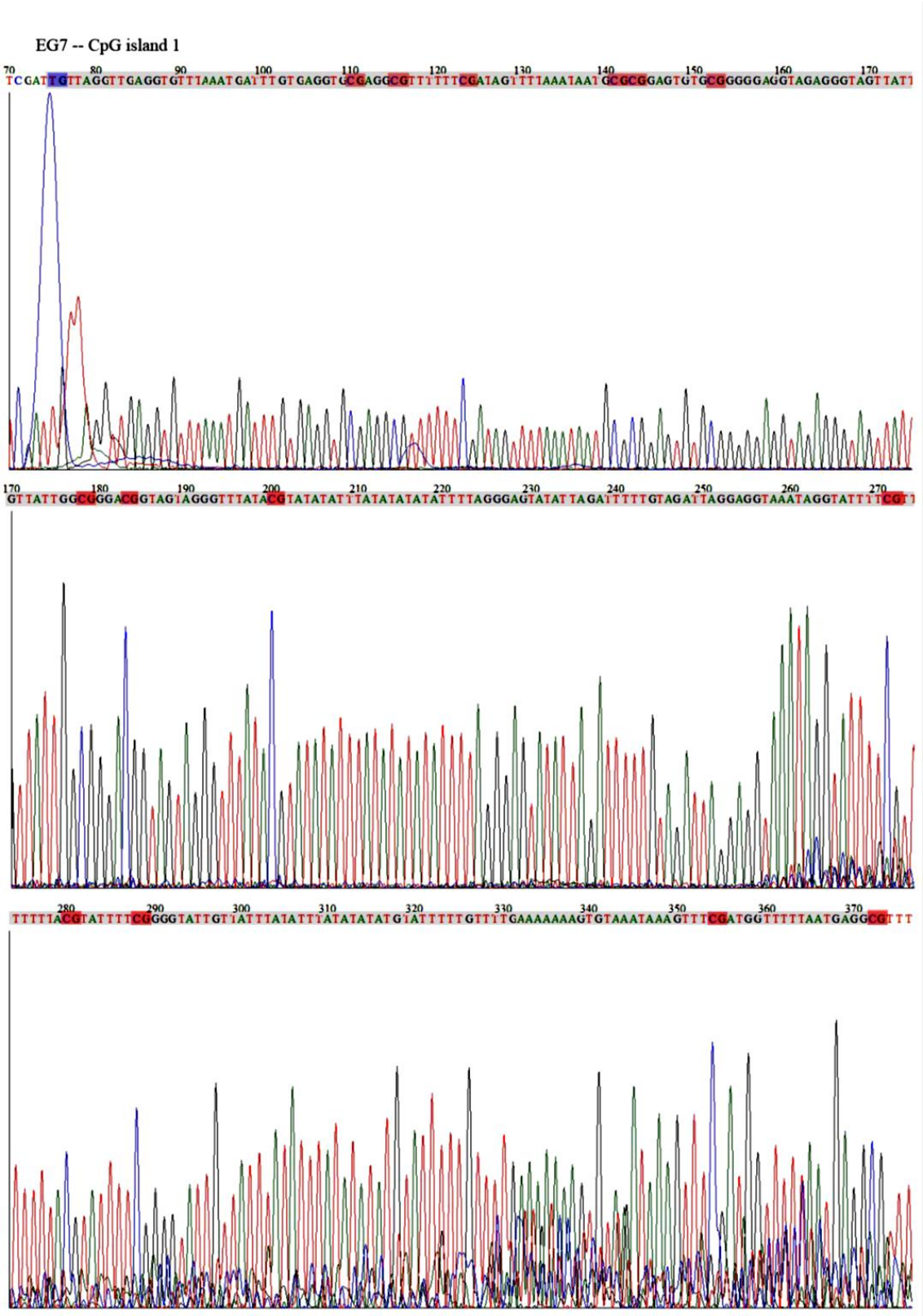

Appendix 10

DNA sequence chromatogram of *Hoxa2* promoter CpG island 1 from EG7 cell line genomic DNA

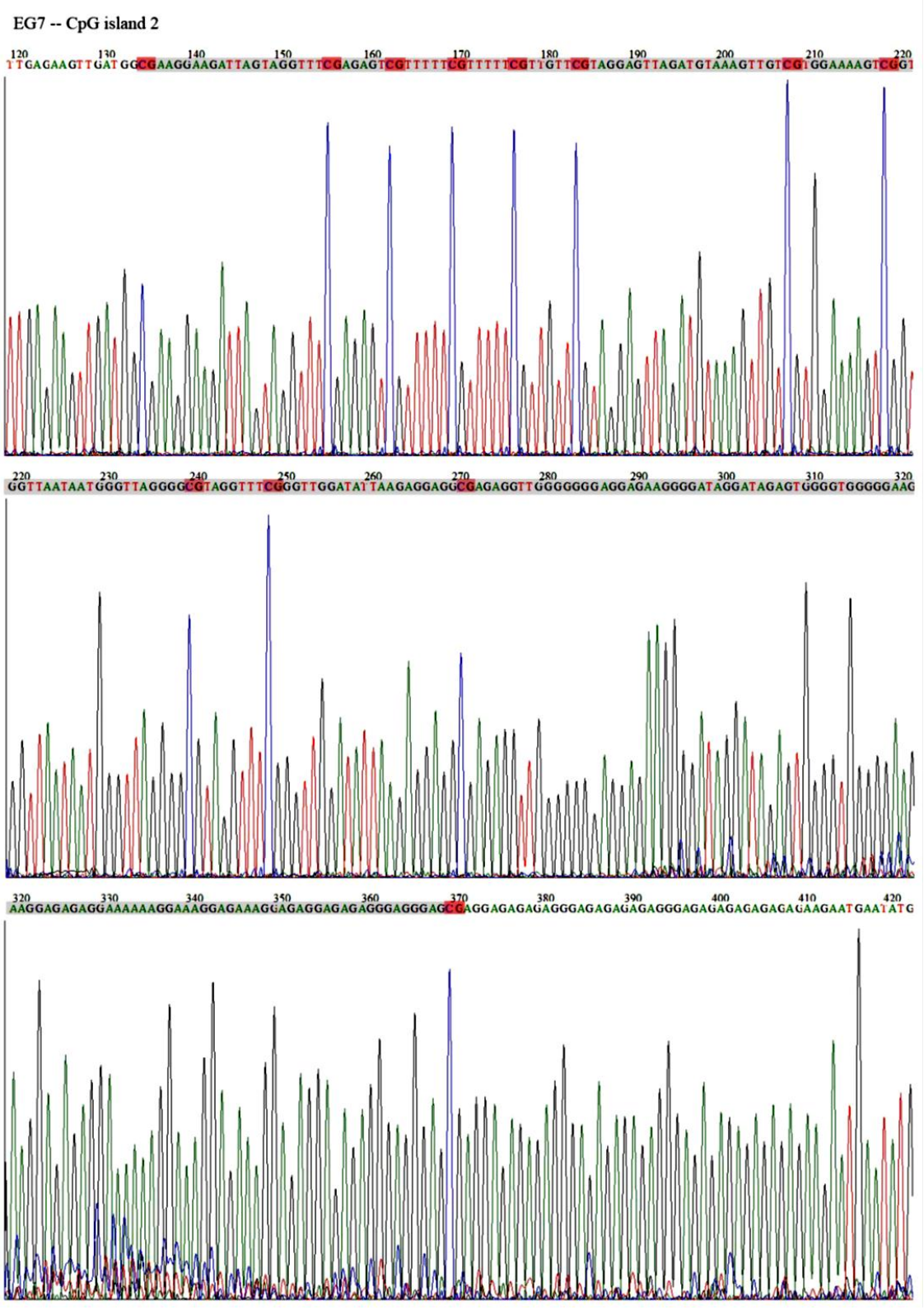

Appendix 11

DNA sequence chromatogram of *Hoxa2* promoter CpG island 2 from EG7 cell line genomic DNA

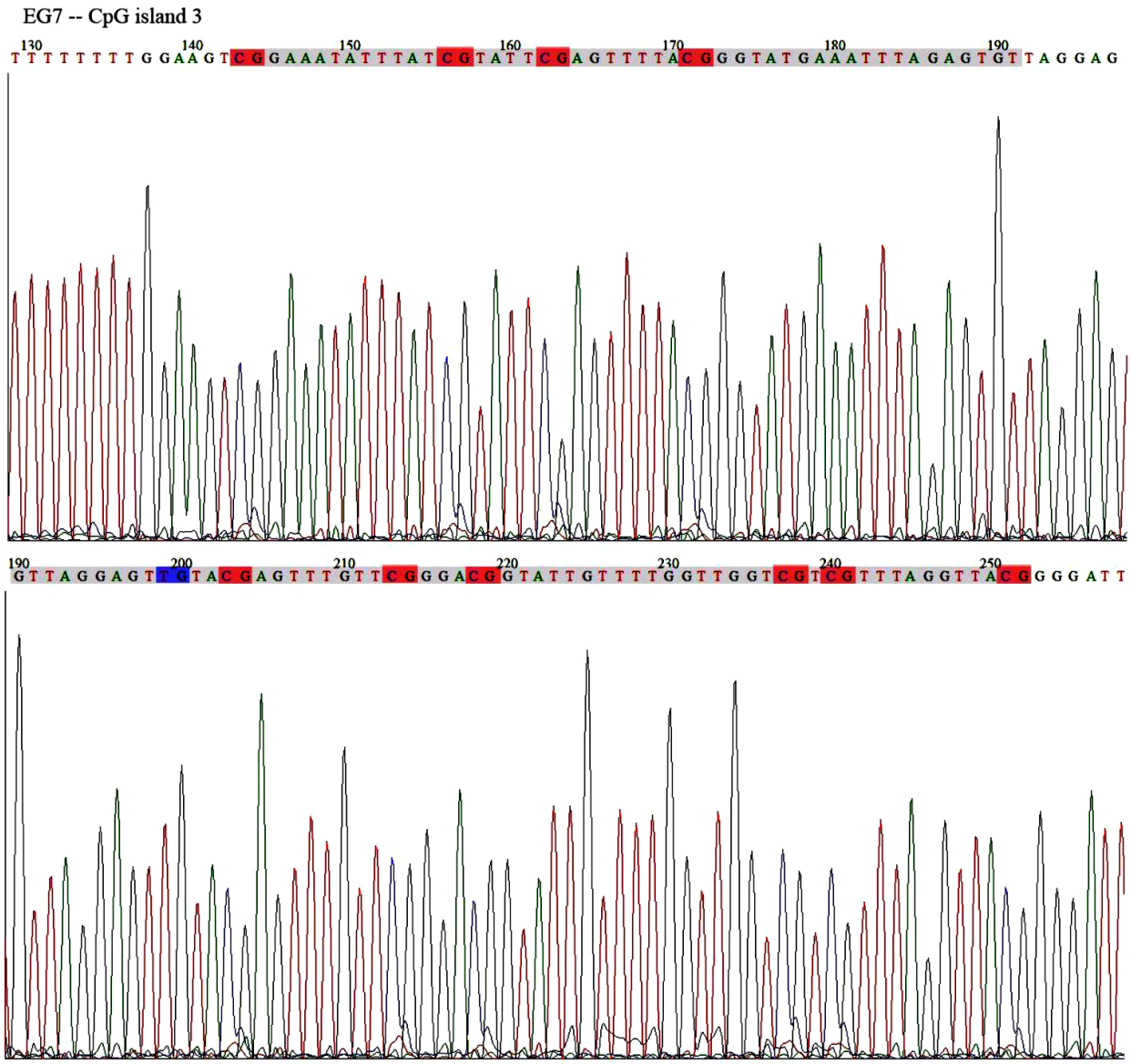

Appendix 12

DNA sequence chromatogram of *Hoxa2* promoter CpG island 3 from EG7 cell line genomic DN

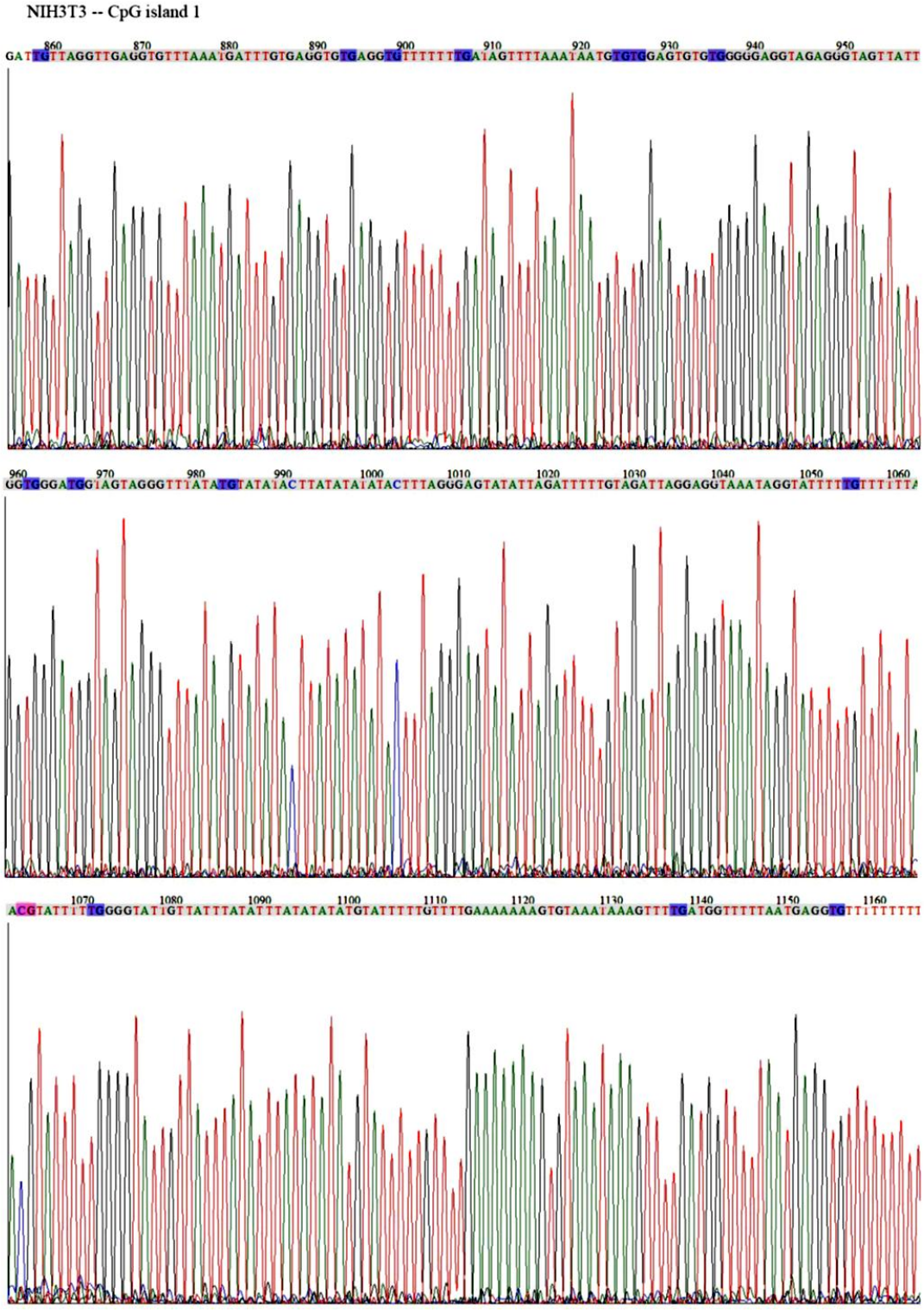

Appendix 13

DNA sequence chromatogram of *Hoxa2* promoter CpG island 1 from NIH3T3 cell line genomic DN

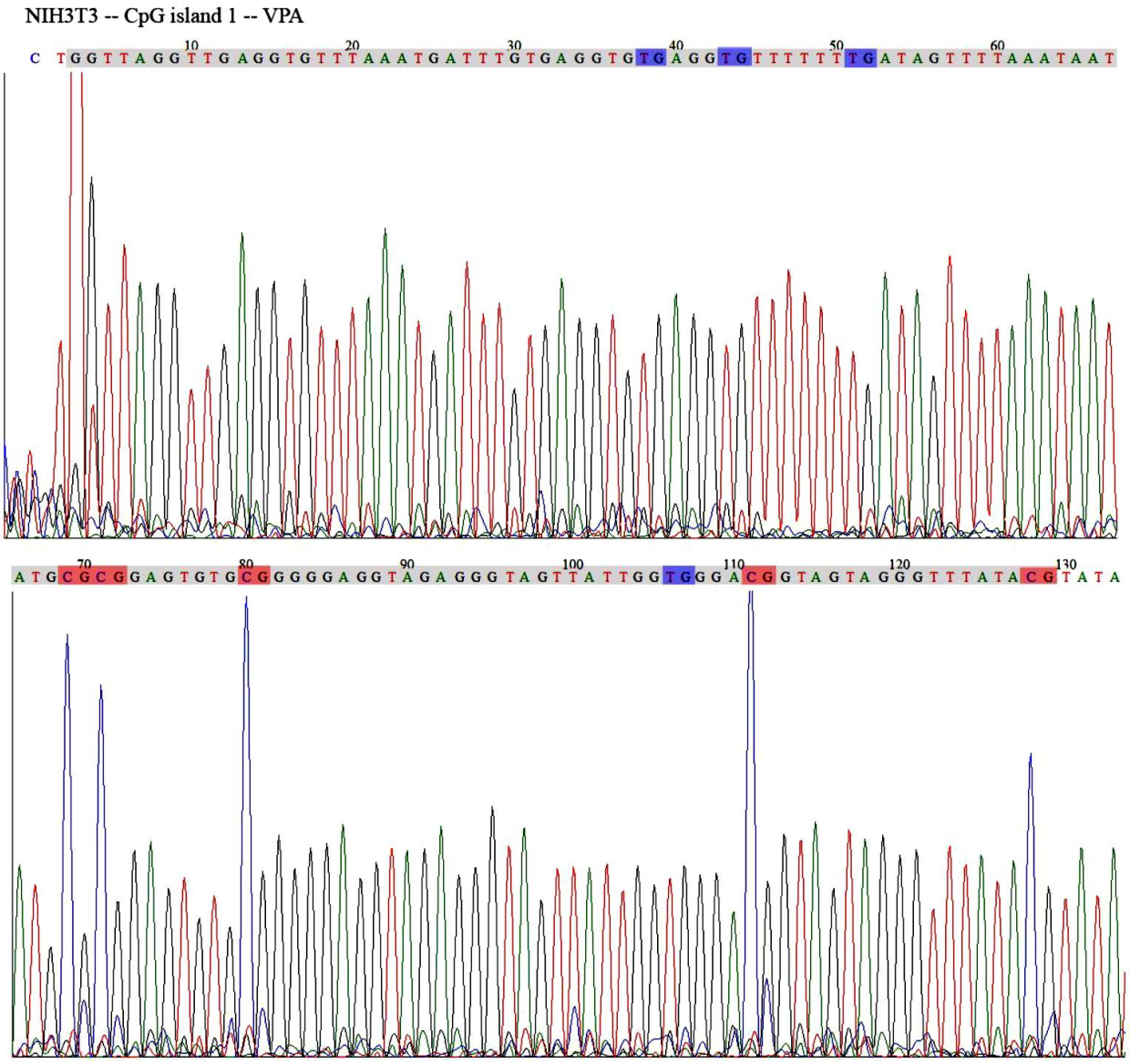

Appendix 14

DNA sequence chromatogram of *Hoxa2* promoter CpG island 1 from VPA treated NIH3T3 cell line genomic DNA (NIH3T3 cells treated with VPA (100 µg/mL) for 24 h)

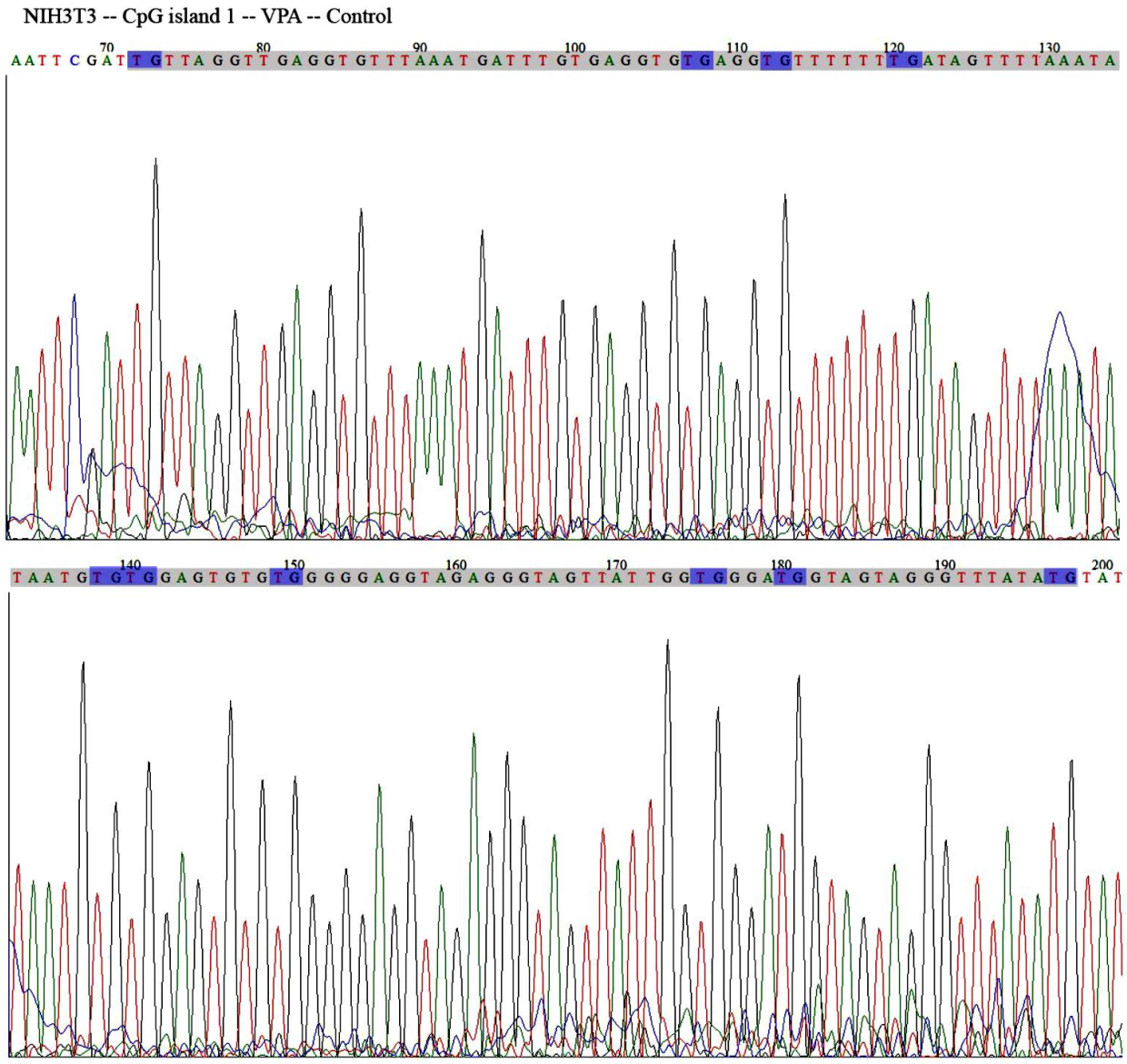

Appendix 15

DNA sequence chromatogram of *Hoxa2* promoter CpG island 1 from untreated control NIH3T3 cell line genomic DNA

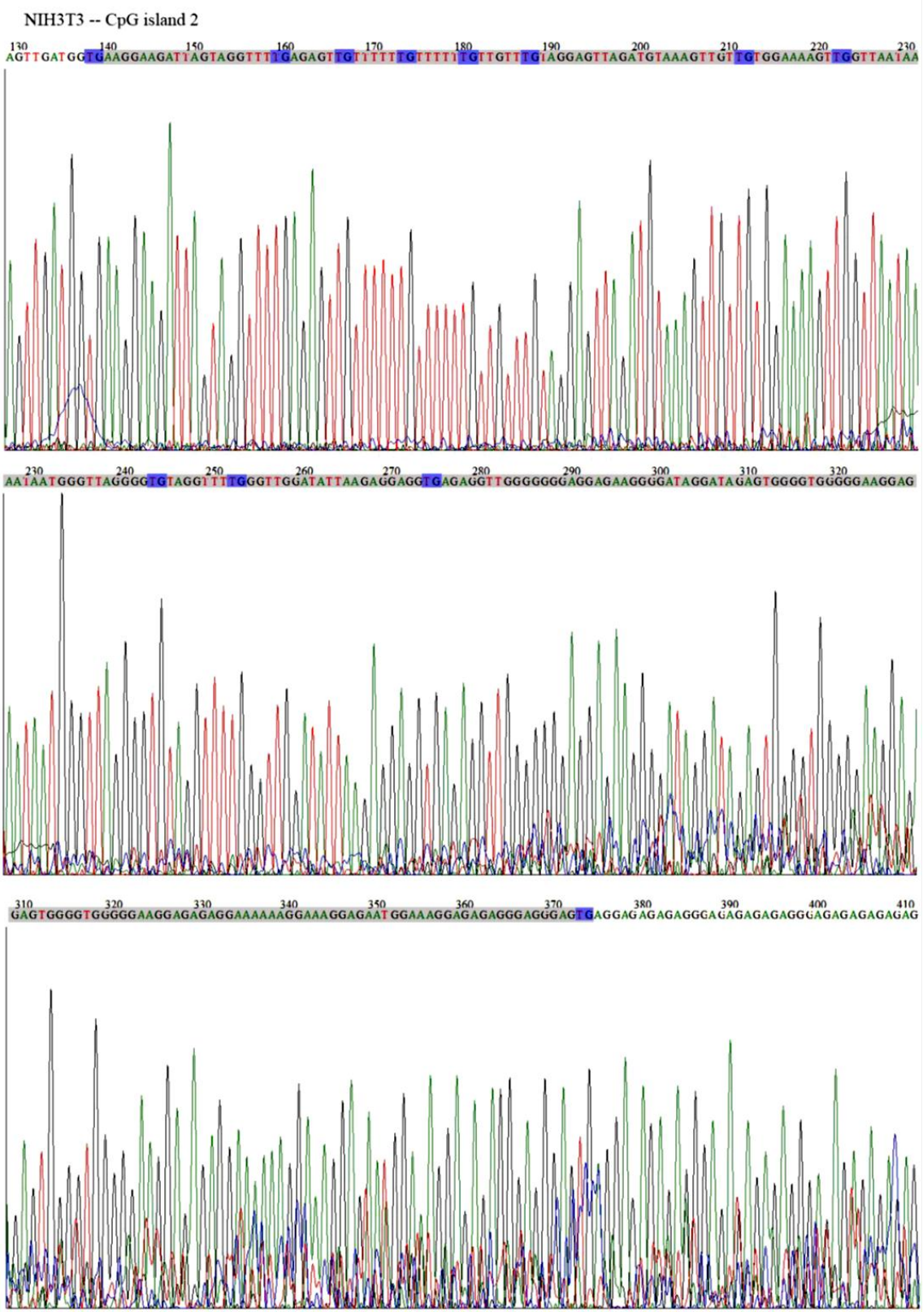

Appendix 16

DNA sequence chromatogram of *Hoxa2* promoter CpG island 2 from NIH3T3 cell line genomic DNA

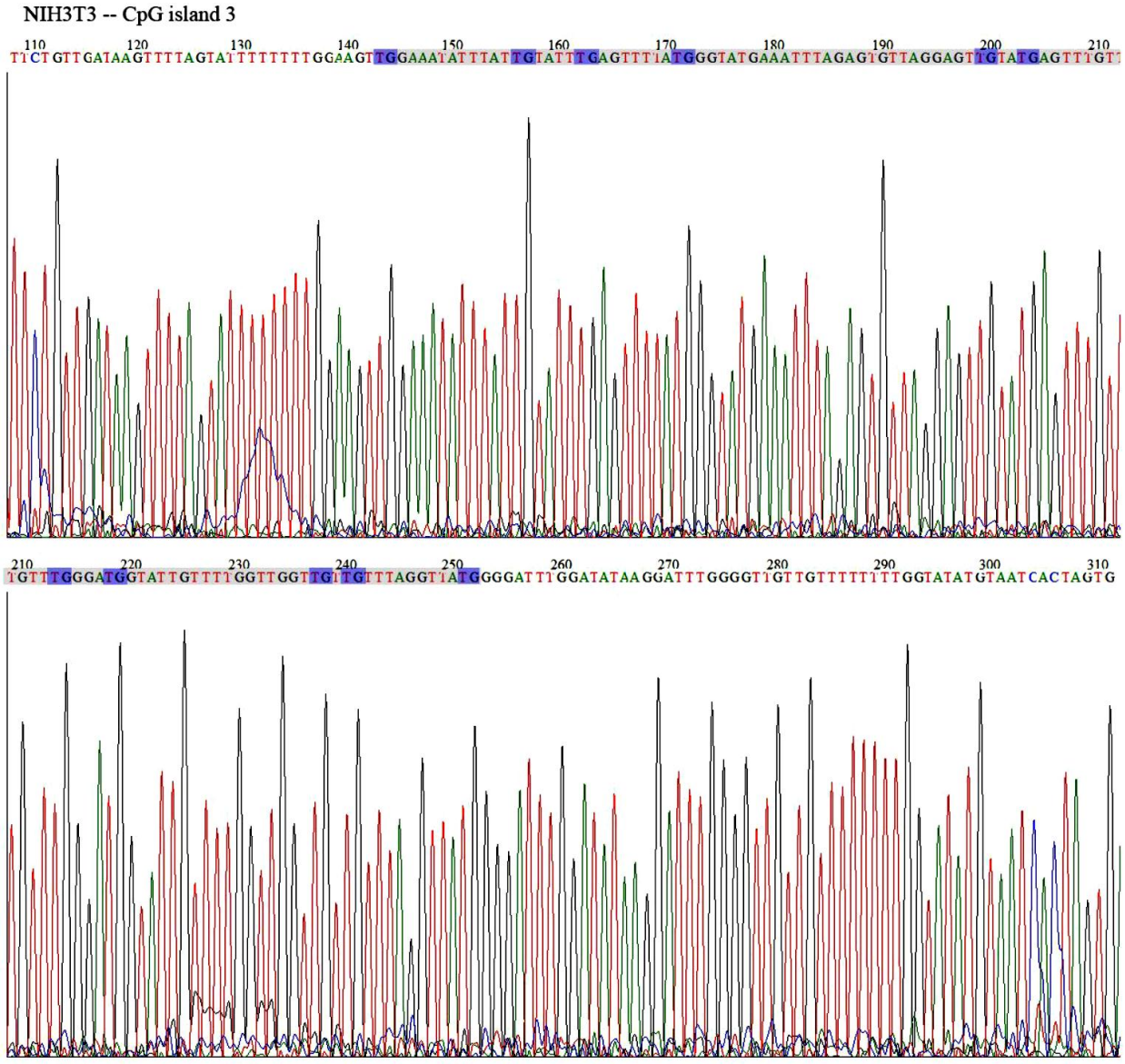

Appendix 17

DNA sequence chromatogram of *Hoxa2* promoter CpG island 3 from NIH3T3 cell line genomic DNA